Production of Hydrogen and 5-Aminolevulinic Acid by Photosynthetic Bacteria from Palm Oil Mill Effluent

Maneewan Suwansaard

A Thesis Submitted in Partial Fulfillment of the Requirements
for the Degree of Doctor of Philosophy in Biotechnology
Prince of Songkla University
2010

Thesis Title	Production of Hydrogen and 5-Aminolevulinic Acid by Photosynthetic Bacteria from Palm Oil Mill Effluent
Author	Miss Maneewan Suwansaard
Major Program	Biotechnology

Major Advisor :	**Examining Committee :**
……..……	…….……Chairperson
(Assoc. Prof. Dr. Poonsuk Prasertsan)	(Assoc. Prof. Dr. Duangporn Kanthachote)
Co-advisors :	…….…….
	(Assoc. Prof. Dr. Poonsuk Prasertsan)
……..……	…….…….
(Prof. Dr. Jill H. Zeilstra-Ryalls)	(Prof. Dr. Jill Zeilstra-Ryalls)
……..……	…….…….
(Assoc. Prof. Dr. Wanna Choorit)	(Dr. Piyarat Boonsawang)
	…….…….
	(Assoc. Prof. Dr. Lerluck Chitradon)

The Graduate School, Prince of Songkla University, has approved this thesis as partial fulfillment of the requirements for the Doctor of Philosophy Degree in Biotechnology

...……..
(Assoc. Prof. Dr. Krerkchai Thongnoo)
Dean of Graduate School

ชื่อวิทยานิพนธ์ การผลิตไฮโดรเจนและกรด5-อะมิโนลีวูลินิกโดยแบคทีเรียสังเคราะห์แสงจากน้ำทิ้งโรงงานสกัดน้ำมันปาล์ม

ผู้เขียน นางสาวมณีวรรณ สุวรรณสะอาด

สาขาวิชา เทคโนโลยีชีวภาพ

ปีการศึกษา 2552

บทคัดย่อ

ในการวิจัยและพัฒนากระบวนการผลิตก๊าซไฮโดรเจนจากน้ำทิ้งของโรงงานสกัดน้ำมันปาล์มจากการหมักแบบไร้แสง (dark fermentation) พบว่ามีกรดไขมันระเหยง่ายเหลืออยู่ ซึ่งสามารถใช้เป็นสารตั้งต้นสำหรับการผลิตก๊าซไฮโดรเจนจากแบคทีเรียสังเคราะห์แสง งานวิจัยนี้เริ่มจากการแยกเชื้อแบคทีเรียสังเคราะห์แสงจากตัวอย่างน้ำในทะเลสาบสงขลาในภาคใต้ของประเทศไทยจำนวน 34 ตัวอย่าง โดยเลี้ยงเชื้อในอาหารเลี้ยงเชื้อ modified GA ที่มีปริมาณกรดอะซิติก 20 มิลลิโมลาร์ เป็นแหล่งคาร์บอนภายใต้สภาวะไร้อากาศ-มีแสง โดยให้แสงที่ความเข้มแสง 3,000 ลักซ์ อุณหภูมิ 30 องศาเซลเซียส สามารถคัดแยกเชื้อได้ 19 สายพันธุ์ ที่มีความสามารถในผลิตก๊าซไฮโดรเจนได้ 4-326 มิลลิลิตรต่อลิตรต่อวัน โดยสายพันธุ์ TN1 เป็นสายพันธุ์ที่ให้อัตราการผลิตก๊าซไฮโดรเจนได้สูงสุด (43 มิลลิลิตรต่อลิตรต่อชั่วโมง$^{-}$) โดยให้ผลผลิต 1.85 โมลไฮโดรเจนต่อโมลอะซิเตท และมีประสิทธิภาพการใช้แสงที่ร้อยละ 1.07 นอกจากนี้สายพันธุ์ TN1 ยังมีคุณสมบัติที่เป็นมิตรต่อสิ่งแวดล้อมคือค่าพีเอชไม่มีการเปลี่ยนแปลงจากค่าพีเอชเป็นกลางตลอดช่วงเวลาการเลี้ยงเชื้อ และก๊าซชีวภาพที่ผลิตได้มีความบริสุทธิ์สูงโดยที่ปริมาณก๊าซคาร์บอนไดออกไซด์น้อยกว่าร้อยละ 0.1

จากการจำแนกสายพันธุ์ TN1 โดยการศึกษาลักษณะทางสรีรวิทยาร่วมกับการวิเคราะห์ 16S rDNA พบว่าเป็นสายพันธุ์ใหม่ของ *Rhodopseudomonas* (*Rps*.) *palustris* การศึกษาสภาวะที่เหมาะสมต่อการผลิตไฮโดรเจนโดย *Rps. palustris* TN1 พบว่าอาหารเลี้ยงเชื้อที่มีการค่าพีเอชเริ่มต้นเป็น 7 ร่วมกับการบ่มเชื้อภายใต้สภาวะไร้อากาศมีแสงที่ความเข้มแสง 3,000 ลักซ์ ให้ผลผลิตก๊าซไฮโดรเจนสูงสุด (2.5 โมลไฮโดรเจนต่อโมลอะซิเตท) เมื่อศึกษาผลของความเข้มข้นของกรดไขมันระเหยง่ายที่พบเป็นส่วนใหญ่ในน้ำเสียที่ผ่านการบำบัดด้วยกลุ่มจุลินทรีย์แบบไร้อากาศ ได้แก่กรดอะซิติก กรดโพรพิโอนิกและกรดบิวทิริกภายใต้สภาวะที่เหมาะสมดังกล่าว พบว่า

Rps. palustris TN1 สามารถใช้กรดไขมันระเหยง่ายดังกล่าวเพื่อการเจริญเติบโตและการผลิตก๊าซไฮโดรเจน โดยที่ความเข้มข้นของกรดอะซิติก 20 มิลลิโมลาร์ให้อัตราการผลิตก๊าซไฮโดรเจนสูงสุด (38.3 มิลลิลิตรต่อลิตรต่อชั่วโมง) ขณะที่กรดบิวทิริกความเข้มข้น 20 มิลลิโมลาร์ ให้ค่าผลผลิตก๊าซไฮโดรเจนสูงสุด (4.7โมลไฮโดรเจนต่อโมลบิวทิริก) เชื้อสามารถใช้กรดอะซิติกและกรดบิวทิริกได้ทั้งหมด (ร้อยละ 100) ขณะที่ใช้กรดโพรพิโอนิกได้เพียงร้อยละ 85 ประสิทธิภาพการใช้พลังงานแสงของกรดอะซิติกที่ความเข้มข้น 20 มิลลิโมลาร์ เท่ากับร้อยละ 2.0 และของกรดบิวทิริกที่ความเข้มข้น 20 มิลลิโมลาร์ เท่ากับร้อยละ 1.8 สูงกว่าประสิทธิภาพการใช้พลังงานแสงของกรดโพรพิโอนิกที่ความเข้มข้น 20 และ 40 มิลลิโมลาร์(ร้อยละ 0.2) ประมาณ 10 เท่า

วิธีทางสถิติแบบพื้นที่การตอบสนอง Central Composite Design (CCD) ได้นำมาใช้ศึกษาสัดส่วนความเข้มข้นกรดไขมันระเหยง่ายที่เหมาะสมต่อการผลิตก๊าซไฮโดรเจน และการผลิตพอลีไฮดรอกซีแอลคาโนเอต (polyhydroxyalkanoate, PHA) โดย *Rps. palustris* TN1 มีวัตถุประสงค์สองประการคือ หนึ่ง เพื่อหาสัดส่วนความเข้มข้นกรดไขมันระเหยง่ายที่เหมาะสมเมื่อต้องการให้ได้การผลิตก๊าซไฮโดรเจนสูงสุดและการผลิต PHA ต่ำสุด และเพื่อหาสัดส่วนความเข้มข้นกรดไขมันระเหยง่ายที่เหมาะสมเมื่อต้องการให้ได้การผลิตก๊าซไฮโดรเจนต่ำสุดและการผลิต PHA สูงสุด สมการลำดับที่สองใช้ในการอธิบายผลของกรดไขมันระเหยง่ายแต่ละชนิดและผลของอิทธิพลร่วมต่อการผลิตก๊าซไฮโดรเจนและ PHA จากการทดลองพบว่าอิทธิพลร่วมระหว่างกรดอะซิติกกับกรดบิวทิริกและกรดโพรพิโอนิกกับกรดบิวทิริกมีความสำคัญอย่างมีนัยสำคัญทางสถิติ (P<0.05) ขณะที่อิทธิพลร่วมระหว่างกรดอะซิติกกับกรดโพรพิโอนิกไม่มีความสำคัญในเชิงสถิติ ผลการคำนวณหาพื้นที่การตอบสนองที่เหมาะสมของกรดไขมันระเหยง่ายแต่ละชนิด โดยใช้โปรแกรม Design Expert (Stat-Ease) เวอร์ชั่น 7 พบว่าความเข้มข้นที่เหมาะสมของกรดไขมันระเหยง่ายเมื่อต้องการให้เชื้อผลิตก๊าซไฮโดรเจนได้สูงสุด ประกอบด้วย กรดอะซิติก 52 มิลลิโมลาร์ กรดโพรพิโอนิก 16 มิลลิโมลาร์ และกรดบิวทิริก 25 มิลลิโมลาร์ เชื้อผลิตก๊าซไฮโดรเจนได้สูงสุดที่ 1,278 ± 39.3 มิลลิลิตรต่อลิตร และสามารถผลิต PHAได้ 1.70 ± 0.24 กรัมต่อลิตร ซึ่งให้ค่าที่ได้จากการทดลองใกล้เคียงกับค่าทำนายจาก CCD (ก๊าซไฮโดรเจน 1,356 มิลลิลิตรต่อลิตร และ PHA 1.59 กรัมต่อลิตร) อีกทั้งยังได้ค่าประสิทธิภาพการผลิตก๊าซไฮโดรเจนเท่ากับร้อยละ 63.7 และให้ค่าประสิทธิภาพการใช้พลังงานแสงเท่ากับร้อยละ 0.69 สำหรับความเข้มข้นที่เหมาะสมของกรดไขมันระเหยง่ายเมื่อต้องการให้เชื้อผลิต PHAได้สูงสุดประกอบด้วยกรดซิติก 73 มิลลิโมลาร์และกรดโพรพิโอนิก 34 มิลลิโมลาร์ ภายใต้ความเข้มข้นดังกล่าวเชื้อผลิต PHA 1.83 ± 0.63 กรัมต่อลิตร

และผลิตไฮโดรเจน 970 ± 184 มิลลิลิตรต่อลิตร ค่าดังกล่าวมีความแตกต่างจากค่าที่ทำนายโดย CCD คิดเป็นร้อยละ 3.2 และร้อยละ 23.9 ตามลำดับ การผลิต PHA โดยใช้ความเข้มข้นกรดอะซิติกและกรดโพรพิโอนิกในสัดส่วนที่เหมาะสมนี้ ให้ผลผลิต PHA เพิ่มขึ้นร้อยละ 23.7

วิธี Plackett-Burman ได้นำมาใช้ศึกษาผลของปัจจัยภายใน (องค์ประกอบของอาหารเลี้ยงเชื้อ) และปัจจัยภายนอก (พีเอชเริ่มต้นและความเข้มแสง) เพื่อคัดเลือกปัจจัยที่มีอิทธิพลต่อการผลิตก๊าซไฮโดรเจนด้วยเชื้อ *Rps. palustris* TN1 เลี้ยงเชื้อภายใต้สภาวะไร้อากาศ-มีแสง (3,000 ลักซ์) และมีกรดไขมันระเหยง่าย (กรดอะซิติก 52 มิลลิโมลาร์ กรดโพรพิโอนิก 16 มิลลิโมลาร์ และ กรดบิวทิริก 25 มิลลิโมลาร์) เป็นแหล่งคาร์บอน พบว่าอาหารเลี้ยงเชื้อที่มีองค์ประกอบของยีสต์สกัด โซเดียมไบคาร์บอเนต รวมทั้งค่าพีเอชเริ่มต้นของอาหารเลี้ยงเชื้อ เป็นปัจจัยที่มีความสำคัญทางสถิติ (P<0.05) จากนั้นนำปัจจัยที่มีความสำคัญดังกล่าวมาศึกษาสัดส่วนที่เหมาะสมด้วยวิธีการออกแบบพื้นที่การตอบสนอง (Response surface methodology, RSM) ผลการทำนายพื้นที่การตอบสนองพบว่าองค์ประกอบของอาหารที่มียีสต์สกัด 2.3 กรัมต่อลิตร และโซเดียมไบคาร์บอเนตเท่ากับ 0.63 กรัมต่อลิตร ร่วมกับการปรับพีเอชอาหารเลี้ยงเชื้อเริ่มต้นเป็น 7.07 ให้ปริมาณก๊าซไฮโดรเจนที่ผลิตได้เท่ากับ 2,214 มิลลิลิตรต่อลิตร (R^2 = 0.98) เมื่อนำสภาวะดังกล่าวไปใช้เพื่อผลิตก๊าซไฮโดรเจน พบว่า *Rps. palustris* TN1 สามารถผลิตก๊าซไฮโดรเจนได้เท่ากับ 2,618 ± 273 มิลลิลิตรต่อลิตร ประสิทธิภาพการผลิตก๊าซไฮโดรเจนคิดเป็นร้อยละ 62.6 และค่าประสิทธิภาพการใช้พลังงานแสงเท่ากับร้อยละ 0.7 การผลิตก๊าซไฮโดรเจนในสภาวะที่เหมาะสมนี้สามารถเพิ่มปริมาณการผลิตก๊าซได้ถึงสองเท่ารวมทั้งเชื้อสามารถใช้กรดไขมันระเหยง่ายทั้งหมด เพิ่มขึ้นร้อยละ 40

การศึกษาความสามารถในการผลิตก๊าซไฮโดรเจนจากน้ำทิ้งรวมของโรงงานสกัดน้ำมันปาล์มโดย *Rps. palustris* TN1 ที่ระดับความเจือจางต่างๆ พบว่าการเลี้ยงเชื้อภายใต้สภาวะไร้อากาศโดยการเติมก๊าซอาร์กอน เชื้อสามารถผลิตก๊าซไฮโดรเจนได้ 29-865 มิลลิลิตรต่อลิตร นอกจากนี้เมื่อเลี้ยงเชื้อภายใต้สภาวะมีอากาศเล็กน้อย (ปราศจากการเติมก๊าซอาร์กอน) ในน้ำทิ้งรวมที่ไม่มีการเติมอาหารเสริมและมีการเติมอาหารเสริม (ยีสต์สกัดและโซเดียมไบคาร์บอเนต) และเจือจางน้ำทิ้งรวมในระดับความเจือจางไม่เจือจางจนถึงระดับความเจือจาง 1 ต่อ 20 พบว่าน้ำทิ้งรวมระดับความเจือจาง 1 ต่อ 2 ให้ผลลิตก๊าซไฮโดรเจนสูงสุด 2.64 และ 2.34 โมลไฮโดรเจนต่อโมลกรดไขมันระเหยง่ายทั้งหมด ตามลำดับ การศึกษาค่าทางจลนพลศาสตร์พบว่า การผลิตไฮโดรเจนที่ระดับความเจือจาง 1 ต่อ 2 ที่ไม่มีการเติมและเติมอาหารเสริมให้ปริมาณการผลิตก๊าซสูงสุด 2,906 และ 3,090 มิลลิลิตรต่อลิตรด้วยอัตราการผลิตก๊าซสูงสุด 32.5 และ 41.5 มิลลิลิตรต่อลิตรต่อ

ชั่วโมงตามลำดับ ประสิทธิภาพการใช้กรดไขมันระเหยง่ายทั้งหมดในสองสูตรอาหารมีค่ามากกว่าร้อยละ 85 ผลการทดลองในหัวข้อนี้บ่งชี้ว่าแบคทีเรียสังเคราะห์แสงสามารถเจริญและผลิตไฮโดรเจนจากน้ำทิ้งรวมของโรงงานสกัดน้ำมันปาล์ม

การปรับปรุงสายพันธุ์แบคทีเรียสังเคราะห์แสงเพื่อเพิ่มศักยภาพในการผลิตกรด 5 อะมิโนลีวูลินิก (5-aminolevulic acid, ALA) โดยใช้เทคนิคทางด้านพันธุวิศวกรรมดัดแปรยีน *hemB* ของสายพันธุ์ *Rhodobacter* (*Rbs*.) *sphaeroides* SH5 ยีน *hemB* เป็นยีนที่เกี่ยวข้องกับการสังเคราะห์เอนไซม์ porphobilinogen synthase (PBGS) ซึ่งใช้ ALA เป็นสารตั้งต้นในการผลิตไพโรลในวิถีการสังเคราะห์สารเตตระไพโรลอันได้แก่ ฮีม แบคเทอริโอคลอโรฟิลล์และวิตามินบีสิบสอง ลักษณะโครงสร้างโปรตีนของเอนไซม์ PBGS แสดงให้เห็นว่า เอนไซม์มีกิจกรรมการทำงานที่สูงเมื่ออยู่ในรูปมัลติเมอร์ และประสิทธิภาพการทำงานของเอนไซม์ลดลงเมื่ออยู่ในรูปไดเมอร์ โครงสร้างโปรตีนดังกล่าวได้นำมาใช้ในการทำนายว่า การลดจำนวนกรดอะมิโนที่เกี่ยวข้องกับการรวมตัวเป็นมัลติเมอร์ จำนวน 15-27 หน่วย มีความเป็นไปได้ในการลดกิจกรรมการทำงานของเอนไซม์ พลาสมิด *hemB* ดัดแปร (pMS3)ได้พัฒนาจากพลาสมิดดั้งเดิม pBBR1-MCS2 โดยลดลำดับนิวคลีโอไทด์ที่เกียวข้องจากข้อมูลเบื้องต้น พลาสมิดทั้งสองถูกถ่ายโอนไปยัง *Rba. sphaeroides* SH5 เพื่อศึกษากิจกรรมการทำงานของเอนไซม์ PBGS ผลการทดลองพบว่ากิจกรรมการทำงานของเอนไซม์ใน *Rba. sphaeroides* SH5 (pMS3) เทียบกับ *Rba. sphaeroides* SH5 (pBBR1-MCS2) มีกิจกรรมการทำงานลดลง 7 เท่าในสภาวะมีอากาศ-ไร้แสง (จาก 0.158 ลดลงเป็น 0.024 ไมโครโมลต่อชั่วโมงต่อมิลลิกรัมโปรตีน) และกิจกรรมการทำงานลดลง 27 เท่าในสภาวะไร้อากาศ-มีแสง (จาก 0.414 ลดลงเป็น 0.015 ไมโครโมลต่อชั่วโมงต่อมิลลิกรัมโปรตีน) ผลการทดสอบความสามารถในการผลิต ALA โดยการปลดปล่อยออกนอกเซลล์เมื่อเลี้ยงเชื้อทั้งสองสายพันธุ์ในอาหาร modified GA พบว่าไม่มีการปลดปล่อย ALA ออกนอกเซลล์ในทั้งสองสายพันธุ์เมื่อเลี้ยงเชื้อภายใต้สภาวะมีอากาศ-ไร้แสง ในขณะที่การปลดปล่อย ALA ภายนอกเซลล์เพิ่มขึ้นสองเท่าในสายพันธุ์ *Rba. sphaeroides* SH5 (pMS3) (6.28 ไมโครโมลาร์) เมื่อเทียบกับ *Rba. sphaeroides* SH5 (pBBR1-MCS2) (3.16 ไมโครโมลาร์) ภายใต้สภาวะไร้อากาศ-มีแสง

การวิเคราะห์หาปริมาณ ALA โดยวิธีทางชีวภาพได้คิดค้นขึ้นมาใหม่ในงานวิจัยชิ้นนี้เพื่อลดต้นทุนในการวิเคราะห์หาปริมาณ ALA ที่เชื้อปลดปล่อยออกนอกเซลล์ การวิเคราะห์อาศัยหลักการการเจริญของแบคทีเรียสังเคราะห์แสง *Rba. sphaeroides* AT1 ต้องการ ALA เพื่อการเจริญ ผลของการศึกษาความสัมพันธ์ระหว่างความเข้มข้นของ ALA ต่อการเจริญของ *Rba.*

sphaeroides AT1 พบว่ามีความแม่นยำสูง (R^2=0.89) การตรวจสอบความเที่ยงของวิธีวิเคราะห์ทางชีวภาพและวิธีวิเคราะห์โดยใช้ HPLC พบว่าค่าที่วิเคราะห์ได้มีความแตกต่างน้อยกว่าร้อยละ 15 ผลการทดลองบ่งชี้ว่ามีความเป็นไปได้ในการวิเคราะห์ ALA ด้วยวิธีทางชีวภาพ

การศึกษาความสามารถในการผลิต ALA โดยเชื้อ *Rba. sphaeroides* SH5 (pMS3) และ *Rba. sphaeroides* SH5 (pBBR1-MCS2) จากน้ำทิ้งรวมโรงงานสกัดน้ำมันปาล์มที่ไม่มีการเติมอาหารเสริม ที่ความเจือจาง 2 ระดับคือ ไม่เจือจางและเจือจาง 1 ต่อ 2 พบว่าอัตราการเจริญจำเพาะของทั้งสองสายพันธุ์ในน้ำทิ้งรวมทั้งสองระดับความเจือจางไม่มีความแตกต่างอย่างมีนัยสำคัญทางสถิติ (P>0.05) บ่งชี้ว่าองค์ประกอบในน้ำทิ้งไม่ส่งผลต่อการเจริญของสายพันธุ์ที่ได้รับการปรับปรุงพันธุ์ (*Rba. sphaeroides* SH5 (pMS3)) ความเข้มข้นของ ALA ที่เชื้อ *Rba. sphaeroides* SH5 (pMS3) ปลดปล่อยออกนอกเซลล์สูงสุดในน้ำทิ้งที่ไม่เจือจางและ ระดับความเจือจาง 1 ต่อ 2 มีค่า 36.3 และ 61.0 ไมโครโมลาร์ ตามลำดับ เมื่อทำการเลี้ยงเชื้อเพียง 6 ชั่วโมง ขณะที่ความเข้มข้นของ ALA ปลดปล่อยออกนอกเซลล์ของ *Rba. sphaeroides* SH5 (pBBR1-MCS2) มีค่าสูงสุด 2.9 ไมโครโมลาร์ ณ เวลา 12 ชั่วโมงของการเลี้ยงเชื้อและไม่พบการปลดปล่อย ALA ออกนอกเซลล์เมื่อเลี้ยงในน้ำทิ้งรวมที่ระดับการเจือจาง 1 ต่อ 2 ตลอดระยะเวลาการเลี้ยงเชื้อ 48 ชั่วโมง ความสามารถในการปลดปล่อย ALA ออกนอกเซลล์ของ *Rba. sphaeroides* SH5 (pMS3) สูงกว่าการปลดปล่อยออกนอกเซลล์ของ *Rba. sphaeroides* SH5 (pBBR1-MCS2) ถึง 19 เท่าในน้ำทิ้งที่ไม่มีการเจือจาง ดังนั้นน้ำทิ้งโรงงานสกัดน้ำมันปาล์มสามารถบำบัดด้วย *Rba. sphaeroides* SH5 (pMS3) และได้ผลผลิต ALA เป็นผลิตภัณฑ์มูลค่าเพิ่ม

ความเป็นไปได้ในการผลิตผลิตภัณฑ์มูลค่าเพิ่มไฮโดรเจนและALA โดยเชื้อแบคทีเรียสังเคราะห์แสงสองสายพันธุ์ร่วมกัน โดยศึกษาในอาหารสังเคราะห์ที่มีกรดอะซิติกความเข้มข้น 20 มิลลิโมลาร์เป็นแหล่งคาร์บอนหลักและโซเดียมกลูตาเมต 5 มิลลิโมลาร์เป็นแหล่งไนโตรเจนหลักเลี้ยงเชื้อภายใต้สภาวะไร้อากาศ-มีแสง (3,000 ลักซ์) ขั้นต้นศึกษาผลของความเข้มข้นของ ALA (0-1 มิลลิโมลาร์) ต่อการเจริญของเชื้อ *Rps. palustris* TN1 (pBBR1-MSC2) และการผลิตก๊าซไฮโดรเจน พบว่า ความเข้มข้นต่าง ๆ ของ ALA ไม่มีผลต่อน้ำหนักเซลล์แห้งที่ได้ แต่มีผลให้การผลิตไฮโดรเจนเพิ่มขึ้นถึง 1,075 มิลลิลิตรต่อลิตรในอาหารที่มีการเติม ALA เข้มข้น 1 มิลลิโมลาร์ ขั้นต่อมาศึกษาความเป็นไปได้ในการเลี้ยงเชื้อสองสายพันธุ์ร่วมกัน พบว่าหลังการเลี้ยงเชื้อ 48 ชั่วโมง ไม่พบการเจริญของเชื้อ *Rps. palustris* TN1 (pBBR1-MSC2) ในอาหารที่มีการเติมเชื้อ 2 สายพันธุ์พร้อมกัน อย่างไรก็ตาม สามารถพบการเจริญของทั้งสองสายพันธุ์ เมื่อเลี้ยง *Rps.*

palustris TN1 (pBBR1-MSC2) ก่อนเป็นระยะเวลา 24 ชั่วโมง แล้วจึงเติม *Rba. sphaeroides* SH5 (pMS3) ดังนั้นกระบวนการแบบ 2 ขั้นตอนจึงมีศักยภาพในการเปลี่ยนแปลงสารอินทรีย์ที่เหลือเป็นก๊าซไฮโดรเจน และ ALA โดยผลิตก๊าซไฮโดรเจนโดยเชื้อ *Rps. palustris* TN1 1 เป็นลำดับแรก จากนั้นเติมแบคทีเรียสังเคราะห์แสงสายพันธุ์กลาย *Rba. sphaeroides* SH5 (pMS3) เพื่อผลิต ALA เป็นลำดับต่อไป

Thesis Title	Production of Hydrogen and 5-Aminolevulinic Acid by Photosynthetic Bacteria from Palm Oil Mill Effluent
Author	Miss Maneewan Suwansaard
Major Program	Biotechnology
Academic Year	2009

ABSTRACT

Research directed towards development of processes to produce hydrogen from palm oil mill effluent (POME) revealed that, following the application of existing biotreatment processes, there were residual volatile fatty acids (VFA) which could potentially be used as substrates for hydrogen production by photosynthetic bacteria. In this study, 34 samples were taken from Songkhla Lake in southern Thailand and purple non-sulfur photosynthetic bacteria were enriched for using modified GA medium containing 20 mM acetate as the major carbon source. From cultivation under anaerobic-low light (3,000 lux) conditions at 30°C for 96 h, 19 hydrogen producing isolates with productivities between 4 and 326 ml $l^{-1}d^{-1}$ were obtained. The isolate TN1 was the most efficient producer at a rate of 43 ml l^{-1} h^{-1} with a yield of 1.85 mol H_2 mol $acetate^{-1}$ and light conversion efficiency of 1.07%. Additional environmentally desirable features of photohydrogen production by isolate TN1 included the absence of pH change in the cultures and no detectable residual CO_2.

Morphological, physiological, and 16S rDNA analyses identified the isolate TN1 as a new strain of *Rhodopseudomonas* (*Rps*.) *palustris*. The optimal pH and light intensities for H_2 production by TN1 were found to be 7.0 and 3,000 lux, respectively. Its phototrophic H_2 production from various concentrations of the three predominant volatile fatty acids (VFAs) present in processed POME was investigated. The highest hydrogen production from each substrate was achieved at a concentration of 20 mM. The highest rate of hydrogen production was by TN1 grown with acetate

(38.3 $ml^{-1}l^{-1}h^{-1}$) while the highest hydrogen yield was by TN1 grown with butyrate (4.7 mol H_2 mol $substrate^{-1}$). TN1 consumed 100% of these VFAs but only 85% of the propionate. The maximum light conversion efficiencies when TN1 was grown with 40 mM acetate and 20 mM butyrate (2.0 and 1.8%) were about 10 times higher than that when grown with 20 and 40 mM propionate (0.2%).

A central composite design was employed with the aim of (i) optimizing hydrogen production and minimizing polyhydroxyalkanoate (PHA), and (ii) maximize PHA production and minimizing hydrogen production. Response surface plots were generated. Based on the experimental results, the statistically significant terms ($P<0.05$) describing the effects of the VFAs could be approximated with a second-order model. The interactive effects between acetate and butyrate, and propionate and butyrate were significant ($P<0.05$), while the interactive effects between acetate and propionate were insignificant. For a mixture of VFAs that are predicted to be optimal for maximum hydrogen production and minimum PHA formation, 52 mM acetate, 16 mM propionate, and 25 mM butyrate, the expected hydrogen production was 1,356 ml l^{-1} and the expected PHA production was 1.59 g l^{-1}, respectively. These predicted values were validated experimentally, as the actual values measured for hydrogen evolution were 1,278 ± 39.3 ml l^{-1} and 1.70 ± 0.24 g l^{-1} for PHA formation. The hydrogen production and light conversion efficiencies were 63.7% and 0.69 %, respectively. For a mixture of VFAs that are predicted to be optimal for maximum PHA formation and minimum hydrogen production, 73 mM acetate and 34 mM propionate, the expected PHA production was 1.89 g l^{-1} and the expected hydrogen production was 1,273.9 ml l^{-1}. Subsequent experimental measurements using this mixture of VFAs revealed the level of PHA formation was 1.83 ± 0.63 g l^{-1} and hydrogen production was 970 ± 184 ml l^{-1}. The devaiations between the expected and observed values were 3.2% and 23.9%, respectively. Under these conditions, PHA content increased 23.7%.

To determine the effect of intrinsic (medium compositions) and extrinsic parameters (initial pH and light intensity) on hydrogen production by *Rps. palustris* TN1 under photosynthetic conditions with the optimum mixture of the three VFAs as substrates, the statistical model of Plackett-Burman within the Design Expert

program (Stat-Ease, Version 7) was used to screen for important parameters. The optimal condition was then predicted using response surface methodology (RSM). The concentration of $NaHCO_3$, the amount of yeast extract, and the initial pH were found to be significant ($P<0.05$) with respect to their effects on hydrogen production, and the optimal medium condition was predicted to be 0.63 g l^{-1} $NaHCO_3$, 2.3 g l^{-1} yeast extract, and initial pH of 7.07. Under those conditions, hydrogen productivity was expected to be 2,214 ml l^{-1} with the determination coefficient value (R^2) of 0.98. The performance of the model was tested experimentally, and the average value for hydrogen evolution from three replicates was 2,618 ± 273 ml l^{-1}; the efficiency of hydrogen was 62.6% and the light conversion efficiency was 0.7%. The deviation between predicted and experimental values of hydrogen production were 18.2%. The improvement in hydrogen production achieved with these modifications to the amounts of yeast extract and $NaHCO_3$ was greater than 2-fold. Furthermore, these modifications improved total VFA consumption from 29% without supplementation to 72% with supplementation.

Samples of palm oil mill effluent (POME) and anaerobically digested POME (Biogas reactor effluent) from two different sources were used as substrates for hydrogen production by *Rps. palustris* TN1. When anaerobic conditions were established by flushing cultures with argon gas, POME was found to be suitable substrate for hydrogen production, and among the dilutions of the POMEs tested the range of hydrogen produced was 29-865 ml l^{-1}. Hydrogen production by TN1 from diluted POMEs with or without nutrient supplementation was also investigated for a series of dilutions from no dilution to 1/20 dilution without flushing the cultures with argon to establish anaerobic conditions. The maximum hydrogen yields were obtained from cultures in 1/2 dilutions of unsupplemented and supplemented POME with values of 2.64 and 2.34 mol H_2 mol VFA^{-1}, respectively. By evaluation of the kinetics, the maximum hydrogen productions (H_{max}) for the 1/2 dilutions of unsupplemented and supplemented POME were calculated to be 2,906 ml l^{-1} and 3,090 ml l^{-1}, respectively, and the corresponding maximum hydrogen production rates

(R_{max}) were calculated to be 32.5 ml l^{-1} h^{-1} and 41.5 ml l^{-1} h^{-1}, respectively. In those dilutions, more than 85% of total VFA were consumed. Based on these results, POME is considered to be a promising source of electrons for hydrogen production by photosynthetic bacteria.

A genetic engineering approach targeting the *hemB* gene, coding for porphobilinogen synthase (PBGS), was used towards strain improvement of 5-aminolevulinic acid (ALA) production by *Rhodobacter* (*Rba.*) *sphaeroides* SH5. A mutant gene coding for a protein having a deletion of amino acid residues 15-27 was constructed. On the basis of enzymatic and structural data for other PBGSs, it was predicted that the mutant protein would be unaffected in its ability to dimerize, but reduced in its ability to form higher order multimers that are known to be necessary for 100% activity. If this polypeptide encoded by the mutant allele borne on a plasmid interacted with the wild type polypeptide produced from the intact chromosomal *hemB* gene, it would then reduce the amount of active enzyme in the cell. As predicted, when placed in multicopy (plasmid pMS3) in *Rba. sphaeroides* SH5, the defective gene behaved in a dominant-negative fashion, as the PBGS activity was reduced by approximately 7-fold (0.158 to 0.024 μmoles h^{-1} mg $protein^{-1}$) under aerobic-dark conditions and 27-fold (0.414 to 0.015 μmoles h^{-1} mg $protein^{-1}$) under anaerobic-light (3,000 lux) conditions, compared to control cells having only the wild type *hemB* gene. For both *Rba. sphaeroides* SH5 with pMS3 and with the empty vector pBBR1-MCS2 (Kovach *et al*., 1994) in modified GA medium under aerobic-dark conditions the extracellular levels of ALA were undetectable; however, the concetration was 2-fold higher for cells with pMS3 *versus* pBBR1-MCS2 under anaerobic-light conditions (3.16 *versus* 6.28 μM).

Towards simplifying and reducing the cost of assessing improved extracellular production of ALA by SH5 (pMS3) and other potentially improved strains, a novel bioassay was developed based on the ALA requirement of *Rba. sphaeroides* AT1 (Neidle and Kaplan, 1993) for growth. The determinant coefficient R^2 of the fitted standard curve of *Rba. sphaeroides* AT1 cell density *versus* ALA

concentration was 0.89. The deviation between HPLC-determined extracellular ALA and extracellular ALA measured using the bioassay produced by SH5 (pMS3) was less than 15%.

The potential for using POME as a cost-effective medium for growth of the ALA production strain *Rba. sphaeroides* SH5 (pMS3) was investigated using the dilution of unsupplemented POME that was optimal for hydrogen production by *Rps. palustris* TN1. The specific growth rates of *Rba. sphaeroides* SH5 (pBBR1-MSC2) and *Rba. sphaeroides* SH5 (pMS3) cultured in undiluted POME and 1/2 dilution POME were very similar (P>0.05), indicating POME does not contain components that negatively affect growth of the bacteria. The maximum levels of extracellular ALA produced by *Rba. sphaeroides* SH5 (pMS3) cultured in undiluted POME and 1/2 diluted POME were observed after 6 h of cultivation with the concentration of 36.3 and 61.0 μM, respectively. The maximum extracellular level of ALA for *Rba. sphaeroides* SH5 (pBBR1-MCS2) were measured in a 12 h culture in undiluted POME, and was found to be 2.9 μM, while ALA remained undetectable even after 48 h of culturing in the 1/2 dilution of POME. These studies reveal that *Rba. sphaeroides* SH5 (pMS3) produces approximately 19-fold more extracellular ALA than *Rba. sphaeroides* SH5 (pBBR1-MSC2) when grown in POME. Based on these results, *Rba. sphaeoides* SH5 (pMS3) could be used as bioremediator for POME treatment while also producing ALA.

Hydrogen and ALA production from co-cultures of the genetically engineered ALA-overproducing strain *Rba. sphaeroides* SH5 (pMS3) and *Rps. palustris* TN1 with the plasmid vector of pMS3, pBBR1-MCS2 (Kovach *et al.*, 1994), was investigated. First, the effect of ALA (0-1 mM) on cell growth and hydrogen production by *Rps. palustris* TN1 was investigated. Dry cell weights did not vary significantly for cells cultured in media with varying ALA concentrations. However, hydrogen production increased in the presence of added ALA, up to 1,075 ml l^{-1} with 1 mM ALA. Then the growth of each bacterium was evaluated when co-cultured in synthetic medium using 20 mM acetate as a carbon source and 5 mM glutamate as a nitrogen source under anaerobic-light condition (3,000 lux). After 48 h of incubation,

the concentration of *Rps. palustris* TN1 (pBBR1-MCS2) cells was below detectable levels, while the numbers of SH5 (pMS3) cells had increased significantly; i.e. the *Rba. sphaeroides* bacteria had overgrown the culture. However, when *Rps. palustris* TN1 (pBBR1-MCS2) was inoculated 24 h before the addition of *Rba. sphaeroides* SH5 (pMS3), both bacteria were detectable at the end of the incubation period (48 h). These outcomes contraindicate co-culturing. However, a two-staged process could successfully be used to improve the bioconversion of organic wastes to ALA and hydrogen by photosynthetic bacteria. First TN1 (pBBR1-MCS2) would be used for hydrogen production. Then through the subsequent addition of SH5 (pMS3), production would shift to ALA.

ACKNOWLEDGEMENT

This thesis could not successfully complete without the kindness of advisor's team. First and foremost, I am indebt to my major advisor, Assoc.Prof. Dr. Poonsuk Prasertsan, for pushing me to reach my potential. I appreciate her confidence in me as her graduate student to make my own mistakes and learn from them. She faced the hard time with me throughout my whole study and thesis writing. She opened me to biotechnological world and provided lots of good idea and advice. It's difficult to overstate my gratitude to my co-advisor, Prof. Dr. Jill Zeilstra-Ryalls. With her enthusiasm, her inspiration, and her great efforts to explain things clearly and simply, she helped to make molecular biology to be fun for me. Special thanks to my co-advisor, Assoc. Prof. Dr. Wanna Choorit, for all comments and suggestions.

Many thank to my fellow lab mates in environmental biotechnology laboratory: A, P' Noi, and N' Meow, for the stimulating discussions, for the sleepless nights we were working together before deadlines, and for all the fun we have had during my Ph. D study. Also I thank P' Sa, P' Pan, and P' Da, and in Scientific Equipment Center (SEC), Prince of Songkla University for all technical suggestions.

I would like to express my sincere appreciation to The Royal Golden Jubilee (RGJ) Ph.D. Program of Thailand Research Fund (TRF), The Joint Graduate School of Energy and Environment (JGSEE) and Graduate School of Prince of Songkla University, Thailand for the research grant.

Lastly, and most importantly, I am grateful to my wonderful family, parents Chaiwat -Suneerat Suwansaard, and brother Saranyoo Suwansaard. They provided the unconditional love, supports, and encouragement to help me learn that I can truly accomplish anything. To them I dedicate this thesis

Maneewan Suwansaard

CONTENT

CONTENT (Cont.)

LIST OF TABLES

LIST OF TABLES (Cont.)

LIST OF TABLES (Cont.)

LIST OF TABLES (Cont.)

LIST OF FIGURES

LIST OF FIGURES (Cont.)

LIST OF FIGURES (Cont.)

LIST OF FIGURES (Cont.)

LIST OF FIGURES (Cont.)

LIST OF FIGURES (Cont.)

LIST OF ABBREVIATIONS AND SYMBOLS

A	Irradiated area
ALA	5-Aminolevulinic acid
ALAS	ALA synthase
An-L	Anaerobic-Light condition
Ae-D	Aerobic-dark condition
ATP	Adenosin triphosphate
Bchl	Bacteriochlorophyll
BCIP	5-bromo-4-chloro-3-indolyphosphate
BOD	Biological oxygen demand
CCD	Central composite design
COD	Chemical oxygen demand
CO_2	Carbon dioxide
CO	Carbon monoxide
C/N	Carbon to nitrogen ratio
C.V.	Coefficient of variation
°C	Degree celcious
D	Diameter
Da	Dalton
DCW	Dry cell weight
EDTA	Ethylenediaminetetraacetic acid
GluRs	Glutamyl-tRNA synthetases
GSA-AM	Glutamate-1-semialdehyde 2, 1-aminomutase
GA	Glutamate-acetate medium
GG	Glutamate-glucose medium
GM	Glutamate-malate medium
GSY	Glutamate glucose salt yeast extract medium
H_2	Hydrogen
HAT	Hydroxyamino-tetrahydropyranone

LIST OF ABBREVIATIONS AND SYMBOLS (Cont.)

H_{max}	Maximum hydrogen production
I	Light intensity
kDa	Kilo Dalton
klux	Kilolux
LA	Levulinic acid
MGSY	Monosodium glutamate glucose salt yeast extract medium
MSGE	Monosodium glutamate effluent medium
$MgCl_2$	Magnesium chloride
$NaHCO_3$	Sodium hydrogen carbonate
NH_4Cl	Ammonium chloride
NH_4^+	Ammonium ion
$(NH_4)_2SO_4$	Ammonium sulfate
NaCl	Sodium chloride
NBT	Nitroblue tetrazolium
η	Light conversion efficiency
P	Maximum cumulative hydrogen production
PAR	Photosynthetically active radiation
PAP	Pyridoxamine 5'-phosphate
PBD	Plackett-Burman design
PBGS	Porphobilinogen synthase
PHB	Poly-3-hydroxybutyrate
PLP	Pyridoxal phosphate
PNSB	Purple non-sulfur bacteria
POME	Palm oil mill effluent
PSB	Photosynthetic bacteria
PPIX	Protoporphyrin IX
ppm	Part per million
rpm	Round per minute
R_{max}	Maximum hydrogen production rate

LIST OF ABBREVIATIONS AND SYMBOLS (Cont.)

RSM	Response Surface Methodology
SCP	Single cell protein
VFA	Volatile fatty acid
V_{H_2}	Volume of hydrogen production
w/v	Weight by volume
λ	Lag time
ρ_{H_2}	Density of hydrogen production

CHAPTER 1

INTRODUCTION

The palm oil industry is one of the major agro- industries of southern Thailand. The average quantity of palm oil mill effluent (POME) generated in Thailand is 0.87 m^3 per ton of fresh fruit bunch (H-Kittikun *et al.,* 1994). Unfortunately, POME is a significant source of pollution, as much of the effluent is discharged into rivers without treatment. While most POME is treated in anaerobic digestion ponds by fermentative bacteria, this is also problematic, as these ponds emit not only several gases but also volatile fatty acids (VFAs) into the environment (Borja, 1995). Therefore, new and more effective methods of treatment, and especially those that would convert POME to valuable products, are highly desirable.

One such method could involve alternative approaches for hydrogen evolution from POME by the activities of microorganisms. The anoxygenic purple non sulfur photosynthetic bacteria (PNSB) have the potential to produce hydrogen under light-fermentative conditions. By utilizing energy from the sun to drive thermodynamically unfavorable reactions, PNSB can potentially divert 100% of electrons from an organic substrate to H_2 production (Harwood, 2008). This is a considerable advantage over fermentative bacteria, which can only divert a theoretical 1/3 of electrons from high-carbohydrate waste streams for H_2 production (Angenent *et al*. 2004). PNSB can therefore utilize the VFAs that are often produced but not metabolized, during anaerobic fermentation. Thus, waste streams from photofermentation contain less VFAs, which are fully reduced to form H_2 and CO_2 and other valuable products. Moreover, photofermentation out-performs anaerobic fermentation in purity of biogas. PNSB produce a net gas product of 95% H_2 and 5% CO_2 plus water vapor (James *et al*., 2009), which is suitable for use in polymer electrolyte membrane (PEM) fuel cells without purification (Nakada *et al*., 1999; He *et al*., 2005). The considerable promise of hydrogen production by PNSB for fuel by has already been documented (Das and Veziroglu, 2001; Levin *et al*., 2004; Ni *et al*., 2006; He *et al*., 2005). Hydrogen yield depends on the composition of the organic

source, light intensity, and type of PNSB, (Barbosa *et al*., 2001; Oh *et al.*, 2004; Fang *et al*., 2005).

In addition to hydrogen, photosynthetic bacteria also produce 5-aminolevulinic acid (ALA) in large amounts, as it is the metabolic precursor to the photopigment bacteriochlorophyll. ALA is a bioactive compound that has very broad applications including medical, pharmaceutical and agricultural. Among the agricultural applications, ALA is not only used as a bioherbicide, bioinsecticide and growth promoting factor, but has also been found to confer salt and cold temperature tolerance in plants (Sasaki *et al*., 2002).

The extracellular ALA production by natural isolated PNSB has been developed in our laboratory (Environmental biotechnology laboratory, Department of industrial biotechnology, Prince of Songkla University (Madmarn, 2002; Sattayasamithstid, 2002; Riansa-ngawong, 2004; Suwansaard, 2004; Chaikritsadakarn, 2004; Sawangsaeng, 2005; Tangprasitipap, 2005). This particularly extracellular ALA by natural isolated PNSB was applied in agricultural fields as an immune stimulator in shrimp and fish (Tangprasitipap, 2005; Madmarn, 2002), a plant growth promoter (Suwansaard, 2004), and a bioinsecticide (Riansa-ngawong, 2004). The strain improvements by chemical and physical techniques were studied (Tangprasitipap, 2005; Madmarn, 2002; Sawangsaeng, 2005). However, the amounts of extracellular ALA were low. Therefore, another approach for enhancement extracellular ALA production should be used.

This research aims to investigate the production of hydrogen and ALA from selected strains of photosynthetic bacteria. The study further includes strain improvement by genetic engineering, optimization of production conditions, and process scale-up**.**

Review of literature

1. Classification of anoxygenic photosynthetic bacteria.

The anoxygenic photosynthetic bacteria can be found in fresh waters, salt waters, acidic water, basic water, and also in various wastewaters. These bacteria play important roles in CO_2 assimilation and nitrogen fixation (Lascelles, *et al*., 1978). They are divided into two major groups, the so-called green and purple photosynthetic bacteria.

1.1 Green photosynthetic bacteria

1.1.1 Green sulfur bacteria

Chlorobium thiosulfatophilum and *Chlorobium vibrioforme* can use both sulfur compounds as well as organic hydrogen as electron donors (Blankenship *et al*., 1995). The reaction center of green sulfur bacteria is similar to the photosystem I reaction center of oxygenic photosynthetic organisms i.e. plant and algae (Lascelles, *et al*., 1978). Since the FeS centers in the reaction center can reduce NAD^+ (or $NADP^+$) by ferredoxin and the ferredoxin-NAD $(P)^+$ oxidoreductase enzyme, green sulfur bacteria do not depend upon reverse electron flow for carbon reduction. The antenna system of the green sulfur bacteria contains bacteriochlorophyll (Bchl) and carotenoids housed in complex structures known as a chlorosomes that are attached to the surface of the photosynthetic membrane. This antenna arrangement is similar to the phycobilisomes of cyanobacteria. It has been proposed that they accomplish carbon fixation by using the respiratory chain that normally oxidizes carbon (Krebs cycle) and results in the release of CO_2. With the input of energy, this process can be run in the reverse direction, resulting in the uptake and reduction of CO_2. All species of green sulfur bacteria are strict anaerobes and obligate phototrophs. No member of this group has been found suitable for any practical application (Blankenship *et al*., 1995).

1.1.2 Green gliding bacteria

Green gliding bacteria (*Chloroflexus aurantiacus*), also known as green filamentous bacteria, can grow photosynthetically under anaerobic conditions or

in the dark by respiration under aerobic conditions. Like the green sulfur bacteria, green gliding bacteria harvest light using chlorosomes. The green gliding bacteria appear to have reaction centers similar to those of the purple bacteria, but there are several notable differences. For example, instead of two monomer Bchl molecules, *C. aurantiacus* has one Bchl and one bacteriopheophytin, and the metal between the two quinones is Mn rather than Fe (Feick *et al*., 1995). *C. aurantiacus* appears to fix CO_2 by a scheme that does not involve the Calvin cycle or the reverse Krebs cycle (Ivanovsky *et al*., 1993). Perhaps their most distinctive characteristic is the arrangement of the bacteria in multicellular filaments that are capable of gliding motility. The green gliding bacteria are also thermophilic, and their potential to produce valuable thermotolerant enzymes like amylase and protease has been noted (Sasikala and Ramana, 1995).

1.1.3 Heliobacteria

The Heliobacteria (*Heliobacterium chlorum* and *Heliobacillus mobilis*) are in the phylum of Gram Positive Bacteria that are strict anaerobes. Although the heliobacterial reaction center is similar to photosystem I in that it can reduce NAD^+ (or $NADP^+$), it contains the distinctive chlorophyll, Bchl *g* (Lascelles, *et al*., 1978). This is in contrast to the green bacteria which have Bchl *c, d,* or *e* and the purple bacteria which have Bchl *a* or Bchl *b*. This group is strictly anaerobic and obligatorily photoorganotrophic. Nevertheless, the member species are highly tolerant to oxygen exposure and also drying conditions (Lascelles, *et al*., 1978). These bacteria are valued for their ability to fix atmospheric nitrogen and so biofertilize (Sasikala and Ramana, 1995).

1.2 Purple photosynthetic bacteria

The purple bacteria are a small group of Gram-negative eubacteria, consisting of only about 30 species. They are unicellular, reproduce by binary fission, and in most cases are motile by flagella. All purple bacteria are capable of growing anaerobically in the light with CO_2 as the carbon source and reduced inorganic compounds as the electron donor. The only pathway for carbon fixation by purple bacteria is the Calvin cycle (Madigan *et al*., 2009). There are two divisions of

photosynthetic purple bacteria, the purple sulfur bacteria and the purple non-sulfur bacteria (Blankenship *et al*., 1995).

1.2.1 The purple sulfur bacteria

1.2.1.1 The family *Chromatiaceae*

The purple sulfur bacteria use an inorganic sulfur compound such as hydrogen sulfide as the electron donor. These organisms are predominately aquatic, found in sulfate-rich environments, and are mostly strictly anaerobes that require vitamin B_{12} as the only growth factor. This group has been exploited for their ability to purify sulfide wastes, as a single cell protein source (SCP) due to the high protein content of their biomass, and their ability to produce biopolyester (Madigan *et al*., 2009).

1.2.1.2 The family *Ectothiorhodospiraceae*

This family is distinguished from the *Chromatiaceae* by the fact that they deposit sulfur outside the cells. These sulfur depositions are oxidized to sulfate. Other characteristics of the bacteria include their requirement for saline and alkaline growth conditions and the presence of intracytoplasmic membrane arranged in lamellar stacks. The *Ectothiorhodospiraceae* are able to grow by photoautotrophic and/or photoorganotrophic processes, which can be used in the anaerobic purification of sulfide wastes in high saline and alkaline environments (Lascelles, *et al*., 1978).

1.2.1.3 The family *Rhodospirillaceae* (the purple non-sulfur bacteria)

The purple non-sulfur bacteria (PNSB) use various organic compounds as electron donors (H_2A) including fatty acids, other organic acids such as succinate or malate, primary and secondary alcohols, carbohydrates and even aromatic compounds, and they can also use hydrogen gas. Most purple non-sulfur bacteria have a predominantly photoheterotrophic mode of metabolism. Their growth is typically inhibited by sulfide, even though many can oxidize sulfide anaerobically in the light if the concentration is kept very low. The PNSB have been classified as anoxygenic phototrophic bacteria, and are divided into 6 genuses (Imhoff *et al*., 1984).

a. The genus *Rhodospirillum*

Rhodospirillum (*Rsp.*) cells are spiral shaped, and 0.5 to 1.5 μm wide. This genus uses polar flagella for motility. The bacteria have intracytoplasmic photosynthetic membranes arranged in vesicles, lamellae, or stacks, but not as finger-like intrusions of cytoplasmic membrane. *Rsp. rublum*, *Rsp. fulvum*, *Rsp. oxigens, Rsp. photometricum,* and *Rsp. melischianum* belong in this genus.

b. The genus *Rhodopseudomonas*

The *Rhodopseudomonas* (*Rps.*) cells are rod shaped and display polar growth, dividing asymmetrically. They use flagella for motility. These bacteria contain intracytoplasmic photosynthetic membranes. *Rps. palustris*, *Rps. acidophila*, *Rps. rutica*, and *Rps. viridis* belong in this genus.

c. The genus *Rhodomicrobium*

The bacteria in this genus are ovoid. Their peritrichously arranged flagella are used for motility. Reproduction of these organisms occurs by budding. Members of this genus have stacked intracytoplasmic membranes. *Rhodomicrobium* (*Rmi.*) *vannielii* is a member of the genus.

d. The genus *Rhodopila*

The cells in this genus are spherical to ovoid. They use flagella for motility. The photosynthetic membranes of these bacteria are vesicular. The *Rhodopila* can grow at low pH, and biotin and *p*-aminobenzoic acid are required as growth factors. These cells are sensitive to oxygen. *Rhodopila globiformis* is a member of the genus.

e. The genus *Rhodocyclus*

Rhodocyclus (*Rcy*.) bacteria are slender, curved cells, and are 0.3-0.7 μm in diameter. The bacteria in this genus are nonmotile or motile by polar flagella. They have intracytoplasmic membranes which form small finger-like intrusions of the cytoplasmic membrane. *Rcy. tenuis, Rcy. gelatinosus,* and *Rcy.purpureus* are members of this genus.

f. The genus *Rhodobacter*

The genus *Rhodobacter* (*Rba*.) was formerly included in the genus *Rhodopseudomonas* but is now differentiated by their invaginating intracytoplamic membranes that can appear vesicular in thin sections. The cells are ovoid to rod-

shaped and the bacteria multiply by binary fission. They can be motile or nonmotile. All species require thiamine, and most of them require biotin. Additional vitamin requirements are variable among the species. The photosynthetic pigments are Bchl *a* and carotenoid of the spheroidene group. *Rba. sphaeroides*, *Rba. sulfidophilus*, *Rba. capsulatus, Rba. blasticus*, and *Rba. adriaticus* are the member species of this genus.

2. Hydrogen production

Currently, hydrogen constitutes approximately 3% of energy consumption (Das and Veziroglu, 2001). Commercial production of hydrogen is from fossil fuels, biomass, and water through a variety of processes in which 90% of hydrogen is evolved by natural gas via steam reforming processes. However, these thermo-chemical and electrochemical processes generate pollutants and are also expensive. By comparison, biological processes employ mild reaction conditions, are less energy intensive, and are environmental acceptable.

The microorganisms involved in biological hydrogen production process are algae, cyanobacteria, fermentative bacteria, and PNSB. The biological production process can be classified according to the type of microorganism involved. Their relative advantages and disadvantages are summarized in Table 1.

Table 1. A comparison of biological hydrogen production processes.

Microorganisms	Advantages	Disadvantages
Green algae	- Can produce H_2 directly from water and sunlight.	- Requires high intensity of light. - O_2 can be dangerous for the system. - Lower photochemical efficiency
Cyanobacteria	- Can produce H_2 directly from water and sunlight. - Has nitrogenase enzyme to fix N_2 from atmosphere.	- Uptake hydrogenase consumes hydrogen. - Nitrogenase is affected by O_2
PNSB	- Can use light energy to produce hydrogen. - Can use small-chain organic compounds as electron donors. - Some specie can use CO as sole carbon source to produce hydrogen under dark condition. - High theoretical hydrogen yield. - O_2 has no inhibitory effect on nitrogenase	- Light conversion efficiency is very low. - Uptake hydrogenase consumes hydrogen.
Fermentative bacteria	- Do not need light for cell growth and hydrogen production. - A variety of complex substances can be used as substrates.	- Relatively lower H_2 yield. - Produce metabolites such as acetic, propionic, butyric, acid. - Biogas contains either H_2 or CO_2

Sources: Das and Veziroglu (2001) and Nath and Das (2004)

2.1 Hydrogen production by algae

Green algae are capable to convert solar energy into chemical energy in the form of hydrogen (photolysis):

$$2H_20 \xrightarrow{solar\ energy} 2H_2 + O_2$$

Two photosynthetic systems are responsible for photosynthesis process: (i) photosystem I (PSI) involving CO_2 reduction and (ii) photosystem II (PSII) splitting water and evolving oxygen (Lehniger *et al*., 2008). In the biophotolysis process, two photons from water can yield either CO_2 reduction by PSI or hydrogen formation with the presence of hydrogenase. In green plants, due to the lack of hydrogenase, only CO_2 reduction takes place (Ramachandran and Menon 1998). Green algae, however, possess hydrogenase and so have the ability to produce hydrogen. In this process, electrons are generated when PSII absorbs light energy. The electrons are then transferred to the ferredoxin (Fd) using the solar energy absorbed by PSI (Benemann, 1997). The hydrogenase accepts the electrons from Fd to produce hydrogen as shown in Fig. 1.

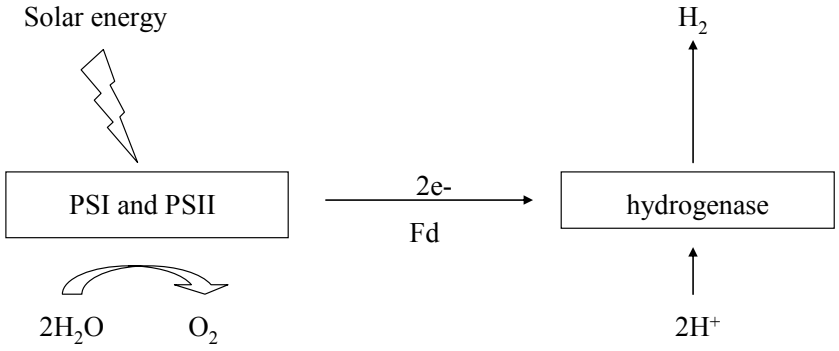

Figure 1. Biophotolysis hydrogen production by algae.
Source: Modified from Ni *et al*. (2006)

Since hydrogenase is sensitive to oxygen, it is necessary to maintain the oxygen content at a low level, under 0.1%, so that hydrogen production can be sustained (Halenbeck and Benemann, 2002). This condition can be met by the green algae *Chlamydomonas reinhardtii* that can deplete oxygen during oxidative respiration (Melis *et al*., 2000). However, due to the significant amount of substrate being respired and consumed during this process, the efficiency is low. Recently, mutants derived from microalgae were reported to have good O_2 tolerance giving higher hydrogen production. The mutant of *Chlamydomonas reinhardtii* with had H_2-evolving activities of up to 10 times the O_2-tolerance compared to the wild-type (Flynn *et al*., 2002).

2.2 Hydrogen production by Cyanobacteria

Cyanobacteria (blue-green algae) perform oxygenic photosynthesis. Cyanobacteria contain photosynthetic pigments, such as chl *a*, carotenoids, and hycobiliproteinsand. The nutritional requirements for cyanobacteria are air (N_2 and O_2), water, mineral salts and light (Hansel and Lindblad, 1998).

There are several enzymes involve in hydrogen metabolism and synthesis of H_2 as shown in Fig.2. These include nitrogenases which catalyze the production of H_2 as a by-product of nitrogen reduction to ammonia, uptake hydrogenases which catalyze the oxidation of H_2 synthesized by the nitrogenase, and bi-directional hydrogenases which have the ability to both oxidize and synthesize H_2 as follow (Tamagnini *et al*, 2002):

$$12H_2O + 6CO_2 \xrightarrow{light\ energy} C_6H_{12}O_6 + 6O_2$$
$$C_6H_{12}O_6 + 12H_2O \xrightarrow{light\ energy} 12H_2 + 6CO_2$$

Among species of cyanobacteria, *Synechococcus* spp., *Alphanocapsa* spp., *Noctoc* spp., and *Anabaena* spp. were found to possess higher hydrogen production rates (Howarth and Codd, 1985; Masukawa *et al*., 2001).

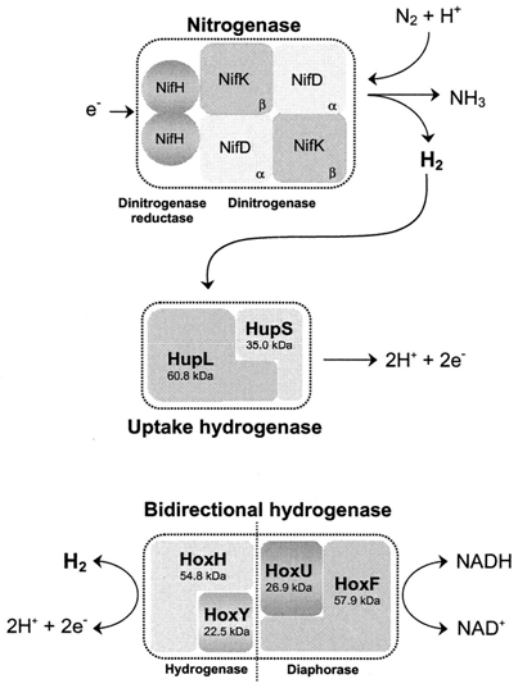

Figure 2. Enzymes in hydrogenproduction in cyanobacteria.
Source: Tamagnini *et al*. (2002)

2.3 Hydrogen production by fermentative bacteria

Biohydrogen production by fermentative bacteria is carried out by glycolysis or by the Embden-Meyerhoff-Parnas pathway in which organic materials is converted to hydrogen, carbon dioxide, organic acids, and solvent (Kirk *et al*., 1985). The majority of microbial hydrogen production in dark fermentations is driven by the anaerobic metabolism of pyruvate, formed during the catabolism of various substrates (Hallenbeck and Benemann, 2002). Fermentative bacteria grown on carbohydrate-rich substrates produce organic fermentation end products, hydrogen, and carbon dioxide. Hydrogen producing bacteria including *Enterobacter* (Fabiano and Perego, 2002) and *Clostridium* (Taguchi *et al*., 1992) have been found to produce hydrogen during fermentation. Some *Enterobacter* species can degrade soluble starch (Yokoi *et al*., 1997; Kumar and Das, 2001), while some *Clostridial* species are able to degrade soluble starch without pretreatment. Among the hydrogen producing strains, *Clostridium butyricum* has been studied most extensively (Karube *et al*., 1976, Hallenbeck and Benemann, 2002).

To enhance hydrogen production, thermophilic anaerobic bacteria have been investigated, as they have high yields (83-100%) (de Vrije *et al*., 2002). In this regard, *Thermoanaerobacterium* spp. has been found to be a dominant species. *Thermoanaerobacterium thermosaccharolytic* PSU2 isolated from a biohydrogen reactor fed with POME produced hydrogen 2.53 mol H_2 mol hexose^{-1} (O-Thong *et al*., 2008).

2.4 Hydrogen production by PNSB

PNSB are among the most promising microbes for biological production of hydrogen for the reasons as described in Table 1.

There are two processes by which PNSB can generate hydrogen: the water-gas shift reaction and photodecomposition of organic compounds, or photo-fermentation.

2.4.1 Process of hydrogen production by PNSB

2.4.1.1 The water-gas shift reaction of PNSB

Some *Rhodospirillaceae* can survive in the dark using CO as the sole carbon source. They generate ATP by coupling oxidation to the release of H_2 and CO_2 (Das and Veziroglu, 2001; Levin *et. al*., 2004; Ni *et al*., 2006). This process is called the water-gas shift reaction:

$$CO\ (g) + H_2O\,(l) \rightarrow CO_2(g) + H_2(g), \quad \Delta G^0 = -20 \quad kJ\,mol^{-1}$$

The enzyme that oxidizes CO is carbon monoxide dehydrogenase, which is a membrane bound protein complex (Das and Veziroglu, 2001). Under anaerobic conditions, CO induces the synthesis of several proteins, including CO dehydrogenase, Fe-S protein and CO-tolerant hydrogenase. Electrons produced from CO oxidation are conveyed via the Fe-S protein to the hydrogenase for hydrogen production (Ni *et al*., 2006).

Hydrogen production via the water-gas shift reaction has been described for *Rhodocyclus gelatinosus* (*Rubrivivax* (*Rvi*.) *gelatinosus*) CBS, which was found to have a doubling time of 7 h in light when CO served as the only carbon source (Maness and Weave, 2001). The hydrogen production rate was 96 mmol H_2 g^{-1} DCW h^{-1} when cultured with stirring at a high rate (250 rpm) and supplementing

with 20% CO in the gas phase (Maness and Weave, 2001). In the presence of organic substrates together with CO, *Rvi. gelatinosus* will use both substrates (Maness and Weave, 2001)

2.4.1.2 Photodecomposition of organic compounds, or photo-fermentation

Photo-fermentative hydrogen production by PNSB from organic wastes as substrate occurs through the action of nitrogenase under anaerobic light conditions (Fig. 3).

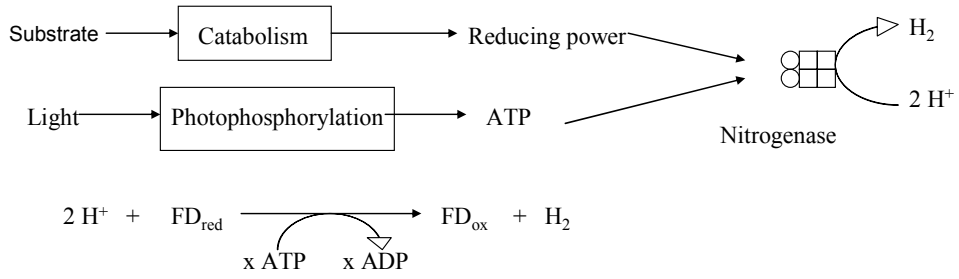

Figure 3. Photodecomposition of organic compounds.
Source: Modified from Kawaguchi *et al*. (2002)

2.4.2 Enzymes involved in hydrogen production by PNSB

Many microorganisms contain enzymes having hydrogenase activity; i.e. they either oxidize hydrogen to protons and electrons or reduce protons and thus release molecular hydrogen. With respect to bioproduction of hydrogen two enzymes of particular importance having these activities are nitrogenase and (uptake) hydrogenase.

2.4.2.1 Nitrogenase

Hydrogen production occurs by the activity of nitrogenase in the photo-fermentation pathway. This enzyme synthesizes hydrogen when nitrogen (N_2) is absent as follows:

$$2H^+ + 2e^- + 4ATP \rightarrow H_2 + 4ADP + 4P_i$$

In this reaction, hydrogen production by nitrogenase requires large amounts of ATP and reducing power where growth is nitrogen-limited. The nitrogenase complex must be saturated with ATP and also NADH for optimal activity. Hence, H_2 photoproduction occurs most rapidly under saturating light intensity at the expense of organic electron donors. The primary inhibitor of nitrogenase activity is oxygen, which irreversible destroys the enzyme. Ammonium, the salts of which are frequently used as the nitrogen sources in the cultivation of PNSB, is the second inhibitor of concern (Das and Veziroglu, 2001; Ni *et al*., 2006). It both represses the synthesis of nitrogenase and inhibits nitrogenase activity. This inhibition is reversible; however, as the nitrogenase activity recovers after the ammonium is consumed or removed. There are several different nitrogenases present in PNSB, all of which are capable of producing hydrogen. One contains molybdenum centers, and thus the availability of molybdenum can affect nitrogen fixation and hydrogen production, as has been reported for *Rba*. *sphaeroides* (Yakunin *et al*., 1991 cited by Koku *et al*., 2002). Further evidence of tight control is noted in a study of *Rba. capsulatus* grown on lactate and glutamate. If lactate is exhausted earlier than glutamate, the net formation of ammonia occurs, which eventually leads to inhibition of nitrogenase (Hillmer and Gest, 1977). Also, in the presence of nitrogen gas, the nitrogen fixation reaction dominates and hydrogen production is insignificant (Sasikala *et al*., 1990).

Nitrogenase synthesis may be strongly stimulated by light, resulting in a corresponding increase in nitrogenase acitivity as observed in continuous cultures of *Rba. capsulatus* (Jouanneau *et al*., 1985). Interestingly, a diurnal pattern of illumination (alternating periods of light and dark) results in more stable nitrogenase activity (Meyer *et al*., 1978), suggesting the presence of circadian regulation as well.

2.4.2.2 Hydrogenase

Hydrogenases have been found to be widely distributed among PNSB (Vignais *et al*., 1985; Türkarslan *et al*., 2002; Gogotov, 1986). In vitro studies show the hydrogenase of *Rba. capsulatus* is capable of both hydrogen production and consumption. However, production is apparently predominantly via nitrogenase, and hydrogen-producing activity by hydrogenase is minor, if there is any at all. As reported by Gogotov (1986) and Zorin (1986), the hydrogen producing activity of

hydrogenase is less than 10% of hydrogen consuming activity, and the maximum activity for hydrogenase occurs under conditions that only favor hydrogen uptake. Therefore, hydrogenase is generally accepted to be the metabolic antagonist of nitrogenase, and to function in the direction of hydrogen uptake. The terms hydrogenase and uptake hydrogenase are used interchangeably in reference to this enzyme (Klemme, 1993).

Hydrogenase is inhibited primarily by carbon monoxide and oxygen, although oxygen tolerance of this enzyme is considerably higher than that of nitrogenase. Hydrogenases are nickel enzymes, and limitation of nickel may attenuate the synthesis of this enzyme (Fissler *et al*., 1994). Consistent with this thinking, the presence of the chelating agent ethylenediaminetetraacetic acid (EDTA) is also known to inhibit hydrogenase activity (Kern *et al*., 1994; Fissler *et al*., 1994). The synthesis of hydrogenase in *Rsp. rubrum* and *Rba. capsulatus* is repressed by high concentrations of organic compounds, while synthesis of hydrogenase in *Rba. sphaeroides* 2R occurs in the presence of hydrogen, whether organic compounds are present or not (Gogotov *et al*., 1986). This explains why hydrogen production by *Rba. sphaeroides* O.U.001 is reported to be partially inhibited in a pure hydrogen atmosphere (Sasikala *et al*, 1990), whereas no such inhibition has been observed for production by *Rba. capsulatus* (Hillmer and Gest, 1977) or *Rsp. rubrum* (Gest and Kamen, 1949 cited by Koku *et al*., 2002). The properties of nitrogenase and hydrogenase are summarized in Table 2.

Table 2. Comparative properties of nitrogenase and hydrogenase.

Product	Nitrogenase	(uptake)Hydrogenase
Substrates	ATP, H^+, or N_2 electron	H_2
Products	H_2 or NH_4^+	ATP, H^+, electrons
Number of protein	Two (Mo-Fe) and Fe	One
Metal components	Mo, Fe	Ni, Fe, S
Optimum temperature	30 °C (*Azotobacter (A.) vinelandii*)	55 °C (*Rsp. rubrum*)
		70 °C (*Rba. capsulatus*)
Optimum pH	7.1-7.3 (*A. vinelandii*)	6.5-7.5 (*Rps. sulfidophilus*)
Inhibitors, repressors	N_2, (of H_2 production only), NH_4^+, O_2, High N to C ratio	CO, EDTA, O_2, presence of organnic compounds
Stimulators	Light	H_2 (*Rba. sphaeroides*), absence of organic compounds (*Rsp. rubrum, Rba. capsulatus*)

Source: Ni *et al*. (2006)

2.4.3 The photosystem of the PNSB

The photosystem of PNSB converts light energy into the chemical bond of high-energy compounds by a two-step process. First, light energy (photon) strikes the pigments of antenna complexes within the cell membrane of the PNSB and the pigment within the complex is activated by the light into an excited state. Second, the excited pigment transmits electrons from donors to acceptors at the reaction center and the light energy is converted into a high-energy chemical bond of ATP (Fig. 4).

Reducing power (from reversed electron flow) and ATP generated from light energy are transferred to the enzyme systems for hydrogen production, hydrogenase or nitrogenase. However, the supply of reducing power and/or ATP for hydrogenase or nitrogenase is not always directly dependent on photosynthetic energy-production, and can sometimes involve the decomposition of the carbohydrates that have been photosynthetically produced. On the other hand, the process of carbon fixation reduces the conversion efficiency of light to hydrogen (Miyake *et al*., 1999) by consuming those same resources.

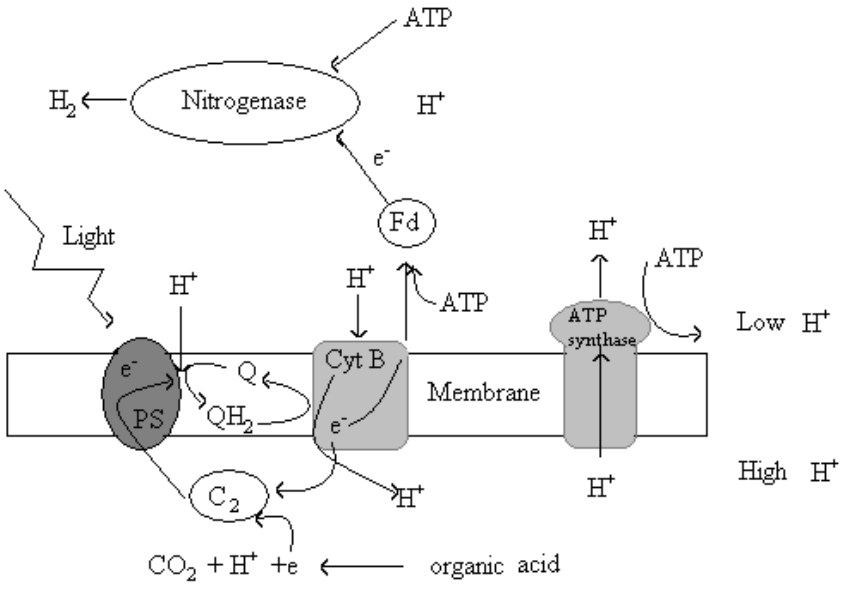

Figure 4. Photofermentation by PNSB.

Source: Akkerman *et al*. (2002)

2.4.4 Hydrogen metabolism of PNSB

The ability to produce hydrogen from a given organic compound depends upon the carbon metabolism of the organism. Among the PNSB, carbon utilization pathways are different among different species, and even among different strains of the same species of PNSB. Koku *et al* (2002) proposed a generalized scheme of carbon flow in PNSB that is shown in Fig 5. Some compounds can be utilized by this pathway; however, DL-malate follows different route (Koku *et a*l., 2002). When substrates, such as butyrate or glycerol, are more reduced than cell material, the excess electrons are disposed of by photoreduction of CO_2 (Gest *et al*., 1951).

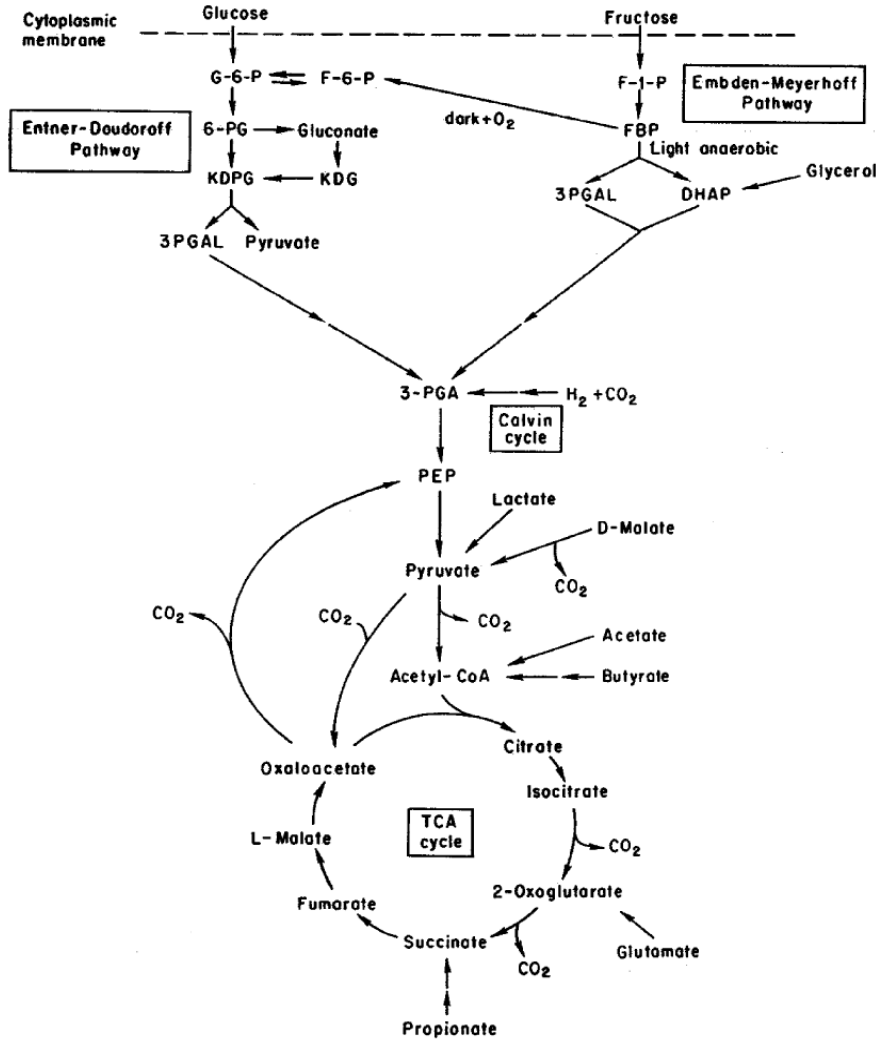

Figure 5. Carbon metabolism in PNSB.

Source: Koku *et al*. (2002)

2.4.4.1 Assimilation of acetate in PNSB

In many bacteria, acetate is assimilated via the tricarboxylic acid cycle (TCA) cycle. Many acids in this cycle are expended for biosynthetic purposes and are replenished via the glyoxylate shunt (Cronan and LaPorte, 1996), which is primarily an oxidative pathway. Acetyl-CoA is generated from the oxidation of acetate, which usually is derived from the oxidation of fatty acids (Lehninger *et al*., 2008). Some bacteria also possess the glyoxylate shunt. The key enzymes in the shunt are isocitrate lyase, which splits isocitrate into glyoxylate and succinate, and malate synthase, which synthesizes malate from glyoxylate and acetyl-CoA that can be generated during the degradation of fatty acids (Cronan and LaPorte, 1996) as shown in Fig 6a.

Rhodospirillacae grow on acetate anaerobically in the light and also aerobically. *Rsp. tenue*, *Rps. palustris*, and *Rmi. vanneilii* have an incomplete TCA cycle, but possess the enzymes isocitrate lyase and malate synthase and use glyoxylate shunt to convert acetyl-CoA into anapleurotic and gluconeogenic compunds (Fig 6a). *Rsp. rubrum* and *Rba. sphaeroides* lack isocitrate lyase, although they contain malate synthase (Alber and Gottschalk, 1976).

A new pathway for acetate assimilation in *Rba sphaeroides* was purposed by Alber *et al*., (2006), which is called ethylmalonyl-CoA (EM) pathway. Assimilation begins with the condensation of two molecules of acetyl-CoA to form acetoacetyl-CoA, which undergoes reduction to β-hydroxybutyryl-CoA. β-Hydroxybutyryl-CoA is in turn activated and carboxylated to form the novel intermediate mesaconyl-CoA. Hydration of mesaconyl-CoA yields β-methylmalyl-CoA, which undergoes cleavage to glyoxylate and propionyl-CoA. Condensation of glyoxylate with acetyl-CoA yields malate, while the typical reactions of propionate metabolism result in carboxylation and conversion of propionyl-CoA to succinate (Fig. 6b). Thus, via this new pathway, CoA-activated esters of conventional and novel C3-C5 compounds serve as substrates for a series of condensation, rearrangement and carboxylation reactions that form two C4 gluconeogenic precursors from three acetyl-CoA and two CO_2 molecules as summarized as follows:

$$3 \text{ Acetyl CoA} + 2\ CO_2 \rightarrow \text{L-malate} + \text{succinate}$$

Filatova *et al*. (2005) have proposed another metabolism, the citramalate(CM) pathway, for acetate assimilation in *Rsp. rubrum*. In this pathway, acetate is oxidized to glyoxylate in the following reaction demonstrated in Fig.6C. Citramalate is produced by the condensation of pyruvate and acetyl-CoA through several reactions. Citramalate is converted into propionyl-CoA and glyoxylate then condenses with another acetyl-CoA to form malate, which is catalyzed by malate synthase. Pyruvate, which serves as the acetyl-CoA acceptor in the reaction catalyzed by citramalate synthase, is replenished through the carboxylation of propionyl-CoA. This carboxylation leads to the formation of methylmalonyl-CoA, which transforms into succinate. Succinate is then converted to oxaloacetate via the TCA cycle. The oxaloacetate is then decarboxylated, forming phosphoenolpyruvate (PEP). The conversion of PEP to pyruvate completes the citramalate cycle (Fig. 6c). Acetate assimilation in *Rsp. rubrum* takes place only in the presence of high concentrations of bicarbonate, due to the reaction of propionyl-CoA carboxylation in the citramalate cycle.

2.4.4.2 Assimilation of propionate in PNSB

van Niel (1944) reported that *Rps. palustris* and *Rba. capsulatus* could grow on medium containing fatty acid as a sole carbon source, but *Rba. sphaeroides* and *Rcy. gelatinosa* [*sic.*] could not (Maruyama and Kitamura, 1975). However, Maruyama (1979) found that *Rba. sphaeroides* 0 (van Niel strain, IFO, No. 12203) and *Rba. sphaeroides* S grew on propionate medium at a very slow rate in either aerobic-dark or anaerobic-light conditions. *Rba. sphaeroides* S assimilates propionate very rapidly in the presence of acetate or $NaHCO_3$ (Maruyama, 1979). Another species of PNSB, *Rsp. rubrum*, is known to metabolize propionate via methylmalonyl-CoA to succinyl Co-A. The methylmalonyl CoA metabolism includes CO_2 fixation catalyzed by propionyl CoA carboxylase (PCC) as follow (Maruyama and Kitamura, 1975):

$$propionate \rightarrow propionyl-CoA \xrightarrow{CO_2} D-methylmalonyl-CoA \rightarrow$$
$$L-methylmalonyl-CoA \rightarrow Succinyl-CoA \rightarrow TCA\ cycle$$

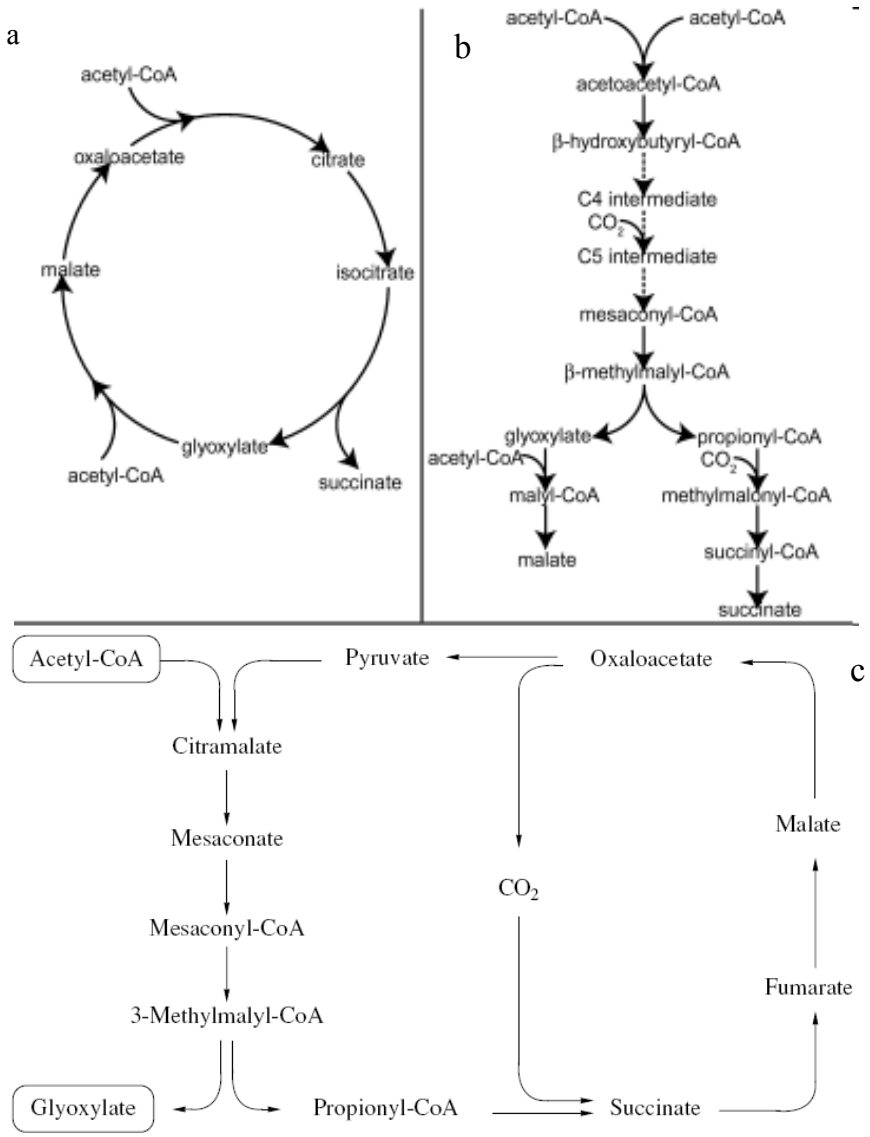

Figure 6. Pathways of acetate assimilation present among PNSB. (a) The glyoxylate cycle, (b) the alternate glyoxylate pathway (ethylmalony Co-A) of *Rba. sphaeroides*, and (c) the alternative glyoxylate cycle (citramalate cycle) of *Rsp. rubrum*.

Source: [a b] Modified from Ensign (2006) and [c] Filatova *et al*. (2005)

PCC plays important role in the reaction of propiony-CoA carboxylation of propionate assimilation (Berg *et al*., 2002). This enzyme functions in catabolism of odd-chain fatty acid and several amino acids (Lehninger *et al*., 2008).

PCC is also involved in the citramalate cycle, the anaplerotic pathway proposed for *Rsp. rubrum* (Ivanovsky *et al*., 1993; Filatova *et al*.; 2005; Berg and Ivanosky, 2009.

2.4.4.3 Assimilation of butyrate in PNSB

Ogata and Yamanaka (1982) reported that butyrate assimilation in *Rps. palustris* No.82 takes place in a process beginning with its convesion to butyryl-CoA. The butyryl-CoA then undergoes β-oxidation to form acetyl-CoA. It was found that *Rba. capsulatus*, another PNSB, consumed 0.2% butyrate in the presence of 1.0 % $NaHCO_3$ for cell growth (Shively *et al*., 1984)

2.4.4.4 Overall metabolism of hydrogen in PNSB

The carbon source is fed into the (alternate) glyoxylate shunt and/or TCA cycle where it is oxidized to produce CO_2 and electrons. Working in parallel is the photosynthetic membrane apparatus, which converts light energy into ATP (Koku *et al*., 2002). This ATP is channeled into the nitrogenase along with the protons and electrons. Nicotinamide adenine dinucleotide (NAD) and ferredoxin (Fd) are used as electron carriers by their oxidation/reduction (Madigan *et al*., 2009). Protons are supplied in part by the glyoxylate shunt and/or TCA cycle, and the remainder is supplied by the action of ATP synthase working as a part of the photosynthetic apparatus, which can be considered as a part of the photosynthetic apparatus, might function reversibly to generate ATP from a proton gradient, or to create a proton gradient by consuming ATP (Madigan *et al*., 2009). Finally, the nitrogenase reduces the protons to hydrogen. The function of hydrogenase is hydrogen consumption, which also produces ATP, protons and electrons. Therefore, the net amount of hydrogen produced is the amount of hydrogen produced by nitrogenase minus the amount of hydrogen consumed by hydrogenase. The overall metabolism of hydrogen in PNSB is shown in Fig 7.

2.4.5 The relationship of hydrogen production and polyhydroxyalkanoates (PHAs)

2.4.5.1 PHAs

Accumulating PHAs is a natural way for bacteria to store carbon and reducing power, when nutrient supplies are imbalanced. These polyesters are accumulated as when bacterial growth is limited by depletion of nitrogen,

phosphorous (Koller *et al*. 2008) or oxygen and an excess amount of a carbon source is still present (Anderson and Dawes, 1990).

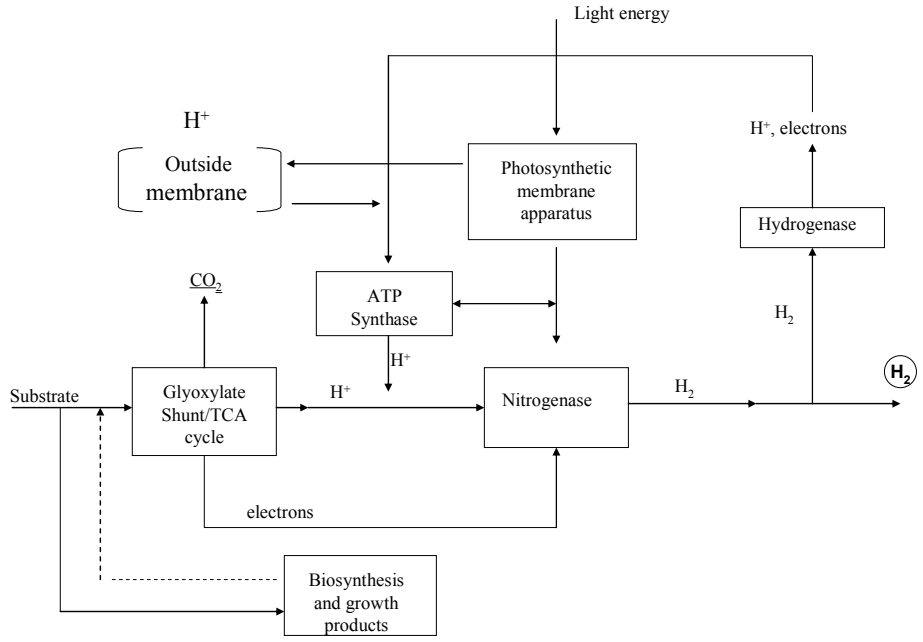

Figure 7. Overall hydrogen metabolism in PNSB.
Source: Modified from Koku *et al.* (2002)

As PHAs are insoluble in water, the polymers are accumulated in intracellular granules inside the cells. It is advantageous for bacteria to store excess nutrients inside their cells as polymers, as this minimizes changes in the osmotic state. Further, the larger polymeric state prevents leakage of these valuable compounds out of the cell, and the nutrient stores will remain securely available at a low maintenance cost (Peters and Rehm, 2005).

The first PHA to be discovered was poly(3hydroxybutyrate) or PHB from *Bacillus megaterium* (Lemoigne, 1926), which is a homopolymer. Copolymers are formed when mixed substrates are used. *Ralstonia eutropha* converts a mixture of glucose and valerate into short-chain-length PHAs such as poly(3-hydroxybutyrate-co-3-hydroxyvalerate) (PHBV) or poly(3-hydroxybutyrate-co-4-hydroxybutyrate) (PHB4B) (Yan *et al*., 2005).

Many genera of PNSB such as *Rba sphaeroides*, *Rba. capsulatus*, *Rsp. rubrum*, and *Rps. palustris* have been demonstrated to accumulate PHAs as

intracellular storage material under either aerobic-dark or anaerobic-light conditions (Sangkharak and Prasertsan, 2007; Kranz *et al*., 1997; Brandl *et al*., 1989; Mukhopadhyay *et al*., 2005). PHA biosynthesis is a multistep pathway involving the formation of the monomeric units β-hydroxybutyryl-CoA, which is derived from acetoacetyl-CoA that is converted from acetyl Co-A. Polymerization is mediated by PHA synthase. In *Rba. sphaeroides* 2.4.1, the production of monomers can apparently occur via two pathways, one of which requires NADPH, while the other uses NADH (Fales *et al*., 2001) as shown in Fig. 8.

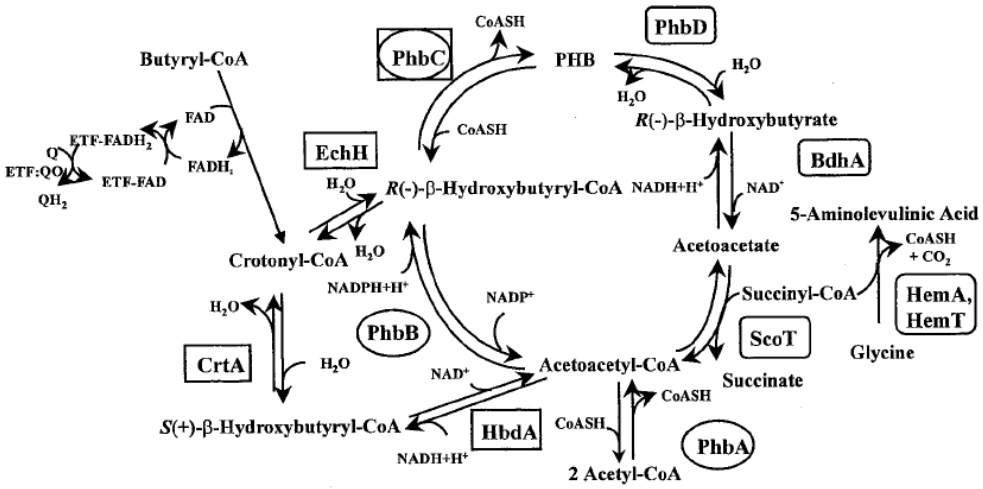

Figure 8. Schematic diagram of proposed dual pathway for polyhydroxybutyrate biosynthesis in *Rba. sphaeroides* 2.4.1. Enzymes catalyzing the reactions have been abbreviated as follows: PhbA, 3-ketothiolase; PhbB, acetoacetyl-CoA reductase; PhbC, polyhydroxybutyrate synthase; CrtA, *S*-(1)-b-hydroxybutyryl-CoA dehydratase (crotonase); EchH, enoyl CoA hydratase; HbdA, *S*-(1)-b-hydroxybutyryl-CoA dehydrogenase; PhbD, polyhydroxybutyrate depolymerase; BdhA, *R*-(2)-b-hydroxybutyrate dehydrogenase; ScoT, 3-oxoacid CoA-transferase (succinyl-CoA–acetoacetate transferase); HemA and HemT, ALA synthases.

Source: Fales *et al.* (2001)

2.4.5.2 Relationship between hydrogen and PHA production in PNSB

Both hydrogen and PHA production take place under physiological conditions of excess energy and reducing power, or high carbon to nitrogen ratios. Since, as is true of hydrogen, PHA also has commercial value as a biodegradable polymer. Therefore, any determination of the best economic value of microbial bioconversions of any given substrate should include consideration of the production of both hydrogen and PHA. Franchi *et al*., (2004) summarized hydrogen and PHAs production in PNSB in a schematic diagram (Fig. 9). This includes H_2 production, mediated by the enzyme nitrogenase; H_2 uptake (recycling), catalyzed by a membrane-bound uptake hydrogenase that reduces the net amount of gas evolved; and biosynthesis of alternative electron sinks for reductants, in particular, PHAs in the form of cytoplasmic granules.

The partition between hydrogen and PHA production depends related to substrates, which are easily converted to acetyl unit without forming pyruvate such as acetate, propionate, and butyrate (Doelle, 1969). In the presence of acetate, hydrogen production competes with PHA synthesis in *Rps. palustris* (De Philippis *et al*., 1992), *Rba. sphaeroides*, and *Rsp. rubrum* (Hustede *et al*.,1993) because of competition for the assimilation of reducing equivalents.

Metabolic mutant strains of *Rba. sphaeroides* RV were constructed towards improving hydrogen production (Franchi *et al*., 2004). One mutant is disabled in a PHA synthase gene, another mutant lacks uptake hydrogenase, and so hydrogen recycling is abolished, and a third mutant has both of these two mutations. Interestingly, hydrogen production was only improved by the absence of the hydrogen uptake hydrogenase, achieving 1.55 l l^{-1} day^{-1} (Franshi *et al*., 2004).

PHAs can themselves be used as endogenous substrates for hydrogen production. Maeda *et al*., (1997) reported that *Rhodovulum* (*Rdv.*) *sulfidophilum* W-1S utilized intracellular PHAs as electron donors for hydrogen production. Intracelluar PHA in *Rdv. Sulfidophilum* W-1S was more efficiently converted to hydrogen than succinate (Maeda et al., 2003)

pH is another factor determining the relative amount of PHAs. *Rba. sphaeroides* cultures that were buffered to prevent alkalination were found to produce

more hydrogen and less PHA (Husted *et al*, 1993). Khatipov *et al.* (1998) found that when the initial pH of the medium was increased to 7.5 from 6.8, hydrogen production decreased 7 times and the amount of accumulated PHA tripled.

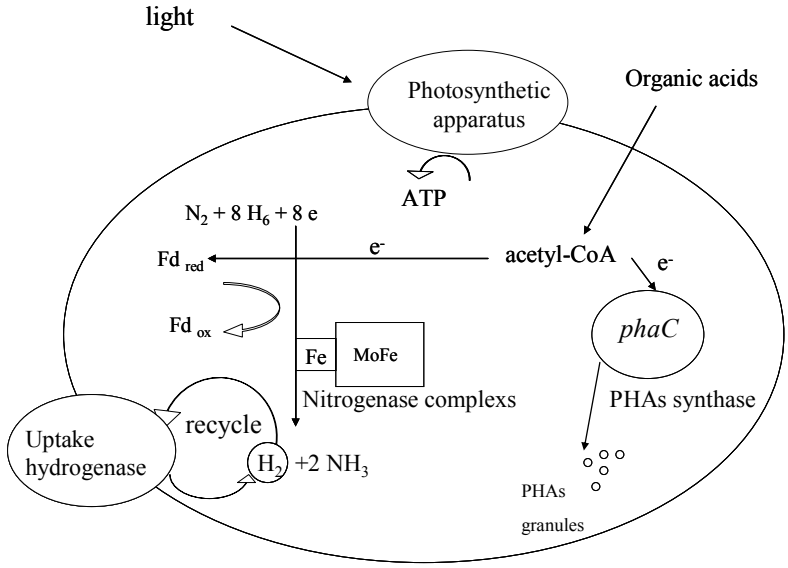

Figure 9. Schematic diagram of relationship between production of hydrogen and PHA in PNSB.

Source: Franchi *et al*. (2004)

2.4.6 Factors affecting hydrogen production by PNSB

PNSB can use a wide variety of substrates. Some photosynthetic bacteria can convert organic acids (acetic, lactic and butyric) [to hydrogen (H_2) and carbon dioxide (CO_2) under anaerobic conditions in the presence of light.

2.4.6.1 Carbon sources

The carbon sources for hydrogen production by PNSB can be organic acids, such as acetate, propionate, butyrate, and lactate that are present in various wastewaters (Pansomboon, 1998; Yetis *et al*., 2000; Lee *et al*., 2002; Takabatake *et al*., 2004). The main carbon components of several wastewaters are volatile fatty acids (VFAs), which are produced from the fermentation of the organic acids (Pansoomboon, 1998; Takabatake *et al*., 2004; Lee *et al*., 2002).

The criteria used to evaluate the hydrogen production performance of substrate are (i) hydrogen production rate, which is the rate of gas production

(amount/time) on a basis of the amount of culture or the amount of bacterial dry weight and (ii) efficiency of hydrogen production (%), which is a measure of how much of the substrate has been utilized for hydrogen production (rather than growth or alternative biosynthesis), which is called Hydrogen yield. It is the ratio of the actual moles of hydrogen produced to the theoretical amount that would have been obtained if all of the substrate was used for hydrogen (and carbon dioxide) production according to the following hypothetical reaction (Sasikala *et al*., 1993):

$$CxHyOz + (2x - z)H_2O \rightarrow (y/2 + 2x - 2)H_2 + xCO_2:$$

The efficiency of hydrogen production can be express as (Chen *et al*., 2007)

$$H_2(\%) = \frac{Amount\ of\ H_2\ produced\,(mol) / Amount\ of\ substrate\ consumed\,(mol)}{Theoretical\ amount\ of\ H_2\ produced\,(mol) / Amount\ of\ substrate\ consumed\,(mol)} \times 100$$

Table 3 shows hydrogen production rate, efficiency of hydrogen production with different type of VFAs and strains of PNSB. However, it should be noted that other parameters such as the age and the past growth history of the culture, the basal medium composition and the reactor geometry may also be important for hydrogen production behavior by PNSB.

Glutamate can also be used as a carbon and nitrogen source. Koku *et al.* (2003) reported that hydrogen production and cell growth of *Rba. sphaeroides* O.U. 001 was observed when 2 mM glutamate was the sole carbon and nitrogen source (Koku *et al*., 2003). Hydrogen production by *Rba. marinum* A-501 from lactate as a major carbon source and glutamate as major nitrogen source has also been demonstrated (Kawaguchi *et al*., 2002). Lactate was found to be utilized not only as the source for hydrogen production but also for supplementing the reducing power in the hydrogen production process. Glutamate was found to be a growth-limiting substrate, and was apparently used as both carbon and nitrogen source. It was thought that glutamate was completely consumed for cell mass production. The addition of algal extract increased the hydrogen production rate and the hydrogen yield from lactate significantly, and it was also consumed for cell mass production.

2.4.6.2 Hydrogen production from wastewaters

The ability to use wastewaters as a source of nutrients for microbial hydrogen production is of considerable economic interest. A number of studies involving hydrogen production by PNSB have been reported in the literature.

The effect of mixtures of volatile fatty acid from anaerobic acidogenesis of organic waste on hydrogen production has been investigated. The effluent from a dairy factory in China contains approximately 1.8 g l^{-1} of acetate, 0.2 g l^{-1} of propionate and 1.0 g l^{-1} of butyrate (Shi and Yu, 2005). The consumption by *Rps. capsulate* [*sic*] of the volatile fatty acids occurred in the order acetate, then propionate, then butyrate (Shi and Yu, 2004).

Hydrogen production from tofu wastewater treatment by cells of *Rba. sphaeroides* entrapped in agar was also investigated. Hydrogen was produced with a high yield (1.9 ml ml^{-1}wastewater) and 41% total organic carbon removal was observed (Zhu *et al*., 1999).

Sasikala *et al*. (1991) used the wastewater of a lactic acid fermentation plant for hydrogen production by *Rba. sphaeroides* O.U. 001. Eroglu *et al*. (2006) used diluted olive mill wastewater as substrate for hydrogen production by *Rba. sphaeroides O.U. 001*. Growth was observed for dilutions of 1–20%, while hydrogen production was detected for dilutions below 4%.

Tao *et al*. (2008) used effluents from succinate wastewater, anaerobic fermentation of wastewater from a fuel ethanol manufacturer, and kitchen waste as substrates for hydrogen production by their new isolate of *Rba. sphaeroides*, ZX5. Hydrogen production was reported to be at the level of 25 l H_2 per liter of succinate wastewater with a hydrogen production rate of 55 ml H_2 l^{-1} h^{-1}, at the level of 20 l H_2 per liter of anaerobic fermentation of wastewater from a fuel ethanol manufacturer with a production rate of 48 ml H_2 l^{-1} h^{-1}, and at the level of 91 l H_2 per liter of kitchen waste with a rate of 45 ml H_2 l^{-1} h^{-1}.

Table 3. Hydrogen production by PNSB in VFAs.

Carbon source	Concentration (mM)	Organism	H_2 yield (mol H_2 mol VFA $^{-1}$)	efficiency of H_2 production (%)	Maximum H_2 production rate (ml l^{-1} h^{-1})	Light conversion efficiency (%)	Process	References
Acetate	22	*Rps.* sp.	2.912	72.8	25.2	0.9	Batch	Barbosa *et al*., 2001
	22	*Rps. palustris*	0.592	14.8	2.2	0.1	Batch	Barbosa *et al*., 2001
	12- 55	*Rps. palustris* P4	2.4-2.8	60-70	NA	NA	Batch	Oh *et al*., 2004
	10	*Rba. capsulatus*	2.1	52.5	7.9	NA	Batch	Fang *et al*., 2005
	30		1.4	35	6	NA	Batch	
	40		1.3	32.5	7.5	NA	Batch	
	50		1.2	30	8.2	NA	Batch	
	60		1.1	27.5	8.8	NA	Batch	
	20	*Rba. capsulatus*	0.65	16.25	16.4	NA	Batch	Shi and Yu, 2006
	40		0.46	11.5	17.7	NA	Batch	
	30	*Rba. capsulatus* B100	2.12	53	NA	NA	Batch	Ooshima *et al*., 1998

Table 3. Hydrogen production by PNSB in VFAs (Cont.).

Carbon source	Concentration (mM)	Organism	H_2 yield (mol H_2 mol VFA $^{-1}$)	efficiency of H_2 production (%)	Maximum H_2 production rate (ml l^{-1} h^{-1})	Light conversion efficiency (%)	Process	References
Acetate	30	*Rba. capsulatus* ST410	3.36	84	NA	NA	Batch	
	35	*Rba. sphaeroides* ZX5	2.76	69	90	NA	Batch	Tao *et al*., 2008
	21	*Rba. sphaeroides* IL106	2.7	67.5	NA	NA	Batch/Immobilization	Asada *et a.,* 2008
	42		3.03	75.75	NA	NA	Batch/Immobilization	
	21	*Rba. sphaeroides* S	2.7	67.5	NA	NA	Batch/Immobilization	
	42		2.48	62	NA	NA	Batch/Immobilization	
	32.5	*Rps. palustris* WP 3-5	2.96	74	32.2	1.93	Batch/Illumination systems	Chen *et al*., 2006

Table 3. Hydrogen production by PNSB in VFAs (Cont.).

Carbon source	Concentration (mM)	Organism	H_2 yield (mol H_2 mol VFA $^{-1}$)	efficiency of H_2 production (%)	Maximum H_2 production rate (ml l^{-1} h^{-1})	Light conversion efficiency (%)	Process	References
Acetate	32.5	*Rps. palustris* WP 3-5	2.96	74	32.2	1.93	Batch/Illumination systems	Chen *et al*., 2006
	15.62	*Rps. palustris* WP 3-5	3.63	90.8	43.8	2.34	Batch/Illumination systems/ Immobilization	Chen and Chang 2006
	15.62	*Rps. palustris* WP 3-5	3.56	89.1	44	2.31	Continuous/Illumination systems/Immobilization	
	20	*Rhodopseudomonas* spp.	0.82	20.6	NA	NA	Batch	Wu *et al*., 2010
	20	*Rps. palustris* W004	0.17	4.4	NA	NA	Batch	

Table 3. Hydrogen production by PNSB in VFAs (Cont.).

Carbon source	Concentration (mM)	Organism	H_2 yield (mol H_2 mol VFA $^{-1}$)	efficiency of H_2 production (%)	Maximum H_2 production rate (ml l^{-1} h^{-1})	Light conversion efficiency (%)	Process	References
Propionate	20	*Rba. capsulatus*	0.28	4	12.6	NA	Batch	Shi and Yu, 2006
	40		0.25	3.5	16	NA	Batch	
Butyrate	20	*Rba. capsulatus*	0.24	2.4	5.8	NA	Batch	Shi and Yu, 2006
	40		0.1	1	5.7	NA	Batch	
	27	*Rps.* spp.	0.84	8.4	7.6	NA	Batch	Barbosa *et al*., 2001
	20	*Rba. capsulatus*	0.24	2.4	5.8	NA	Batch	Shi and Yu, 2006

Table 3. Hydrogen production by PNSB in VFAs (Cont.).

Carbon source	Concentration (mM)	Organism	H_2 yield (mol H_2 mol substrate^{-1})	efficiency of H_2 production (%)	Maximum H_2 production rate (ml l^{-1} h^{-1})	Light conversion efficiency (%)	Process	References
Butyrate	10	*Rba. capsulatus*	2.8	28	12.8	NA	Batch	Fang *et al*., 2005
	15		2.9	29	6.2	NA	Batch	
	30		1.9	19	7.5	NA	Batch	
	40		1.6	16	9.4	NA	Batch	
	60		1.3	13	9.4	NA	Batch	
	50	*Rba. sphaeroides* ZX5	7.15	71.5	118	NA	Batch	Asada *et al*., 2008
	20	*Rps.* spp.	3.02	30.2	NA	NA	Batch	Wu *et al*., 2010
	20	*Rps. palustris* W004	1.50	14.5	NA	NA	Batch	

2.4.6.3 Nitrogen sources

The PNSB can use both organic and inorganic nitrogen sources. They also have the ability to fix nitrogen gas under anaerobic-light conditions (Stiffler and Gest, 1954). Hydrogen production by these bacteria is predominantly catalyzed by nitrogenase, which is strongly inhibited in the presence of excess amounts of NH_4^+ ions. However, dinitrogen does not inhibit this activity (Kim and Takahashi, 1980; Ni *et al*., 2006). Another way that ammonium reduces nitrogenase activity is through increased glutamine synthetase activity, which is the key enzyme in the assimilation of ammonium (Sweet and Burris, 1981; Tubb. 1974; Toch and Cantu, 1980). Thus, the type and concentration of nitrogen source is critical to the efficiency of photohydrogen production and also cell growth.

The effect of various nitrogen sources on hydrogen production, cell growth and acetate consumption by *Rps. palustris* was studied by supplementing an acetate minimal salt medium with such nitrogen sources as glutamate, NH_4Cl and yeast extract (Oh *et al*., 2004.). The initial concentration of the nitrogen source was 5 mM for glutamate and NH_4Cl, or 3 g l^{-1} for yeast extract. Light-grown cells were used as inoculum. H_2 produced over a period of 220 h in the presence of these nitrogen sources was as follows, in descending order: none (control) > yeast extract > glutamate > NH_4Cl. The NH_4Cl was most inhibitory and H_2 production stopped at an early stage, approximately 50 h after the start of cultivation, although cell growth continued to a much later period. The results suggest that *Rps. palustris* P4 relies on its nitrogenase for the photosynthetic H_2 production. In addition, they indicate that, in order to be used in a fermentation broth for photosynthetic H_2 production, the broth from a dark-fermentation should have low residual nitrogen content.

Takabatake *et al.* (2004) reported hydrogen production was possible from mixed cultures in wastewater having high ammonium content when albumin and sodium carbonate were added. Sodium carbonate increased hydrogen production when acetate was used as sole carbon source, but depressed the hydrogen production when propionic acid or butyric acid was used as sole carbon source.

In addition to the particular nitrogen source, the ratio of carbon to nitrogen (C/N ratio) was found to be an important parameter affecting hydrogen production by PNSB. The study by Eroglu *et al*. (1999) indicated that the hydrogen

production rate depended upon the L-malic acid to sodium glutamate ratio. The maximum hydrogen production rate was observed for growth medium containing 15 mM L-malic acid and 2 mM sodium glutamate.

2.4.6.4 Light intensity

PNSB can absorb visible wavelengths of light (Madigan *et al*., 2009). The photosynthetically active radiation (PAR) range of the PNSB is any wavelength between 400-950 nm, as well as the entire spectrum (Akkerman *et al*., 2002). The performance of PNSB with respect to biological hydrogen production can be evaluated by the light energy efficiency, in which hydrogen production rate is compared to the energy of illumination; i.e. the ratio of the total energy value of the hydrogen produced (heat of combustion) to the total energy input to the photobioreactor (PBR) by solar radiation.

The theoretical maximum photosynthetic efficiency is considered to exceed 10% (Akkerman *et al*. 2002), but the photosystems of PNSB saturate at low light intensity, leading to low light conversion efficiency under high light intensity, such as in solar PBRs (Wakayama and Miyake 2002). PNSB can adapt to photosynthesis at low light intensities by using large arrays of light harvesting complexes to capture diffuse light energy and conduct it into the reaction centre (Akkerman *et al*., 2002). The range of adaptability can be deduced from studies of hydrogen production versus changes in light intensities. A decrease in light intensity from 180 to 5.5 lux applied to a culture of *Rps.* spp. led to an increase in efficiency of light from 0.5 to 1.8% (Koku *et al*., 2002), while a reduction in light intensity from 34 to 24 klux resulted in an increase in light efficiency from 0.9 to 6.2% (Barbosa *et al*., 2001).

Shi and Yu (2005) found that increasing light intensity decreased the light efficiency of hydrogen production by *Rsp. capsulate* [*sic*]. The light intensity also affected butyrate consumption by this strain. Below 4,000 lux, butyrate was not consumed completely within 190 hrs, while above 4,000 lux, butyrate was consumed completely within the same period of time.

2.4.6.5 pH

The initial pH is reported to impact PNSB growth and hydrogen production. *Rba.* sp. M-19 can produce hydrogen from starch manufacturing waste.

Yokoi *et al*. (2002) found that the maximum hydrogen yield of 7.2 mol H_2 mol^{-1} glucose was obtained from a culture with an initial pH of 7.5. For this same organism, the optimum pH of nitrogenase activity reported by Koku *et al*. (2002) was 6.5-7.5, which is consistent with the idea that this enzyme is responsible for most of the hydrogen production. Another study found that the optimal initial pH for hydrogen production, both rate and yield, by *Rba. capsulatus* was in the range of 7.0-8.0 (Fang *et al*., 2005). Arix *et al*. (1996) evaluated hydrogen production by *Rba. sphaeroides* O.U.001 under anaerobic conditions, and with a fixed light intensity (50.2 lux) The optimum initial pH was between 7.3 and 7.8, and the maximum hydrogen production rate obtained was 0.047 l^{-1} h^{-1} gas produced per unit volume of culture with 99% purity. However, the literature is not completely in agreement as to the relationship between pH and hydrogen production. One study by Tsygankov and Gogotov (1982) reported the optimal initial pH range for pure cultures of *Rba. capsulatus* is pH 6.5-7.5.

3. 5-Aminolevulinic acid production

3.1 Structure and properties of ALA

ALA is an amino-keto acid with a molecular weight of 131.2 Da and 167.6 in hydrochloride form (Dawson *et al*., 1987; Fukada *et al*., 2005). One molecule of ALA contains five carbon, three oxygen, one nitrogen and nine hydrogen atoms. The structure of ALA is such that the end groups can form COO^- and NH_3^+, depending on pH solution; thus ALA is a zwitter ionic compound. The dissociation constants of ALA are pK_a1 = 3.90 and pK_a2 = 8.05 at 25°C (Dawson *et al*., 1987; Elfsson *et al*., 1998; Fukada *et al*., 2005).

3.2 Biosynthesis and cellular utilization of ALA

ALA can be chemically synthesized from levulinic acid, 2-hydroxypyridine, furfural, furfurylamine, tetrahydro- furfurylamine, 5-hydroxy-2-pyridone, N- methoxycarbonyl-piperidinones and succinic acid (Sasaki *et al*., 2002; Bozell *et al*., 2002). Among these, the majority of chemically produced ALA is

derived from furfurylamine (Bozell *et al*., 2002). Commercial ALA produced by chemical processes involves many steps, and has a relatively low yield, which contributes to its high cost. While medical usage of ALA supports expensive production methods, cost can be prohibitive for the many other non-medical potential uses. A number of other less-expensive approaches have been investigated for their potential to produce ALA. Among them, biological production of ALA is regarded as an attractive alternative.

ALA formation takes place in virtually every organism, as it serves as the common precursor for the synthesis of all tetrapyrroles, including heme, corrin, chlorophyll, and vitamin B_{12}. The production of tetrapyrroles begins with the condensation of two molecules of ALA to form the pyrrole ring structure of porphobilinogen (PBG). Four molecules of PBG are then joined together to form the tetrapyrrole ring. Subsequent decarboxylations produce protoporphyrinogen IX, and final products are formed by further modifications and the addition of a metal ion ligand (Fukada *et al.,* 2005). There are two biochemical pathways by which ALA can be synthesized, and both are represented among the PNSB.

3.2.1 The C4 pathway (Shemin pathway) of ALA formation

ALA is produced by the C4 pathway in animals, fungi and the alpha-proteobacteria. In this pathway, ALA is synthesized from the condensation of glycine and succinate, which is catalyzed by ALA synthase using pyridoxal phosphate as a cofactor (Nishikawa *et al*., 1999). ALA is formed when C-2 of glycine, together with its associated amino group, is transferred to succinyl CoA, thereby becoming C-5 of ALA (Fig. 10) (Avissar and Moberg, 1995).

3.2.2 The C5 pathway of ALA formation

The C5 pathway of ALA formation is present in the chloroplasts of plants, algae cyanobacteria, most eubacteria, and some anoxygenic photosynthetic bacteria (Rieble *et al*., 1989). It is composed of three steps (Fig. 4), and involves glutamyl-$tRNA^{GLU}$ (Tait, 1973). The glutamate becomes the 5-carbon skeleton of ALA (Avissar and Moberg, 1995)

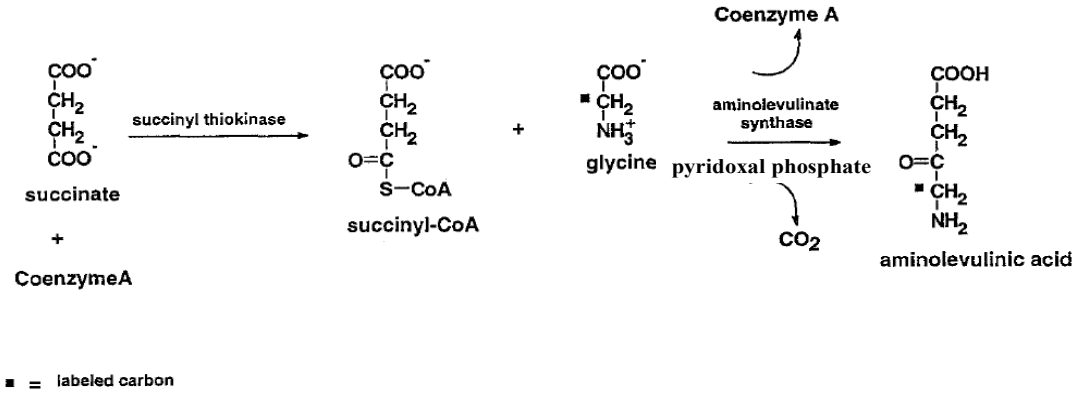

Figure 10. ALA biosynthesis via the Shemin pathway.
Source: Avissar and Moberg (1995)

The first reaction of the pathway links glutamate, through its carboxyl group, to its cognate transfer RNA. The glutamyl-tRNA synthetase catalyzing this step is not dedicated to ALA formation (Eisenberg, 2002). The carboxyl group of glutamyl-tRNA^{Glu} is activated and then reduced by NADPH to form glutamate 1-semialdehyde, with the release of tRNA^{Glu}. This reaction is catalyzed by an enzyme that is dedicated to ALA biosynthesis, glutamyl-tRNA reductase . Glutamate-1-semialdehyde may also exist in a cyclic form, hydroxyamino-tetrahydropyranone, and both compounds are converted to ALA by a second dedicated enzyme, glutamate-1-semialdehyde 2,1-aminomutase. Some investigators consider glutamate-1-semialdehyde to be the first committed precursor of porphyrin synthesis in organisms and organelles that use this pathway (Jahn *et al*., 1992).

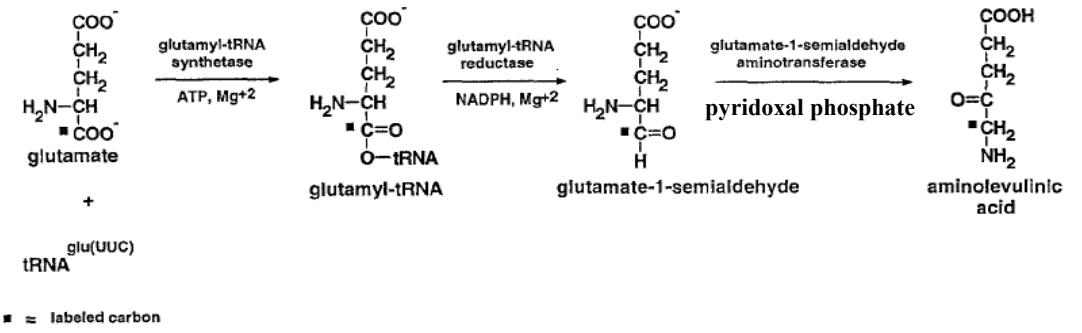

Figure 11. ALA formation via the C-5 pathway.
Source: Avissar and Moberg (1995)

3.3 Enzymes involved in ALA production and utilization

3.3.1 ALA synthase (C4 pathway)

ALA synthase (ALAS) catalyzes the condensation of glycine and succinyl coenzyme A with pyridoxal phosphate as a cofactor to 5-aminolevulinic acid, carbon dioxide and CoA (Zeilstra-Ryalls and Kaplan, 1995). This reaction is the first and rate-limiting step in tetrapyrrole biosynthesis (Freist *et al*., 1997). All purified ALAS enzymes were found to be homodimers with subunits in the range of 40-60 kDa (Avissar and Moberg, 1995). *Rba. sphaeroides* strains have either one or two ALA synthase genes. Other PNSB have as many as four ALA synthase genes (Zeilstra-Ryalls, 2008).

3.3.2 Glutamyl-tRNA synthetase (C5 pathway)

Glutamyl-tRNA synthetases belonging to the class I aminoacyl-tRNA synthetases are responsible for the formation of Glu-$tRNA^{Glu}$ from glutamate and $tRNA^{Glu}$ in the presence of ATP. Among the twenty aminoacyl-tRNA synthetases, glutamyl-tRNA synthetase occupies a special position. It is one of only two enzymes of this family which is not found in all organisms, being mainly absent from gram positive eubacteria and archaebacteria (Neidle and Kaplan, 1993; Freist *et al.,* 1997).

3.3.3 Glutamyl-tRNA reductase (C5 pathway)

Glutamyl-tRNA reductase catalyzes the reduction of glutamyl-$tRNA^{GLU}$ to glutamate 1-semialdehyde with the release of the intact tRNA (Loida *et al*., 1999). The reaction is the first committed step in tetrapyrrole biosynthesis in plants and most prokaryotes (Moser *et al.,* 2001). In *Chlamydomonas*, the activity is associated with a monomeric protein of 130 kDa, while the *E. coli* enzyme is composed of two polypeptides with individual molecular masses of 45 kDa (GluTR45) and 85 kDa (GluTR85) (Beale, 1999).

3.3.4 Glutamate 1-semialdehyde aminomutase (C5 pathway)

Glutamate 1-semialdehyde aminomutase (GSA) is encoded by the *hemL* gene and catalyses the transamination of glutamate 1-semialdehydeto ALA (Loida *et al.,* 1999) in the presence of pyridoxal 5'-phosphate or pyridoxamine 5'-phosphate. This enzyme has been purified from bacteria and chloroplasts of higher plants, and the genes encoding this protein have been characterized. Most of the

enzymes have a homodimeric structure with subunit molecular masses of 44-46 kDa (Jahn *et al*., 1992).

3.3.5 Porphobilinogen synthase

Regardless of which pathway cells employ to synthesize ALA, it is the substrate of porphobilinogen synthase (PBGS), which is then the second enzyme involved in the biosynthesis of natural tetrapyrroles compounds. This enzyme consumes two molecules of ALA in condensing them through a nonsymmetrical pathway to the pyrrole PBG (Jarret *et al.,* 2000), (Fig. 12). The two ALA substrate molecules are named the A and P-side-ALA, based on the acetic acid and propanoic acid side-chains that they contribute to the product. The corresponding binding sites of PBGS are termed A-site and P-site, respectively (Frere *et al*., 2002).

Many PBG synthases are metallo-enzymes and are divided into two major classes. The Zn^{2+}-dependent enzyme is found in mammals, yeast and some bacteria including *Escherichia (E.) coli*, while the Mg^{2+} dependent PBGS is present in plants and other bacteria (Frankenberg *et al*., 1999). Bollivar et al. (2004) reported that the PBGS of *Rba. capsulatus* does not utilized metal ion (Zn^{2+} or Mg^{2+}). It was also reported that, while the dimeric form of the enzyme had less activity, it was most active as either a hexamer or octamer (Bollivar *et al*., 2004).

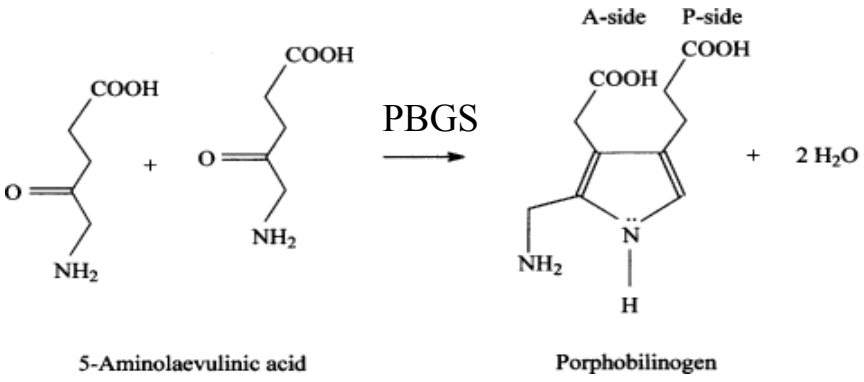

Figure 12. PBG formation. Two molecules of ALA condense to form PBG.
Source: Erskine *et al*. (2003)

3.4 Genes associated with ALA metabolism

3.4.1 The ALA synthase genes

The ALA synthase-encoding *hemA* gene is only found in the alpha-proteobacteria. That this gene is necessary and sufficient for ALA formation was demonstrated by virtue of the fact that it can complement ALA auxotrophs of *E. coli* (Tai *et al*., 1988) even though that organism normally uses the C5 pathway (Beale, 1999). Some strains of *Rba. sphaeroides* such as 2.4.1 harbor a second ALA synthase gene, *hemT* (Tai et al., 1988). Either gene, when expressed is capable of meeting all of the cellular requirements for ALA in that organism (Neidle and Kaplan, 1993).

3.4.2 The glutamyl-tRNA reductase genes

In bacteria other than the C4 pathway-utilizing alpha-proteobacteria, ALA is produced via the C5 pathway. Unfortunately, before the distribution of these completely different biosynthesis pathways among bacteria was known or appreciated, the gene for glutamyl-tRNA reductase gene of *E. coli* had been named *hemA* (Drolet *et al*., 1989). Thus, the ALA synthase-encoding *hemA* gene and the glutamyl-tRNA reductase-encoding *hemA* genes are completely different.

3.4.3 The *hemL* genes

The *hemL* genes, encoding GSA, have been cloned from several bacteria, and from barley, soybean and *Arabidopsis*. In higher plants the gene is present in nuclear DNA. The deduced amino acid sequences of all of the gene products have extensive homology. For example, there is 70% similarity between barley and *Synechococcus* enzymes. This degree of similarity is far greater than that which exists among glutamyl-tRNA reductase proteins (Ilag *et al*., 1994).

3.4.4 The *hemB* genes

The *hemB* genes, encoding PBGS, have been characterized from numerous sources, including bacteria, algae, pea, soybean, and spinach. Alignment of sixteen derived PBGS polypeptide sequences from various organisms indicates the presence of a conserved lysine residue at the active site (Gibbs and Jordan, 1986) and a zinc binding site in enzymes from animals and bacteria, including the PNSB (Hansson, 1994 cited by Avissar and Moberg, 1995).

3.5 Strain improvements for increased ALA production

Towards improved production of ALA by PNSB, the chemical N-methyl-N'-nitro-N nitrosoguanidine (NTG) has been the preferred mutagen. The desired mutant characteristics are low PBGS activity and excretion of ALA without requiring the addition of LA to inhibit PBGS when cells are grown under aerobic condition and without illumination (Tanaka *et al*., 1991: Tanaka *et al*., 1994; Nishikawa *et al*., 1999).

3.5.1 Outcomes of chemical mutagenesis

Whereas ALA accumulation from the wild type strain of *Rba. sphaeroides* CR-001 was found to be less than 15.0 μM when cultured under aerobic-dark conditions, the mutant derivative CR-17 secreted 32.0 μM ALA under microaerobic-dark conditions and as much as 64.5 μM when cultured under anaerobic-light conditions. *Rba. sphaeroides* CR-17 could excrete ALA without LA addition, and with the addition of 15 mM LA these bacteria secreted 82.5 μM of ALA when cultured under aerobic-dark conditions (Tanaka *et al*., 1991). Nishigawa *et al*. (1999) generated an industrial strain by sequentially mutating *Rba. sphaeroides* CR-001 using NTG. Following mutagen treatment, mutant strains were screened for by cultivation of individual colonies in 96-well microtiter plates in the absence of light, followed by assaying for ALA using the Ehrlich reaction. The mutant strain CR-606 accumulated 11.2 μM ALA in 50 mM, glucose, 60 mM glycine, 5 mM LA and 1% (w/v) yeast extract with an aeration rate of 0.2 vvm in normal air and agitation speed of 300 rpm.

3.5.2 The application of recombinant technology for improved ALA production

Several recombinant bacteria have been recently developed for the mass production of ALA. Van der werf and Zeikus (1996) cloned a *Rba. sphaeroides hemA* gene into plasmid pUC19, such that transcription emanated from the *lac* promoter. Under optimized conditions (in the presence of 50 mM succinate and 25 mM glycine, and with the addition of 50 mM LA addition and ATP), ALA production by *Escherichia coli* DH1 with the plasmid was 22.5 mM. Another *E. coli* recombinant was engineered by introducing a plasmid bearing the *Bradyrhizobium*

japonicum hemA gene into strain BL21 (DE3). In these bacteria, the ALA synthase gene was transcribed from the T7 promoter. Optimized culture conditions were MS8 medium supplemented with 15 mM glycine and 30 mM succinate (pH 6.5) in shaking flasks at 37°C and 180 rpm. When, at the end of log phase (about 15 h), 30 mM LA was added the extracellular ALA concentration was found to be as high as 1.3 g l^{-1} (Chung *et al*., 2005).

3.6 Factors affecting ALA production by PSB

3.6.1 The effect of carbon and nitrogen sources on ALA production by PNSB

Among carbon sources that could be used for industrial production of ALA by bacteria, glucose has the advantage of being inexpensive. In batch fermentation with glucose as a carbon source, *Rba. sphaeroides* mutant strain CR-606 accumulated 20 mM ALA after 18 h with the production rate of 1.1 mM h^{-1}. The yield coefficient for ALA was 40% mol mol^{-1} glucose (Nishikawa *et al.*, 1999). However, the ability to metabolize glucose is not universal among PNSB.

Volatile fatty acids produced from anaerobic digestions represent another cost-effective carbon source for ALA synthesis. Sasaki *et al*. (1987) reported that *Rba. sphaeroides* can utilize volatile fatty acid (VFA) such as acetic, propionic, and butyric acid as carbon and energy sources. Tanaka *et al.* (1994) found, using VFAs present in the anaerobic digestion liquor of sewage sludge in combination with the addition of glycine and glutamic acid as the nitrogen source, *Rba. sphaeroides* produced up to 9.2 mM ALA.

3.6.2 The effect of precursor concentrations on ALA production by PNSB

In ALA biosynthesis by the C4 pathway, glycine and succinate (succinyl CoA) are the direct precursors. Nishikawa *et al*. (1999) reported that the addition of glycine to cultures of *Rba. sphaeroides* mutant strains (isolated following NTG mutagenesis), grown under aerobic-dark conditions, was extremely effective in increasing ALA accumulation, whereas no significant effect was found following the addition of succinate.

3.6.3 The effect of inhibition of PBGS on ALA production by PNSB

Levulinic acid (LA) is a competitive inhibitor of PBGS. It has been reported that the addition of LA to mid-log phase cultures effectively blocked ALA metabolism, resulting in the retardation of cellular growth and excretion of the ALA produced by the cells (Sasaki *et al*., 1987). Addition of LA to cultures of *Rba. sphaeroides* was required for extracellular ALA production (Sasaki *et al*., 1987), and only moderately suppressed cell growth. However, concentrations higher than 50 mM LA completely suppressed both growth and ALA formation (Sasaki *et al*., 1987), and the most cost-effective concentration of LA for ALA production was determined to be 30 mM (Sasaki *et al*., 1990).

3.6.4 The effect of metal ions on ALA production by PNSB

The availability of metal ions, particularly iron and cobalt, is an important factor in regulating tetrapyrrole biosynthesis in microorganisms. Co^{2+} is essential for vitamin B_{12} biosynthesis, Fe^{2+} or Fe^{3+} is necessary for the conversion of coproporphyrinogen III to protoporphyrinogen IX and for the formation of heme, and bacteriochlorophyll is derived from the Mg^{2+} chelate of protoporphyrin IX. Under conditions of iron (Fe^{2+} and Fe^{3+}) sufficiency, ALA synthase activity levels are negatively affected by heme compounds, either through feedback inhibition or by transcription repression (Sasaki *et al*., 1991). These findings argue that ALA production medium should contain limiting amounts of cobalt, iron, and magneisum in order to enhance ALA accumulation (Sasikala *et al*., 1995).

3.6.5 The effect of light intensity on ALA production by PNSB

Both growth and ALA production by PNSB correlate with light intensity. Sasaki *et al.* (1987 and 2002) report that maximum levels of ALA in *Rba. sphaeroides* were excreted for cells grown in the presence of light with an intensity of 3 klux. Higher illuminations, over 5 klux diminished ALA production. Of course, at very low light intensities, below 1 klux, the growth rate was negatively affected, as was ALA production.

Consistent with those observations Firsow and Drews (1977) report a similar diminution of photopigment synthesis at very high light intensities, which correlated with both diminished ALA production and lower growth rates.

Tungsten lamps are suitable for illumination of PNSB because they generate emissions in the near infra-red (IR) region of 800-900 nm. These wavelengths of light are very efficiently absorbed by the Bchl *a* present in these bacteria.

3.6.6 The effect of pH on ALA production by PNSB

ALA production by *Rba. sphaeroides* has been investigated at various initial pHs, but also with the addition of LA. The extracellular ALA production was reported to be as much as 16 mM at neutral pH (6.7 and 7.0) whereas low production of ALA (<3.5 mM) was observed at an acidic pH (lower than 6.5), and less than 3.9 mM of ALA was produced at an alkaline pH (higher than 7.5) (Sasaki *et al*., 1990).

3.7 Uses of ALA

ALA is useful in a variety of agricultural applications that include use as an herbicide, insecticide and growth promoting factor (Rebeiz *et al*., 1984; Rebeiz *et al*., 1988; Tanaka *et al*., 1992). It has also been found to improve salt and cold temperature tolerance in plants (Kuramoci *et al*., 1997). ALA also has several medical applications including tumor diagnosis and cancer treatment (Kaneko *et al*., 1998). It is the only naturally occurring photodynamic compound, which converts molecular oxygen into singlet oxygen when excited by the absorption of light (Rebeiz *et al*., 1984) and can be used as an effective biodegradable herbicide/insecticide. Other features of ALA increasing its agricultural usefulness, is its biodegradability, and the absence of any known adverse effects on the environment (Van der Werf and Zeikus, 1996).

3.8 Measurements of ALA levels

3.8.1 Chemical assay

The principle of the chemical assay for ALA is to detect the pyrrole (2-methyl-3-acetyl-4-(3 propionic acid) formed from the condensation reaction that takes place in the presence of acetylacetone (Nishikawa *et al*., 1999). The pyrrole detection follows reaction with Ehrlich reagent, in which the amine of the pyrrole is reacted with the aldehyde of *p*-dimethylamino benzaldehyde (DMAB) in acid solution to form a purple red compound (Mauzerall and Granick, 1956; Nishikawa *et*

al., 1999; Di Venosa *et al*., 2004). However, this method is not sensitive enough to measure ALA below concentrations of 500 μg l^{-1} (2.9 μM) (Sithisarankul *et al*., 1999). This chemical assay is showed in Fig. 13. It has been used as a means to quantitate biological ALA production by *Rba. sphaeroide*s and recombinant *E. coli* strains (Sasaki *et al*., 1987; Sasaki *et al*., 1990; Sasaki *et al*., 2002; Nishikawa *et al*. 1999; Chung *et al*., 2005).

3.8.2 High-performance liquid chromatography (HPLC) detection

ALA determination by HPLC has been used in clinical research (Sithisarankul *et al*., 1999; Dalton *et al*., 2002; Lee *et al*., 2004). The method is based on detection of fluorescent derivatives of ALA prepared via the Hantzch reaction (Sithisarankul *et al*., 1999; Dalton *et al*., 2002; Lee *et al*., 2004). The Hantzch reaction for ALA detection was developed by Oishi *et al*. (1996). Formaldehyde reacts with acetylacetone in the presence of amine group of ALA which formed the fluorescence product of 3,5-diactyl-1,4-dihydrolutidine (DDL) (Li *et al*., 2008), as showed in Fig 14. The maximum absorption wavelength of the product occurs at 368 nm, and the maximum excitation and emission wavelengths are found at 370 and 470 nm, respectively.

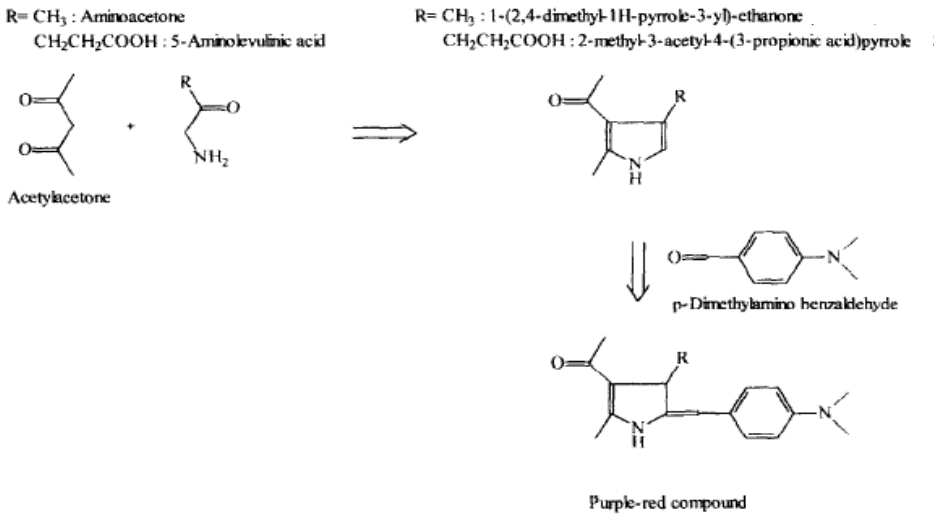

Figure 13. Schematic diagram for ALA determination by colorimetric method. Source: Nishikawa *et al*. (1999)

3.8.3 Capillary electrophoresis detection

A capillary electrophoresis system has been described for resolving and identifying ALA in a solution that also contained 2, 5-dicarboxyethyl-3,6-dihydropyrazine (DHPY) and 2,5-dicarboxyethylpyrazine (PY). These were dissolved in 200 mM phosphate buffer at pH 7.4. Separation of the chemicals was optimal when electrophoresing in borate buffer of pH 9.4 and applying a voltage of 20 kV. The solution separated within 7 min and the relative standard deviation (R.S.D.) of ALA, DHPY, and PY were 0.75, 3.18, and 1.50%, respectively (Bunke *et al*., 2000).

For ALA detection in culture broth, the optimum separating conditions in culture broth were electrophoresing in a 30 mM of sodium borate running buffer with a voltage of 20kV and current of 150 μA. Using this system, ALA, PBG, LA, and glycine in culture broth could be resolved and detected. Other detectable compounds present in the broth consisted of minerals, vitamins, and organic acids (Kim *et al*., 2001

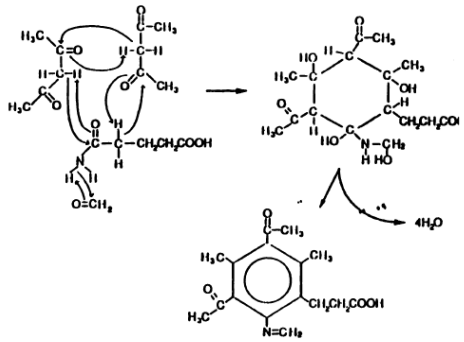

Figure 14. Reaction of ALA with formaldehyde and acetylacetone.
Source: Okayama *et al.* (1990)

3.9 Hydrogen and ALA production by PNSB

Sasaki (1998) have studied the characteristics of hydrogen and ALA production by *Rba. sphaeroides* S in separate parallel processes. It was observed that the hydrogen production rate from acetate and propionate was 30.0 ml (g cell)$^{-1}$ h^{-1}. 5-aminolevulinic acid (ALA) was produced extracellularly from a VFA medium prepared from a post-anaerobic digestion liquor of swine waste and sewage sludge

using the cells of *Rba. sphaeroides* with a dense resting cell system. Approximately 9 mM ALA was produced after six days of incubation.

3.10 Previous research on ALA production by PNSB

ALA production and/or its application have been investigated for PNSB collected in the Environmental Laboratory of the Department of Industrial Biotechnology, Faculty of Agro-Industry, Prince of Songkla University, Thailand. Some of the findings from those studies are summarized here, and the data are reported in Table 4.

Tangprasitipap (2005) examined intracellular ALA production by the PNSB *Rba. sphaeroides* SH5. This strain was found to accumulate the highest intracellular ALA concentration (226 μM) when 10 mM levulinic acid was added to cultures grown under aerobic-dark conditions. Another component of this study was to examine the toxicity of ALA in the black tiger shrimp, *Penaeus monodon*. The study involved the application of ALA in amounts of 0-3,300 ppm for 7 days to these organisms (average weight 15 ± 2 g). Based on the results, the ALA LD_{50} was estimated to be 113.33 ppm. Even low concentrations of analytical grade of ALA (66,660 ppb) were found to increase total haemocyte count, phenoloxidase activity and survival of shrimp infected white spot syndrome virus. When ALA (10-1,000 ppm) was added to cultures of haemocytes (*in vitro*), degranulation increased, which was thought to indicate that ALA could act as an immunostimulant (Johansson *et al*., 2000; Lee and Söderhäll 2002).

Madmarn (2002) used chemical mutagenesis to improve ALA production by PNSB. Using NTG, a collection of mutant strains were generated from the wild type strain *Rba. sphaeroides* ES16. Among them, mutant strain N20 was found to excrete the highest extracellular ALA concentration (180.97 μM; Table 4). The effect of medium composition on growth and ALA production was also examined for *Rba. sphaeroides* N20 (Suwansaard, 2004). Cultures grown in glutamate glucose (GG) medium with 3% NaCl under aerobic-dark conditions had specific growth rates of 0.28 h^{-1}, and the ALA production level was 42.79 μM. When cultivated in glutamate malate (GM) medium with 3% NaCl under aerobic-

dark conditions ALA production was 45.78 μM. The effect of magnesium chloride ($MgCl_2$) supplementation on ALA production was evaluated as well. For GG the optimal concentration of $MgCl_2$ was 10 mM and resulted in ALA production levels of 63.69 μM. The optimal concentration of $MgCl_2$ in GM medium was 15 mM, and 48.48 μM ALA was produced.

Riansa-ngawong (2004) examined the effects of protein hydrolysate on production of ALA from the wild *Rba. sphaeroides* strain ES16 and the mutant derivative U7, which was identified as a halotolerant isolate following UV mutagenesis (Madmarn, 2002). The optimal concentration of protein hydrolysate for both strains was 0.1% (w/v), and the amount of ALA produced was 50.54 and 44.21 μM, respectively.

Rba. capsulatus strain SS3 was also investigated with respect to ALA production by Sattayasmithstid (2002). In a comparison of ALA produced by the bacteria cultured in GM medium supplemented with a variety of nutrients, with optimized supplementation the highest extracellular ALA concentration was found to be 976 μM (Table 4). However, ALA produced by cultivation of *Rba. capsulatus* SS3 in monosodium glutamate wastewater was, at best, approximately 40-fold lower than in the synthetic medium (Chaikritsadakarn, 2004). This strain was subjected to NTG treatment for strain improvement (Sawangsaeng 2005). The mutant strain *Rba. capsulatus* SN28 was found to produce approximately 3-fold higher amounts of extracellular ALA than the parent strain in GM medium.

Table 4. Extracellular ALA production by the purple non-sulfur bacteria (PNSB) in the collection of the Environmental Biotechnology Laboratory, Faculty of Agro-Industry, PSU.

Strains	ALA Concentration (μM)	Time (h)	Production rate (μM h^{-1})	Medium	Condition (37 °C)	References
Rba. sphaeroides ES16	24.94	24	1.04	GM	Aerobic (200 rpm)-dark	Tangprasitipap, 2005
Rba. sphaeroides ES16	23.04	24	0.96	GM	Anaerobic-light (3 klux)	Tangprasitipap, 2005
Rba. sphaeroides ES16	27.91	72	0.39	GM	Aerobic (150 rpm)-dark	Madmarn, 2002
Rba. sphaeroides ES16	50.54	96	0.53	GG[a]	Aerobic (200 rpm)-dark	Riansa-ngawong, 2004
Rba. sphaeroides N20	43.75	72	0.61	GM	Aerobic (150 rpm)-dark	Madmarn, 2002
Rba. sphaeroides N20	44.87	72	0.62	GG	Aerobic (150 rpm)-dark	Madmarn, 2002
Rba. sphaeroides N20	40.94	72	0.57	MGSY	Aerobic (150 rpm)-dark	Madmarn, 2002
Rba. sphaeroides N20	180.97	24	7.54	GSY	Aerobic (300 rpm)-dark	Madmarn, 2002
Rba. sphaeroides N20	45.67	60	0.76	GM	Anaerobic-light (3 klux)	Suwansaard, 2004
Rba. sphaeroides N20	42.79	60	0.71	GG[b]	Aerobic (200 rpm)-dark	Suwansaard, 2004
Rba. sphaeroides N20	48.48	72	0.67	GM[b]	Anaerobic-light (3 klux)	Suwansaard, 2004
Rba. sphaeroides N20	63.91	84	0.76	GG	Aerobic (200 rpm)-dark	Suwansaard, 2004
Rba. sphaeroides U7	60.42	72	0.84	GM	Aerobic (150 rpm)-dark	Madmarn, 2002

Table 4. Extracellular ALA production by additional PNSB in the collection of the Environmental Laboratory, Faculty of Agro-Industry, PSU (Cont.).

Strains	ALA Concentration (μM)	Time (h)	Production rate (μM h^{-1})	Medium	Condition (37 °C)	References
Rba. sphaeroides U7	44.21	96	0.46	GG[a]	Aerobic (200 rpm)-dark	Riansa-ngawong, 2004
Rba. capsulatus SS3	976.00	60	16.27	GM[a]	Facultative-light (3 klux)	Sattayasmithstid, 2002
Rba. capsulatus SS3	0.20	20	0.01	MSGE	Aerobic (150 rpm)-dark	Chaikritsadakarn, 2004
Rba. capsulatus SS3	40.00	60	0.67	GSY	Aerobic (150 rpm)-dark	Chaikritsadakarn, 2004
Rba. capsulatus SS3	18.60	36	0.52	MSGE[a]	Aerobic (150 rpm)-dark	Chaikritsadakarn, 2004
Rba. capsulatus SS3	24.00	36	0.67	MSGE[b]	Aerobic (150 rpm)-dark	Chaikritsadakarn, 2004
Rba. capsulatus SS3	22.34	18	1.24	GM	Aerobic (200 rpm)-dark	Sawangsaeng, 2005
Rba. capsulatus SN28	64.77	60	1.08	GM	Aerobic (200 rpm)-dark	Sawangsaeng, 2005

Table 4. Extracellular ALA production by additional PNSB in the collection of the Environmental Laboratory, Faculty of Agro-Industry, PSU (Cont.).

Strains	ALA Concentration (μM)	Time (h)	Production rate (μM h^{-1})	Medium	Condition (37 °C)	References
Rba. capsulatus SN28	97.13	60	1.62	GG	Aerobic (200 rpm)-dark	Sawangsaeng, 2005
Rba. capsulatus SN28	129.37	60	2.16	GG[c]	Aerobic (200 rpm)-dark	Sawangsaeng, 2005
Rba. capsulatus SN28	308.72	72	4.29	GG[d]	Aerobic (200 rpm)-dark	Sawangsaeng, 2005
PNSB sp. FS5	7.54	24	0.31	GM	Aerobic (200 rpm)-dark	Tangprasitipap, 2005
PNSB sp. FS5	6.44	24	0.27	GM	Anaerobic-light (3 klux)	Tangprasitipap, 2005
Rba. sphaeroides SH5	8.04	24	0.34	GM	Aerobic (200 rpm)-dark	Tangprasitipap, 2005
Rba. sphaeroides SH5	32.94	24	1.37	GM	Anaerobic-light (3 klux)	Tangprasitipap, 2005

Note: GM: glutamate-malate medium; GM[a]: GM supplemented with 15 mM levulinic acid, 30 mM glutamate, 7.5 mM malic acid, 0.5 g l^{-1} propionic acid, 15 mM $MgCl_2$, 10 μM pyridoxal phosphate and pH 6.5; GM[b]: GM medium supplemented with 15 mM $MgCl_2$; GG: glutamate-glucose medium; GG[a]: GG medium supplemented with 0.1% protein hydrolysate; GG[b]: GG medium supplemented with 10 mM $MgCl_2$; GG[c]: GG medium supplemented with 15 mM levulinic acid; GG[d]: GG medium supplemented with 5 mM levulinic acid, 0.5 g/l butyric acid, 15 mM $MgCl_2$, 2% NaCl, and pH 7; GSY: glutamate-glucose salt yeast extract medium; MGSY: monosodium glutamate glucose salt yeast extract medium; MSGE: monosodium glutamate effluent (COD 220,100 mg l^{-1}); MSGE[a]: monosodium glutamate effluent (COD 15,200 mg l^{-1}); MSGE[b]: monosodium glutamate effluent (COD 15,000 mg l^{-1})

OBJECTIVES

1. To screen and isolate PNSB strain from Songkla Lake having high hydrogen production from acetate.
2. To identify the PNSB isolate from Songkla Lake having maximum hydrogen production.
3. To optimize the types and concentrations of volatile fatty acid (VFA), and medium compositions for hydrogen production by the PNSB isolate having maximum hydrogen production using statistical methodology.
4. To determine the hydrogen productivity of the PNSB isolated from Songkla Lake using palm oil milling effluent (POME) as a substrate.
5. To improve 5-aminolevlulinic acid (ALA) production by previously isolated and characterized PNSB bacteria by recombinant methods.
6. To investigate ALA production by the recombinant strain using POME as a substrate.
7. To evaluate the feasibility of hydrogen and ALA production in a one-stage process using POME as growth medium.

CHAPTER 2

MATERIALS AND METHODS

1. Strains and plasmids

New natural isolates of hydrogen-producing purple non-sulfur photosynthetic bacteria (PNSB) were enriched from mud and water samples taken from Songkhla Lake, Songkhla and Phatthalung Provinces, Thailand. Stock cultures of *Rhodobacter* (*Rba.*) *sphaeroides* strains ES16, N20, U7, FS3, FS4, FS5 and SH5 and *Rba. capsulatus* strains SN28 and SS3 were obtained from Environmental Biotechnology Laboratory, Department of Industrial Biotechnology, Faculty of Agro-Industry, Prince of Songkla University, Hatyai, Thailand. Other stock cultures of *Rba. sphaeroides* strains, *Rhodopseudomonas (Rps.) palustris* strains, and *Escherichia (E.) coli* strains and plasmids used in this study are listed in Table 5 and 6, together with their relevant characteristics and sources.

Table 5. Bacterial strains used in this study.

Bacterial strain	Relevant characteristic(s)	Reference(s) or source(s)
E. coli		
DH5	F^-ϕ80d*lac*ZΔ(*lac*ZYA-*arg*F)*U169 recA1 endA1 hsdR1 supE44 thi-1 gyrA96 relA1 deoR*	Jessee, 1986
DH5αphe	DH5α with *phe*::Tn*10d*Cm^r	Eraso and Kaplan, 1994
HB101	F^- Δ(*gpt-proA*)*62 leuB6 supE44 ara-14 galK2 lacY1*	Ditta *et al*., 1980

Table 5. Bacterial strains used in this study (Cont.).

Bacterial Strain	Relevant characteristic(s)	Reference(s) or source(s)
E. coli		
S17-1	Conjugal donor; C600::RP4-(Tc::*Mu*)(Km::Tn*7*) *pro res mod*$^+$ (Tp^r Sp^r)	Simon *et al*., 1983
XL1-Blue	F'::Tn*10 proA*$^+$*B*$^+$ *lacI*^{q} Δ(*lacZ)M15/recA1 endA1 gyrA96 (Nal*^{r}*) thi hsdR17* ($r_K^-m_K^+$) *glnV44 relA1 lac*	Stratagene
Rba. sphaeroides		
2.4.1	Wild type	van Neil, 1944
HemAT1	2.4.1 derivative, *hemA*::ΩKn^r and *hemT*:: ΩSt^r-Sp^r	Neidle and Kaplan, 1993
ATCC17029	Wild type	ATCC
Tc^r	(pUI1007-×SH5) mutant, Tc^r	This study
Tc^s	(pUI1007-×SH5) mutant, Tc^s	This study
Rps. palustris		
CGA009	Wild type	Kim and Harwood, 1991

Table 6. Plasmids used in this study.

Plasmid	Relevant characteristic(s)	Reference(s) or source(s)
pBSIISK$^+$	Ap^r	Stratagene
pBBR1-MCS2	Kn^r	Kovach *et al*., 1994
pSUP202	pBR325 derivative, Mob$^+$ Ap^r Cm^r Tc^r	Simon *et al*., 1983
pUI1087	pBSIISK$^+$ with modified polylinker, Ap^r	Zeilstra-Ryalls and Kaplan, 1995
pUI1007	pSUP202 derivative with *hemA*::ΩKn^r	Neidle and Kaplan, 1993
pUI1992	wild type *hemB* from *R. sphaeroides* 2.4.1 in pUI1087	Zeilstra-Ryalls, unpublished
pUI1638	source of Ω Sp^r-St^r cassette	Eraso and Kaplan, 1994
pMS1	Δ(15-27)*hemB* in pUI1992, Ap^r	This study
pMS2	XbaI-HindIII fragment containing *hemB* from pUI1992 in pBBR1-MCS2; Kn^r	This study
pMS3	XbaI-HindIII fragment containing Δ*hemB* from pMS1 in pBBR1-MCS2; Kn^r	This study
pMS4	XhoI fragment containing Ω from pU1638 in ScaI- site SH5 *hemA* of pSUP202	This study

2. Media

Basal medium (Barbosa *et al*., 2001), Glutamate-Malate (GM) (Tangprasitipap, 2005), modified Glutamate-Acetate (GA) (This study), and Sistrom's succinic acid minimal (SIS) medium (Sistrom, 1960) were used for growth of PNSB. Luria Bertani (LB) was used for *E. coli* growth (Bertani, 1951). The media compositions are listed below.

Table 7. Media used in this study.

Composition ($g\ l^{-1}$)	Basal medium	Glutamate-Malate (GM)[a]	Modified Glutamate-Acetate (GA)[a]	Sistrom's succinic acid minimal (SIS) medium[b]	Luria Bertani (LB)
KH_2PO_4	0.5	0.5	0.5	2.72	-
K_2HPO_4	0.6	0.5	0.6	-	-
NaCl	0.4	0.4	0.4	0.5	5
$(NH)_2SO_4$	-	0.8	-	-	-
NHCl	-	-	-	0.195	-
$MgSO_4.7H_2O$	0.2	0.2	0.2	0.3	-
$CaCl_2.2H_2O$	5×10^{-2}	5.3×10^{-2}	5×10^{-2}	3.34×10^{-2}	-
$FeSo_4.7H_2O$	1×10^{-3}	-	1×10^{-3}	7×10^{-3}	-
$Na_2MoO_4 \cdot 2H_2O$	7.5×10^{-3}	-	7.5×10^{-3}	-	-
$(NH_4)_6Mo_7O_{24} \cdot 4H_2O$	-	-	-	2×10^{-4}	
$CoCl_2.6H_2O$	1×10^{-5}	-	1×10^{-5}	-	-
$ZnCl_2$	1×10^{-4}	-	1×10^{-4}	-	-
$CuCl_2$	1×10^{-5}	-	1×10^{-5}	-	-
H_3BO_3	2×10^{-3}	-	2×10^{-3}	1.14×10^{-3}	-
EDTA-2Na	2×10^{-3}	-	2×10^{-3}	1.76×10^{-2}	-

Table 7. Media used in this study (Cont.).

Composition ($g\ l^{-1}$)	Basal medium	Glutamate-Malate (GM)[a]	Modified Glutamate-Acetate (GA)[a]	Sistrom's succinic acid minimal (SIS) medium[b]	Luria Bertani (LB)
$ZnSO_4.7H_2O$	-	-	-	0.11	-
$MnSO_4.H_2O$	-	1.2×10^{-2}	-	1.54×10^{-2}	-
$CuSO_4.5H_2O$	-	-	-	3.92×10^{-3}	-
$Co(NO_3)_2.6H_2O$	-	-	-	2.48×10^{-3}	-
Nicotinic acid	-	1×10^{-3}	-	1×10^{-2}	-
Thiamine. HCl	1×10^{-3}	1×10^{-3}	1×10^{-3}	5×10^{-3}	-
biotin	1.5×10^{-5}	1.5×10^{-5}	1.5×10^{-5}	1×10^{-4}	-
Yeast extract	-	2	1	-	5
Sodium- L-glutamate	-	3.8	0.94 (5mM)	-	-
D,L-Malic acid	-	2.7	-	-	-
$CH_3COONa.3H_2O$	-	-	2.72 (20 mM)	-	-
Tryptone	-	-	-	-	10
Succinic acid	-	-	-	4	-
L-Glutamic acid	-	-	-	0.1	-
L-Aspatic acid	-	-	-	4×10^{-2}	-
Nitrilotriacetic acid	-	-	-	0.2	-

[a] adjusted to pH 7 by 5 N NaOH.

[b] adjusted to pH 7 by KOH pellets.

3. Instruments

The instruments used in this work were supported by the Department of Industrial Biotechnology, Faculty of Agro-Industry, Scientific Equipment Center (SEC), Prince of Songkla University (PSU), Hatyai, Thailand, or the Department of Biological Sciences, Bowling Green State University (BGSU), Ohio, USA. The instruments are listed in Tables 8 and 9.

Table 8. Description of instruments used in Thailand.

Instruments	Model	Company
Electronic balance	BP 221S	Satorius, Germany
Shaker	SK3-PO Seiker	Welsource Co., Ltd., China
Spectrophotometer and microplate reader	Zenyth200rt	Anthos Labtec Instruments, Austria
Hot air oven	ULM.500	Memmert, USA
Gas Chromatography equipped with flame ionization detector	GC 6850	Hewlett Packard, USA
High performance liquid chromatography equipped with fluorescence or refractive index detector	1100	Hewlett Packard, USA
Transmission electron microscopy	H-7100	Hewlett Packard, USA
Scanning electron microscopy	960	Hewlett Packard, USA
Lux meter	LX-50	Hitachi, Japan
Micro centrifuge	a 14	Jouan, France
Refrigerated centrifuge	Universal 32 R	DWYER Instruments, Inc, USA
Fermentor	MDL 300	B.E. Marubishi, Japan
Gas detector	Oldham MX 2100	Cambridge Sensotec Ltd., England

Table 9. Description of instruments used in the USA.

Instruments	Model	Company
Electronic balance	CP 42025	Sartorius, Germany
Electronic balance	AL54	Mettler Toledo, USA
Waterbath shaker	Gyrotry® G76	New Brunswick scientific, USA
Incubation shaker	Innova 4200	New Brunswick scientific, USA
pH meter	125	Denver Instrument, USA
Double beam Spectrophotometer	U-2000	Hitachi, Ltd., USA
Waterbath (Isothermal)	202	Fisher Scientific, USA
Waterbath	VWR	VWR International, USA
Microcentrifuge	Minispin plus	Eppendorf, USA
Refrigerated Centrifuge	5810 R	Eppendorf, USA
Electrophoresis system		OQ scientific, USA
Western Blotting System		Hoefer, Inc., USA
Thermo cycle		Bio Rad

4. Analytical methods

4.1 Monitoring Cell Growth

Cell densities were monitored by measuring light scattering at 660 nm with a spectrophotometer or microplate reader. Dry cell weights (DCW) were calculated from a standard curve that was generated for each isolate by the method of Sasaki *et al*. (1987).

4.2 Determination of biogas and hydrogen content

The biogas production in each culture vial was measured by a syringe technique described by Owen *et al*. (1979). Hydrogen content of the biogas was determined using a gas detector.

4.3 Volatile fatty acid (VFA) analysis

VFAs were measured by determining free fatty acid concentrations in samples of the cultures using a Gas Chromatography equipped with FID and a 30 m × 0.25 mm × 0.25 μm capillary packed with crossbond®-acid-deactivate Carbowax® polyethyleneglycol (Stabilwax®-DA, Restek GC columns, USA). The samples were first centrifuged at 10,502×*g* for 5 min, acidified by using 0.1 M phosphoric acid, and then passed through a 0.2 μm nylon membrane. The operational temperatures at the injection port and detector were 230 and 250°C, respectively. The oven was programmed as follows: (i) hold at 70°C for 3 min, (ii) ramp for 5 min at 20°C min^{-1} to a final temperature of 235°C, (iii) hold at 235°C for 3 min. Helium was used as carrier gas with a flow rate of 1.2 ml min^{-1}.

4.4 Calculation of hydrogen yield and production efficiency

Hydrogen yield was expressed as the ratio of the actual moles of H_2 produced to the theoretical moles of H_2 produced. The efficiency of hydrogen production was defined as indicated in Eq. 1 (Chen *et al*., 2007):

$$H_2(\%) = \frac{Amount\ of\ H_2\ produced\,(mol) / Amount\ of\ substrate\ consumed\,(mol)}{Theoretical\ amount\ of\ H_2\ produced\,(mol) / Amount\ of\ substrate\ consumed\,(mol)} \times 100 \quad (1)$$

4.5 Kinetic analysis

A modified Gompertz equation (Eq. 2) (Miyake and Kawamura, 1987) was used to fit the cumulative hydrogen production data for TN1 cultures to obtain *P*, R_{max}, and λ:

$$H = H_{\max} \exp\{-\exp\left[\frac{R_{\max} e}{H_{\max}}(\lambda - t) + 1\right]\} \quad (2)$$

H: cumulative H_2 production (ml l^{-1}), *P*: maximum cumulative H_2 production (ml l^{-1}), R_{max}: maximum H_2 production rate (ml $l^{-1}h^{-1}$), λ: lag time (h), t: culture time (h), and *e*: irrational constant (2.718) (Jerrold and Weinstein, 1985).

The kinetic parameters were determined by best-fitting the hydrogen production data for Eq. 2 using Sigma Plot version 9.0 (Systat Software, Inc., Chicago, IL, USA).

4.6 Light conversion efficiency

Light conversion efficiency (η) is defined as the efficiency by which the light energy can be transformed into H_2 (Miyake and Kawamura, 1987). The η value was calculated using the following equations:

$$\eta(\%) = \frac{H_2\ energy\ content \times H_2\ output}{light\ energy\ input} \times 100 \quad (3)$$

$$= \frac{241.83\,(kJmol^{-1})2(g_{H_2}mol^{-1})\rho(gl^{-1})V(l)}{I(Js^{-1}m^{-2})t(h)3600(sh^{-1})A(m^2)} \times 100$$

$$= \frac{33.6\rho_{H_2}V_{H_2}}{ItA} \times 100 \quad (4)$$

where, ρ_{H_2} is the density of H_2 production (g l^{-1}), V_{H_2} is the volume of H_2 production (l), *I* is the light intensity in W m^{-2} (1 lux = 0.0161028 W m^{-2}), t is the duration time of H_2 production (h), *A* is the irradiated area (m^2). $A = \pi \times H \times D$, where the *H* is the height of volume of culture broth and *D* is the diameter of the serum vial. The enthalpy of water formation in the gas phase is 241.83 kJ mol^{-1} (Miyake and Kawamura, 1987).

4.7 Immunoblot analyses

Crude cell lysates were prepared by passaging cells suspended in 0.1 M sodium phosphate ($NaPO_4$) buffer, pH 7.7, through a French pressure cell at 700 lb in^{-2} followed by centrifugation at 13,000× *g* for 15 min at 4°C. Samples were then subjected to immunoblot analysis according to standard procedures (Harlow and lane, 1999). Nitrocellulose membranes (Micron Separations Inc., Westboro, USA) were prepared by electrophoretic transfer of proteins resolved by polyacrylaminde gel electrophoresis using 12% gels from Invitrogen (Carlsbad, USA). The membranes were then probed with 1:10,000 dilution of anti-HemA, 1:2,000 dilution of anti-HemT, or 1:10,000 dilution of anti-HemB rabbit antisera. Alkaline phosphatase-conjugated goat anti-rabbit antisera (Sigma-Aldrich Co.) were used as the secondary antibody and immuno-complexes were detected using the 5-bromo-4-chloro-3-indolyphosphate (BCIP)/nitroblue tetrazolium (NBT) liquid substrate system (Sigma-Aldrich Co.).

4.8 Protein concentration determination

The protein concentration in samples subjected to spectral analysis or analyzed by immunoblotting were determined with the Pierce bicinchoninic acid (BCA) Protein Assay Protocol (Rockford, USA) and bovine serum albumin was used as a standard in all cases (Zeilstra-Ryalls and Kaplan, 1995).

4.9 Porphobilinogen synthase activity

The porphobilinogen (PBG) synthase assay is a colorimetric assay based on the reaction between 5-aminolevulinic acid (ALA) and 4-(dimethylamino)benzaldehyde (Ehrlich's reagent) to form PBG. (Mauzerall and Granick, 1956). Crude lysate samples (prepared as described in section 4.6) were pre-incubated in a total volume of 900 µl of 0.1 M Bis-Tris propane (BTP) buffer pH 8.5 for 10 min at 37°C. The enzyme reaction was initiated by the addition of 0.1 M (commercial) ALA-HCl (Sigma-Aldrich Co.) to a final concentration of 10 mM and was allowed to run for 5 min in a final volume of 1 ml. The reaction was stopped by the addition of 0.5 ml of 20% Trichloroacetic acid (TCA). After centrifugation at 2,040×*g* for 3 min, the PBG was then quantified by reaction of the stopped assay

mixture with an equal volume of modified Ehrlich's reagent and the absorbance was measured at 555 nm approximately 7-8 minutes later. All assays were performed in triplicate. If the amount of product resulted in an absorbance above 1.0 OD, the stopped assay mixture was diluted prior to the addition of modified Ehrlich's reagent. The extinction coefficient of the pink complex formed (ε555) is 63,000 m^{-1}. (This protocol was modified from Gacond *et al.*, 2007).

4.10 Extracellular 5-aminolevulinic acid (ALA) assay

4.10.1 Chemical ALA assay

Extracellular ALA was determined by a colorimetric method (Mauzerall, and Granick, 1956). The supernatant of bacterial cells culture (0.5 ml) was decanted into a new test tube containing 1 ml of 1 M acetate buffer pH 4.7. Then 25 µl of acetyl acetone (2,4-pentanedione) was added and the tubes capped were heated at 100 °c for 15 min and quick-chilled. Modified Ehrich's reagent (1.75 ml) was added and after 20 min the optical density at 553 nm was determined. The amount of ALA was then determined by comparing the OD_{553} to a standard curve generated by assaying known concentrations of (commercial) ALA-HCl (Tangprasitipap, 2005).

4.10.2 Biological ALA assay

200 µl of a fresh culture of the *Rba. sphaeroides* ALA auxotrophic mutant strain AT1 (Neidle and Kaplan, 1993) diluted to an optical density (660 nm) of 0.5 was added to the supernatant to be tested for extracellular ALA. 5 µl of a 50 mg ml^{-1} stock solution containing Spectinomycin (Sp) and Streptomycin (St) was used to prevent growth of the bacterial cells present in the supernatant. *Rba. sphaeroides* AT1 growth was then determined after 24 h cultivation by measuring the absorbance at 660 nm. The ALA concentration was determined by comparing the culture density to a standard curve of the optical density of cultures of *Rba. sphaeroides* AT1 grown in SIS medium supplemented with a range of known concentrations of (commercial) ALA-HCl.

4.10.3 High performance liquid chromatographic (HPLC) ALA assay

A fluorescent derivative of ALA was prepared based on the Hantzsch reaction of formaldehyde, in which acetylacetone in the presence of the amine group

of ALA forms the fluorescent product 3,5-diactyl-1,4-dihydrolutidine (DDL) (Li *et al*., 2008). 50 µl of the culture supernatant was reacted with 3.5 ml of acetylacetone reagent, acetylacetone:ethanol:water (15:10:75 by vol) containing 0.4% NaCl, and 0.45 ml formaldehyde solution (8.5% v/v). This mixture was heated for 30 min at 100°C and then cooled in an ice bath. It was left to stand in the dark until analysis by HPLC with a fluorescence detector (Hewlett-Packard, Agilent 1100, USA). 20 µl of the reaction mixture was injected into the Inertsil ODS-3 column (5 µm, 250 × 150 mm) (GL Science Inc, Tokyo, Japan). The mobile phase was methanol and 2.5% (w/v) acetic acid in the ratio of 60:40 v/v, the operating temperature was controlled at 40°C, and the flow rate was set at 0.6 ml min^{-1}. Standard ALA-HCl was run under the same conditions. The eluate was monitored at an excitation and emission wavelength of 363 and 473 nm, respectively.

4.11 Spectral analysis of membrane fractions and photopigments

Crude cell-free lysates of *Rba. sphaeroides* were prepared as described in section 4.6. Spectra were recorded over a range 350 to 950 nm. The B875 and B800-850 pigment-protein complex levels were determined by the method of Meinhardt *et al.* (1985) from the spectral data. Relative amounts of total pigments were compared by extraction from equivalent numbers (based on optical densities) of whole cells using methanol:acetone in the ratio 7:2 and examined spectrophotometrically over the range of 350-800 nm.

4.12 Determination of polyhydroxyalkanoate (PHA) concentration

A gravimetric method was used for quantitative determination of PHA (Grothe *et al*., 1999). A sodium dodecyl sulfate (SDS) solution (1% w/v SDS 10 ml, pH 10) was added to the biomass pellet obtained as described for cell concentration. The mixture was incubated on an orbital shaker (60 min, 200 rpm 37^{o}C). The solids were recovered by centrifugation (4 min, 7,000 × *g*) and washed with commercial sodium hypochlorite solution (1 ml, 5.64% sodium hypochlorite) that was diluted to 20 ml. The pellet was centrifuged (4 min, 7,000 × *g*), washed with deionized water (20 ml) and centrifuged again. The final pellet was dried (105^{o}C, 24 h) to constant weight in pre-weighed tube. The PHA content relative to biomass was calculated as

the mass of PHA obtained per unit dry cell weight. Measurements were performed in duplicate.

4.13 Determination of wastewater characteristics

Chemical oxygen demand (COD), biochemical oxygen demand (BOD), pH, suspended solids (SS), total suspended solids (TSS), oil concentration, total phosphorus and total Kjeldahl nitrogen (TKN) were determined in accordance with the procedures described in the Standard Methods (APHA, 1999). Ammonium-nitrogen and phosphate concentrations were analyzed using commercial test kits from Spectroquant (Merck Ltd., Germany). The sugar contents were analyzed by HPLC (section 4.13).

4.14 Sugar analysis

Sugar was determined by using HPLC with a Zorbax NH_2 column (4.6×250 mm, 5-Micron, Agilent, USA) combined with RI detector (Sreenath *et al*., 2001). The mobile phase was acetonitrile and water in the ratio 75:25 (v/v), the operating temperature was controlled at 25°C, and the flow rate was set at 0.7 ml min^{-1}. Standard sugars were run under the same condition (Rahman *et al*., 2006).

5. Methods

5.1 Isolation of hydrogen producing by nonsulfur photosynthetic bacteria (PNSB)

A total of 34 water and lake bed samples were collected from Songkhla Lake in Phatthalung and Songkhla Provinces, Southern Thailand. Purple non-sulfur photosynthetic bacteria (PNSB) were enriched by inoculating each sample into 50 ml serum vials that had been completely filled with modified GA medium, which is modified from basal medium (Shi and Yu, 2006) by the addition of 20 mM acetate as a major carbon source and 5 mM glutamate as a major nitrogen source. Anaerobic conditions were established by flushing the sealed vials with argon gas. The vials were incubated at room temperature (30 ± 2°C) under anaerobic-light conditions (3,000 lux). After 10 days of incubation, the cultures varied in color, and included

dark red, pink, brown and yellow. Bacteria from each culture were restreak-purified on GA agar plates that were then incubated in anaerobic jars with a CO_2 generator (AnaerocultA system, Merck, Germany) placed in front of a tungsten lamp. One isolated colony from each plate was cultured on GA agar plates. Stock cultures were prepared from samples of these cultures.

5.2 Culturing of natural isolates of PNSB

Each permanent stock culture was used to inoculate three 50 ml serum vials completely filled with modified GA medium and closed with a silicon stopper flushed with argon. The vials were incubated under anaerobic-light conditions for 2 days in a at 30°C water bath to cut off infrared wavelength from the tungsten lamp irradiation. Because nitrogenase, a hydrogen-producing enzyme, is inhibited by ammonium (Yokoi *et al*., 2002), the modified GA medium was modified by substituting Na_2MoO_4 for $(NH_4)_6Mo_7O_{24}$ at a concentration of 0.75 mg l^{-1}.

5.3 Identification of the selected PNSB isolate TN1

Morphological and biochemical characteristics of the isolate used for subsequent studies were determined according to Bergey's Manual of Systematic Bacteriology (Imhoff and Trüper, 1992). The morphological studies were performed using an Eclipse E200 Nikon light microscope (Nikon Instruments Inc**.**, Melville, USA), and by scanning and transmission electron microscopy (SEM and TEM) of the selected strain (performed at the Scientific Equipment Center, Prince of Songkla University, Thailand). To evaluate the metabolic capabilities of the selected strain defined media as described by Watanabe *et al.* (1981) were used.

Spectral analyses of photosynthetic pigment-protein complexes were performed on crude membrane preparations. The 16S rDNA sequencing was performed at the Mahidol University-Osaka University Collaborative Research Center for Bioscience and Biotechnology, Thailand, and sequence results were then compared to the publicly available databases via the BLAST server at http://www.ncbi.nlm.nih.gov. Nucleotide sequences were aligned using the ClustalX and Bioedit programs. The phylogenetic tree was created using the NJPLOT program.

5.4 Preparation of starter cultures of PNSB

Starter cultures of *Rps. palustris* TN1 were prepared by inoculating TN1 from stock cultures into modified GA medium filled in 50 ml serum vial closed with a silicon stopper flushed with argon. The vials were incubated under anaerobic-light conditions (3000 lux) at 30°C for 18-24 h (exponential phase). The starter culture cells were collected by centrifugation at 8307 x *g*. The cell pellets were resuspended in sterilized 0.01 M potassium phosphate buffer, pH 7 and again collected by centrifugation. This was repeated twice, and the final pellet was resuspended in fresh medium, the optical density at 660 nm determined, and then diluted to a density of 0.5 before use.

For *Rba. sphaeroides* strains, the stock cultures were used to inoculate 250 ml flasks containing 100 ml GM medium and incubated under aerobic-dark (150 rpm) conditions at 30°C for 12-18 h (exponential phase). The starter culture cells were collected, washed (twice), and resuspended to a final optical density of 0.5, as described for *Rps. palustris* TN1.

The starter cultures of the genetically engineered strains were prepared as described previously, with the exception that kanamycin (Kn) was added (working concentration 50 μg ml^{-1}) for plasmid maintenance.

5.5 Effect of types and concentrations of volatile fatty acid on hydrogen production by the selected strain

The selected PNSB isolate, *Rps. palustris* TN1, was grown in a basal medium (Barbosa *et al*., 2001) modified by the addition of 5 mM glutamate as a major nitrogen source and acetate (20, 40, 60, or 80 mM), propionate (20 or 40 mM), or butyrate (20, 40, 60, or 80 mM) as a major carbon source. Unless otherwise indicated, the pH of these media was adjusted to 7 prior to sterilization. Cultures were incubated at room temperature (30 ± 2°C) in low light (3,000 lux), unless otherwise indicated. All experiments were carried out in 50 ml vial bottles. Anaerobic conditions were established by flushing the sealed vials with argon gas. Samples were taken every 6 h to determine total biogas (ml), H_2 content (ppm), volatile fatty acid residues (g l^{-1}), DCW (g l^{-1}) and pH.

5.6 Optimization of *Rps. palustris* TN1 hydrogen production using volatile fatty acids (VFAs) as electron donors by statistical methodology

5.6.1 Experimental design

The ranges of the VFAs used in this study, 0-80 mM acetate, 0-40 mM propionate and 0-80 M butyrate, were based on concentrations of these VFAs generated from anaerobic-dark fermentative treatments of palm oil milling wastewaters using *Thermoanaerobacterium thermosaccharolyticum* PSU-2 (O-Thong *et al*., 2008) A central composite design (CCD) (Box *et al*., 1978) was used to determine the optimum concentrations of mixtures of the VFAs for maximum hydrogen production and minimum PHA production, and for minimum hydrogen production and maximum PHA production. Experiments were performed in 50 ml serum bottles containing a 40 ml working volume with 10% (v/v) inoculums. Unless otherwise indicated, anaerobic conditions were established by flushing the sealed vials with argon gas. The vials were incubated at room temperature (30 ± 2°C) under light (3,000 lux) conditions.

5.6.2 Response Surface Methodology (RSM)

RSM uses a collection of statistical tools and techniques for constructing and exploring an approximate functional relationship between a response variable and set of design variables (Xu *et al*.,, 2008). The basic strategy of RSM has four principles (i) to move variables and responses into the optimum region, (ii) to examine the variables behavior of the response in the optimum region, (iii) to estimate optimum conditions, and (iv) to subject the model to experimental verification (Xu *et al*.,, 2008).

The variable levels *Xi* were designated. as χ_i according to the following equation such that *Xo* corresponded to central values:

$$\chi_i = \frac{Xi - Xo}{\Delta Xi}, \; i = 1, 2, 3, ..., \; k \quad ..... \quad (4)$$

where χ_i denotes the code value of the i^{th} test variable, *Xi* is a value of the i^{th} test variable, *Xo* is the value of *Xi* at the center point of the experiment, and *ΔXi* is the step change value.

Central composite design (CCD) is one type of RSM. It is particularly useful in identifying the important parameters and interactions between two or more

parameters, involving relatively few experiments compared to conventional methods. The number of experiments can be reduced by using only part of the CCD without losing the information about the main effects (Luengo *et al*., 2003; He *et al*., 2004).

In order to describe the effects of VFAs (acetate, propionate, butyrate) on hydrogen production in batch culture, 20 batch experiments were conducted by 2^n CCD (2^3 = 8 factor points) plus 2n (2 x 3 = 6: axial points, with $\alpha = \sqrt{3}$) and six replicates at the center points (n_0 = 6). The concentration ranges of acetate (X_1), propionate (X_2), butyrate (X_3) were 0-80 mM (central value = 40 mM), 0-40 mM (central value = 20 mM), and 0-80 mM (central value = 40 mM), respectively. The concentrations used in each experiment were designed by Eq. 4 .

The experimental design for X_1 (acetate), X_2 (propionate), and X_3 (butyrate) are described in Table 10. Stepwise regression analysis was carried out by generating the second order model as follows (Eq. 5):

$$Y = \beta_0 + \beta_1 X_1 + \beta_2 X_2 + \beta_3 X_3 + \beta_{11} X_1^2 + \beta_{22} X_2^2 + \beta_{33} X_3^3 + \beta_{12} X_1 X_2 + \beta_{13} X_1 X_3 + \beta_{23} X_2 X_3 \quad \text{..... .....(5)}$$

where Y is the expected response value predicted from RSM, and β_i, β_j and β_{ij} are the parameters estimated from regression results. Design expert software version 7.0 (Stat-Ease. Inc., MN, USA) was used for regression and graphical analysis of the experimental data.

Table 10. Levels of factors used for optimization of hydrogen production.

Variable	Label	Level		
		Low (-1)	Medium (0)	High (1)
X_1	Acetate (mM)	0	40	80
X_2	Propionate (mM)	0	20	40
X_3	Butyrate (mM)	0	40	80

5.6.3 Model validation and confirmation

The optimum conditions predicted using the RSM were tested experimentally to confirm the model. The experiment was performed in a 3-l fermentor. The samples were taken every 12 h to determine OD660, pH, H_2 content,

and VFA and PHA as described previously (section 4.1, 4.2, 4.3, and 4.12). The percentage of deviation between the predicted and experimental values was determined.

5.7 Optimization of medium compositions and environmental conditions for hydrogen production by statistical methodology

5.7.1 Plackett-Burmann design (PBD) for screening of the importance of medium components and growth conditions

PBD is a screening design which considerably diminishes the number of experiments necessary for, and gives as much as possible information for the evaluation the target factors. Using PBD, those factors that significantly positively affect the response are identified, and can then be investigated further for optimization; factors with less significant effects or with high negative effects on the response value may be omitted from further experiments (Plackett and Burman, 1944). PDB is usually used as the first step in RSM to screen the most important variables. In this study, PBD was used to screen for important medium components with respect to their individual effects, but not interactive effects between them (Plackett and Burman, 1944). This design is particularly useful when the investigator is confronted with a large number of variables, and is uncertain as to which values are likely to produce optimal or near optimum responses (Strobel and Sullivan, 1999). PBD comprises one type of a two-level screening design. The different variables were studied in two levels (Table 7); a negative sign (-) indicates a low level and a positive sign (+) indicates high level (Plackett and Burman, 1944). Plackett–Burman experimental design is based on the first order model:

$$Y = \beta_0 + \sum \beta_i x_i \qquad (6)$$

where Y is the response, β_0 is the model intercept and β_i is the linear coefficient and x_i is the level of the independent. The maximum number of variables that can be evaluated in this design is equal to the total number of experiments minus one.

The variables were chosen based on literature pertaining to PNSB hydrogen production. Nitrogen and mineral sources, other nutritional components, and environmental conditions, were investigated by PBD in order to then optimize

those among them that were found significant for maximum hydrogen production and minimal PHA production by *Rps*. *palustris* TN1. A total of 9 growth factors were tested: glutamate (A), yeast extract (B), $NaHCO_3$ (C), $FeSO_4.7H_20$ (D), $NaMoO_4.2H_20$ (E), EDTA-2Na (F), initial pH (G), light intensity (H), and initial cell concentration (J). The medium components and test levels for the PBD experiments are described in Table 11. A set of 12 experiments, nine assigned variables and three unassigned variables, commonly referred as dummy variables, were designed using the Design Expert 7 software (Stat-Ease Corporation, USA). The hydrogen production response was determined by *t*-values analysis.. The significant variables, which were those having 95% significance level in the screening experiments, were further optimized by using CCD.

The experiments were performed in duplicate in 50 ml serum bottles containing a 40 ml working volume of the previously optimized mixture of the volatile fatty acids acetate, butyrate, and propionate (section 5.6) and with 10% (v/v) inoculums, over the course of 96 h.

5.7.2 Optimization by CCD of factors that significantly affect hydrogen production

Using CCD, the significant variables identified from the screening experiments (PDB) were optimized for maximum hydrogen production and minimum PHA production (section 5.6) by the Design Expert 7 software (Stat-Ease Corporation, USA). The experiments were performed in duplicate in 50 ml serum bottles containing a 40 ml working volume of previously optimized mixture of the volatile fatty acids acetate, butyrate, and propionate (section 5.6), unless otherwise indicated. A 10% (v/v) starter culture was used as inoculum. Samples were taken every 12 h to determine OD660, pH, H_2 content, and VFA and PHA as described previously (section 4.1, 4.2, 4.3, and 4.12).

Table 11. Medium components and environmental conditions with test levels for Plackett-Burman experiment.

Components	unit	Levels	
		low (-)	high (+)
glutamate (A)	mM	5	15
yeast extract (B)	g l^{-1}	1	3
$NaHCO_3$ (C)	g l^{-1}	0	1.5
$FeSO_4.7H_20$ (D)	g l^{-1}	1	3.2
$NaMoO_4.2H_20$ (E)	g l^{-1}	0.5	1
EDTA-2Na (F)	g l^{-1}	2	5
initial pH (G)		6.5	7
light intensity (H)	lux	3000	5000
initial cell concentration (J)	g l^{-1}	1.2	0.8

5.7.3 Model validation and confirmation

The optimum conditions predicted using the RSM were tested experimentally to confirm the model. The experiments were performed in a 3-l fermentor with the significant variables identified by PBD. Samples were taken every 12 h to determine OD660, pH, H_2 content, and VFA and PHA as described previously. The percentage of deviation between the predicted and experimental values was determined.

5.8 Hydrogen production by *Rps. palustris* TN1 using palm oil mill effluent (POME) as substrate

5.8.1 Characteristics of palm oil mill effluent

POME and anaerobically digested POME were obtained from J.K Industry Import and Export Co., Ltd. (Songkhla, Thailand) and Thaksin Palm Co., Ltd. (Suratthani, Thailand). The pH, biological oxygen demand (BOD), chemical oxygen demands (COD), and total nitrogen content (APHA, 1998) were determined for each sample. Volatile fatty acids (VFAs) were identified and quantitated in the

samples by GC as described in section 4.3. Sugar contents were analyzed as described in section 4.14.

5.8.2 Production of hydrogen from POME

A starter culture (10% v/v) was used to inoculate different dilutions of sterile POME in sealed 50 ml serum bottles that were made anaerobic (unless otherwise indicated) by flushing with argon. Cultivation was conducted under anaerobic-light condition (3,000 lux), pH 7.0 for 144 h. Samples were taken at appropriate time intervals to determine pH, OD_{660}, hydrogen production, and volatile fatty acid consumption.

5.9 Strain improvement for ALA production

5.9.1 Bacterial strains, plasmids, and growth conditions

The bacterial strains and plasmid used in this study are listed in Table 1 and 2. Unless otherwise indicated, *Rba. sphaeroides* strains were grown in Sistrom's succinic acid minimal medium A (Sistrom, 1960; Table 7) and *E. coli* were grown in Luria-Bertani (LB) medium or on LB agar (Bertani, 1951) at 37°C. For *Rba. sphaeroides*, aerobic-dark conditions were established by culturing in test tubes with shaking at 30°C. Semi-aerobic culturing of *Rba. sphaeroides* was performed in 250 ml flasks containing 100 ml of Sistrom's succinate minimal medium with antibiotics, as appropriate, that were placed in a Gyrotory® water bath shaker, set at the speed of 2.5 and temperature of 30°C. Anaerobic-light conditions were established by either completely filling screw-capped tubes and placing them in front of incandescent lights (approximately 625 Lux or 10 W $(m^2)^{-1}$) at 30°C or by sparging illuminated 100 ml liquid cultures with a mixture of 98% nitrogen and 2% carbon dioxide.

Media were supplemented with antibiotics as necessary for the maintenance of plasmids or selection of recombinant strains. For *Rba. sphaeroides*, final concentrations were 0.8 μg ml^{-1} of tetracycline (Tc), 50 μg ml^{-1} of Kn, and 50 μg ml^{-1} Sp and St (together). For *E. coli*, the final concentrations were 15 μg ml^{-1} of Tc, 50 μg ml^{-1} of Kn, 50 μg ml^{-1} of Sp and St (together), and 100 μg ml^{-1} of ampicillin. All antibiotics were of reagent-grade (Sigma-Aldrich Co.).

5.9.2 Conjugations and transformations

Mobilizations of plasmids into *Rba. sphaeroides* and *Rps. palustris*

were performed as previously described (Davis *et al*., 1988; Ditta *et al*., 1980; Figurski and Helinski, 1979). Transformations of *E. coli* were performed using $CaCl_2$-treated cells prepared according to standard procedures (Sambrook *et al*., 1989).

5.9.3 DNA manipulations and DNA sequence analysis

Chromosomal DNA was isolated from *Rba. sphaeroides* using the GenElute ™ Bacterial Genome DNA kit (Sigma-Aldrich Co.). Plasmid DNA isolation, restriction endonuclease treatment, and other enzymatic treatment of DNA fragments and plasmids were performed according to standard protocols (Sambrook *et al*., 1989) or manufacturers' instructions, with enzymes purchased from New England Biolabs, Inc. (Beverly, Mass). DNA was analyzed by standard electrophoretic techniques (Sambrook *et al*., 1989). Isolation of DNA from agarose was performed using the Zymoclean Gel DNA Recovery Kit (Zymo Research Co, USA).

DNA sequencing was performed offsite at Geneway Research (Hayward, USA). DNA sequences were analyzed by using the BLAST server at the National Center of Biotechnology Information (Bethesda, USA.) and the BLASTX program (Altschul *et al*., 1997).

5.9.4 DNA amplifications and oligonucleotide-directed mutagenesis

Purified genomic DNA was used as template in amplification reactions. In all cases, dimethyl sulfoxide was added at a final concentration of 5% to improve extensions using the high G+C *Rba. sphaeroides* DNA. PCR was performed using *Pfu* Turbo (Stratagene) in a Bio-Rad MyCycler (Hercules, USA). The Quikchange Site-Directed Mutagenesis Kit (Stratagene, La Jolla, USA) was used to carry out oligonucleotide-directed mutagenesis. The integrity of the relevant sequences was confirmed by DNA sequencing. Oligonucleotides were purchased from Integrated DNA Technologies, Inc. (Coralville, USA).

5.10 ALA production by the genetically engineered strain of *Rba. sphaeroides* SH5(pMS3) using POME as substrate

Starter cultures were prepared as described in Section 5.4. Cultivation was carried out in sterile POME with different dilution under anaerobic-light (3,000 lux) and aerobic dark (150 rpm) conditions at 30°C. This experiment was carried in

50 ml with 40 ml working volume. Samples were taken every 6 h during log phase then every 12 h for up to 48 h of cultivation to measure pH, OD_{660}, and extracellular ALA levels.

5.11 One-stage process of hydrogen and extracellular ALA production

5.11.1 Effect of ALA concentration on hydrogen production by *Rps. palustris* TN1

Starter cultures were prepared in modified GA medium under anaerobic-light (3,000 lux) incubation for 18-24 h and then used as a 10% (v/v) inoculum. Commercial ALA (0-2 mM) was used in this study. Samples were taken every 6 h for up to 48 h cultivation to measure pH, OD_{660}, dry cell weight, extracellular ALA levels, and hydrogen production**.**

5.11.2 Co-culturing the hydrogen production PNSB *Rps. palustris* TN1(pBBR1-MCS2) and the ALA production PNSB *Rba. sphaeroides* SH5(pMS3)

Rps. palustris TN1 (pBBR1-MCS2) and *Rba. sphaeroides* SH5(pMS3) (Table 1) were cultured individually and together in GA medium under anaerobic-light conditions. Samples were taken every 6 h up to 48 h cultivation to measure pH, OD_{660}, dry cell weight, extracellular ALA levels, and hydrogen production**.** Viable cell counts were performed using modified GA medium and serially diluted cultures.

CHAPTER 3

RESULTS AND DISCUSSION

Purple non-sulfur photosynthetic bacteria (PNSB) can produce hydrogen from metabolizing volatile fatty acids (VFAs) such as acetate via photo-fermentation (Fig. 3). Since VFAs are generated from the dark fermentations of many organically rich substrates by anaerobic bacteria, the hydrogen-generating capacity of PNSB could be exploited as a means to enhance microbial conversions of agro-waste such as palm oil milling effluent (POME) to useful products. These same bacteria can also synthesize 5-aminolevulinic acid (ALA), another product having wide-ranging uses. This metabolic capability further expands the economic potential of POME. Sections 1, 2 and 8 present results and discussions of studies directed towards the isolation or bioengineering of PNSB that demonstrate that potential. The results and discussions of studies that define optimum parameters for hydrogen production by PNSB identified in this work are presented in sections 3-6. In sections 7 and 9 results and discussions of studies of hydrogen and ALA production from POME by the PNSB are presented. The results and discussions pertaining to the development of a novel cost-saving bioassay for extracellular ALA detection are presented in section 10. Finally, the results and discussions of an investigation of the co-culturability of the hydrogen and ALA-producing PNSB in POME are presented in section 11.

1. Isolation of H_2-producing purple non-sulfur photosynthetic bacteria, and initial investigations of their productivity using the volatile fatty acid (VFA) acetate as substrate

1.1 Assembling a collection of high hydrogen-producing PNSB

An assessment of the acetate-based hydrogen-producing capacities of PNSB strains from the collection of the Environmental Biotechnology Laboratory (Faculty of Agro-Industry, Prince of Songkla University, Thailand) revealed that all had capacities that were low (6.6-16 ml l^{-1} d^{-1}). With the goal of obtaining new

natural isolates that have higher capacities and are well-suited to conditions that would prevail in an applied situation in which the PNSB would be used for generating hydrogen from VFAs, modified GA medium that contains 20 mM sodium acetate as a major carbon source was used to enrich for PNSB from 34 individual samples of Songkhla Lake waters and lake bed sediments. Among the independent PNSB isolates obtained from these samples, 19 could produce hydrogen with a range of 4-326 ml l^{-1} d^{-1} (Table 12). The top six hydrogen-producing isolates, designated SL2, SL3, SL8, SL15, SL24, and TN1 had production rates of 326, 305, 308, 157 and 301 ml l^{-1} d^{-1}, respectively, with hydrogen yields of 543, 564, 424, 209, and 456 ml g DCW^{-1}, respectively. Cultures of isolate SL8 were not consistent with respect to hydrogen production, and so this isolate was not examined further. The remaining five were studied in more detail.

1.2 Growth, acetate consumption, and hydrogen production of high-hydrogen producing PNSB isolates

To be useful in a two-stage biohydrogen production process in which the first stage would be an anaerobic-fermentative biotreatment of POME, the PNSB should grow well in low light and in media with acetate, and hydrogen production should be dependent upon acetate availability. The top five hydrogen producers isolated from the Songkhla Lake environ were evaluated with respect to these parameters (Table 13 and Fig. 15). Measurements were performed on triplicate cultures of each isolate over the entire duration of logarithmic growth, a period of 72 hours.

The specific growth rates of the five high-hydrogen producers varied. The lowest rate was 0.0269 h^{-1} for the isolate SL15 and the highest rate was 0.0475 h^{-1} for the isolate SL24. For all of the high-hydrogen producers, acetate was depleted within 48 h (Fig. 15) with a concomitant accumulation of hydrogen. H_2 yield or efficiency of H_2 production can be employed to evaluate the H_2 production potential of substrate (Koku *et al*., 2002). The efficiency of hydrogen production from acetate among the natural isolates was determined by comparing the theoretical yield to the measured amount of hydrogen produced by these isolates (Table 13). Isolate TN1 had a hydrogen production efficiency of 46.31%, which was the highest of the five. The

corresponding light conversion efficiencies calculated from the amount of hydrogen produced during 72 hours ranged from <0.01-1.07% (Table 13). It was found that, while isolate SL24 had the highest specific growth rate, it also had the lowest hydrogen production efficiency from acetate. By contrast, isolate TN1 had a relatively high specific growth rate (0.0328 h^{-1}) and also the highest production efficiency (46.31%).

Table 12. Hydrogen production by new PNSB isolates in 20 mM sodium acetate under anaerobic-light conditions (3,000 lux) at 30°C.

Strain	Color	DCW ($g\ l^{-1}$)	Total biogas ($ml\ l^{-1}\ d^{-1}$)	Total H_2 ($ml\ l^{-1}\ d^{-1}$)	% H_2 content	$Y_{p/x}$ ($ml\ H_2\ g\ DCW^{-1}$)
SL1	Red-pink	0.78	24	22	91.67	14.10
SL2	Red-pink	0.30	350	326	93.14	543.33
SL3	Pink	0.27	337	305	90.50	564.81
SL6	Pink	0.30	22	20	90.91	33.33
SL7	Pink	0.28	22	19	86.36	33.33
SL8	Orange-pink	0.28	183	167	91.26	303.64
SL10	Red-pink	0.24	131	96	73.28	200.00
SL14	Orange-pink	0.67	38	28	73.68	20.90
SL15	Pink	0.24	215	208	96.74	424.49
SL19	Orange-pink	0.52	104	92	88.46	88.46
SL21	Red-pink	0.78	22	4	18.18	2.56
SL24	Orange-pink	0.27	190	157	82.63	290.74
TN1	Orange-pink	0.33	341	301	90.27	456.06
TN3	Orange-pink	0.81	38	36	94.74	22.22
TN4	Orange-pink	0.74	30	20	66.67	13.51
TN5	Red	0.57	131	96	73.28	84.21
TN6	Red	0.82	22	20	90.91	12.20
TN7	Brown	0.74	36	34	94.44	22.97
TN8	Brown	0.87	23	20	86.96	11.49

Table 13. Growth and hydrogen production of the top five H_2-producing PNSB.

Strains	Specific growth rate (h^{-1})	H_2 yield (mol H_2 mol acetate^{-1})[a]	Efficiency of H_2 production (%)[a]	Light conversion efficiency (%)[a]	Final pH[a]
SL2	0.0300	1.37	34.17	0.63	8.06
SL3	0.0298	1.09	27.34	0.33	7.39
SL15	0.0269	0.56	13.91	0.10	9.22
SL24	0.0475	0.09	2.23	<0.01	9.48
TN1	0.0328	1.85	46.31	1.07	7.05

[a]Determined after 72 h of cultivation.

1.3 pH of the culture

It was found that there was a close correspondence between pH changes of the culture (Fig. 15) and hydrogen productivity (Table 13). Thus, the greatest pH change occurred in the cultures of isolates SL15 and SL24, which also had the lowest efficiencies of hydrogen production. The pH changed by less than 0.1 units in the culture of isolate TN1, which exhibited the highest efficiency of hydrogen production. Perhaps the lack of pH change observed for the TN1 culture reflects a particularly high capacity of this isolate to minimize pH change through the use of alternate electron sinks for reductants; in particular, poly-3-hydroxyalkanoates (PHAs) (Franchi *et al*., 2004; Fang *et al*., 2005). A negative impact of elevated pH on hydrogen production has been reported for various PNSB (Sasaki *et al*., 1987; Zabut *et al*., 2006). It may be that these high pHs are suboptimal for the hydrogen-producing nitrogenase (Ni *et al*., 2006).

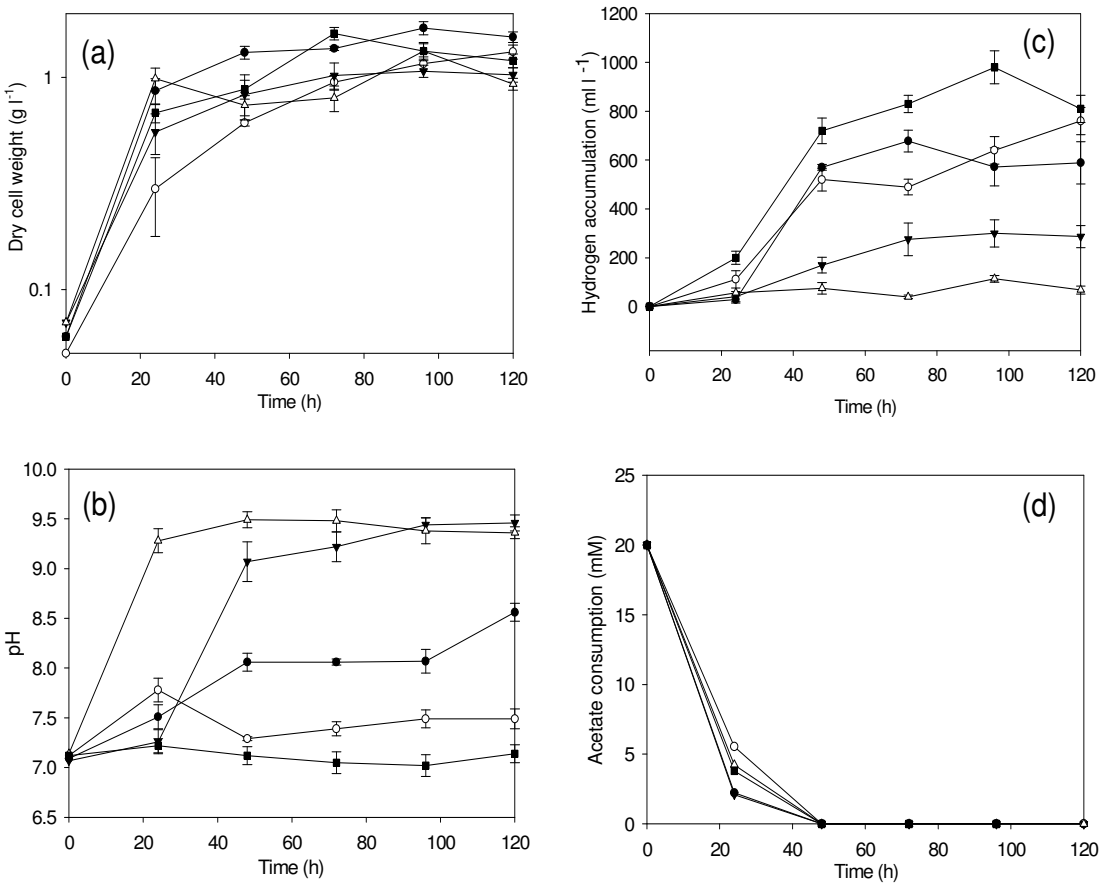

Figure 15. Time course of photohydrogen production by new natural isolates under anaerobic-low light conditions (3,000 lux) at 30°C. (a) Cell growth, (b) pH change, (c) hydrogen accumulation, and (d) acetate utilization. In each panel, symbols are ● SL2, ○ SL3, ▼ SL15, △ SL24, and ■ TN1.

1.4 Evaluation of the kinetics of hydrogen production by isolate TN1

Among the five high-hydrogen producers, the yield of hydrogen was the greatest for isolate TN1, which generated the most hydrogen per mol of acetate in the medium (1.85 mol H_2 mol acetate^{-1}), and so also had the highest light conversion efficiency. In order to further investigate its suitability for producing hydrogen from anaerobically treated POME, the kinetics of hydrogen production by isolate TN1 were evaluated using a modified Gompertz equation (Miyake and Kawamura, 1987; Mu *et al*., 2006; He *et al*., 2005), as described in Eq. (2). Isolate TN1 was again cultured in triplicate under anaerobic-light (3,000 lux) conditions in modified GA medium and

measurements of growth, acetate utilization, hydrogen production, and pH were taken every 6 hours over the course of 2 days. The inverse correlation between the amount of acetate available and the amount of hydrogen produced was observed again, as was a lack of change in pH of the cultures, which remained at pH 7.0 throughout. As shown in Fig. 16 by the solid line, there was a good fit of the hydrogen production data to the modified Gompertz equation, with a coefficient of determination value, R^2, of 0.995. The R_{max} value defined by the equation was 43 ml l^{-1} h^{-1}. It was also found that hydrogen production began during exponential phase. The short lag phase for cell growth could probably be attributed to the fact that pre-cultured inoculums in mid-exponential phase (18-24 h), prepared as described in Chapter 2 section 4, had been used. Pertinent reports in the literature are consistent with the idea that the age of inoculums culture is critical for the initiation of hydrogen production. The best hydrogen production was observed when the inoculums at mid-exponential phase were used (Koku *et al*., 2003).

1.5 Performance assessment of photohydrogen production from acetate by isolate TN1

Based on these analyses, the PNSB TN1 possesses the following attributes with respect to photohydrogen production from acetate:

- TN1 produces high amounts of hydrogen from acetate with an efficiency of 46.31%. A recent survey of the ability to use cultures to generate hydrogen for electricity found the best rate for photo-fermentation among PNSB was 0.16 mmol l^{-1} h^{-1} (Levin *et al*., 2007). TN1 compares favorably with a rate of 1.73 mmol l^{-1} h^{-1} (converted from the R_{max} value using a factor of 24.8 ml $mmol^{-1}$ at 30^{o}C and 1 atm pressure (Levin *et al*., 2007)).
- The pH of the isolate TN1 culture remains near neutral, which is desirable in terms of environmental impact and downstream applications.
- When cultured in modified GA medium (20 mM acetate), there was no detectable CO_2 in the biogas when all of the acetate had been utilized (results not shown). Therefore the hydrogen content of the biogas is very high. This could simplify the downstream purification step to obtain hydrogen suitable for fuel cell use in generating electricity (Manish and Banerjee, 2008).

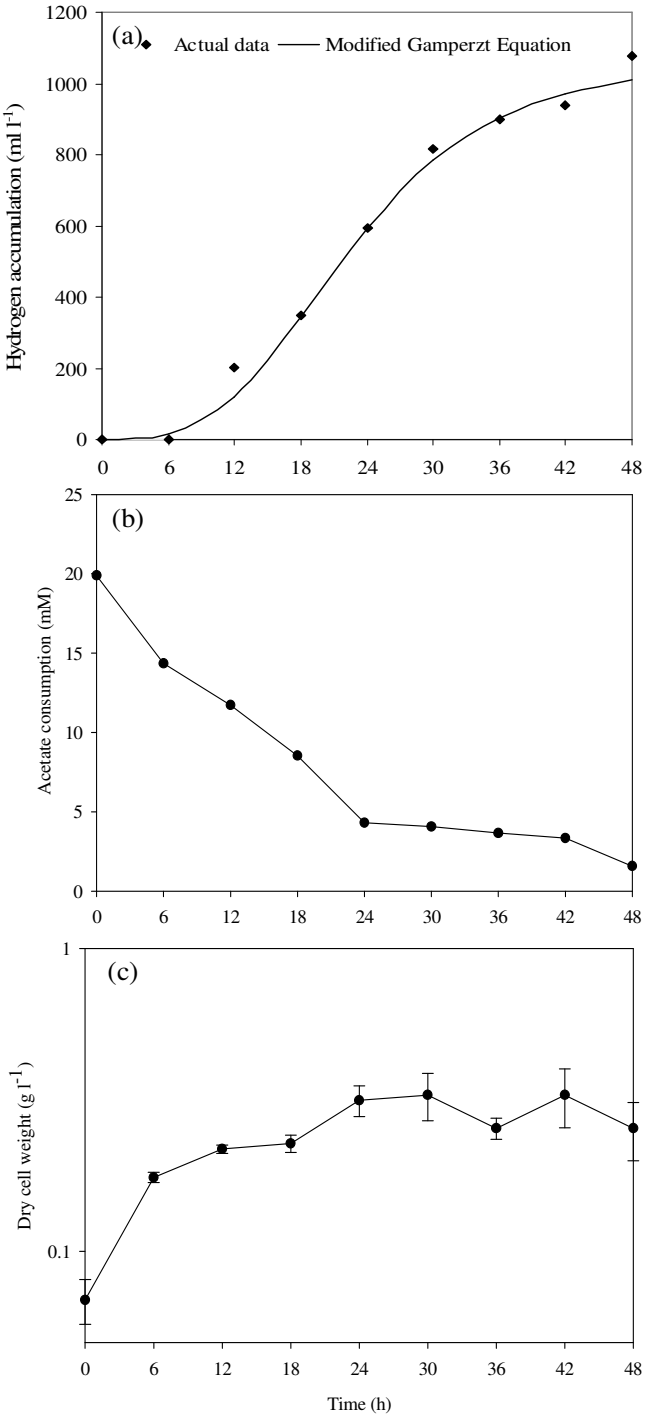

Figure 16. Evualuation of the kinetics of hydrogen production by TN1. (a) Hydrogen accumulation data fitted to the modified Gompertz equation, (b) acetate consumption, and (c) dry cell weight for triplicate cultures of the isolate TN1 cultivated for 48 h in modified GA medium under anaerobic-light conditions (3000 lux).

2. Taxonomic determination of the PNSB isolate TN1

The PNSB TN1 is a motile, Gram negative rod, 0.5 μm wide and 2.2 μm long, and it multiplies by budding. The internal photosynthetic membranes appear to be arranged in parallel lamellae and there are visual inclusions in cells that likely contain the intracellular storage material polyhydroxyalkanoate, PHA (Fig. 17). After growing under anaerobic-photoheterotrophic conditions for 24 h, the cell suspension was red and the absorption spectra of a crude cell lysate had maxima of bacteriochlorophyll *a* (380, 477, 504, 591, 807, and 866) (Imhoff and Trüper, 1989). The spectral profile of the TN1 sample is compared to a sample prepared from *Rhodopseudomonas* (*Rps.*) *palustris* strain CGA009 in Fig. 18. All of these properties identified the isolate TN1 as *Rps.* sp. (Imhoff and Trüper, 1989). Isolate TN1 assimilates organic compounds containing thiosulfate or sulfide in a basal medium with $(NH_4)_2SO_4$ as a nitrogen source under anaerobic-light conditions (Table 14). None of the vitamins in the basal medium were necessary for growth. Under photoheterotrophic conditions, isolate TN1 consumed acetate, propionate, butyrate, valerate, lactate, malate, tartrate, succinate, citrate, glutamate, benzoate, glucose, fructose, manitol, sorbitol and glycerol. Thiosulfate was used as an electron donor under photoautotrophic conditions. These results indicated that isolate TN1 was most closely allied to *Rps. palustris* although *Rps. palustris* has not been shown to utilize tartrate under anaerobic-light conditions (Imhoff and Trüper, 1989).

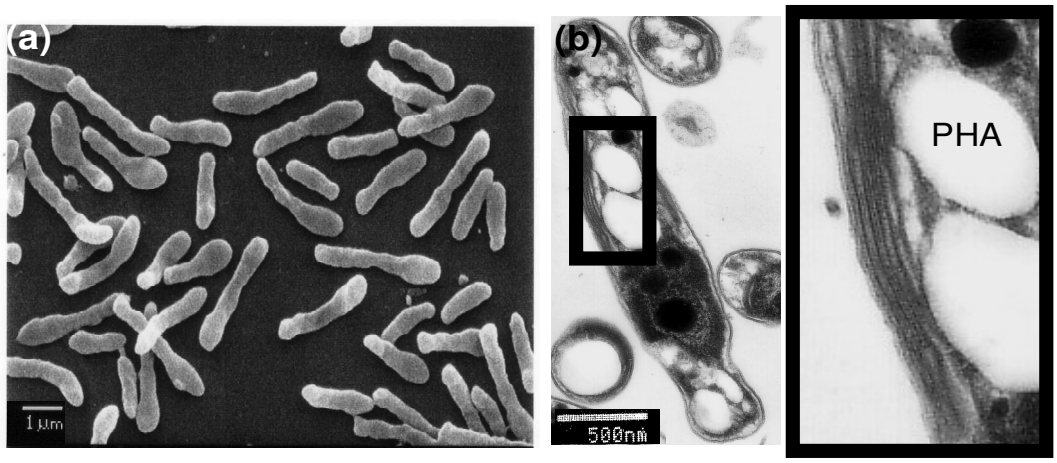

Figure 17. Electron micrographs of TN1. (a) Scanning electron micrograph (10,000 X magnification), (b) transmission electron micrograph (15,000 X magnification) with enlargement to show the lamellar arrangement of the cytoplasmic membrane and PHA inclusions.

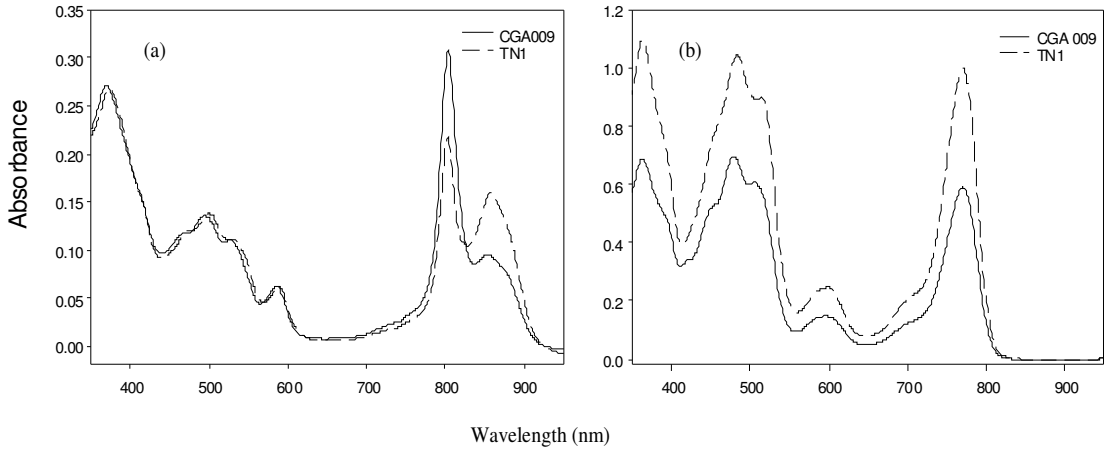

Figure 18. Spectral analyses of crude lysates prepared from *Rps. palustris* strain CGA009 (kindly provided by C. Harwood, University of Washington, USA) and isolate TN1. The spectra are scans of (a) equivalent amounts (total protein) of crude membrane preparations and (b) pigments extracted from equivalent numbers of cells.

2.1 16S rRNA determination of TN1

DNA sequence analysis of the genes coding for the 16S RNA of ribosomes has become an important tool in bacterial identification (Rossello-Mora

and Amann, 2001). The DNA sequence of the 16S rRNA gene of isolate TN1 was determined and submitted to NCBI (Gen Bank accession number GU723303) for searching the closest matches using the BLAST tool (Zhang *et al*., 2000).The sequence was most similar (99%) to *Rps. palustris*. A phylogenetic analysis of the 16S rDNA sequence of TN1 (Fig. 19) also indicated that TN1 is a newly isolated strain of *Rps. palustris.*

2.2 Characteristics of TN1, a new natural isolate of *Rps. palustris*

Based on morphological, biochemical, and 16S rRNA analyses, TN1 is a natural isolate of *Rps. palustris.* Distinctive characteristics of this strain include the following:

1. Absorption peaks of the protein-pigment complexes of the photosynthetic apparatus are different from *Rps. palustris* wild type strain CGA009 (Fig. 18a).
2. TN1 can use tartrate, and has no vitamin requirement (Table 14).
3. TN1 has a high hydrogen-generating capacity from acetate.
4. Cultures of TN1 maintain a constant pH.
5. TN1 cultures possess an unusual fluorescence.
6. TN1 appears to have substantial PHA formation capacity.

As is true of other strains of *Rps. palustris*, it is likely that the newly identified strain TN1 has the capacity to degrade aromatic organic compounds. It would be interesting to examine this metabolic possibility in future.

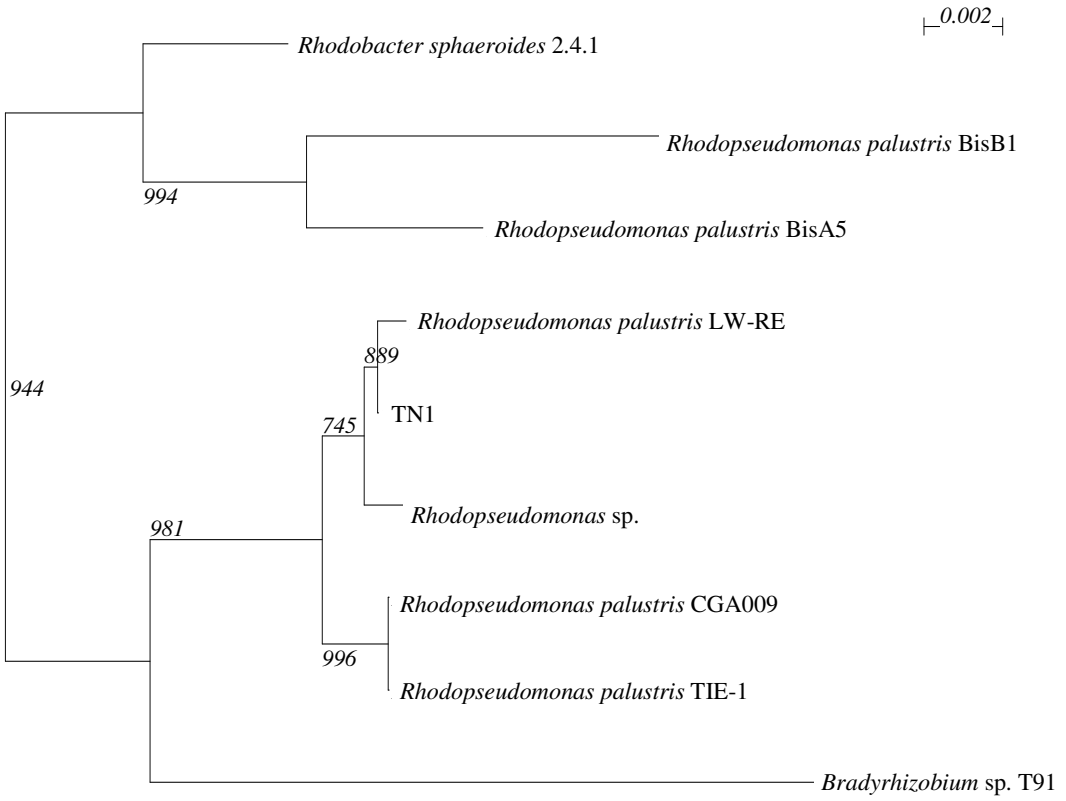

Figure 19. Phylogenetic relationship of strain TN1 to previously described strains of *Rps. palustris*, to *Rhodobacter sphaeroides* 2.4.1, and to *Bradyrhizobium* sp. T91, based on partial 16S rRNA gene sequences.

Table 14. Taxonomical and biochemical characteristics of isolated TN1 and *Rps. palustris* ATCC17001^T used in Bergey's manual (Imhoff and Trüper, 1989).

Characteristics	Results	
	TN1	*Rhodopsuedomanas palustris* ATCC17001^T
1. Growth form	Photoheterotroph Chemoheterotroph	Photoheterotroph Chemoheterotroph
2. Growth on sulfide and thiosulfate		
- Sulfide	+	+
- Thiosulfate	+	+
3. Gram stain	negative	negative
4. Cell shape	Rod	Rod
5. Cell size (μm)	0.5x 2.5 μm	0.6-0.9 x 1.2-2.0 μm
6. Motility	+	+
7. Gelatin degradation	-	-
8. Vitamin requirement	no	*p*-aminobenzoate and biotin
9. Electron donor		
- Acetate, propionate, lactate, malate, succinate, butyrate, valerate, glutamate, benzoate, glycerol, sorbitol	+	+
- Tartrate	+	-
- Citrate, glucose, fructose, mannitol	+	±
10. Bacteriochlorophyll	*a*	*a*

3. Effect of types and concentrations of volatile fatty acid on H_2 production

Following a first stage of biohydrogen production from POME by *Thermobacterium (T.) thermosaccharolyticum* PSU-2 under dark fermentation conditions, acetate, propionate and butyrate are the predominant VFAs with concentration ranges of 0 to 70 mM (O-Thong *et al*., 2008). The present investigation examined the H_2 production by *Rps. palustris* TN1 using different types and concentrations of VFAs. Results are summarized in Table 15, together with the initial and final pHs of the cultures. The best fits of the hydrogen accumulation to a modified Gompertz equation are illustrated in Fig. 20. Using acetate, propionate and butyrate as a carbon source, the values for the maximum rate of H_2 production (R_{max}), the maximum H_2 production (H_{max}) and lag time (λ) are listed in Table 16.

Among these results, the following points are considered to be most significant with respect to the use of *Rps. palustris* TN1 for biohydrogen production from the effluent of anaerobically treated POME. The maximum hydrogen yields were observed with 20 mM butyrate, acetate, and propionate with the values of 4.7, 2.5 and 1.7 mol H_2 mol substrate^{-1}, respectively. However, the maximum rate of hydrogen production (R_{max}) was observed in the order acetate, butyrate and propionate (38.3, 22.7 and 16.0 ml l^{-1} h^{-1}, respectively), corresponding to hydrogen production efficiencies of 61.9, 47.3 and 23.8%, respectively. This indicates that acetate had the highest H_2 production potential among the three VFAs. The maximum hydrogen production (H_{max}) was observed for the culture with 40 mM acetate (2,107 ml l^{-1}), followed by cultures with 20 mM butyrate (1,778 ml l^{-1}) and 20 mM propionate (608 ml l^{-1}), respectively. The same order was observed for the light conversion efficiencies; 2.0, 1.8 and 0.2%, respectively.

Among PNSB, the substrate ranges are strain specific (Tao *et al*., 2008) and the biochemical pathways of carbon metabolism are as yet uncertain for many of these bacteria. However, it is well-established that the PSNB derive reductant from VFAs and capture energy from light for cell growth and biosynthetic products. Further, hydrogen production involves photo-fermentation as described in section 2.4.1.2 of Chapter 1.

Table 15. Hydrogen production by *Rps. palustris* TN1 from individual VFAs.

Volatile fatty acid (VFA)	Concentration (mM)	Initial pH	Final pH[a]	Specific growth rate ($h^{-1} \times 10^{-3}$)	VFA depletion Consumption (%)[a]	H_2 Yield (mol H_2 mol VFA^{-1})[a]	Efficiency (of H_2 production; (%)[a,]	Light conversion efficiency; (%)[a]
Acetate	20	7.0	7.0	6.28	100	2.5	61.9	1.0
	40	7.0	7.0	6.13	100	1.8	45.5	2.0
	60	6.9	7.5	10.3	87	1.1	27.7	1.3
	80	7.0	7.5	8.08	50	1.0	6.9	1.4
Propionate	20	7.2	7.3	6.13	85	1.7	23.8	0.2
	40	7.2	7.4	1.0	85	0.8	10.8	0.2
Butyrate	20	7.1	6.9	6.16	100	4.7	47.3	1.8
	40	7.0	6.8	6.12	79	1.4	35.8	0.6
	60	7.0	6.8	10.7	53	1.1	10.6	0.5
	80	7.0	6.7	14.0	46	1.0	11.2	0.6

[a]Determined at the end of the cultivation period. In all cases, the measurements used to determine specific growth rates, H_2 yield, efficiency of hydrogen production, and light efficiencies varied by less than 10%.

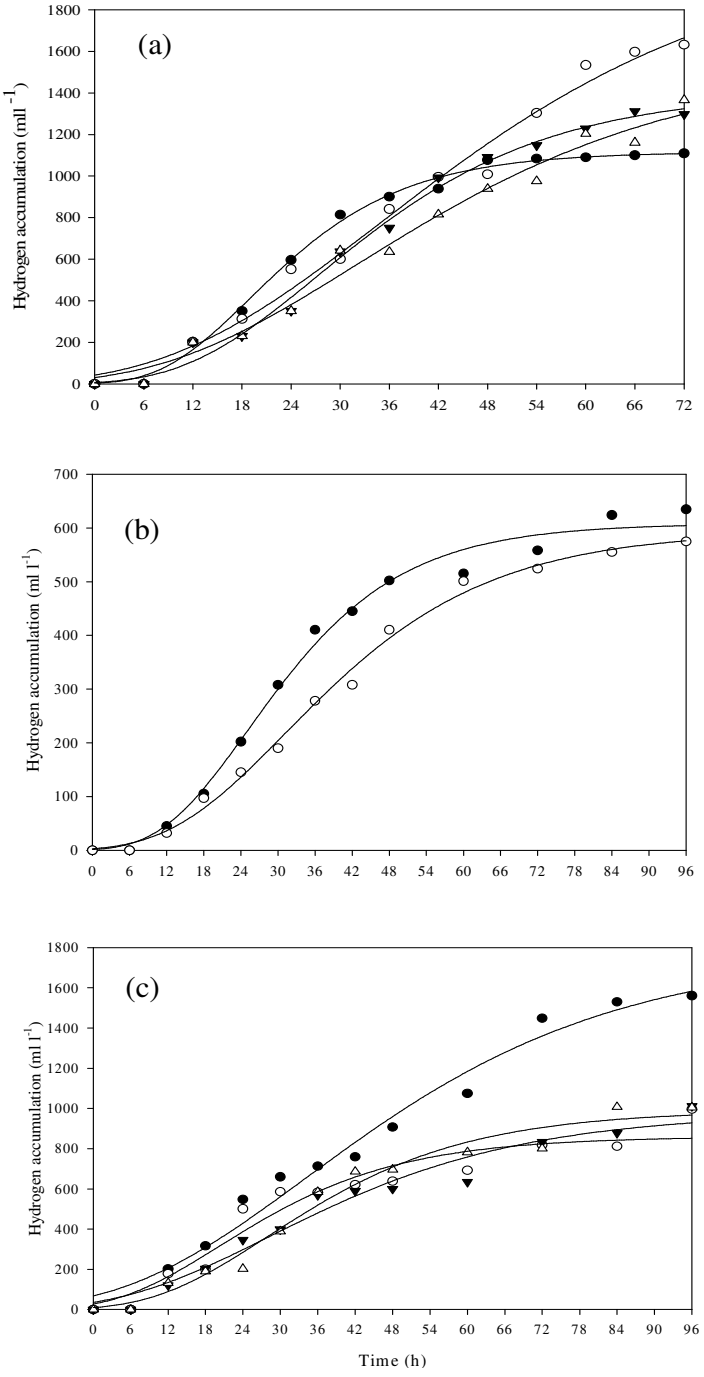

Figure 20. Hydrogen accumulation data for *Rps. palustris* TN1 fitted to a modified Gompertz equation generated from cultures with (a) acetate, (b) propionate, and (c) butyrate. In each panel, symbols are ♦ 20 mM, ◊ 40 mM, ▼ 60 mM, and △ 80 mM concentrations of the respective VFAs.

Table 16. Evaluation of the kinetics of hydrogen production by *Rps. palustris* TN1 from individual volatile fatty acids[a].

Volatile fatty acid	Concentration (mM)	λ (h)	R_{max} (ml l^{-1} h^{-1})	H_{max} (ml l^{-1})	R^2
Acetate	20	8	38.3	1,116	0.996
	40	9	30.2	2,107	0.987
	60	11	32.2	1,408	0.993
	80	9	24.5	1,556	0.983
Propionate	20	11	16	608	0.992
	40	13	11.7	595	0.996
Butyrate	20	5	22.7	1,778	0.989
	40	4	19.3	860	0.941
	60	5	15.4	981	0.978
	80	10	20.0	990	0.986

[a]All assays were performed in triplicate; values varied less than 10%. H_{max} (maxiumum H_2 production), R_{max} (maximum rate of H_2 production) and λ (lag time) and R^2 (goodness of fit) values were determined by best-fitting the cumulative H_2 production data to a modified Gompertz equation (Eq. 2).

The useful ranges of VFA concentrations for hydrogen production from *Rps. palustris* TN1 were 20-40 mM acetate, 20 mM butyrate and <20 mM propionate (Table 15). High levels of VFAs are reported to inhibit hydrogen production by PNSB (Stewart, 1975, Zheng and Yu, 2005; Shi and Yu, 2006), and Fang *et al*. (2005) reported hydrogen yields by PNSB decreased with increasing acetate and butyrate concentrations. The data from the present study were consistent with those reports. Also in agreement with the data from the present study, Barbosa *et al*. (2001) found that *Rps.* sp. has a higher efficiency of H_2 production (72.8%) from acetate than from butyrate (8.4%). The efficiency of H_2 production decreased with increasing propionate concentrations from 20 mM (4.0%) to 40 mM (3.5%). Among the *Rhodopseudomonads*, a higher hydrogen yield has been reported for an undefined

species from 22 mM acetate; however, its rate of H_2 production, 25.2 ml l^{-1} h^{-1} (Barboso *et al*., 2001), is lower than that of TN1 (Table 3).

The effect of VFAs on cell growth was characterized in terms of specific growth rates. Rates of growth within the range typically reported for PNSB (Neidle and Kaplan, 1993) were measured for cultures in media with 20-60 mM acetate, 20 mM propionate, and 20-80 mM butyrate. However, the results indicate that concentrations higher than 60 mM acetate and 20 mM propionate are inhibitory for cell growth. They also indicate that butyrate is predominantly used for cell growth rather that hydrogen production (Table 15). These findings are similar to a former study of *Rps. faecalis* RLD, in which butyrate was used for cell growth while acetate was converted to hydrogen (Ren *et al*., 2008). However, Shi and Yu reported that another PNSB, *Rps.* [*sic.*] *capsulata*, used acetate and propionate for cell growth rather that for hydrogen production, while the organism used butyrate for hydrogen production rather that cell growth (Shi and Yu, 2006).

As indicated in Table 15, the size and direction of any change in pH of the cultures was substrate- and concentration-dependent. However, regardless of which substrate was provided, the size of the change in pH of the cultures correlated inversely with H_2 productivity; the smaller the change from pH 7.0, the greater the productivity. This observed relationship is consistent with reports of the optimum pH ranges for hydrogen production by nitrogenase activities in other PNSB. Thus, the optima reported for *Rps. acidophila* and *Rhodopila globiformi*s is 6.5-7 (Ormerod and Gest, 1962), while the optimum pH range for nitrogenase activity in *Rps. sulfidophilus* was reported by Ni *et al*. (2006) to be 6.5-7.5.

The final pHs of cultures containing acetate and propionate were in the range of 7-7.5. However, the final pHs of cultures containing butyrate were between 6.7 and 6.9. These more acidic pHs may come about through the generation of acetate as butyrate is consumed; (as shown in the following reaction) although the acetate can be used to produce hydrogen (Shi and Yu, 2006) these pHs might reduce the nitrogenase activity and so hydrogen production would also be lessened.

$$CH_3(CH_2)_2COOH + H_2O \rightarrow 2H_2 + 2CH_3COOH$$

4. Effect of light intensity and pH on H_2 production

Anaerobic-fermentative cultures of *T. thermosaccharolyticum* PSU-2 in POME are very opaque (O-Thong et al., 2008), so light penetration is very limited. Therefore, the ability of PNSB to capture photonic energy with high efficiency through the deployment of high numbers of light-harvesting complexes (Kaplan, 1978) is a distinctly positive attribute for their use in photo-hydrogen production from treated POME. The measurements of the light efficiencies of hydrogen production for TN1 reflect this capability; at light intensities that are lower (2,000 lux) or higher (4,000 lux) than the optimum level (3,000 lux), hydrogen production was no more than 10% lower than the maximum value. Even under very low light conditions (1,000 lux) as would be expected to exist in the treated POME, H_2 production remained as high as 70% of the maximum value (Fig. 21a).

Hydrogen production by *Rps. palustris* TN1 was maximal for media with initial pHs of 7.0 (Fig. 21b). The optimum initial pH of 7.0 was the same as that previously reported for another PNSB, *Rhodocyclus gelatinosus* R7 (Prasertsan *et al*., 1993). Hydrogen production by *Rhodobacter* (*Rba.*) *sphaeroides* O.U. 001 was optimal at pH 7.0 (Sasikala *et al*., 1991). Also Fang *et al*. (2005) reported that the optimum initial pH for hydrogen production by PNSB is in the range of 7.0-8.0 (Fang *et al*., 2005). Initial pHs at which hydrogen production was not observed for TN1 were in the range 5-5.5. Since a lower pH results in a lower production of ATP in the cell, it is expected that hydrogen production would be lower (Bowles and Ellefson, 1985). At alkaline pHs, hydrogen evolution from cultures of TN1 was slowed down drastically. Because the uptake hydrogenase functions optimally at high pH (Sasikala *et al*., 1991), an initial pH of 8.5-9.0 is expected to be unfavorable for H_2 production.

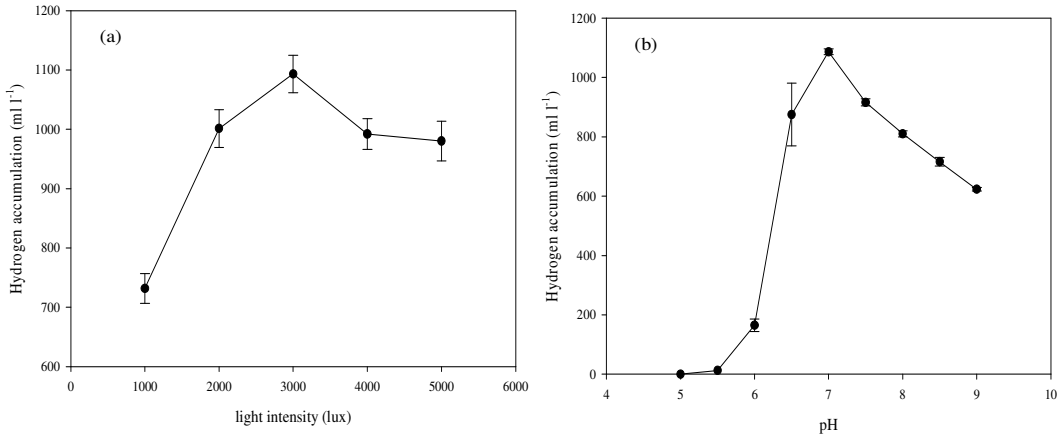

Figure 21. Effects of physical parameters on hydrogen accumulation from cultivation of *Rps. palustris* TN1. Parameters are (a) light intensities and (b) initial pHs.

5. Optimization of VFA composition for hydrogen and polyhydroxyalkanoate (PHA) production by *Rps. palustris* TN1 using response surface methodology (RSM)

In preceding sections of this thesis, the ability of PNSB to produce hydrogen and also accumulate PHA as intracellular storage material under photoheterotrophic conditions has been described. Based on the presumed metabolic capabilities deduced from the characterizations of *Rps. palustris* TN1 (section 2), both hydrogen and PHA production are possible for this organism. This section details the application of RSM to determine the optimum mixtures of the three predominant VFAs present following anaerobic-fermentative treatment of POME (O-Thong *et al*., 2008) for each of these two products. Both H_2 and PHA production take place under physiological conditions of excess energy and reducing power, or high carbon to nitrogen (C/N) ratios (Eroglu *et al*., 2004). H_2 and PHA both have commercial value; therefore, the conversion of VFA by the PNSB to each of these products was investigated in order to make feasible an assessment of the total economic impact of these bioprocesses. First, the optimum mixture of VFAs that would maximize hydrogen production and minimize PHA production was determined. Then the

optimum mixture of VFAs that would minimize hydrogen production and maximize PHA production was determined. Towards further defining the optimum conditions for hydrogen production, other studies were directed towards identifying additional nutritional and physical factors that play a role.

5.1 Central composite experimental design (CCD) to examine the relationships between VFAs and hydrogen and PHA production.

In optimization studies, a classical method is often used for experimental design, in which one factor is changed at a time while other factors are kept fixed. It is time consuming and incapable of reaching the true optimum, since this method ignores interactions that can exist among the variables (Shi and Yu, 2005). To avoid these problems, a 2^3-factorial central composite experimental design (CCD) with six axial points and six replications at the center point leading to a total number of twenty experiments was used to develop models that would (1) describe the optimum concentrations of the three predominant VFAs present in pre-treated POME, acetate, propionate, and butyrate, and their possible interactions such that hydrogen production is maximized and PHA production minimized and (2) describe the optimum concentrations of the three predominant VFAs present in pre-treated POME, acetate, propionate, and butyrate, and their possible interactions such that hydrogen production is minimized and PHA production maximized.

The experimental conditions and the hydrogen and PHA production levels for each of the trial experiments prescribed by the CCD are given in Table 17. The hydrogen production ranged from 485-1,323 ml l^{-1}, and the maximum value (1,323 ml l^{-1}) was obtained in trial experiments 15-20 that used intermediate concentrations of VFAs. Higher concentrations of VFAs had a negative effect on hydrogen production (for example, trial experiment 8).

In the absence of acetate, propionate and butyrate (trial experiment 1), hydrogen was still produced. Cell growth and hydrogen production were probably being sustained by the glutamate present in the medium. According to Fuji *et al*, (1987) one mole of glutamate can produce nine moles of hydrogen.

Table 17. The CCD for response surface analysis of the optimimum concentrations of VFAs used for H_2 and PHA production using response surface methodology.

Trial Experiment	(X_1) Acetate (mM)	(X_2) Propionate (mM)	(X_3) Butyrate (mM)	(Y_1) Hydrogen production (ml l^{-1})	(Y_2) PHB (g l^{-1})
1	0	0	0	730	0.05
2	80	0	0	1212	0.18
3	0	40	0	623	0.17
4	80	40	0	1145	0.18
5	0	0	80	745	0.12
6	80	0	80	485	0.14
7	0	40	80	508	0.13
8	80	40	80	232	0.12
9	0	20	40	1038	0.12
10	80	20	40	1073	0.17
11	40	0	40	1182	0.14
12	40	40	40	934	0.17
13	40	20	0	1316	0.19
14	40	20	80	901	0.16
15	40	20	40	1300	0.22
16	40	20	40	1250	0.23
17	40	20	40	1323	0.21
18	40	20	40	1289	0.22
19	40	20	40	1273	0.22
20	40	20	40	1300	0.23

For these same concentrations of VFAs, PHA production varied between 0.05 and 0.23 g l^{-1} (Table 17). The maximum PHA production levels (0.23 ml l^{-1}) were also measured in trial experiments 15-20, which had intermediate concentrations of the three VFAs. In contrast to hydrogen, very little PHA is produced in the absence of acetate, propionate and butyrate (trial experiment 1). Li and Fang (2008) similarly found that *Rubrivivax gelatinosus* L31 could not produce PHA using glutamate as a carbon source. This may be a consequence of the prevailing low C/N ratio, rather than a metabolic deficit, as PHA production is reported to improve in medium containing higher C/N ratios (Sangkharak and Prasertsan, 2007).

5.2 Modeling the effect of VFA concentrations on hydrogen and PHA production by regression equation and response surface analysis.

5.2.1 Modeling of the effect of VFA concentrations on hydrogen production

The useful features of RSM include (1) that it contains a satisfactory distribution of information across the experimental region, (2) that it provides a means to assess lack of fitness, (3) that the design is described by a minimum number of higher order terms, and (4) that there is good correlation between predicted outcomes and experimental tests (Jo *et al*., 2006). The hydrogen production data of the trial experiments in Table 17 were used to construct the RSM model. First the data were fitted to a regression equation using a least-squares method. All terms, regardless of their significance, were included in the following equation (Eq. 7).

$$Y_1 \text{ (ml l}^{-1}) = 609 + 18.29X_1 + 24.46X_2 + 10.19X_3 - 0.024X_1X_2 - 0.13X_1X_3 - 0.066X_2X_3 - 0.14X_1^2 - 0.61X_2^2 - 0.11X_3^2 \quad (7)$$

This quadratic polynomial equation was chosen to represent the hydrogen production. According to Eq. 7, hydrogen production (Y_1) is a function of acetate (X_1), propionate (X_2), and butyrate (X_3) concentrations. Further, propionate and butyrate concentrations have significant effects (P<0.0001) on hydrogen production,

while acetate concentration has a smaller but still significant effect (P<0.0006). An analysis of variance (ANOVA) was used to identify terms in this equation that were not statistically significant (P value less than 0.05) (Table 18).

The RSM model was then generated from the equation and the overall model was tested by ANOVA (Box and Behnken, 1960). Those values are presented in Table 19. Based on the Fischer's F-test having a low probability value (P<0.0001) the model is significant. The value of the regression-based coefficient of determination, R^2, was 0.995, and therefore the model explains 99.5% of the variability in hydrogen production with respect to the independent variables, leaving less than 1% of the total unexplained by the model. The value of the coefficient of variation (C.V.) was 3.34%, indicating a high reliability of the model. The lack of fit P-value was 0.17, which indicates that the model equation accurately predicts the hydrogen production for any value of the variables.

Table 18. Coefficient estimations and p-values of each term in equation 7.

Term	Hydrogen production	
	Coefficient estimate	Probability $(P)>F$
intercept	609	
X_1	18.29	0.0006 [a]
X_2	24.46	< 0.0001 [a]
X_3	10.19	< 0.0001 [a]
X_1X_2	-0.024	0.2803
X_1X_3	-0.13	< 0.0001 [a]
X_2X_3	-0.066	0.0049 [a]
X_1^2	-0.14	< 0.0001 [a]
X_2^2	-0.61	< 0.0001 [a]
X_3^2	-0.11	< 0.0001 [a]

[a] Statistically significant (P <0.05).

The contour plots and response surfaces based on Eq. 7, with one variable held constant at its optimum value and the other two variables at values within the range of the trial experiments, are shown in Fig. 22. Each plot has a distinct maximum, which suggests that the optimum value is within the CCD boundary. The shapes of the contour plots, which could be circular, elliptical, or saddle, are all eliptical, indicating that the interactions between each pair of variables are significant (Celik *et al*., 2004). These shapes also indicate that the concentration of each VFA alone significantly affects hydrogen production (Fig 22a-c).

The surfaces predict that a significant increase in hydrogen production could be achieved when the values of acetate propionate and butyrate are increased from from 40 to 60, 10 to 20, and 20 to 40 mM, reaching a maximum of 1,168-1,318 ml l^{-1} hydrogen production. Further increases in VFA concentrations are predicted to decrease hydrogen production, which could arise through substrate inhibition (Fang *et al*, 2005; Shi and Yu, 2005).

Table 19. ANOVA for response surface quadratic model of equation 7.

Statistic report	Value
P -value	
• model	0.0003[a]
• Lack of Fit	0.17
R^2	0.995
C.V.	3.34

[a]Statistically significant (P <0.05).

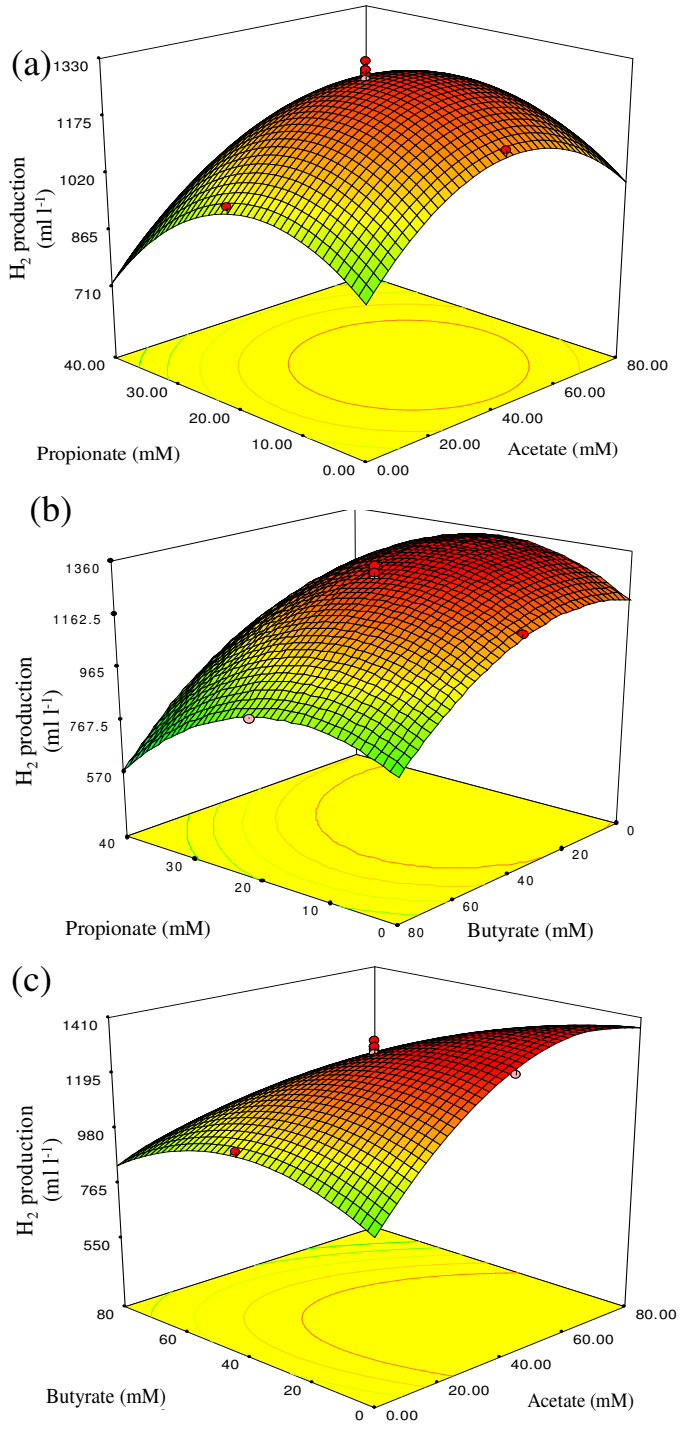

Figure 22. Response surfaces of hydrogen production by *Rps. palustris* TN1 as a function of acetate (mM), propionate (mM) and butyrate (mM) concentrations, based on the central composite experimental results.

5.2.2 Modeling of the effect of VFA concentrations on PHA production

The least squares method was also used to describe the response surface of PHA production using the productivity data from the trial experiments based on the CCD (Table 17). All terms were included in the following equation:

$$Y_2\ (\text{g l}^{-1}) = 1.37 + 0.0088X_1 + 0.014X_2 - 0.0062X_3 - (3.65 \times 10^{-6})X_1X_2 - (6.90 \times 10^{-5})X_2X_3 - (9.32 \times 10^{-5})X_2X_3 - (6.12 \times 10^{-5})X_1^2 - (2.39 \times 10^{-4})X_2^2 + (1.15 \times 10^{-4})X_3^2 \quad (8)$$

For PHA production, a quadratic model was also chosen to describe the response surface. As was found for hydrogen production, PHA production (Y_2) is apparently also a function of acetate (X_1), propionate (X_2), and butyrate (X_3) concentrations. An ANOVA was used to identify terms in this equation that were not statistically significant (P value less than 0.05) (Table 20).

Table 21 summarizes the values of the statistical parameters from an ANOVA test of the model generated from the equation. The value of R^2 was 0.89, and so 89% of variation for PHA production is attributable to the independent variables, while 11% of the total cannot be explained by the model. The C.V. value is 10.29%, indicating with respect to the model. The lack of fitness P-value is 0.17, which indicates that the model equation accurately predicts the PHA production for any value of the variables.

The contour plots and response surfaces for PHA production based on Eq. 8, holding one variable constant at its optimum value while the other two variables are changed over the range of the trial experiments, are shown in Fig. 23. The elliptical shape of the contour plot for varying concentrations of propionate and acetate at the optimum concentration of butyrate indicates that acetate and propionate have significant and interactive effects on PHA production (Fig 23a). The saddle shapes of the other two contour plots indicate that butyrate has no interactive influence (Fig 23b-c) However, each of the VFAs appear to have significant individual influences. This result agrees with that of Kemavongse *et al*. (2008), who

demonstrated that acetate and propionate induced the accumulation of poly-β-hydroxybutyrate-co-β-hydroxyvalerate (PHBV) in *Rba. sphaeroides* U7.

Table 20. Coefficient estimations and *p*-values of each term in equation 8.

Term	PHA production	
	Coefficient estimate	Probability *(P)>F*
intercept	1.37	
X_1	0.0088	0.003[a]
X_2	0.014	0.0244[a]
X_3	0.0062	0.0001[a]
$X_1 X_2$	3.65×10^{-6}	0.7980
$X_1 X_3$	6.90×10^{-5}	< 0.0001[a]
$X_2 X_3$	9.32×10^{-5}	< 0.0001[a]
X_1^2	6.12×10^{-5}	< 0.0001[a]
X_2^2	2.39×10^{-4}	< 0.0001[a]
X_3^2	1.15×10^{-4}	< 0.0001[a]

[a]Statistically significant (P <0.05).

Table 21. ANOVA for response surface quadratic model of equation 8.

Statistic report	Value
P -value	
• model	<0.0001[a]
• Lack of Fit	0.17
R^2	0.89
C.V.	10.29

[a]Statistically significant (P <0.05).

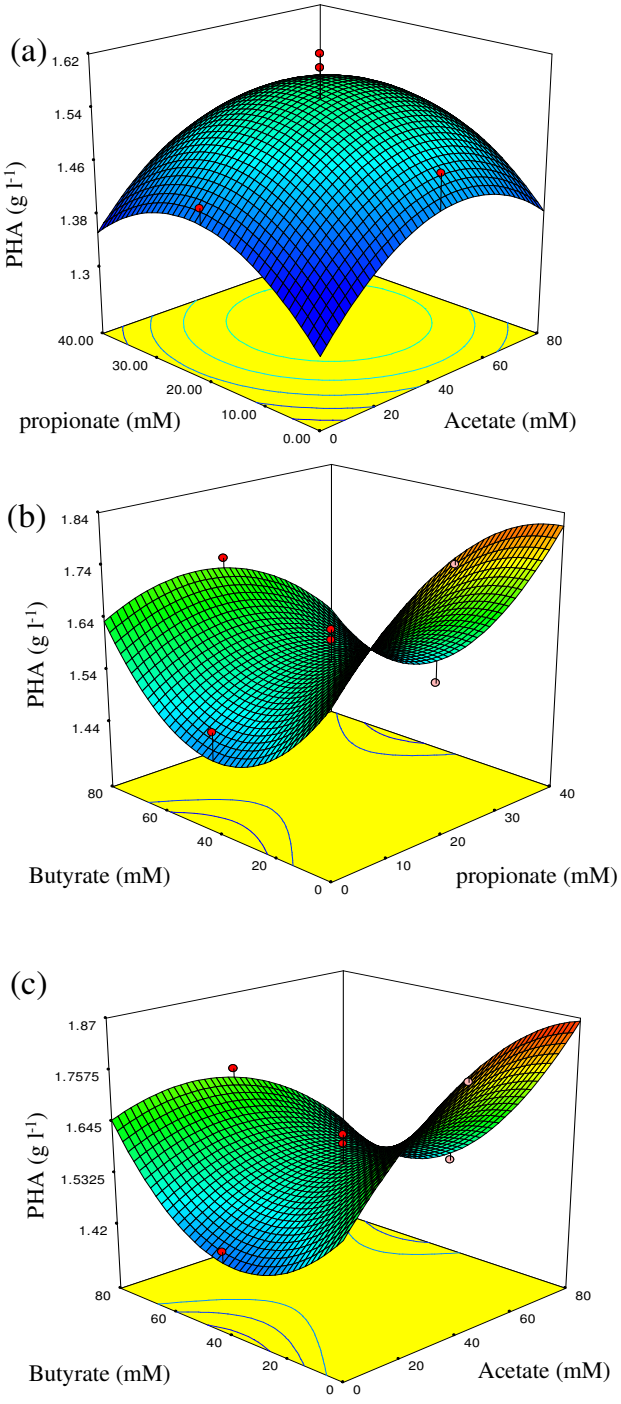

Figure 23. Response surfaces of PHA production by *Rps. palustris* TN1 as a function of acetate (mM), propionate (mM) and butyrate (mM) concentrations, based on the central composite experimental results.

5.3 Predicted optimum VFA concentrations and their experimental validation for hydrogen and PHA production by *Rps. palustris* TN1

5.3.1 Optimized VFA concentrations for maximum hydrogen production and minimum PHA production

In order to predict the optimum concentrations of VFAs for maximal hydrogen production and minimal PHA production Design Expert Software (Stat-ease) version 7.0 was used to solve the regression equation generated from the RSM, Eq. 7. The solution predicts the optimum mixture is 52 mM acetate, 16 mM propionate, and 25 mM butyrate, and the amount of hydrogen and PHA produced would be 1,365.6 ml l^{-1} and 1.59 g l^{-1} respectively. This prediction was tested experimentally in order to assess the performance of the RSM model. For the predicted optimum VFA mixture, the hydrogen accumulation and PHA production by cultures of *Rps. palustris* TN1 were 1,278 ± 39.3ml l^{-1} and 1.70 ± 0.24 g l^{-1}, with deviations between the predicted and experimental values of 5.79% and 6.92%, respectively (Table 22 and Fig. 24). The low values of these deviations support the feasibility of using RSM for improving phototrophic hydrogen production with *Rps. palustris* TN1. The R_{max} defined by fitting data to a modified Gompertz equation was 35.4 ml $l^{-1}h^{-1}$ (Fig. 24). Other measurements made using this optimum mixture included VFA consumption, efficiency of hydrogen production, and light efficiency, which were 29% and 8.95%, and 0.14%, respectively. During the incubation period a small decrease in pH of the culture, from pH 7.04 to 6.82, was observed (Table 23), but this remains within the range that is optimal for nitrogenase activity (Zabut *et al*., 2006). Hydrogen was produced during the log-phase of growth. Consistent with this observation, Koku *et al.* (2003) reported hydrogen production by the PNSB *Rba. sphaeroides* O.U. 001 started between the mid-exponential phases.

5.3.2 Optimized VFA concentrations for minimum hydrogen production and maximum PHA production

The optimum concentrations of VFAs for maximal PHA production and solving regression of the model were predicted by using the Design Expert Software (Stat-ease) version 7.0 to solve the regression equation generated from the RSM, Eq. 8. The solution predicts that the optimum mixture is 73 mM acetate and 34

mM propionate. The experimental values for hydrogen accumulation and PHA production were 970 ± 184 ml l^{-1} and 1.83 ± 0.63 g l^{-1}, respectively (Table 22 and Fig. 25) and deviations between the predicted and experimental values were 23.86% for hydrogen accumulation and 3.17% for PHA production. The deviation for PHA production was low; however, the deviation for hydrogen production was quite high. The R_{max} defined by fitting data to a modified Gompertz equation was 34.3 ml l^{-1} h^{-1} (Fig. 25). Under these optimal conditions for PHA production, VFA consumption and the efficiency of hydrogen production were 44% and 5.78%, respectively, with a light efficiency of 0.11%. A small change from pH 7.0 was observed over the course of the incubation period (Table 23). PHA content increased from 48.71% to 63.8% (Fig. 24b and Fig. 25b) under these optimum conditions.

5.3.3 Assessment of the outcomes from optimizing using RSM

In the effluent of anaerobic digestion, acetate, propionate, and butyrate accounted for 70-80% of total VFA (Shi and Yu, 2006; O-Thong *et al*, 2008). The results presented here demonstrate that VFAs can be used for hydrogen production by *Rps. palustris* TN1. The utilization pathways of substrate for hydrogen production by PNSB are extensive and may differ between species or between different strains of the same species (Koku *et al*., 2002). In the present study, the results indicate that, when a VFA mixture consisting of acetate, propionate and butyrate was used as the carbon source, each can be individually utilized for cell growth and hydrogen production. The results also point to the feasibility of converting the effluent of an acidogenic reactor to hydrogen by *Rps. palustris* TN1.

The engineering implication of these results is that the appropriate conditions for hydrogen production are those that generate low propionate and butyrate levels, and concurrently high concentrations of acetate. Further, for PHA production, high acetate and propionate concentrations and the absence of butyrate are suitable in the operation system.

Table 22. Experimental evaluation of the optimal concentrations of VFAs predicted by RSM for hydrogen and PHA production.

Region	VFA concentrations	Condition	Hydrogen production (ml l^{-1})			PHA (g l^{-1})		
			Predicted value	Experimental value[a]	Deviation %	Predicted value	Experimental value[a]	Deviation %
Optimized VFA for H_2 production	52 mM acetate, 15 mM propionate, 25 mM butyrate	Initial pH 7.0 Yeast extract 1.0 g l^{-1}	1,356.6	1,278 ± 39.3	5.79	1.59	1.70 ± 0.24	6.92
Optimized VFA for PHA production	73 mM acetate, 34 mM propionate	Initial pH 7.0 Yeast extract 1.0 g l^{-1}	1,273.9	970 ± 184	23.86	1.89	1.83 ± 0.63	3.17

[a]Determined at the end of the cultivation period.

Table 23. Evaluation of the kinetics of hydrogen production at optimal concentrations of acetate, propionate and butyrate.

Region	VFA concentration	Initial pH	Final pH[a]	Condition	Total VFA Consumption (%)[a]	H_2 yeild (mol H_2 mol VFA^{-1})[a]	Efficiency of H_2 production (%)[a]	Light conversion efficiency (%)[a]
Optimized VFA concentrations for maximum H_2 production	52 mM acetate, 15 mM propionate, 25 mM butyrate	7.04	6.82	Initial pH 7.0, 1.0 g l^{-1} yeast extract	29	0.63	8.95	0.14
Optimized VFA concentrations for maximum PHA production	73 mM acetate, 34 mM propionate	7.04	7.24	Initial pH 7.0, 1.0 g l^{-1} yeast extract	44	0.40	5.78	0.11

[a]Determined at the end of the cultivation period. In all cases, the measurements used to determine H_2 yield, efficiency of hydrogen production and light efficiencies varied by less than 10%.

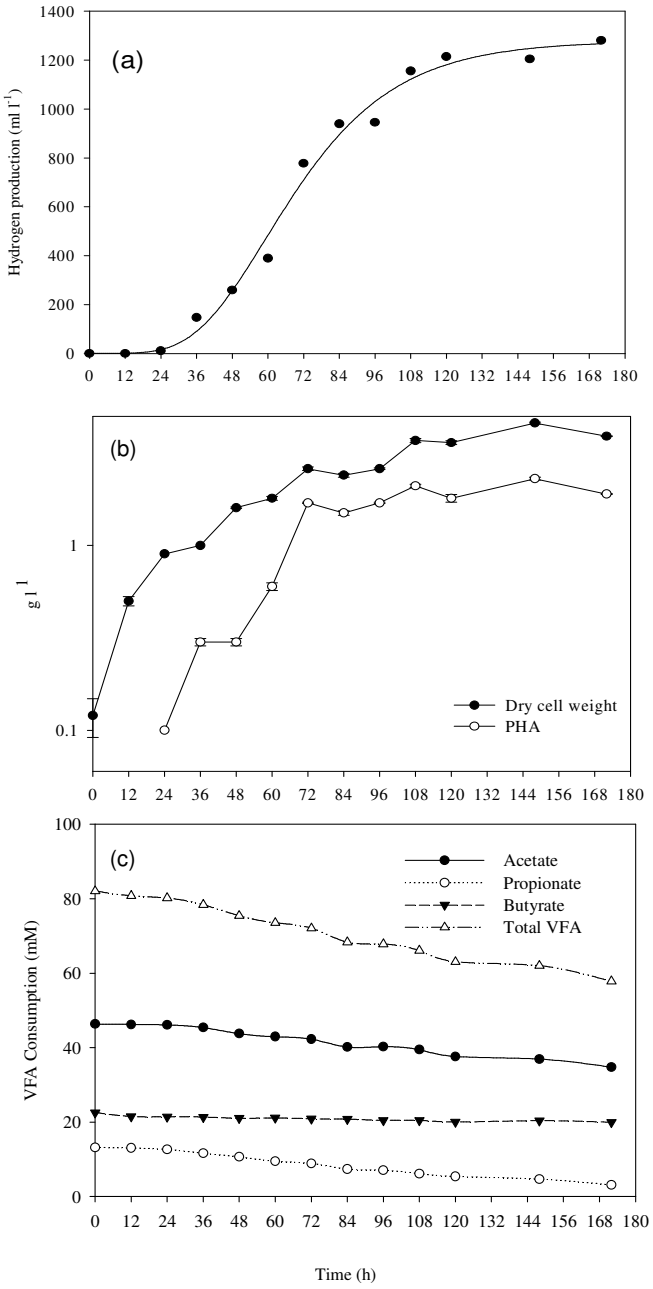

Figure 24. Time course of photohydrogen and PHA production at the optimum concentrations of VFAs for maximum hydrogen production and minimum PHA production (52 mM acetate, 15 mM propionate and 25 mM butyrate) by *Rps. palustris* TN1 under anaerobic-light (3,000 lux) conditions at 30°. Panels are (a) hydrogen production data fitted to the modified Gompertz equation, (b) VFA consumption, and (c) Dry cell weight and Biomass production.

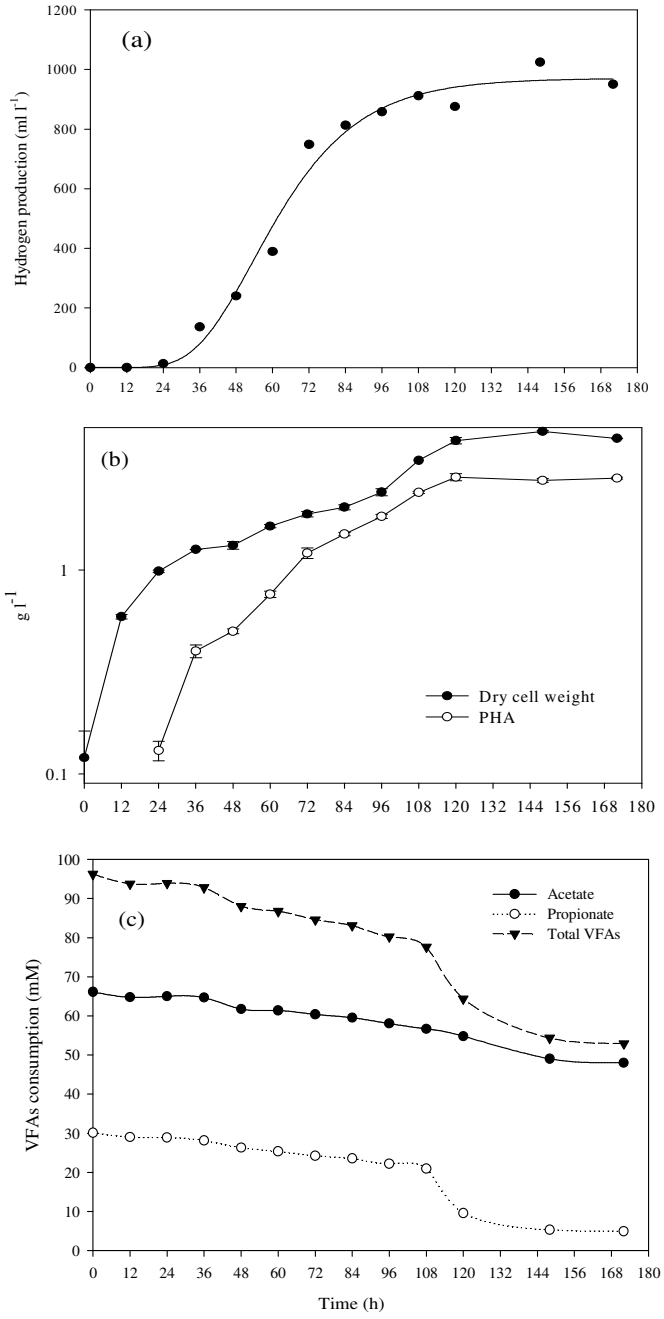

Figure 25. Time course of photohydrogen and PHA production at the optimum concentrations of VFAs for maximum PHA production and minimum hydrogen production (73 mM acetate and 34 mM propionate) by *Rps. palustris* TN1 under anaerobic-light (3,000 lux) conditions at 30°. Panels are (a) hydrogen production data fitted to the modified Gompertz equation, (b) VFA consumption, and (c) Dry cell weight and Biomass production.

6. Optimization of medium composition and environmental parameters for hydrogen production using statistical methodology

Productivity of microbial metabolites can be increased by manipulating nutritional requirements, physical parameters and genetic make up of the producing strain (Greasham, 1983). Initial screening of the components is necessary in order to determine their significance with respect to product formation. Those having the greatest effect are then investigated in detail towards optimization of culture conditions (Greasham, 1983; Naveena *et al*., 2005; Ganapathy *et al*., 1998). Having established the optimal mixure of VFAs for maximum hydrogen production by *Rps. palustris* TN1, this approach, involving a Plackett-Burman design (PBD) and response surface methodology (RSM), was used in order to determine what other modifications, aside from genetic manipulations, could further enhance hydrogen production. As established in previous sections, there is an inverse relationship between hydrogen and PHA production. By extension, it is anticipated that parameters affecting hydrogen production will affect PHA production as well. This will also be considered here.

6.1 Identification of important medium components and environmental conditions using Plackett-Burman design (PBD)

This study was performed using the mixture of VFAs (section 5.3.3) determined to be optimal for maximizing hydrogen production: 52 mM acetate, 16 mM propionate, and 25 mM butyrate. The selection of additional parameters to be investigated was based on a review of the literature.

As the nitrogenase driven H_2-producing activity of PNSB (such as *Rps. palustris* WP3-5) is strongly inhibited by NH_4^+ ions, glutamic acid, which has been showed to have a relatively minor inhibitory effect on nitrogenase activity, was provided as a nitrogen source (Chen *et al*., 2008). It has been reported that the absence of nitrogen and oxygen is important for hydrogen production mediated by nitrogenase, especially in the presence of argon (Basak *et al*., 2007; Chen *et al.,* 2006). While yeast extract is a component of the modified basal medium routinely used for culturing TN1 since it is a good source of both nitrogen and also vitamins

that could promote cell growth and metabolite production, high concentrations are reported to be inhibitory for hydrogen production (Gest and Kamer, 1949; Koku *et al*., 2003; Oh *et al.,* 2004). Therefore, its potential effect on hydrogen production by TN1 was evaluated. The presence of $NaHCO_3$ was also evaluated with respect to hydrogen production, since carbonate is required for VFA uptake by PNSB (van Niel, 1944; Omerod, 1956; Stanier *et al*., 1959; Takabatake *et al*., 2004). The trace elements $FeSO_4$ and Na_2MoO_4 are important for nitrogenase and hydrogenase activities, and Fe^{2+} and Mo^{2+} ions are cofactors of nitrogenase-catalyzed hydrogen production in *Rps. palustris* (Oda *et al*., 2005). Moreover, Fe^{2+} is reported to regulate tetrapyrrole biosynthesis in PNSB (Sasaki *et al*., 1987), and varying concentrations have the potential to thereby alter energy-gathering capacities. Consistent with the importance of the metal ions for the hydrogen producing enzymes, the presence of the chelating agent ethylenediaminetetraacetic acid (EDTA) is known to inhibit hydrogenase activity (Kern *et al*., 1994; Fissler *et al*., 1994). Therefore, the presence of both ions and also EDTA were evaluated.

Initial pH has already been established here as affecting both cell growth and hydrogen production (section 4). Therefore, in order to use *Rps. palustris* TN1 for hydrogen production in anaerobic-treated POME, which has an acidic pH of 4.5-5.5 (O-Thong *et al*., 2008), the initial pH should be adjusted to neutral pH 7. Other physical parameters that could impact hydrogen production by *Rps. palustris* TN1 include initial cell concentration and light intensity, since they are reported to affect VFA consumption and hydrogen production by PNSB (Shi and Yu, 2006).

The PBD (Table 24) was used to screen amongst these nutritional and environmental variables for those that significantly affect hydrogen production. The main effect of each variable upon hydrogen production was estimated by the difference between average measurements made at both high levels (+1) and low levels (-1) of that variable (Gue *et al*., 2009). If the sign of the *t*-value of the tested variable is positive, the influence of the variable on hydrogen production is greater at high levels; if it is negative, the influence of the variable is greater at low levels (Plackett-Burman, 1946). It was found that low concentrations of EDTA and $NaHCO_3$, a low initial cell concentration, high concentrations of glutamic acid, yeast extract, $FeSO_4$, and Na_2MoO_4, a neutral initial pH, and high light intensity all enhance

hydrogen production. However, among these parameters, only the amount of yeast extract, the concentration of $NaHCO_3$, and the initial pH value had confidence levels above 95%, indicating they are statistically significant. By this measure, the influences of the rest of the variables were statistically insignificant (Table 25). The variables with insignificant effects were not subjected to optimization, and were used at minimal concentrations for the purposes of economizing the cost of these studies.

Table 24. Culture conditions for screening the importance of parameters with respect to hydrogen production using Plackett-Burman design.

A:Glutamate (mM)	B: Yeast extract ($gl-^{1}$)	C: $NaHCO_3$ ($mg\ l^{-1}$)	D: FeSO4 ($mg\ l^{-1}$)	E: Na_2MoO_4 ($mg\ l^{-1}$)	F: EDTA ($mg\ l^{-1}$)	G: Initial pH	H: Light intensity (lux)	J: Initial cell concentration ($g\ l^{-1}$)	Hydrogen production ($ml\ l^{-1}$)
15 (+)	1 (-)	1.5 (+)	1 (-)	0.5 (-)	2 (-)	7 (+)	5000 (+)	1.2 (+)	767
15 (+)	3 (+)	0 (-)	3.2 (+)	0.5 (-)	2 (-)	6.5 (-)	5000 (+)	1.2 (+)	874
5 (-)	3 (+)	0 (-)	1 (-)	1 (+)	2 (-)	7 (+)	3000 (-)	1.2 (+)	906
15 (+)	1 (-)	0 (-)	3.2 (+)	0.5 (-)	5 (+)	7 (+)	3000 (-)	0.8 (-)	945
15 (+)	3 (+)	1.5 (+)	3.2 (+)	1 (+)	2 (-)	6.5 (-)	3000 (-)	0.8 (-)	730
15 (+)	3 (+)	0 (-)	1 (-)	1 (+)	5 (+)	7 (+)	5000 (+)	0.8 (-)	884
5 (-)	3 (+)	1.5 (+)	3.2 (+)	0.5 (-)	5 (+)	7 (+)	3000 (-)	1.2 (+)	736
5 (-)	1 (-)	1.5 (+)	3.2 (+)	1 (+)	2 (-)	7 (+)	5000 (+)	0.8 (-)	720
5 (-)	1 (-)	0 (-)	3.2 (+)	1 (+)	5 (+)	6.5 (-)	5000 (+)	1.2 (+)	731
15 (+)	1 (-)	1.5 (+)	1 (-)	1 (+)	5 (+)	6.5 (-)	3000 (-)	1.2 (+)	669
5 (-)	3 (+)	1.5 (+)	1 (-)	0.5 (-)	5 (+)	6.5 (-)	5000 (+)	0.8 (-)	781
5 (-)	1 (-)	0 (-)	1 (-)	0.5 (-)	2 (-)	6.5 (+)	3000 (-)	0.8 (-)	640

Table 25. Statistical evaluation of factors screened for their influence on hydrogen production from results of the Plackett-Burman design.

Variables	Standard Error	*t-values*	*p-values*
A, Glutamic acid (mM)	4.12	7.17	0.0882
B, Yeast extract (g l^{-1})	4.12	8.87	0.0415[a]
C, $NaHCO_3$ (mg l^{-1})	5.05	-15.65	0.0406[a]
D, $FeSO_4$ (mg l^{-1})	5.05	7.60	0.0832
E, Na_2MoO_4 (mg l^{-1})	5.05	4.44	0.1411
F, EDTA (mg l^{-1})	5.05	-4.34	0.1442
G, Initial pH	5.05	2.66	0.0297[a]
H, Light intensity (lux)	5.05	8.30	0.0764
J, Initial cell concentration (g l^{-1})	5.05	-6.42	0.0984

[a]Statistically significant (P <0.05).

6.2 CCD to predict the optimum conditions for hydrogen production using RSM

6.2.1 Effect of the amount of yeast extract, the concentration of $NaHCO_3$, and the initial pH on hydrogen production

To determine the optimum conditions involving the significant variables and their potential interactions, i.e. amounts of yeast extract and $NaHCO_3$, and initial pH, a CCD was constructed. Table 26 represents the design matrix of the variables, together with the experimental results. The hydrogen production ranged from 1,079-2,264 ml l^{-1}. A maximal hydrogen production (2,264 ml l^{-1}) was observed in trial experiments 15-20 that used intermediate values of the variables. The higher levels of yeast extract and $NaHCO_3$, and initial pHs different from neutral pH negatively affected hydrogen production (for example, trial experiment 8).

Table 26. The CCD for response surface analysis of the optimum amount of yeast extract, concentration of $NaHCO_3$, and initial pH.

Trial Experiment	(X_1) Yeast extract (g l^{-1})	(X_2) Initial pH	(X_3) $NaHCO_3$ (g l^{-1})	(Y_1) Hydrogen production (ml l^{-1})	(Y_2) PHA (g l^{-1})
1	1	6.5	0	1079	0.18
2	3	6.5	0	1160	0.25
3	1	7.5	0	1233	0.22
4	3	7.5	0	1412	0.46
5	1	6.5	1	1206	0.23
6	3	6.5	1	1493	0.4
7	1	7.5	1	1510	0.52
8	3	7.5	1	1667	0.82
9	1	7	0.5	1858	0.48
10	3	7	0.5	2056	0.96
11	2	6.5	0.5	1497	0.72
12	2	7.5	0.5	1838	1.3
13	2	7	0	1762	0.8
14	2	7	1	1973	1.23
15	2	7	0.5	2264	1.8
16	2	7	0.5	2234	1.82
17	2	7	0.5	2152	1.74
18	2	7	0.5	2251	1.6
19	2	7	0.5	2214	1.64
20	2	7	0.5	2195	1.74

The data from the trial experiments (Table 26) were fitted to a regression equation using a least-squares method. The second-order polynomial equation describing hydrogen production in relation to the variables is as follows:

$$H_2 \text{ production (ml } l^{-1}) = -87{,}967 + 747.2X_1 + 25{,}191X_2 + 878.6X_3 - 8\,X_1X_2 + 46X_1X_3 + 36X_2X_3 - 156X_1^2 - 1{,}782X_2^2 - 982X_3^2 \quad (9)$$

The results of an ANOVA test used to identify terms in this equation that were not statistically significant are presented in Table 27. From this test, it was determined that the linear terms of the variables are significant, as are the square terms of the variables corresponding to the amount of yeast extract and initial pH. However, the interactive terms are not significant.

Table 28 summarizes the values of the statistical parameters from an ANOVA test of the model generated from Eq. 9. The value of R^2 is 0.98, and so 98% of variation for hydrogen production is attributable to the independent variables, while only 2% of the total cannot be explained by the model. The value of C.V. is 4.34%, and the lack of fitness *P*-value is 0.656. Based on these statistical values, one can expect a good agreement between predicted and experimental values, implying that the statistical model is very reliable for projecting hydrogen production.

The response surface plots and the corresponding contour curves described by the regression equation are shown in Fig. 26. As was also true for the optimization of the VFAs, each response surface plot represents the effect of two independent variables at an optimal level of third variable. The response surfaces of hydrogen production have clear peaks, which indicates that the optimum conditions fall inside the design boundaries. The elliptical shape of the contour plots indicate that the amounts of yeast extract and $NaHCO_3$, and the initial pH have significant individual and interactive influences on hydrogen production (Fig. 26a-c). The model indicates that hydrogen production will increase when the amount of yeast extract is increased over the range from 1 to 2 g l^{-1}, but decreased with more yeast extract (from 2 to 3 g l^{-1}); it will increase when the amount of $NaHCO_3$ is increased over the range from 0 to 0.5 g l^{-1}, but decrease as the amount of $NaHCO_3$ is increased from 0.5 to 1.0 g l^{-1}; and increase when the value of the initial pH is increased from 6.5 to 7.0, but

decrease as the pH is further increased from 7.0 to 7.5. The maximum hydrogen productivity that can be achieved according to the model is 2,152- 2,264 ml l^{-1} (Fig. 26).

Table 27. Coefficient estimations and *p*-values of each term in equation 9.

Term	Hydrogen production	
	Coefficient estimate	probability *(P)*>*F*
intercept	2176.20	
X_1	90.20	0.0038 [a]
X_2	122.50	0.0005[a]
X_3	120.30	0.0005 [a]
$X_1 X_2$	-4.00	0.8848
$X_1 X_3$	23.00	0.4129
$X_2 X_3$	9.00	0.7450
X_1^2	-156.00	0.0068
X_2^2	-445.50	< 0.0001[a]
X_3^2	-245.50	0.0003[a]

[a]Statistically significant (P <0.05).

Table 28. ANOVA for response surface quadratic model of equation 9.

Statistic report	Value
P -value	
• model	<0.0001[a]
• Lack of Fit	0.65
R^2	0.98
C.V.	4.34

[a]Statistically significant (P <0.05).

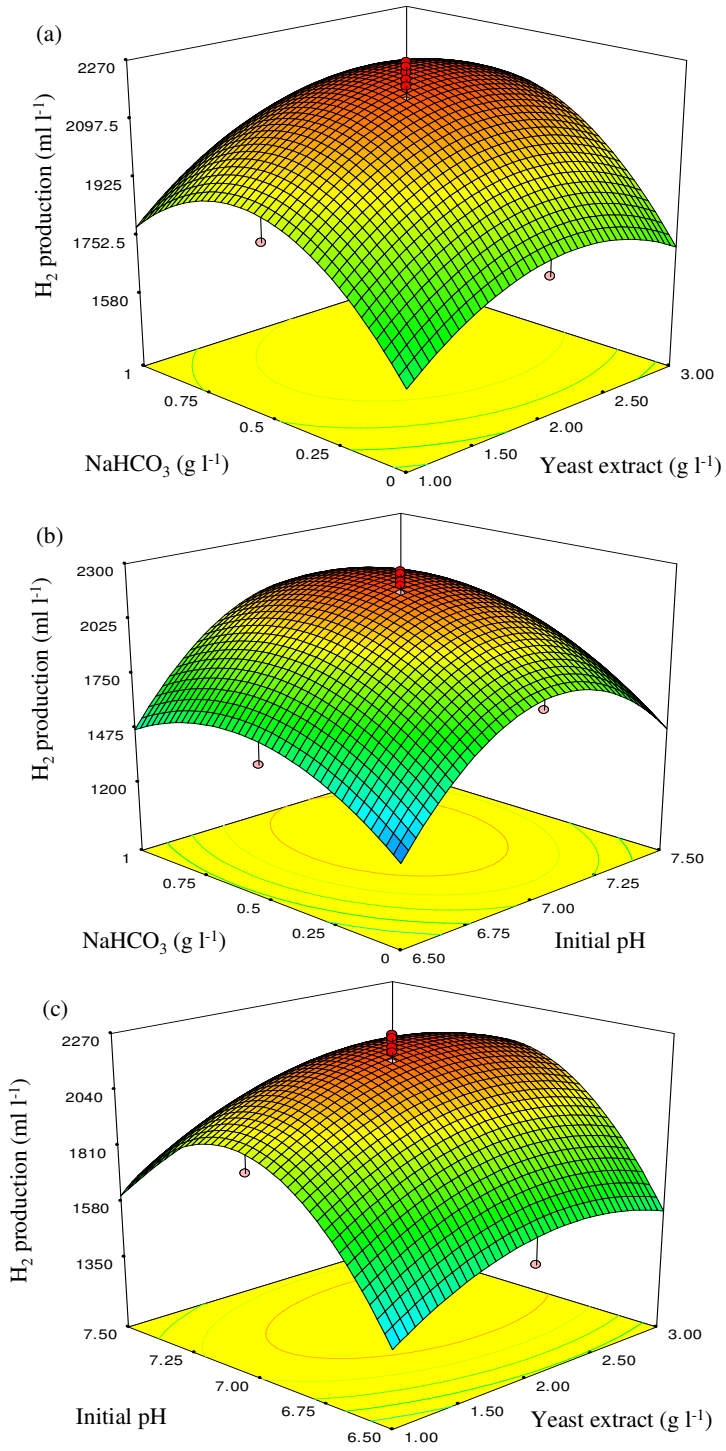

Figure 26. Response surfaces of hydrogen production (ml l^{-1}) by *Rps. palustris* TN1 as a function of initial pH, amount of yeast extract (g l^{-1}) and concentration of $NaHCO_3$ (g l^{-1}) based on the central composite design.

6.2.2 Effect of amount of yeast extract, concentration of $NaHCO_3$, and initial pH on PHA production

The same modeling methods as were used to study nutrient concentrations and initial pH impacts on hydrogen production were also used to examine their effects on PHA production (Table 26). The PHA production values ranged from 0.18-1.82 g l^{-1} and a maximal PHA production (1.82 g l^{-1}) were observed in trial experiments 15-20 involving intermediate conditions. The data from the trial experiments (Table 26) fitted to a regression equation using a least-squares method generated the following second-order polynomial equation:

$$\text{PHA production (g } l^{-1}) = 1.57 + 0.13X_1 + 0.15X_2 + 0.13X_3 + 0.38X_1X_2 + 0.20X_1X_3 + 0.58X_2X_3 - 0.61X_1^2 - 0.32X_2^2 - 0.31X_3^2 \quad (10)$$

An ANOVA test of the terms in Eq. 10 was performed in order to identify those that are significant (Table 29). Only the square term of the variable corresponding to the amount of yeast extract is statistically significant.

Table 30 summarizes the values of the statistical parameters from an ANOVA test of the model generated from Eq. 10. The value of R^2 is 0.91, the value of C.V. is 6.98%, and the lack of fitness *P*-value is 0.42. These values indicate the reliability of the model.

The response surface plots of PHA production are shown in Fig. 27. Their elliptical shapes indicate that the amount of yeast extract, the concentration of $NaHCO_3$, and the initial pH have significant individual and interactive influences on PHA production. They also indicate that PHA production would increase when the amount of yeast extract is increased from 1 to 2 g l^{-1}, but decrease from 2 to 3 g l^{-1}; they would increase as the concentration of $NaHCO_3$ is increased over the range from 0 to 0.5 g l^{-1}, but decrease over the range from 0.5 to 1 g l^{-1}; and increase as the initial pH increases from 6.5 to 7.0, but decrease from pH 7.0 to 7.5. The maximum level of PHA produced is predicted to be 1.60-1.82 g l^{-1} (Fig. 27).

Table 29. Coefficient estimations and *p*-values of each term in equation 10.

Factor	PHA production	
	Coefficient estimate	Probability *(P)>F*
intercept	1.57	
X_1	0.13	0.1493
X_2	0.15	0.0853
X_3	0.13	0.1408
$X_1 X_2$	0.038	0.6863
$X_1 X_3$	0.020	0.8290
$X_2 X_3$	0.058	0.5381
X_1^2	-0.61	0.0027[a]
X_2^2	-0.32	0.0654
X_3^2	-0.31	0.0691

[a]Statistically significant (P <0.05).

Table 30. ANOVA for response surface quadratic model of equation 10.

Statistic report	Value
P -value	
• model	<0.0001[a]
• Lack of Fit	0.42
R^2	0.91
C.V.	6.98

[a]Statistically significant (P <0.05).

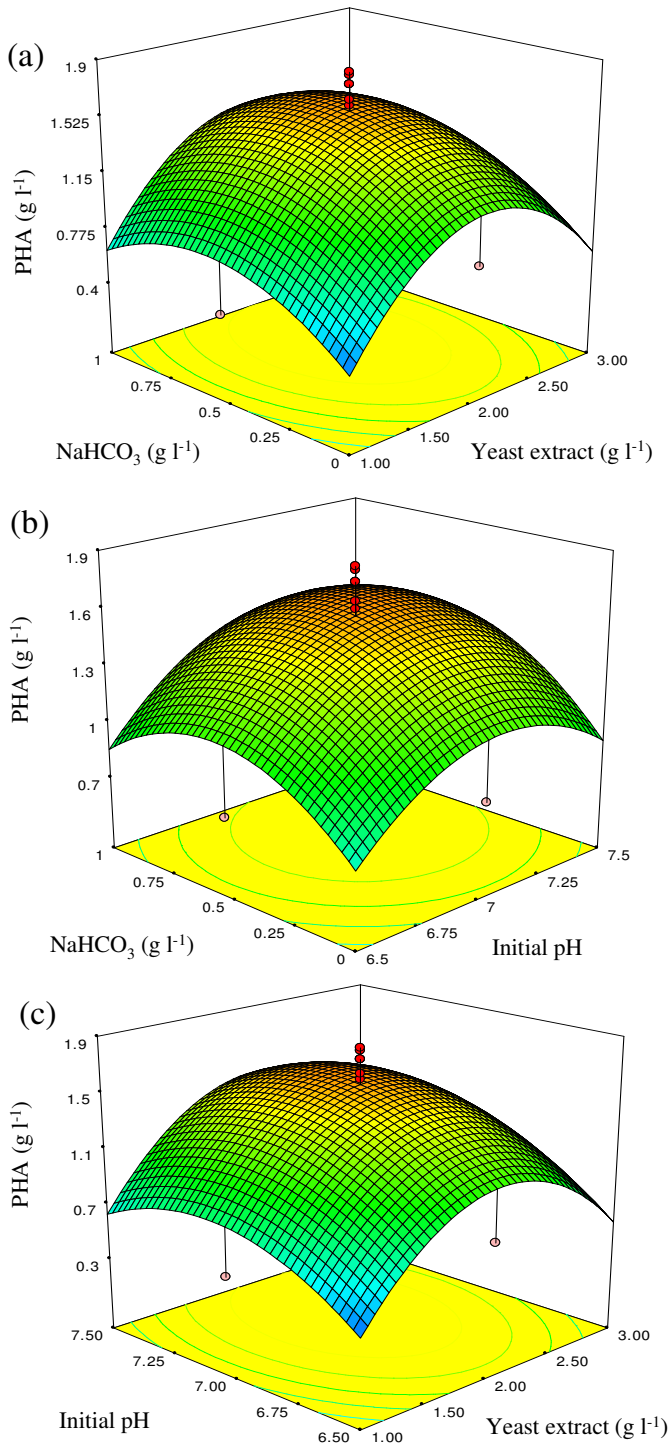

Figure 27. Response surfaces of PHA production (g l^{-1}) by *Rps. palustris* TN1 as a function of initial pH, amount of yeast extract (g l^{-1}) and concentration of $NaHCO_3$ (g l^{-1}), based on the central composite design.

6.3 Predicted optimal amount of yeast extract, concentration of $NaHCO_3$, and initial pH, and their experimental validation for hydrogen and PHA production by *Rps. palustris* TN1

By differentiation of Eqs. 9 and 10 using Design Expert software version 7.0, the predicted optimum values that would achieve the maximum hydrogen production and minimum PHA production were found to be 2.3 g l^{-1} yeast extract, 0.63 g l^{-1} $NaHCO_3$, and an initial pH of 7.07. As may be noted, this condition is very similar to the intermediate conditions of the CCD trial experiments. The hydrogen and PHA production levels predicted by the model are 2,214 ml l^{-1} and 1.58 g l^{-1}, respectively. To verify the reliability of the model, an experiment was performed applying those predicted optimal conditions. The resulting hydrogen and PHA production levels were 2,618 ± 237 ml l^{-1} and 1.22 ± 0.45 g l^{-1}, respectively (Table 31 and Fig. 28). Based on those values, the efficiency of hydrogen production and light conversion efficiency were calculated to be 18.34% and 2.3%, respectively, with 71.9% VFA consumption (Table 32). The deviation between the predicted and experimental values was 18.25% and 22.78% for hydrogen accumulation and PHA production, respectively (Table 32). The R_{max} defined by fitting data to the modified Gompertz equation was 47 ml l^{-1} h^{-1}(Fig. 28).

The improvement in hydrogen production achieved with these modifications to the amounts of yeast extract and $NaHCO_3$ was greater than 2-fold. Furthermore, these modifications improved VFA consumption to 68% of acetate, 100% of propionate and 62% of butyrate (Fig. 28). van Niel (1944) reported that carbonate fixation occurs in PNSB during the uptake of substrates more reduced than cell components and carbonate release takes place during the uptake of the substrates that are more oxidized. Thus, carbonate would serve as an electron acceptor when substrates such as propionate and butyrate, which are more reduced than the cell components, are anaerobically taken up by the cell, while the uptake of acetate, which is more oxidized than the cell components, does not require carbonate (Ormerod *et al*., 1956). This probably means that carbonate plays an important role in maintaining the reduced-oxidized balance of the cell, thereby improving hydrogen production.

Table 31. Experimental evaluation of the optimal conditions predicted by RSM with respect to hydrogen and PHA production.

VFA concentration	Condition	Hydrogen production (ml l^{-1})			PHA (g l^{-1})		
		Predicted value	Experimental value[a]	Deviation %	Predicted value	Experimental value[a]	Deviation %
52 mM acetate, 16 mM propionate, 25 mM butyrate	Initial pH 7.07, 2.30 g l^{-1} yeast extract, 0.63 g l^{-1} $NaHCO_3$	2,214	2,618 ± 273	18.25	1.58	1.22 ± 0.45	22.78

[a]Determined at the end of the cultivation period.

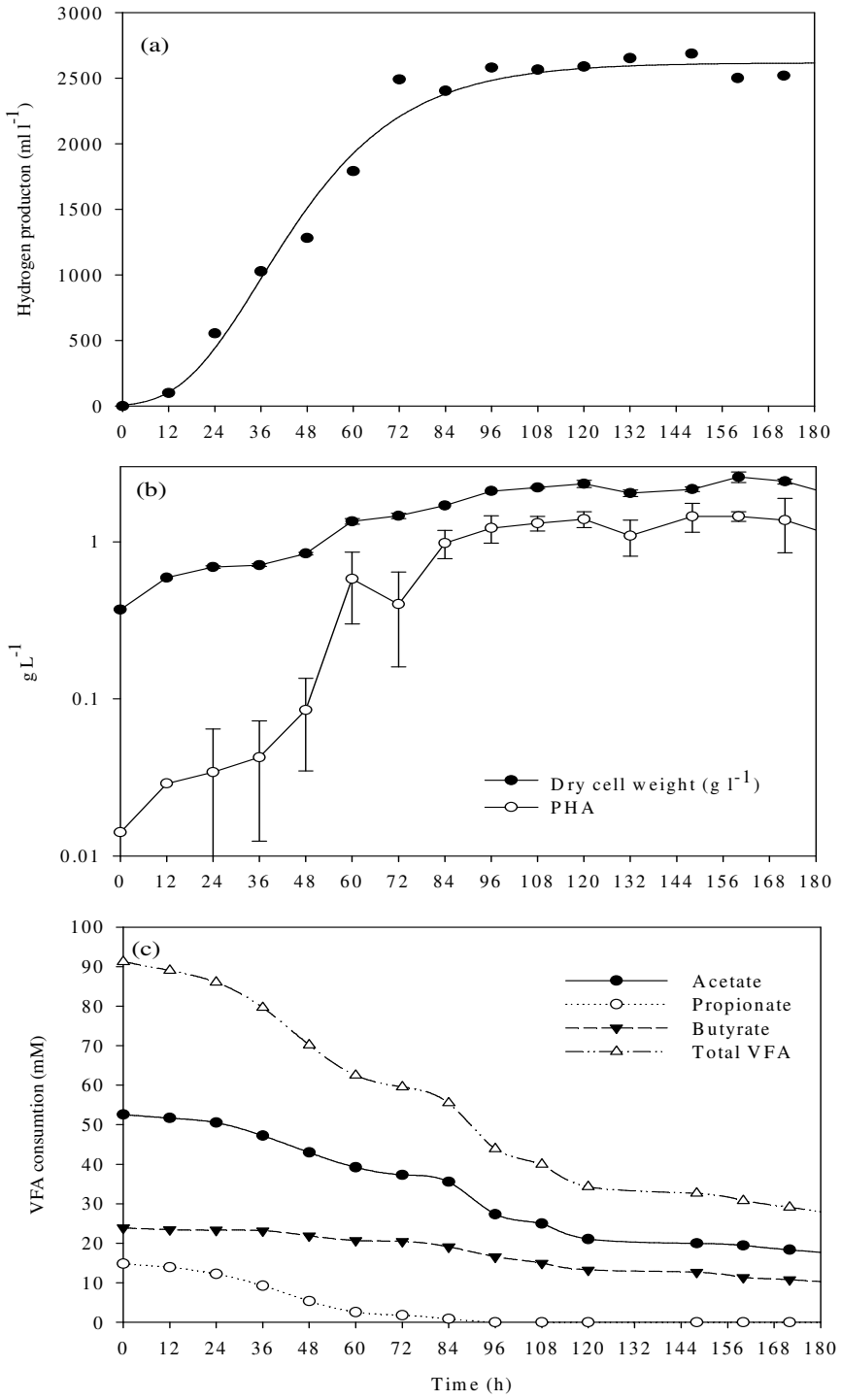

Figure 28. Time course of photohydrogen and PHA production with 2.3 g l^{-1} yeast extract, 0.63 g l^{-1} $NaHCO_3$, and initial pH of 7.07 by *Rps. palustris* TN1 under anaerobic-light (3,000 lux) conditions at 30°. Panels are (a) hydrogen production data fitted to the modified Gompertz equation, (b) Dry cell weight and Biomass production, and (c) VFA consumption.

Table 32. Evaluation of the kinetics of hydrogen production with the optimum amount of yeast extract (2.3 g l^{-1}), $NaHCO_3$ concentration (0.63 g l^{-1}), and initial pH (7.07).

Volatile fatty acid Concentration	Initial pH	Final pH [a]	Total VFA Consumption (%) [a]	H_2 Yield (mol H_2 mol VFA^{-1})[a]	Efficiency of H_2 production (%)[a,]	Light conversion efficiency (%)[a]
52 mM acetate, 16 mM propionate, 25 mM butyrate	7.23	7.49	71.9	1.28	18.34	2.3

[a]Determined at the end of the cultivation period. In this case, the measurement used to determine H_2 yield, efficiency of hydrogen production and light efficiencies varied by less than 10%.

6.4 Assessment of the outcomes from optimizing using RSM

The effluents of anaerobic digestions of wastewaters have acidic pHs (Fang and Yu *et al*., 2001; O-Thong *et al*., 2008). The results presented here demonstrate that the initial pH is an important factor for hydrogen production. The influence of the initial pH on hydrogen production is consistent with results presented in section 4. Therefore, in order to use *Rps. palustris* TN1 for hydrogen production from the effluent of anaerobic digestion, the initial pH should be adjusted to neutral pH 7.

Hydrogen production by *Rps. palustris* TN1 in the medium supplemented with yeast extract and $NaHCO_3$ has advantages that include a higher maximum rate of hydrogen production (R_{max}) and reduced lag time for hydrogen production compared to production in unsupplemented medium (section 5.3.1). Yeast extract would improve production as it can provide many of the basic nutrients for the bacteria, as well as vitamins that promote the growth of PNSB (Koku *et al*., 2003).

The carbonate plays an important role in maintaining the reduced-oxidized balance of the cell for the uptake of VFAs.

7. Hydrogen production by *Rps. palustris* TN1 using palm oil mill effluent (POME) and biogas reactor effluent (BRE) as substrate

A recent technoeconomic analysis of biohydrogen production provides information regarding the value of photofermentation by PNSB. Based on a production rate of 244 ml H_2 l^{-1} h^{-1} and using solar energy, the projected cost is \$10.36 kg^{-1} (James *et al*., 2009). This high production price is primarily due to the cost of feedstock for the PNSB. Therefore, production costs for photofermentation could certainly be reduced by using waste generated by industries as substrate.

Palm oil mill effluent (POME) generated from the milling process to produce crude palm oil, is the largest agro-industrial waste of Southern Thailand. Per ton of fresh fruit bunch milled, the average quantity of effluent is 0.87 m^3 (H-Kittikun *et al*., 1994). POME has a high organic content (75000-96000 mg l^{-1} COD), a BOD of 22000-54000 mg l^{-1}, a total suspended solids (SS) content of 8500-12000 mg l^{-1}, and a total nitrogen content of 830-920 mg l^{-1} (O-Thong *et al*., 2008). So far, biohydrogen production from POME has been carried out by anaerobic bacteria (O-Thong *et al*., 2007, O-Thong *et al*., 2008), while the possibility of photofermentation from POME has not been explored. In this section an evaulation of the potential to use POME for hydrogen production by *Rps. palustris* TN1 is presented.

7.1. Characteristics of POME and BRE

A comprehensive analysis of POME and BRE characteristics are essential because their physico-chemical properties can vary according to palm oil species, harvesting time, cultivation area, and the kind of process used in oil extraction. In this study, POME was collected from JK Import Export Co., Ltd., and biogas reactor effluent (BRE) was collected from Thaksin Palm oil Co., Ltd. Before using for cultivation of PNSB, a pretreatment of POME and BRE was performed, consisting of centrifugation (10,075 x g) and filtration to remove all solids. This is necessary since the sludge inhibits PNSB cell growth (Ali Hassan *et al*., 1997; Azbar

et al., 2009). All investigations used these pretreated effluents, which are referred to simply as POME and BRE.

Table 33 lists characteristics of the POME and BRE. Both effluents had low nitrogen content (460.0 mg l^{-1} for pretreated POME and 10.1 mg l^{-1} for pretreated BRE). The BOD of the pretreated POME was 38,740 mg l^{-1} while that of pretreated BRE was 980 mg l^{-1}. Thus, both of them had a high C/N ratio (>25:1) which is suitable for hydrogen production (Sangkharak and Prasertsan, 2007). These characteristics are similar to those previously reported for POME from Trang, Southern Thailand (O-Thong *et al*., 2007); i.e. it had a high carbon content (BOD>20,000 mg l^{-1}) and a low nitrogen content (<500 mg l^{-1} total nitrogen).

The COD content of the BRE was much less than the POME. However, the major organic acids identified in both effluents were acetate, propionate, and butyrate, and acetate was the predominant major organic acid in POME. Their concentrations were considerably lower in BRE relative to those in POME. In the anaerobic digestion process, the first stage consists of hydrolysis of polymeric materials to monomers such as glucose which are subsequently converted to VFA and hydrogen. In the second stage, hydrogen-producing acetogenic bacteria convert the VFA to hydrogen. Finally, methanogenic bacteria convert the H_2, CO_2 and VFA to methane and CO_2, and the pH becomes neutral (McCarty, 1982). The lower amounts of organic acids detected in the BRE suggests most of them have been consumed by methanogenesis, which is consistent with the neutral pH of the treated effluent. This makes BRE unsuitable as a medium for photohydrogen production. Therefore, exclusively POME was evaluated as a waste source for hydrogen production by *Rps. palustris* TN1.

7.2. Evaluation of POME as a medium for hydrogen production by *Rps. palustris* TN1

This section describes the results of an investigation of hydrogen production by *Rps. palustris* TN1 in different dilutions of POME under anaerobic-light conditions that were achieved by flushing cultures with argon gas. *Rps. palustris* TN1 was also cultured in dilutions of POME and POME supplemented with yeast extract and $NaHCO_3$ under microaerobic-light conditions, in which low oxygen

conditions were established through the aerobic respirations of the microorganism (no argon flushing). Both investigations were carried out in 50 ml serum vials containing 40 ml of varying dilutions of POME that were incubated at a light intensity of 3000 lux. The pH of the POME was adjusted to 7.07 before sterilization.

Table 33. Characteristics of POME and BRE from two palm oil mills.

Characteristic	Units	Source / effluent type	
		JK Import Export Co., Ltd / POME	Thaksin Palm oil Co., Ltd / BRE
pH		4.50	7.37
Color		Brown	Brown
Biochemical oxygen demand (BOD)	mg l^{-1}	38,740	980
Chemical oxygen demand (COD)	mg l^{-1}	50,057	7,540
Total nitrogen	mg l^{-1}	460.0	10.1
Acetate content	mM	76.43	1.03
Propionate content	mM	27.98	0.24
Butyrate content	mM	24.71	1.30

7.2.1 Hydrogen production potential of POME by *Rps. palustris* TN1 cultured under anaerobic-light conditions

Hydrogen production by *Rps. palustris* TN1 was examined for cultures in undiluted POME and up to a 1/100 dilution of POME made with distilled water. Samples were removed and analyzed for a period of 96 h. The amount of hydrogen detected in the POME cultures varied inversely with respect to the dilution of POME, and the maximum value, 826 ± 33 ml l^{-1} was measured for the culture in undiluted POME (Table 34). Likewise, the PHA content was highest for the culture in undiluted POME (38%).

Table 34. Hydrogen produced by *Rps. palustris* TN1 in POME after 96 h of cultivation.

POME dilution	Hydrogen production (ml l^{-1})	DCW (g l^{-1})	PHA (g l^{-1})	PHA content (%)
Undiluted	826 ± 33	1.07	0.4	38
1/10 dilution	865 ± 16	0.40	0.068	17.2
1/20 dilution	781 ± 40	0.33	0.005	13.8
1/60 dilution	656 ± 145	0.17	0.008	4.5
1/100 dilution	29 ± 2	0.09	0.002	2.8

7.2.2 Hydrogen production potential of POME by *Rps. palustris* TN1 cultured under microaerobic-light conditions

Undiluted and diluted POME (dilutions ranging from 1/2 to 1/20) was used as a medium for *Rps. palustris* TN1. A supplemented POME containing 2.3 g l^{-1} yeast extract and 0.63 g l^{-1} $NaHCO_3$ was also used. These supplements were expected to increase hydrogen productivity, based on the studies described in section 6. Micro-aerobic culture conditions were established by relying upon the aerobic respirations of the bacteria to reduce the oxygen content in the sealed vials. This was regarded as a cost-saving measure that would eliminate the need to sparge them with argon, and make the hydrogen production more economical.

The specific growth rates of *Rps. palustris* TN1 cultured in different POME dilutions varied (Table 35). The lowest rate was measured for the bacteria cultured in the 1/20 dilution of POME, and the highest rates were observed in undiluted POME and undiluted supplemented POME (Table 35 and Table 36). This correlation can be explained by the reduction in biologically-digestible compounds in the more dilute POME.

Table 35. Hydrogen production by *Rps. palustris* TN1 in unsupplemented POME.

POME	Initial pH	Final pH	Specific growth rate (h^{-1})	Total VFA consumption (%)[a]	H_2 yield (mol H_2 mol VFA^{-1}) [a]	Efficiency of H_2 production (%)[a]	Light conversion efficiency (%)[a]
Undiluted	6.49	6.43	0.1742	27.75	0	0	0
1/2 dilution	6.96	6.86	0.1310	87.46	2.64	33.98	0.72
1/5 dilution	7.04	6.99	0.1312	100	2.14	22.98	0.27
1/10 dilution	7.03	8.74	0.1232	100	2.34	20.34	0.05
1/20 dilution	7.01	8.02	0.0213	100	0	0	0

[a]Determined at the end of the cultivation period. In all cases, the measurements used to determine H2 yield, efficiency of hydrogen production and light efficiencies varied by less than 10%.

Table 36. Hydrogen production by *Rps. palustris* TN1 in POME supplemented with yeast extract and $NaHCO_3$.

POME	Initial pH	Final pH	Specific growth rate (h^{-1})	Total VFA consumption (%)[a]	H_2 yield (mol H_2 mol VFA^{-1}) [a]	Efficiency of H_2 production (%)[a]	Light conversion efficiency (%)[a]
Undiluted	7.02	6.54	0.1766	45.42	0	0	0
1/2 dilution	7.04	7.34	0.1896	94.37	2.34	20.34	0.26
1/5 dilution	7.25	8.95	0.1897	100	1.44	12.54	0.13
1/10 dilution	7.10	8.72	0.1885	100	2.11	18.40	0.05
1/20 dilution	7.10	8.18	0.1670	100	0	0	0

[a]Determined at the end of the cultivation period. In all cases, the measurements used to determine H2 yield, efficiency of hydrogen production and light efficiencies varied by less than 10%.

The three major VFAs present in POME, acetate, propionate, and butyrate, were consumed at higher rates in the supplemented POME *versus* the unsupplemented POME (Table 37 *versus* Table 39). At the end of the 96 h cultivation period, in undiluted POME 48.3% of the acetate, 26.3% of the propionate, and 24.0% of butyrate remained (Table 38), whereas in undiluted supplemented POME 32.1% of the acetate, 10.8% of the propionate, and 7.2% of the butyrate remained. By contrast, the sugars in both unsupplemented and supplemented POME were completely consumed within 96 h cultivation period (Table 40). As described previously (section 6), carbonate improves uptake of the VFAs (van Neil, 1944), which accounts for these differences.

No detectable hydrogen was produced by cultures in the undiluted and supplemented POMEs. However, hydrogen was detected in cultures of undiluted POME that had been argon-sparged. Evidently, the balance between energy-consuming hydrogen evolution and energy-producing hydrogen uptake is such that uptake predominates in the light-limited micro-aerobic environment of the undiluted POME. As light penetrance improves through dilution of the POME, so too does the cell's ability to harvest photonic energy and now the balance shifts in favor of hydrogen evolution. That the balance is different in the strictly anaerobic cultures achieved by sparging with argon reflects the oxygen sensitivity of the hydrogen-producing nitrogenase enzyme.

The pH change during cultivation of *Rps. palustris* TN1 in unsupplemented POME was in the range of 6.43-8.74 (Table 35). For cultures in undiluted POME or dilutions up to 1/5, the pH change was small (no more than 0.1 pH units). The closer the pH was to neutrality, the higher the level of hydrogen production, which was to be expected since it is the optimal pH for nitrogenase activity. By comparison, the pH of cultures in the 1/10 and 1/20 dilutions of unsupplemented POME changed to alkaline pH by the end of cultivation (Table 35). These alkaline pHs were not suitable for hydrogen production, as has been reported previously (Koku *et al*., 2002). The pH change during cultivation of *Rps. palustris* TN1 in supplemented POME at all dilutions was larger, and the relative level of hydrogen production consistently paralleled the difference in the pH from neutrality.

Table 37. VFA content (mM) of POME.

POME	Acetate	Propionate	Iso butyrate	Butyrate	Isovalerate	Valerate	Isocaproate	Caproate	Heptanoate
Undiluted	73.43	26.33	0.27	24.03	0.35	7.59	0	5.47	0.58
1/2 dilution	35.77	12.16	0	10.98	0.18	4.22	0	3.3	0
1/5 dilution	13.12	4.30	0	3.41	0	2.57	0	0.73	0
1/10 dilution	6.35	1.80	0	1.39	0	0	0	0	0
1/20 dilution	2.77	0	0	0	0	0	0	0	0

Table 38. Residual VFA content (mM) of cultures of *Rps. palustris* TN1 in POME at the end of cultivation.

POME	Acetate	Propionate	Iso butyrate	Butyrate	Isovalerate	Valerate	Isocaproate	Caproate	Heptanoate
Undiluted	48.30	26.33	0.27	24.03	0.35	7.59	0	5.47	0.58
1/2 dilution	1.68	0.29	0	3.2	0.18	1.23	0	3.3	0
1/5 dilution	0.88	0	0	0.64	0	0.6	0	0	0
1/10 dilution	0	0	0	0	0	0	0	0	0
1/20 dilution	0	0	0	0	0	0	0	0	0

Table 39. Residual VFA content (mM) of cultures of *Rps. palustris* TN1 in supplemented POME at the end of cultivation.

POME	Acetate	Propionate	Iso butyrate	Butyrate	Isovalerate	Valerate	Isocaproate	Caproate	Heptanoate
Undiluted	32.1	10.8	0.1	7.2	0.10	6.80	0	5.02	0.56
1/2 dilution	0.86	0	0	0.74	0.33	0.31	0	1.4	0
1/5 dilution	0	0	0	0	0	0	0	0	0
1/10 dilution	0	0	0	0	0	0	0	0	0
1/20 dilution	0	0	0	0	0	0	0	0	0

Table 40. Sugar content of POME and supplemented POME before and after cultivation of *Rps. palustris* TN1.

POME	Sugar content ($g\ l^{-1}$)	Residual Sugar ($g\ l^{-1}$)	
		Unsupplemented POME	Supplemented POME
Undiluted	1.042	0	0
1/2 dilution	0.0571	0	0
1/5 dilution	0.0093	0	0
1/10 dilution	0	0	0
1/20 dilution	0	0	0

The maximum hydrogen yields were obtained from cultures in 1/2 dilutions of unsupplemented and supplemented POMEs with values of 2.64 and 2.34 mol H_2 mol VFA^{-1}, respectively (Tables 35 and 36). The kinetics of hydrogen production was evaluated by fitting data to a modifed Gompertz equation (Figs. 29 and 30) . For all but the 1/2 dilutions of POME and supplemented POME, the coefficients of determination (R^2) for the curves fitted to the modified Gompertz equations were poor (0.91 or less), and so only for that dilution (for unsupplemented POME, R^2 = 0.99 and for supplemented POME, R^2 =0.97) were the calculated kinetic values considered to be reliable. The maximum hydrogen production (H_{max}) for the 1/2 dilutions of unsupplemented and supplemented POME were calculated to be 2,906 ml l^{-1} and 3,090 ml l^{-1}, respectively, and the corresponding maximum hydrogen production rates (R_{max}) were 32.5 ml l^{-1} h^{-1} and 41.5 ml l^{-1} h^{-1}, respectively.

Using the equation for hydrogen production from the RSM (section 5, Eq. 7), the predicted hydrogen production based on the VFA content for undiluted and 1/2, 1/5, 1/10, and 1/20 dilutions of unsupplemented POME are 1,281, 1,141, 1,016, 874, and 778 ml l^{-1}, and for the same dilutions of supplemented POME are 1,297, 1,374, 1,016, 874, and 778 ml l^{-1}. Given the high reliability demonstrated for the RSM when using the artificial media (section 5), the large difference between the predicted and observed hydrogen production levels for POME strongly suggests that there are components present in POME that make an important contribution to hydrogen production, but these are as yet undefined.

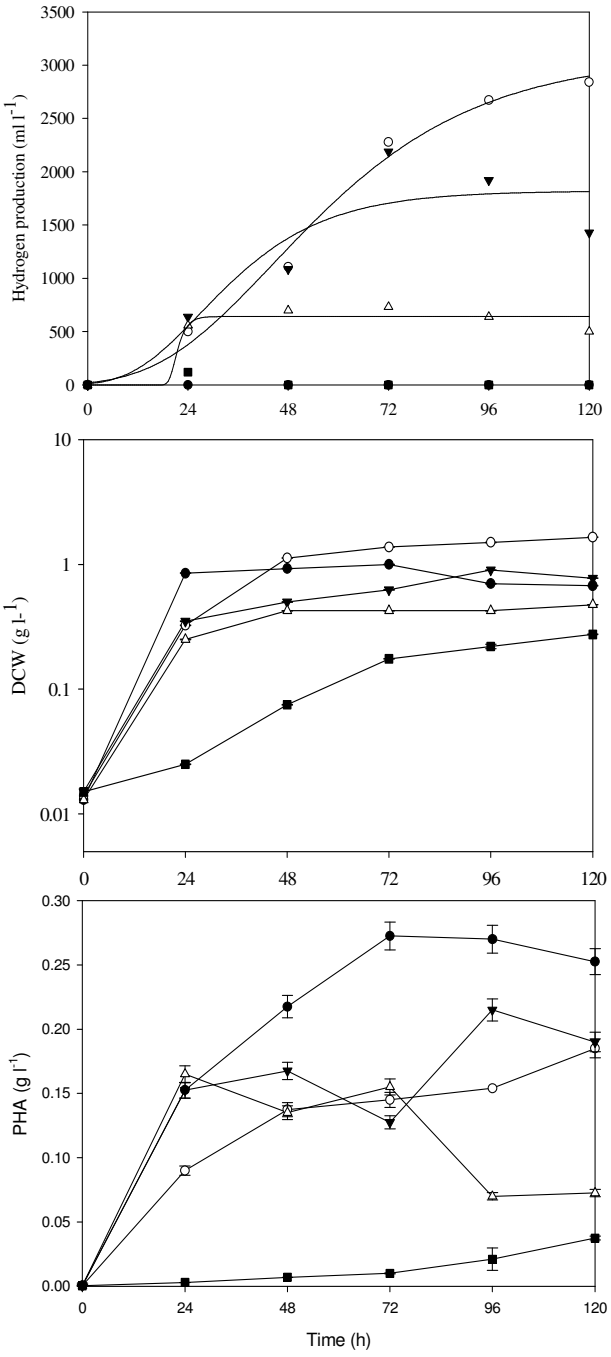

Figure 29. Time course of (top) hydrogen production data fitted to the modified Gompertz equation, (middle) cell growth, and (bottom) PHA content of cultures of *Rps. palustris* TN1 in various dilutions of unsupplemented POME: • undiluted, □ 1/2 dilution, ▼ 1/5 dilution, Δ 1/10 dilution, and ■ 1/20 dilution.

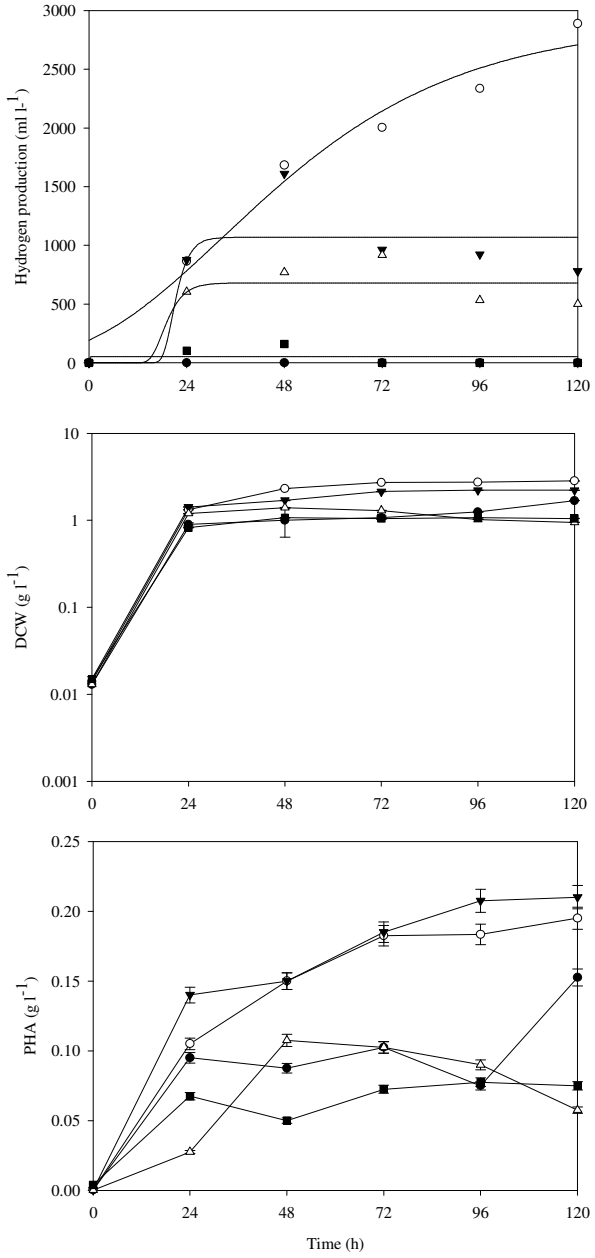

Figure 30. Time course of (top panel) hydrogen production data fitted to the modified Gompertz equation, (middle) cell growth, and (bottom) PHA content of cultures of *Rps. palustris* TN1 in various dilutions of supplemented POME: • undiluted, □ 1/2 dilution, ▼ 1/5 dilution, Δ 1/10 dilution, and ■ 1/20 dilution.

The regression equation for PHA production from the RSM (section 5, Eq. 8) was also used to predict PHA production of the cultures in undiluted and 1/2, 1/5, 1/10, and 1/20 dilutions of unsupplemented and supplemented POME. These were 1.74, 1.66, 1.55, 1.45, and 1.39 g l^{-1}, respectively for the unsupplemented POME, and 1.77, 1.85, 1.55, 1.45, and 1.39 g l^{-1}, respectively, for supplemented POME. Unlike the underestimates of hydrogen production from the RSM predictions, the RSM predictions greatly overestimated PHA production (Table 41). Since the RSM was also proven reliable for predictions of PHA production using artificial media (section 5), these differences provide further evidence that there are critical ingredients in POME influencing PHA production, which are as yet unaccounted for.

Table 41. PHA content of cultures of *Rps. palustris* TN1 in POME and supplemented POME at the end of cultivation.

Dilution	PHA content (%)	
	Unsupplemented POME	Supplemented POME
Undiluted	37.4	9.03
1/2 dilution	11.2	6.84
1/5 dilution	24.5	9.44
1/10 dilution	15.3	6.05
1/20 dilution	13.6	7.14

On the basis of cell growth rates and hydrogen production (H_{max}) (Fig. 19 and Table 20), a 1/2 dilution of unsupplemented POME is the best medium for hydrogen production. The results of this study indicate that the potential for hydrogen production by *Rps. palustris* TN1 in this dilution of POME is quite competitive with the potentials presented in the literature (Table 42).

Table 42. A comparison of hydrogen production from various wastewaters by PNSB.

Organism	Wastewater	H_2 production rate (ml l^{-1} h^{-1})	References
Rps. sp.	Sewage	3	Sunita and Mitra, 1993
Rps. palustris WP3-5	Carbohydrate fed fermentation reactor effluent	8	Lee and Hung, 2006
Rsp. rubrum S1	Lactic acid production wastewater	16-24	Zurrer and Bachofen, 1979
Rsp. rubrum S1	Whey	2-8	Zurrer and Bachofen, 1979
Rba. sphaeroides O.U.001	Olive mill wastewater (OMW)	9	Eroglu *et al*., 2004
Rba. sphaeroides O.U.001	Sugar refinery wastewater	5	Yetis *et al*., 2000
Rba. sphaeroides RV	Tofu wastewater	59	Zhu *et al*., 1999
Rba. sphaeroides O.U.001	Distillery wastewater	22	Sasikala *et al*., 1992
Rps. palustris PBUM001	undiluted POME	10*	Jamil *et al*., 2009
Rps. palustris TN1	1/2 dilution POME	41.3	This study

*VFA content of the POME unknown; cultures were sparged with argon to establish anaerobic conditions.

8. Strain improvement to increase ALA production by PNSB

8.1 Survey of ALA production levels among PNSB of collection of stock cultures of the Environmental Biotechnology Laboratory, Faculty of Agro-Industry, Prince of Songkla University, Thailand

PNSB can be used to produce 5-aminolevulinic acid (ALA), which has many applications (Sasaki *et al*., 2002). As a first step towards exploiting this metabolic capability of PNSB for the production of ALA using POME as substrate, the stock cultures of PNSB in the collection of the Environmental Biotechnology Laboratory, Prince of Songkla University were screened for their extracellular ALA production capacities using modified glutamate-acetate (GA) medium as substrate. The cultures were incubated under aerobic-dark and anaerobic-light conditions.

By chemical assay, the amount of extracellular ALA produced by the stock cultures under aerobic-dark and anaerobic-light condition were determined to be within the range of 7.07-9.27 µM and 5.90-6.85 µM, respectively. However, using HPLC no extracellular ALA could be detected for the cultures incubated under aerobic-dark conditions (Table 43) and the levels were significantly lower for the cultures incubated anaerobically in the light. The results indicated that there is a difference between the chemical assay of ALA and detection by HPLC.

The chemical assay is used to detect pyrrole formed from the condensation of ALA in the presence of acetyl acetone (Nishikawa *et al*., 1999). The amine group of the pyrrole is reacted with the aldehyde of *p*-dimethylamino benzaldehyde (DMAB) in acid solution (Ehrlich's reagent), producing a purple-red compound (Mauzerall and Granick, 1956). Based on the principle of this assay, it can be implied that the Ehrlich's reagent will react with all pyrroles present in the culture broth, or any other compounds having an amine group; for example, Chutmanop *et al*. (2008) reported on the determination of glucosamine concentrations using acetyl acetone and Ehrlich's reagent as an indicator for *Aspergillus oryzae* growth. Unlike the chemical assay, HPLC is reliable and highly sensitive. Most importantly, HPLC determination of ALA content involves detection of fluorescent derivatives of ALA prepared via the Huntzch reaction (Sithisarankul *et al*., 1999; Dalton *et al*., 2002; lee *et al*., 2004), and so avoids the problem of the inability to identify those pyrroles

specifically derived from ALA, which is associated with the chemical assay. An added benefit of HPLC analysis is that it is unaffected by many contaminants that may be present in culture broths, including Na^{+}, Mg^{2+}, ethanol, acetone, and methanol (li *et al*., 2007). For these reasons, HPLC was used for all subsequent measurements of extracellular ALA.

By HPLC analysis, among the stock cultures of wild type strains of PNSB, *Rba. sphaeroides* SH5 secretes the highest amount of extracellular ALA (Table 43). Mutants of PNSB that were isolated following treatments with the chemical mutagen NTG and the physical mutagen UV radiation, were not improved with respect to extracellular ALA production (Table 43). Therefore, a new approach was undertaken that would alter ALA metabolism, by reducing but not eliminating its consumption by porphobilinogen synthase (PBGS) activity. The investigation is detailed in this section.

Table 43. Extracellular ALA levels in cultures of PNSB grown in modified GA medium at 30°C under two different conditions for a 24 h cultivation period.

Strain (lineage)	Aerobic-dark conditions (150 rpm)		Anaerobic-light conditions (3000 lux)	
	Chemical assay (μM)	HPLC (μM)	Chemical assay (μM)	HPLC (μM)
Rba. sphaeroides TK6 (wild type)	9.16±0.05	0	6.85±0.06	3.42±0.03
Rba. sphaeroides FS4 (wild type)	7.70±0.08	0	6.74±0.05	3.32±0.04
Rba. sphaeroides SH5 (wild type)	9.27±0.06	0	6.85±0.03	3.74±0.02
Rba. sphaeroides ES16 (wild type)	7.64±0.04	0	6.40±0.02	3.10±0.02
Rba. sphaeroides U7 (UV mutant of ES16)	7.07±0.04	0	6.63±0.01	2.34±0.01
Rba. sphaeroides N20 (NTG mutant of ES16)	7.75±0.06	0	5.90±0.05	2.68±0.02
Rba. capsulatus SS3 (wild type)	n.a.[a]	n.a.	n.a.	n.a.
Rba. capsulatus SN28 (NTG mutant of SS3)	8.99±0.05	0	6.18±0.04	2.82±0.03
Rps. palustris TN1 (wild type)	0.9±0.03	0	2.13±0.03	1.41±0.02

[a]Not available.

8.2. Engineering an ALA$^-$ mutant strain for isolating *hemB* mutants (by spontaneous and/or forced mutations) coding for PBGS with reduced activity

8.2.1 Attempting the construction of an SH5 *hemA*-disruption mutant strain using a *Rba. sphaeroides* 2.4.1 *hemA* disruption vector

The suicide vector pUI1007 carries the *Rba. sphaeroides* 2.4.1 *hemA* gene within which is inserted the transcription-translation termination omega cassette (Neidle and Kaplan, 1993). It was reasoned that homologous recombination, resulting in replacement of the wild type SH5 *hemA* gene with the 2.4.1 *hemA*-disrupted allele, should be possible, provided the level of similarities between the two genes are sufficiently high. Following mobilizations of pUI1007 into both 2.4.1 and SH5, suitable recombinant candidates (double cross-over candidates would be Kn^r but Tc^s; see Table 5) were identified among exconjugants of both strains. However, by immunoblot analysis, a functional *hemA* gene had been retained in the SH5 candidate (Fig. 31). On the basis of this result, it was concluded that a *hemA*-disrupted mutant derivative of SH5 could not be obtained using the heterologous suicide vector pUI1007.

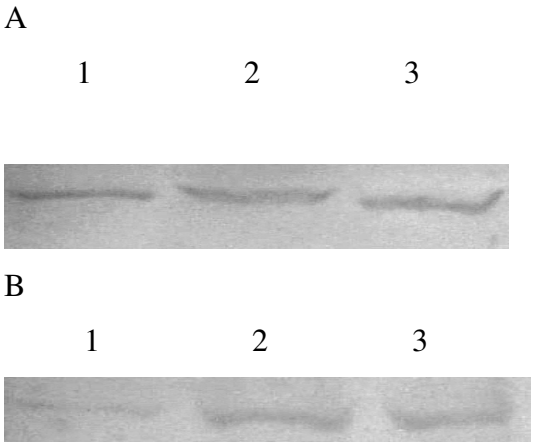

Figure 31. Immunoblots of protein samples probed with (A) anti HemA antisera and (B) anti-HemT antisera. For each blot, lane 1: SH5, lane 2: Tc^r, and lane 3: Tc^s. Equivalent amounts of total protein were used.

The number of ALA synthase genes among wild type strain of *Rba. sphaeroides* is variable. Among the sequenced wild type strains, there are two genes, *hemA* and *hemT*, that encode ALA synthase isoenzymes in *Rba. sphaeroides* strains 2.4.1 and ATCC17029, whereas there is only one ALA synthase gene, *hemA*, in wild type strain ATCC17025. Should SH5 belong to the group having *hemA* alone, elimination of that one gene could be incompatible with viability. Using mono-specific anti-HemT antisera, the status of the *hemT* gene in strain SH5 was evaluated. Based on the presence of immunodetectable HemT protein (Fig. 31B), it can be concluded that *Rba. sphaeroides* SH5 has both *hemA* and *hemT* genes. Therefore, the inability to isolate a *hemA*-disrupted mutant derivative of SH5 must have a different explanation. One possibility is that the number of differences in DNA sequences between the *Rba sphaeroides* 2.4.1 *hemA* gene and the corresponding gene in *Rba. sphaeroides* SH5 precludes successful homologous recombination.

8.2.2 Construction of an Ω cartridge insertion-*hemA* gene disruption plasmid

Using primers HemA-UP and HemA-ALL (Zeilstra-Ryalls and Kaplan, 1995) *hemA* sequences from *Rba. sphaeroides* SH5 were amplified by PCR. DNA sequence analysis of the purified PCR product revealed that, at the nucleotide level, the HemA coding sequences of *Rba. sphaeroides* SH5 are 99% identical to those of *Rba. sphaeroides* 2.4.1. However, among the 96 base pairs of *hemA* upstream sequence there were three mismatches with the corresponding region of 2.4.1. These could be responsible for the inability to obtain recombinants using plasmid pUI1007. Therefore, a non-heterologous suicide vector for disruption of SH5 *hemA* was undertaken. This involved two steps: (1) The SH5 *hemA* PCR product was ligated into *Sca*I-treated pSUP202 (Table 6), which also deletes a 1 kb fragment from the vector. (2) An *Xho*I-ended omega fragment isolated from pUI1638 (Table 6) was ligated into the unique *Xho*I site within the *hemA* sequences carried on the recombinant plasmid from step 1. Following mobilizations of this plasmid, pMS4, into SH5, no suitable recombinant candidates were obtained. While this experimental outcome eliminates the possibility that non-homology is the reason for the lack of

successful recombination, it does not address the possibility that the recombination capacity itself of SH5 is poor.

8.3 Designing and constructing a *hemB* mutant gene encoding an enzyme expected to have reduced activity

8.3.1 Construction of plasmid vectors with wild type or mutant *hemB* genes that can replicate in *Rba. sphaeroides*

Suwanto (2002) had previously used antisense RNA as a means to reduce HemB levels. However, it was reported that the cells are impaired in growth and so this was not a useful approach. Bollivar *et al*. (2004) have examined the oligomeric nature of *Rba. capsulatus* HemB protein *versus* its enzymatic activity. Their data suggest that the dimeric form has lower activity than higher order multimers (Fig. 32). This protein is 71% identical to the *Rba. sphaeroides* 2.4.1 HemB protein. Furthermore, models of the structures of *Rba. sphaeroides* HemB dimers and octamers (kindly provided by E. Jaffe, Fox Chase Cancer Center, PA) suggest that it is very similar in structure to *Rba. capsulatu*s HemB. On the basis of these enzymatic and structural data, a mutant protein was designed that was predicted to be unaffected in its ability to dimerize, but reduced in its ability to form higher order multimers. As shown in the models (Fig. 32), the N-terminal 26 residues comprise a region that is likely to be important for stabilization between dimers, and so it was hypothesized that an internal deletion of amino acid residues 15-27 would reduce or possibly eliminate the formation of oligomers involving dimer-dimer interactions.

Oligonucleotide-directed mutagenesis was used to generate the *hemB* mutant plasmid derivative of pUI1992, pMS1 (Fig. 33). The vector-localized restriction endonuclease sites for XhoI and HindIII that flank the *hemB* sequences were then used to obtain fragments from pUI1992 and pMS1. These were ligated to plasmid pBBR1MCS-2, which is capable of replicating in *Rba. sphaeroides*, that had been treated with the same enzymes used to generate the fragments, creating plasmids pMS2 and pMS3, respectively (Fig. 33).

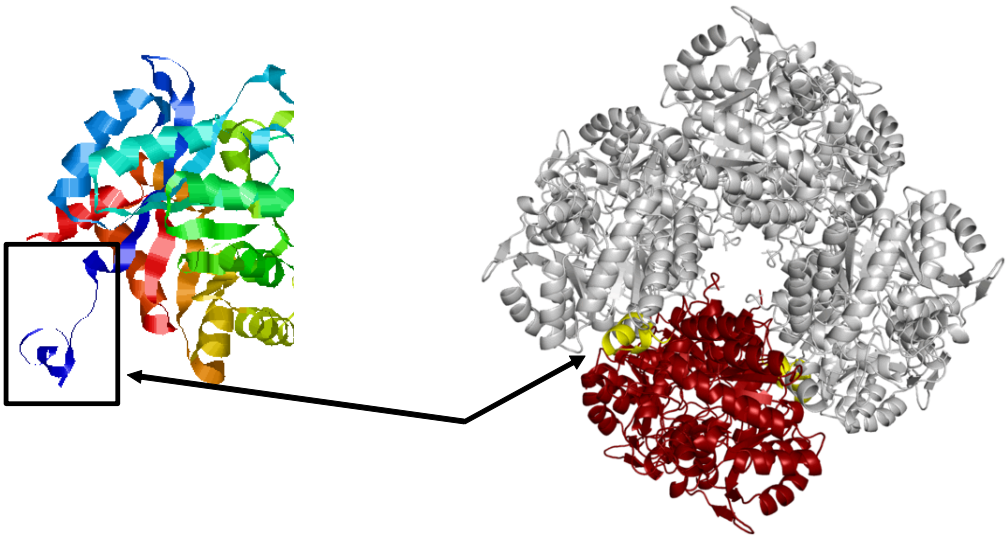

Figure 32. Models of PBGS monomer (left) and octamer (right). The N-terminal region spanning residues 1-26 that is thought to comprise the octamerization domain is boxed in the monomer and highlighted in yellow in the octamer; a single dimer within the octamer is colored red. Monomer and octamer coordinates were kindly provided by E. Jaffe, Fox Chase Cancer Center, PA.

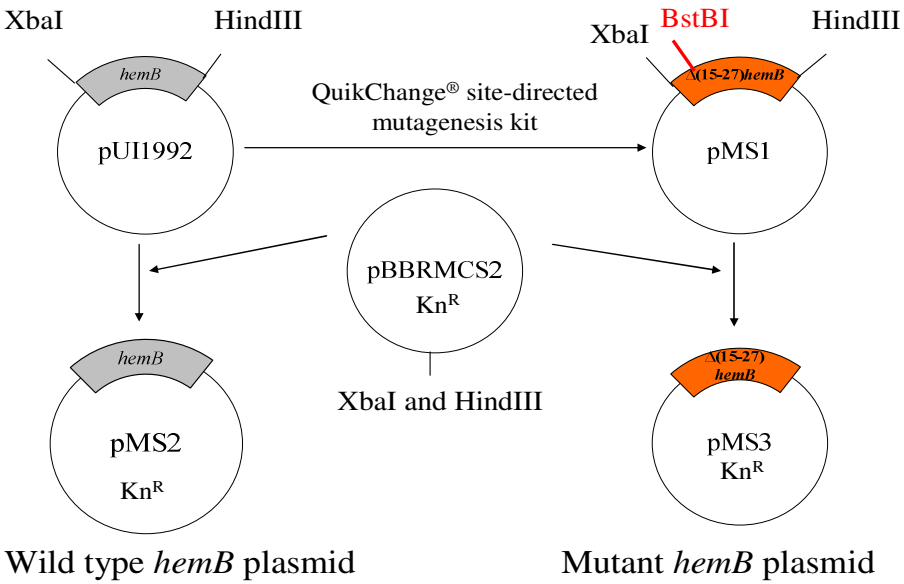

Figure 33. Schematic diagram of constructions of plasmids pMS2, which carries the wild type *hemB* gene, and pMS3, which carries the Δ(15-27) *hemB* mutant allele.

8.3.2 Multicopy analysis

Together with the plasmid vector pBBR1-MCS2, the recombinant plasmids pMS2 and pMS3 were mobilized into *Rba. sphaeroides* wild type strain SH5. The expectation was that, if the mutant *hemB* gene encodes a protein with diminished capacity to participate in oligermization involving dimer-dimer interactions, multiple copies of the defective gene should behave in a dominant-negative fashion. Consequently, the biosynthesis of tetrapyrroles should be reduced, and ALA should accumulate. By reducing, rather than eliminating PBGS activity, it was also predicted that growth would still be sustained. The ability to obtain exconjugants of pMS3 under aerobic-dark conditions already indicated that tetrapyrrole production levels were adequate for growth. Since phototrophic growth conditions have the highest demand for tetrapyrrole production, due to the need for large amounts of bacteriochlorophyll to support photosynthesis, the ability of the pMS3 exconjugants to also grow under anaerobic-light conditions demonstrated that PBGS activity remained sufficient to also meet those needs.

To determine whether or not HemB activity was indeed reduced in the presence of multiple copies of the defective *hemB* gene, PBGS assays were performed using cells that were cultured aerobically in the dark and anaerobically in the light. The results, shown in Fig. 34, reveal that, regardless of growth conditions, the presence of multiple copies of the defective *hemB* gene reduce PBGS activity to levels below that in cells having the single copy of the wild type *hemB* gene alone (SH5 with pBBR1-MCS2 *versus* SH5 with pMS3). This pattern of PBGS activities is precisely what would be predicted if the product of the mutant gene is capable of "poisoning" the wild type protein through the formation of mixed dimers consisting of one mutant and one wild type polypeptide.

To confirm the negative impact of the defective polypeptide on the ability to form higher order oligomers, an immunoblot was prepared from proteins resolved by polyacrylamide gel electrophoresis performed under non-denaturing conditions, and then probed with anti-HemB antisera (Fig. 35). While the dimeric form of the protein could be detected in SH5 with either pMS2 or pMS3, higher molecular weight HemB species was only detected in SH5 with pMS2.

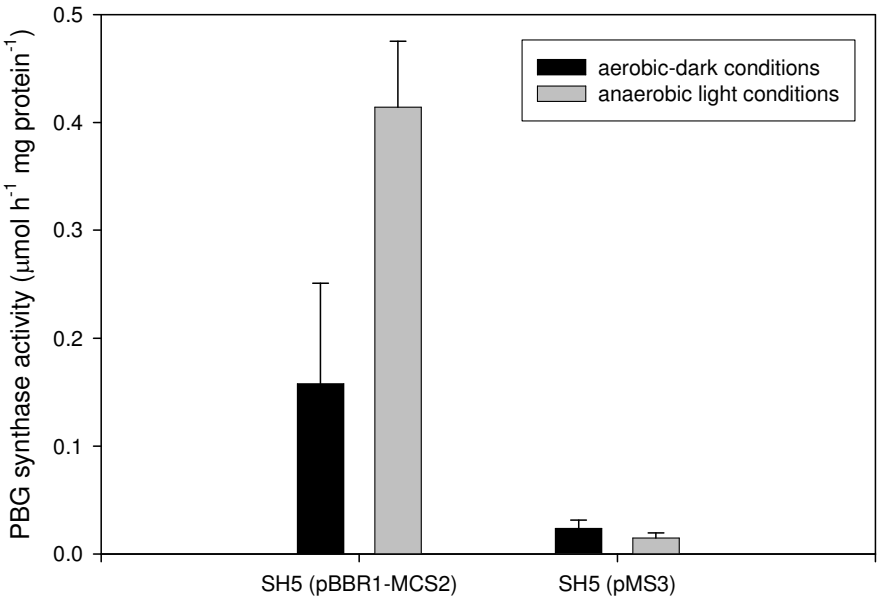

Figure 34. PBG synthase activity in SH5 with the plasmids indicated. Bar heights indicate the average levels of two independent replicates, with the errors indicated.

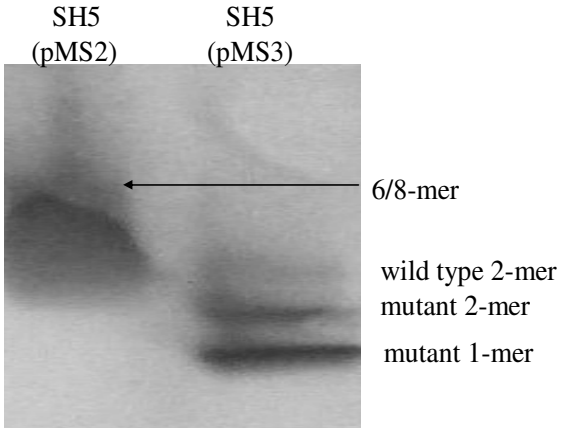

Figure 35. Oligomer analysis of PBGS in *Rba. sphaeroides* SH5 harboring the plasmids indicated. Equivalent amounts of total protein were subjected to non-denaturing polyacrylamide gel electrophoresis, and transferred to a nitrocellulose membrane which was then probed with anti-HemB antisera.

The central question of this study, whether or not reducing HemB activity would increase ALA accumulation, and so also extracellular ALA production, was addressed by comparing the levels of extracellular ALA in cultures of SH5 with pBBR1-MCS2 *versus* SH5 with pMS3. As determined by HPLC, after 24 h of cultivation in modified GA medium under anaerobic-light conditions the concentration of ALA in the culture broth of SH5 with pBBR1-MCS2 was 3.16 μM, while that in the culture broth of SH5 with pMS3 was 6.28 μM. Therefore, the reduction in PBGS activity brought about by the presence of multiple copies of the mutant *hemB* gene nearly doubled the amount of extracellular ALA produced by the cells. Furthermore, this significant increase in ALA production was accomplished with a minimal impact on growth; the specific growth rate of SH5 (pBBR1-MCS2) was 0.386 h^{-1} while the specific growth rate of SH5 (pMS3) was 0.341 h^{-1}.

9. Extracellular ALA production potential of POME

The potential for using POME as a cost-effective medium for growth of the ALA production strain *Rba. sphaeroides* SH5 (pMS3) was investigated. The optimum dilution of unsupplemented POME for hydrogen production by *Rps. palustris* TN1 was 1/2 (section 7). Based on that result, the ability of *Rba. sphaeroides* SH5 (pMS3) to grow and produce extracellular ALA in undiluted POME and 1/2 diluted POME was evaluated. *Rba. sphaeroides* SH5 with pBBR1-MCS2 was used as a control for any consequences associated with the defective *hemB* allele carried on plasmid pMS3. The investigations were carried out in 50 ml serum vials containing 40 ml of undiluted and 1/2 dilution of POME that were incubated micro-aerobically with a light intensity of 3000 lux. The pH of the POME was adjusted to 7.07 before sterilization.

Fig. 36 demonstrates the growth and pH changes of *Rba. sphaeroides* SH5 (pBBR1-MSC2) and *Rba. sphaeroides* SH5 (pMS3) cultured in undiluted POME and 1/2 dilution POME. The pH changes during cultivation of both strains were greater than 2 pH units, and were alkaline pH at the end of cultivation.

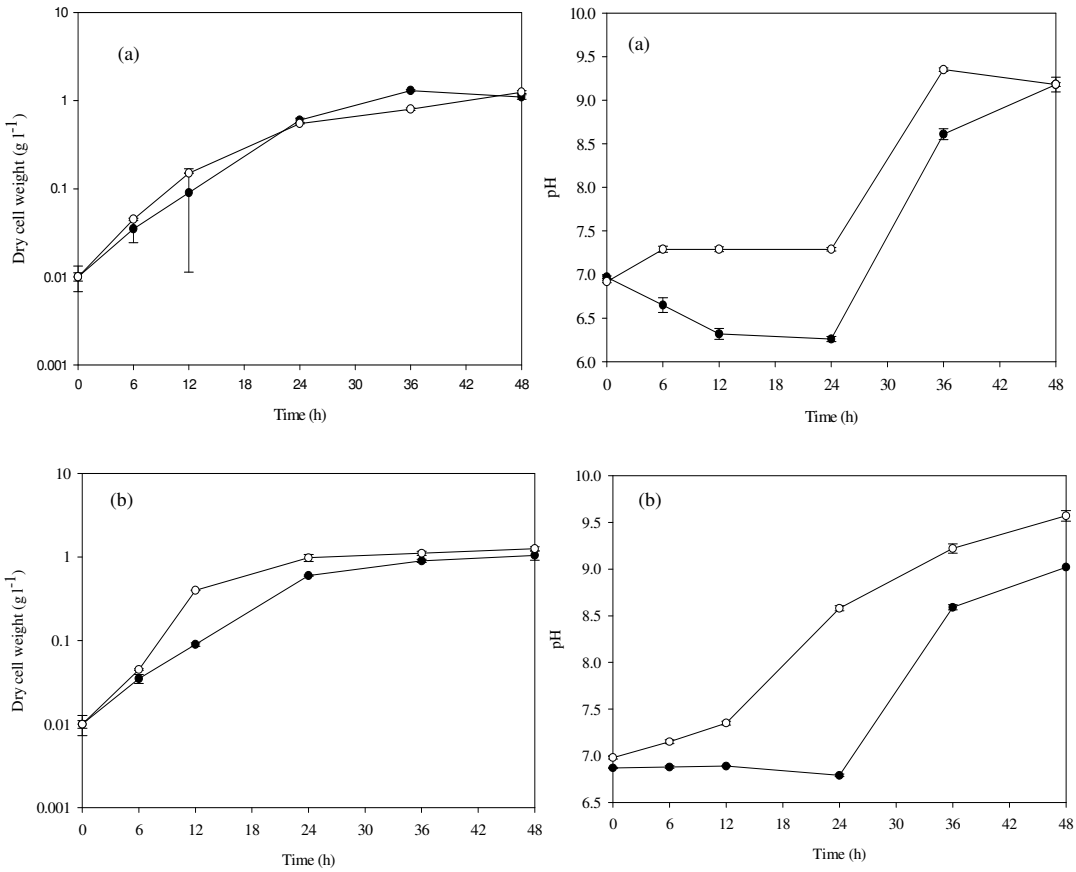

Figure 36. Time course of cell growth and pH change of cultures of (a) *Rba. sphaeroides* SH5 (pBBR1-MSC2) and (b) *Rba. sphaeroides* SH5 (pMS3) in various dilutions of unsupplemented POME: • undiluted, and ○ 1/2 dilution.

The specific growth rates of *Rba. sphaeroides* SH5 (pBBR1-MSC2) and *Rba. sphaeoides* SH5 (pMS3) cultured in undiluted POME and 1/2 dilution POME were very similar (Table 44). The rates are also similar to those measured for the same strains cultured in modified GA medium (section 10; 0.386 h^{-1} and 0.341 h^{-1} for SH5 with pBBR1-MCS2 and pMS3, respectively), indicating that POME does not contain components that negatively affect growth of the bacteria. The maximum levels of extracellular ALA produced by *Rba. sphaeroides* SH5 (pMS3) cultured in undiluted POME and 1/2 diluted POME were observed after 6 h of cultivation with the concentration of 36.3 and 61.0 µM, respectively. The maximum extracellular levels of ALA for *Rba. sphaeroides* SH5 (pBBR1-MCS2) were measured in a 12 h

culture in undiluted POME, while ALA remained undetectable even after 48 h of culturing in the 1/2 dilution of POME (Table 44).

The total amounts of VFA consumed at the times corresponding to the maximum concentrations of ALA were also determined (Table 44). Interestingly, there was no correspondence between VFA consumption and extracellular ALA production levels for either strain. Likewise, there was no correspondence between rates of consumption of individual VFAs consumption (Table 45) and ALA production (Table 46).

These studies reveal that *Rba. sphaeroides* SH5 (pMS3) produces approximately 19-fold more extracellular ALA than *Rba. sphaeroides* SH5 (pBBR1-MSC2), when cultured in undiluted POME. They also indicate that *Rba. sphaeroides* SH5 (pMS3) could be used as bioremediator for POME treatment. Finally, they suggest that culturing these bacteria in POME is a cost-effective means to produce ALA. The low cost of producing ALA in this way has the potential to expand its use in agricultural applications; for example, as a biostimulator for plant growth (Sasaki *et al*., 2002; Suwansaard, 2004).

Table 44. Performance of *Rba. sphaeroides* SH5 with the plasmid vector pBBR1-MCS2 versus SH5 with pMS3 in unsupplemented POME.

POME dilution	Strain (plasmid)	Initial pH	Final pH	Specific growth rate (h^{-1})	Total VFA consumption (%)	Maximum extracellular ALA (μM)
undiluted	SH5 (pBBR1-MCS2)	6.47	9.18	0.183	47.3 (at 12 h)	2.86(at 12 h)
	SH5 (pMS3)	6.52	9.02	0.183	61.6 (at 6h)	36.3 (at 6h)
1/2 dilution	SH5 (pBBR1-MCS2)	6.92	9.18	0.307	40.1 (after 48h)	0 (after 48h)
	SH5 (pMS3)	6.92	9.57	0.307	36.7 (at 6h)	61.05 (after 6h)

Table 45. Consumption of individual VFAs (mM) present in unsupplemented POME after 48 h cultivation.

POME dilution	Strain (plasmid)	Acetate	Propionate	Isobutyrate	Butyrate	Isovalerate	Valerate	Isocaproate	Caproate	Heptanoate
undiluted	SH5 (pBBR1-MCS2)	15.89	2.22	0.25	12.73	0.28	6.43	0	4.29	0.48
	SH5 (pMS3)	20.09	8.42	0.63	11.93	0.48	6.30	0	4.80	0.39
1/2 dilution	SH5 (pBBR1-MCS2)	3.46	2.6	0	4.94	0	2.88	0	2.11	0
	SH5 (pMS3)	1.68	0	0	4.31	0	2.35	0	2.43	0.42

Table 46. ALA production by *Rba. sphaeroides* SH5 with the plasmid vector pBBR1-MCS2 versus SH5 with pMS3 in unsupplemented POME.

Time (h)	Undiluted POME		1/2 dilution POME	
	SH5 (pBBR1-MCS2)	SH5 (pMS3)	SH5 (pBBR1-MCS2)	SH5 (pMS3)
0	0	0	0	0
6	1.77	36.32	0	61.05
12	2.82	1.99	0	4.34
18	0	1.65	0	0
24	0	1.95	0	1.15
36	0	5.15	0	0
48	0	0	0	0

10. Development of a novel bioassay for extracellular ALA detection

The ALA bioassay was developed based on the ALA auxotrophy of *Rba. sphaeroides* AT1 (Neidle and Kaplan, 1993). This mutant strain is a genetically engineered derivative of *Rba. sphaeroides* 2.4.1, which contain two ALA synthase genes, *hemA* and *hemT*. *Rba. sphaeroides* AT1 was constructed by using suicide vectors to replace the wild type genes with the defective alleles *hemA*::ΩKn^r and *hemT* ::ΩSp^r/Sr^r (Neidle and Kaplan, 1993), and so it is incapable of growing in the absence of added ALA. This requirement for ALA suggested the possibility that *Rba. sphaeroides* AT1 growth could be used as a biomeasurement of extracellular ALA produced by *Rba. sphaeroides* SH5. In order to do so, the amount of AT1 growth achieved relative to the amount of ALA added to the medium was first evaluated. The relationship between growth and added ALA (Appendix B) for *Rba. sphaeroides* AT1 cultured in SIS medium under aerobic-dark conditions with Sp/St is approximately linear between 4-20 μM of added ALA (R^2 = 0.89). The growth of *Rba. sphaeroides* AT1 was then measured after culturing the bacteria under the same conditions but with the addition of supernatant from cultures of *Rba. sphaeroides* SH5 (pBBR1-MCS2) and *Rba. sphaeroides* SH5 (pMS3) in modified GA medium. A

similar analysis was performed using the supernatants of SH5 (pBBR1-MCS2) and SH5 (pMS3) grown in POME. The extracellular ALA concentrations deduced from the standard curve (Appendix B) are compared to the concentrations determined by HPLC in Table 47, together with the differences between the two measurements.

The difference between the bioassay and HPLC measurements of extracellular ALA produced by the cultures grown in modified GA medium was less than 15%. However, the difference was larger for cultures grown in POME. It is likely that there are substances in the chemically highly complex POME that are affecting *Rba. sphaeroides* AT1 growth, thus rendering the bioassay less reliable. A more detailed knowledge of the composition of POME should make it possible to modify the bioassay conditions. The cost effectiveness of the bioassay compared to HPLC determination of ALA concentrations warrants such a study.

Table 47. Bioassay *versus* HPLC determination of extracellular ALA in supernatants of SH5 with plasmids pBBR1-MCS2 or pMS3.

Medium	Strain	[ALA] measured by bioassay (μM)	[ALA] determined by HPLC (μM)	Deviation (%)
Modified GA	SH5 (pBBR1-MSC2)	3.67	3.16	14.3
	SH5 (pMS3)	6.28	6.07	3.3
Undiluted POME	SH5 (pBBR1-MSC2)	0.03	1.7	98.2
	SH5 (pMS3)	16.80	36.2	55.5

11. Integrated hydrogen and ALA production by two PNSB

11.1 Effect of ALA concentration on cell growth and hydrogen production by *Rps. palustris* TN1, co-cultured with SH5 (pMS3)

The feasibility of combining hydrogen and ALA production using VFAs as substrates was conducted for cultures grown under anaerobic-light conditions (3,000 lux) conditions. First, the effect of ALA on cell growth and hydrogen production was evaluated. *Rps. palustris* TN1 with the plasmid vector pBBR1-MCS2 was used here, so that it would be capable of growing in the presence of Kn used for maintenance of the plasmid pMS3 in the ALA production strain *Rba. sphaeroides* SH5 (pMS3). The bacteria were co-inoculated into in GA medium containing 20 mM acetate as a carbon source and with Kn (50 μg ml^{-1}). The medium was then further supplemented with commercial ALA varied from 0 to 1 mM.

Hydrogen production for all of the co-cultures, irrespective of added ALA concentrations, was similar (Fig. 37 and Table 48). In all cases hydrogen production was detectable after 8 h, and the maximum hydrogen production rate and the maximum cumulative hydrogen production were not significantly different ($P<0.05$). The maximum hydrogen production rates were in the range of 32.4-39.8 ml l^{-1} h^{-1} and the maximum cumulative hydrogen productions were in the range of 1,233-1,356ml l^{-1}(Table 30). The results indicate that ALA concentration had no effect on hydrogen production. However, the hydrogen production efficiency (72%) and light conversion efficiency (1.40%) were greatest for the culture with 60 μM ALA.

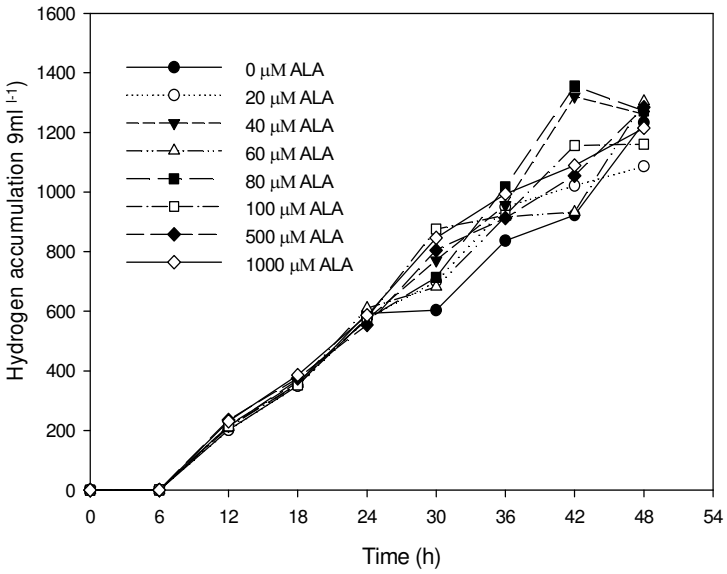

Figure 37. Effect of ALA concentrations on hydrogen production by *Rps. palustris* TN1.

The specific growth rates were variable. The rates increased to a maximum for the culture having 60 μM ALA supplementation (1.3×10^4 h^{-1}) (Table 48), but decreased at higher concentrations. At concentrations up to 60 mM, it may be that ALA is being used as an additional source of carbon and nitrogen, but higher amounts of this acid may have negatively affected growth by lowering the pH. However, even at an ALA concentration of 1 mM, growth was only reduced by 12.2%.

Table 48. Effect of ALA concentrations on hydrogen production by *Rps. palustris* TN1 cultivated in modified GA medium under anaerobic-light condition (3000 lux) at 30 °c.

Initial ALA conc. (µM)	Final ALA conc. (µM)	Final pH	Specific growth rate (h^{-1} x 10^{-3})	Acetate consumption (%)[a]	H_2 Yield (mol H_2 mol acetate^{-1})[a]	H_2 production efficiency (%)[a]	Light conversion efficiency (%)[a]
0	2	7.01	8.20	100	2.53	63.4	1.02
20	7.1	7.00	9.90	100	2.55	63.8	1.26
40	15.3	7.00	11.8	100	2.81	70.4	1.31
60	21.5	7.03	12.9	100	2.90	72.7	1.40
80	35.9	7.02	11.8	100	2.86	71.4	1.34
100	39.3	7.00	10.2	100	2.59	64.8	1.36
500	42.2	6.99	9.8	100	2.59	64.8	1.22
1000	151.5	6.93	7.2	100	2.71	67.8	1.22

[a] Determine at the end of the cultivation period.

Table 49. Evaluation of the kinetics of hydrogen production by *Rps. palustris* TN1 from various ALA concentrations.

ALA conc. (μM)	λ (h)	R_{max} (ml l^{-1} h^{-1})	H_{max} (ml l^{-1})	R^2
0	8	34.3	1,233	0.9865
20	8	35.6	1,671	0.9969
40	8	39.0	1,658	0.9921
60	8	32.4	1,582	0.9861
80	8	39.8	1,742	0.9898
100	8	39.8	1,764	0.9954
500	8	34.6	1,314	0.9950
1000	8	38.6	1,356	0.9978

11.2 Hydrogen and ALA production by co-cultures of the two strains

Having established that the addition of ALA had little effect on hydrogen production or rate of increase in cell density, the effect of inoculum ratios of *Rba. sphaeroides* SH5 to *Rps. palustris* TN1 (1:10, 1:1 and 10:1) on growth of each bacterium was investigated. Dilutions of the culture were spotted onto GA agar in order to determine the numbers of viable cells present at the end of the cultivation period.

For all ratios of inoculums, only an increase in the numbers of *Rba. sphaeroides* SH5 cells was observed. After 48 h cultivation, the numbers of colony forming units present for each culture were as follows: for SH5 alone, $17x10^{-6}$; for TN1 alone, $3x10^{-4}$; for SH5:TN1 inoculum ratio of 1:10, $15x10^{-6}$; for SH5:TN1 inoculum ratio of 1:1, $17x10^{-6}$; and for SH5:TN1 inoculum ratio of 10:1, $21x10^{-6}$ CFU ml^{-1} (Table 50). Other than for the pure culture of TN1 alone, no colonies of TN1 were visible. This result suggests that the *Rps. palustris* TN1 growth was slower than *Rba. sphaeroides* SH5. While in all cases, acetate was completely consumed within the first 12 h of cultivation, as would be expected in the absence of TN1, no hydrogen production was observed and the pH changed from 7 to 9.

Table 50. Effect of inoculum ratios of *Rps. palustris* TN1 (pBBR1-MCS2) and *Rba. sphaeroides* SH5 (pMS3) on the growth of each bacterium.

Co-culture ratio	CFU.ml^{-1} (x 10^6)	SH5 CFU.ml^{-1} (x 10^6)	TN1 CFU.ml^{-1} (x 10^4)
SH5 (1)	17 ± 4	17 ± 4	-
TN1 (1)	0.03 ± 3		13 ± 3
SH5:TN1 (1:10)	15 ± 3	15 ± 3	-
SH5:TN1 (1:1)	17 ± 4	17 ± 4	-
SH5:TN1 (10:1)	21 ± 4	21 ± 4	-

However, when *Rps. palustris* TN1 (pBBR1-MCS2) was inoculated 24 h before the addition of *Rba. sphaeroides* SH5 (pMS3) at the ratio of 1:1, both bacteria were detectable at the end of the incubation period (48 h). Colonies formed from each kind of bacterium are visually distinguishable (Fig. 29).

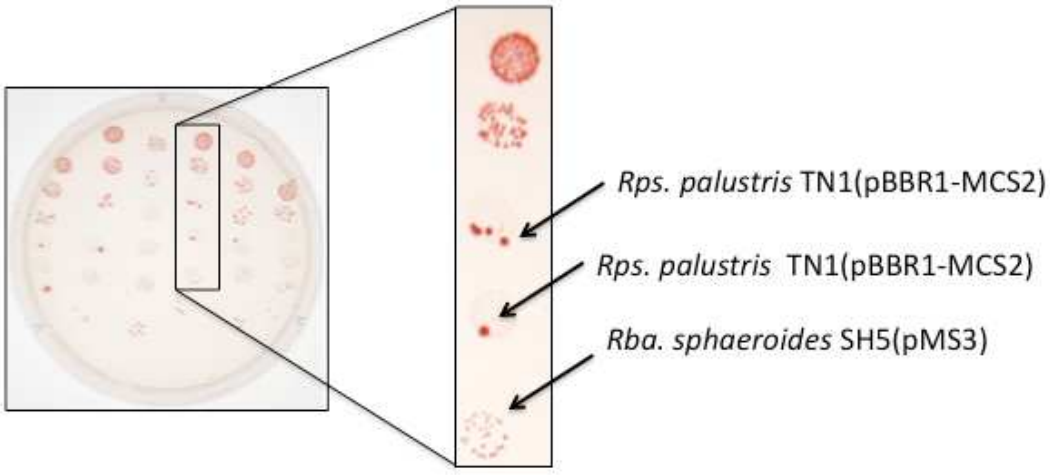

Figure 38. Colonies formed from a mixture of *Rps. palustris* TN1 (pBBR1-MCS2) and *Rba. sphaeroides* SH5 (pMS3) on modified GA agar with Kn.

11.3 Assessment of the outcomes regarding hydrogen and ALA production by co-cultures of two PNSB

The fermentation process by PNSB that is required in order to obtain the commercial bioproducts, hydrogen and ALA, has been established in this section by co-culture of two strains. The outcomes revealed that the difference in growth rates of the strains is prohibitive for successful co-culturing However, a two-staged process could be used to improve the bioconversion of organic wastes to ALA and hydrogen by PNSB. First, *Rps. palustris* TN1 (pBBR1-MCS2) would be used for hydrogen production. Then, through the subsequent addition of *Rba. sphaeroides* SH5 (pMS3), production would be shifted to ALA.

CHAPTER 4

CONCLUSIONS AND SUGGESTIONS

Conclusions

1. Among isolated strains of purple non-sulfur bacteria (PNSB) from Songkhla Lake, the isolate TN1 was chosen for further investigations, because it was found to have the highest hydrogen production capacity.
2. Based on morphological and biochemical tests, TN1 is a *Rhodopseudomonas* sp. strain, and on the basis of its 16s rDNA the bacterium is a newly identified strain of *Rps. palustris* (99% similarity).
3. TN1 produced hydrogen from each of the three predominant VFAs present following anaerobic-dark fermentations of palm oil milling effluent (POME), with optimum concentrations of 20-40 mM acetate, 20 mM butyrate and less than 20 mM propionate.
4. Using Response Surface Methodology (RSM) the optimum mixture of the VFAs for maximum hydrogen production and minimal polyhydroxyalkanoate (PHA) production was 52 mM acetate, 16 mM propionate and 25 mM butyrate, which predicted hydrogen and PHA productions of 1,356 ml l^{-1} and 1.59 g l^{-1}, respectively. These actual values measured for hydrogen evolution were 1,278 ± 39.3 ml l^{-1} and 1.70 ± 0.24 g l^{-1} for PHA formation.
5. To maximize PHA and minimize hydrogen production by RSM, the optimum mixture of the VFAs was 73 mM acetate and 34 mM propionate, the expected PHA production was 1.89 g l^{-1} and the expected hydrogen production was 1,273.9 ml l^{-1}. Under these conditions, PHA content increased 23.7%.
6. A Plackett-Burman statistical model was used to screen for additional important parameters influencing hydrogen production by TN1. Then RSM was used to predict the optima. The model predicts that an initial pH of

7.07, 2.3 g l^{-1} yeast extract and 0.63 g l^{-1} $NaHCO_3$ would be optimal for hydrogen production (2,214 ml l^{-1}). The performance of the model was tested experimentally, and the average value for hydrogen evolution from three replicates was 2,618 ± 273 ml l^{-1}; the efficiency of hydrogen was 62.6% and the light conversion efficiency was 0.7%. The VFA consumption was up to 71.9% when $NaHCO_3$ was supplemented.

6. For TN1 grown in POME, the maximum hydrogen yield of 2.64 and 2.34 mol H_2 mol total VFA^{-1} were obtained at 1/2 dilution of the unsupplemeted and supplemented POME with light conversion efficiency of 0.73 and 0.26%.
7. *Rba. sphaeroides* wild type strain SH5 was improved for higher ALA production by introducing multiple copies of a genetically engineered *hemB* gene that behaved in a dominant negative fashion, reducing porphobilinogen synthase (PBGS) activity present in the cell. PBGS activities in those cells were reduced by approximately 7-fold 0.158 to 0.024 μmoles h^{-1} mg^{-1}) under aerobic-dark conditions and 27-fold (0.414 to 0.015 μmoles h^{-1} mg^{-1}) under anaerobic-light (3,000 lux) conditions compared to control cells having only the wild type *hemB* gene. While extracellular ALA was below detection for cultures grown under aerobic conditions, despite the reduction in PBGS activity, the levels increased by 2-fold (3.16 *versus* 6.28 μM for cultures of the engineered strain grown under anaerobic-light conditions.
8. A novel bioassay for measuring extracellular ALA production was developed based on the ALA requirement of *Rba. sphaeroides* mutant strain for growth. The coefficient of fitness, R^2, for the relationship between growth and ALA concentration was 0.89. The deviation of HPLC extracellular ALA assay and extracellular ALA bioassay was less than 15%.
9. The effect of adding 5-aminolevulinic acid (ALA) (0-1 mM) on the growth of, and hydrogen production by *Rps. palustris* TN1 was investigated. The highest hydrogen production (1,075 ml l^{-1}) was achieved in the medium with the addition of 1 mM ALA.
10. After 48 h cultivation of co-cultures of *Rps. palustris* TN1(pBBR1-MCS2) and *Rba. sphaeroides* SH5(pMS3), no *Rps. palustris* TN1 was detected. However, when *Rba. sphaeroides* SH5(pMS3) was inoculated into a one-day

old growing culture of *Rps. palustris* TN1(pBBR1-MCS2) both bacteteria were detectable after further incubation of the co-culture.

Suggestions

1. Use genetic engineering to disable PHA production, which should improve hydrogen production.
2. Study enzymes involved in hydrogen production such as nitrogenase and hydrogenase by *Rps. palustris* TN1.
3. Develop a suitable bioreactor design for phototrophic hydrogen production.
4. Evaluate large scale production of hydrogen using agro industrial wastes as substrate.
5. Investigate the effect of a light-dark cycle on hydrogen production.
6. Examine the use of sunlight as a light source for hydrogen production.
7. Study parameters affecting PHA production by *R. palustris* TN1.
8. Study the genetic basis for the production of the fluorescent compound by *Rps. palustris* TN1.
9. Investigate the persistence of pH neutrality in *Rba. palustris* TN1 cultures.
10. Develop effective particulate removal methods, such as the use of activated carbon, in order to achieve higher light intensity for hydrogen production from POME.
11. Study in more detail the relationship between hydrogen and PHA production.
12. Investigate ALA recovery and stability produced by the PNSB towards its use in the medical field.

REFERENCES

Akkerman, I., Janssen, M., Rocha, J. and Wijffels, R.H. 2002. Photobiological hydrogen production: photochemical efficiency and bioreactor design. Int. J. Hydrogen Energy 27:1195-1208.

Alber, B.E., Spanheimer, R., Ebenau-Jehle, C. and Fuchs, G. 2006. Study of an alternate glyoxylate cycle for acetate assimilation by *Rhodobacter sphaeroides*. Mol. Microbiol. 61:297-309.

Albers, H. and Gottschalk, G. 1976. Acetate metabolism in *Rhodopseudomonas gelatinosa* and several other *Rhodospirillaceae*. Arch. Microbiol. 111:45–49.

Ali Hassan, M., Shirai, Y., Kusubayashi, N., Ismail Abdul Karim, M., Nakanishi, K. and Hashimoto, K. 1997. The production of polyhydroxyalkanoate from anaerobically palm oil mill effluent by *Rhodobacter sphaeroides*. J. Ferment. Bioeng. 83:485-488.

Altschul, S., Madden, T., Schäffer, A., Zhang, J., Zhang, Z., Miller, W. and Lipman, D. 1997. Gapped BLAST and PSI-BLAST: a new generation of protein database search programs. Nucleic Acids Res. 25:3389-3402.

Anderson, A.J. and Dawes, E.A. 1990. Occurrence, metabolism, metabolic role, and industrial uses of bacterial polyhydroxyalkanoates. Microbiol Rev. 54(4):450–472.

Angenent, L.T., Karim, K., Al-Dahan, M., Wrenn, B.A. and Domiguez-Espinosa, R. 2004. Production of bioenergy and biochemicals from industrial and agricaultural wastewater. Trends Biotechnol. 22:477-485.

APHA. 1998. Standard Methods for Examination of Water and Wastewater, 19th ed. American Public Health Association, USA: Washington DC. p. 1220.

Arix, T., Gunduz, U., Yucel, M., Turker, L., Sediroglu, V. and Eroglu, I. 1996. Photoproduction of hydrogen by *Rhodobactor sphaeroides* O.U. 001. Proceedings of the 11th World Hydrogen Energy Conference. Stuttgart, Germany. 3:2417-2424.

Asada, Y., Ohsawa, M., Nagai, Y., Ishimi, K., Fukatsu, M., Hideno, A., Wakayama, T. and Miyake, J. 2008. Re-evaluation of hydrogen productivity from acetate by some photosynthetic bacteria. Int. J. Hydrogen Energy 33:5147-5150.

Avissar, Y.J. and Moberg, P.A. 1995. The common origins of the pigments of life-early steps of chlorophyll biosynthesis. Photosynth. Res. 44:221-242.

Azbar, N.F., Dokgöz, T., Keskin, F., Eltem, R., Korkmaz, K.S. and Gezgin, Y. 2009. Comparative evaluation of bio-hydrogen production from cheese whey wastewater under thermophilic and mesophilic anaerobic conditions. Int. J. Green Energy 6:192–200.

Barbosa, M.J., Rocha, J.M.S., Tramper, J. and Wijffels, R.H. 2001. Acetate as a carbon source for hydrogen production by photosynthetic bacteria. J. Biotechnol. 85:25-33.

Basak, N. and Das, D. 2007. The prospect of purple non-sulfur (PNS) photosynthetic bacteria for hydrogen production: the present state of the art. World J. Microbiol. Biotechnol. 23:31–42.

Beale, S. I. 1999. Enzymes of chlorophyll biosynthesis. Photosynth. Res. 60:43–73.

Benemann, J. 1997. Feasibility analysis of photobiological hydrogen production. Int. J. Hydrogen Energy 22:979-987.

Berg, I. and Ivanosky, R. 2009. Enzymes of the citramalate cycle in *Rhodospirilum rubrum*. Microbiol. 78.1:16-24.

Berg, I., Ludmila, V., Filatova, R. and Ivanovsky, N. 2002. Inhibition of acetate and propionate assimilation by itaconate via propionyl-CoA carboxylase in isocitrate lyase-negative purple bacterium *Rhodospirillum rubrum*. FEMS Microbiol. Letters. 216:49-54.

Bertani, G. 1951. Studies on lysogenesis. I. The mode of phage liberation by lysogenic *Escherichia coli*. J. Bacteriol. 62:293-300.

Blankenship, R., Madigan, M.T. and Bauer, C. 1995. Anoxygenic Photosynthetic Bacteria. Kluwer Academic, Netherlands.

Bollivar, D., Clauson, C., Lighthall, R., Forbes, S., Kokona, B., Fairman, R., Kundrat, L. and Jaffe, E. 2004. *Rhodobacter capsulatus* porphobilinogen synthase, a high activity metal ion independent hexamer. BMC Biochem. 5:17-25.

Borja, R. 1995. Comparison of an anaerobic filter and an anaerobic fluidize bed reactor treating palm oil mill effluent. Process Biochemistry 30(6):511-521.

Bowles, L.K. and Ellefson, W.L. 1985. Effects of butanol on *Clostridium acetobutylicum*, Appl. Environ. Microbiol. 50: 1165–1170.

Box, G. and Behnken, D. 1960. Some new three level designs for the study of quantitative variables. Technometrics. 2: 455-475.

Box G.E.P., Hunter S.J. and Hunter W.G.. 1978. Statistics for experimenters : An introduction to design, data analysis, and model nuilding. John Wiley & Sons, New York.

Bozell, J., Moens, L., Elliott, D.C., Wang, Y., Neuenschwander, G.G., Fitzpatrick, S.W., Bilski, R.J. and Jarnefeld, J.L. 2002. Production of levulinic acid and use as a platform for derived products. Resou. Conserv. Recy. 28:227-229.

Brandl, H., Knee, Jr., E.J., Fuller, R.C., Gross, R.A. and Lenz, R.W. 1989. Ability of the phototrophic bacterium *Rhodospirillum rubrum* to produce various poly(*β*-hydroxyalkanoates): potential sources for biodegradable polyesters. Int. J. Biol. Macromol. 11:49-55.

Bunke, A., Schimid, H., Burmeister, H., Merkle, P. and Gander, B. 2000. Validation of a capillary electrophoresis method for determination of 5-aminolevulinic acid and degradation products. J. Chromato. A. 883:285-290.

Celik, D., Bayraktar, E. and Mehmetoglu, U. 2004. Biotransformation of 2-phenylethanol to phenylacetaldehyde in a two-phase fed-batch system. Biochem. Eng. J. 17:5-13.

Chaikritsadakarn, A. 2004. Production of 5-aminolevulinic acid from monosodium glutamate effluent by halotolerant photosynthetic bacterium (*Rhodobacter capsulatus* SS3) and its application. Master of Science Thesis in Environmental Technology. The Joint Graduate School of Energy and Environment at King Mongkut's University of Technology Thonburi, Thailand.

Chen, C., Lu, W., Lui, C. and Chang, J. 2007. Improved phototrophic H^2 production with *Rhodopseudomonas palustris* WP3-5 using acetate and butyrate as dual carbon substrates. Biosource Technology 10:10-16.

Chen, C.H., Lu,W.B., Wu, J.F. and Chang, J.S. 2007. Enhancing phototrophic hydrogen production of *Rhodopseudomonas palustris* via statistical experimental design. Int. J. Hydrogen Energy 32:940–949.

Chen, C.-Y. and Chang, J.-S. 2006. Enhancing phototropic hydrogen production by solid-carrier assisted fermentation and internal optical-Fiber illumination. Process Biochem. 4:2041-2049.

Chen, C.-Y., Lee, C.-M. and Chang, J.-S. 2006. Feasibility study on bioreactor strategies for enhanced photohydrogen production from *Rhodopseudomona palustris* WP3-5 using optical-fiber-assisted illumination systems. Int. J. Hydrogen Energy 31:2345-2355.

Chung, S.Y., Seo, K.H. and Rhee, J.I. 2005. Influence of culture conditions on the production of extra-cellular 5-Aminolevulinic acid (ALA) by recombinant *E.coli*. Process Biochem. 40:385-394.

Chumanop, J., Chuichulcherm, S., Chisti, Y. and Srinophakun, P. 2008. Protease Production *by Aspergillus oryzae* in Solid-state Fermentation Using Agroindustrial Substrates. J. Chem. Technol. Biotechnol..83: 1012-1018.

Cronan, J.E. and LaPorte, D. 1996. Tricarboxylic acid cycle and glyoxylate bypass. *In*: *Escherichia coli* and *Salmonella*: *Cellular and Molecular Biology*, Neidhardt, F.C. *et al.*, eds., ASM Press, Washington. pp. 206–216.

Dalton, J.T., Yates, C.R., Yin, D., Straughn, A., Marcus, S.L, Golub, A.L. and Meyer, M.C. 2002. Clinical pharmacokinetics of 5-aminolevulinic acid in healthy volunteers and patients at high risk for recurrent bladder cancer. J. Pharmacol. Exp. Ther. 301:507–512.

Das, D. and Veziroğlu, T.N. 2001. Hydrogen production by biological processes: a survey of literature. Int. J. Hydrogen Energy 28:13-27.

Dawson, R.C., Elliott, D.C. and Jones, K.M. 1987. Data for Biochemical research. 3rd ed., Clarendon Press, Oxford. 561 p.

De Philippis, R., Ena, A., Guastini, M., Sili, C. and Vincenzini, M. 1992. Factors affecting poly-β-hydroxybutyrate accumulation in cyanobacteria and in purple non-sulfur bacteria. FEMS Microbiol. Rev. 103:187–194.

de Vrije, T., de Haas, G.G., Tan, G.B., Keijsers, E.R.P. and Claassen, P.A.M. 2002. Pretreatment of Miscanthus for hydrogen production by *Thermotoga elfii*. Int. J. Hydrogen Energy 27:1381-1390.

Di Venosa, G.D., Fukuda, H., Perotti, C., Batlle, A. and Casas, A. 2004. A method for separating ALA from ALA derivatives using ionic exchange extraction. J. Photochem. Photobiol. B 75:157-163.

Ditta, G., Stanfield, S., Corbin, D. and D. Helinski. 1980. Broad host range DNA cloning system for gram negative bacteria: Construction of a gene bank of *Rhizobium meliloti*. Proc. Natl. Acad. Sci. USA 77:7347-7351.

Doelle, H.W. 1969. Bacterial metabolism. London: Academic Press, Inc.

Drolet, M., Peloquin, L., Echelard, Y., Cousineau, L. and Sasarman, A. 1989. Isolation and nucleotide sequence of the *hemA* gene of *Escherichia coli* K12. Mol. Gen. Genet. 216:347-352

Eisenberg, D. 2002. Metabolism of nitrogenous compounds: Amino acids, porphyrins and neurotransmitters. *In* Biochemistry. (Mathews, K.C., and Holde, V.K.E., ed). Addison Wesley Longman, San Francisco. pp. 746-793.

Elfsson, B., Wallin, I., Eksborg, S., Rudaeus, K. and Ros, A.M. 1998. Stability of 5-aminolevulinic acid in aqueous solution. Euro. J. Pharma. Sci. 7:87–91.

Ensign, S.A. 2006. Revisiting the glyoxylate cycle: alternate pathways for microbial acetate assimilation. Mol. Microbiol. 61:274-276.

Eraso, J. M. and S. Kaplan. 1994. *prrA*, a putative response regulator involved in oxygen regulation in photosynthesis gene expression in *Rhodobacter sphaeroides*. J. Bacteriol. 176:32-43.

Eroglu, E., Eroglu, I., Gunduz, U., Turker, L. and Yucel, M. 2006. Biological hydrogen production from olive mill wastewater with two-stage processes. Int. J.Hydrogen Energy 31:1527-1535.

Eroglu, E., Gunduz, U., Yucel, M., Turker, L. and Eroglu, I. 2004. Photobiological hydrogen production by using olive mill wastewater as a sole substrate source. Int .J. Hydrogen Energy.29**:**163–171.

Eroglu, I., Aslan, K., Gündüz, U., Yüel, M. and Türker, L. 1999. Substrate consumption rates for hydrogen production by *Rhodobacter sphaeroides* in a column photobioreactor. J. Biotechnol. 70:103-113.

Erskine, T.P., Coates, L., Butler, D., Youell, H.J., Brindley, A.A., Wood, P.S., Warren, J.M., Shoolingin-Jordan, M.P. and Cooper, B.J. 2003. X-ray structure of a putative reaction intermediate of 5-aminolaevulinic acid dehydratase. Biochem. J. 373:733-738.

Fabiano, B. and Perego, P. 2002.Thermodynamic study and optimization of hydrogen production *by Enterobacter aerogene*. Int. J. Hydrogen Energy. 27: 149–156.

Fales, L., Kryszak, L., and Zeilstra-Ryalls, J. 2001. Control of *hemA* expression in *Rhodobacter sphaeroide*s 2.4.1: Effect of a transposon insertion in the *hbdA* gene. J. Bacteriol. 183:1568-1576.

Fang H.H.P. and Yu, H. 2002. Mesophilic acidification of gelatinaceous wastewater. J. Biotechnol. 93(2):99-108.

Fang, H.H.P. and Yu, H. 2002. Mesophilic acidification of gelatinaceous wastewater. J. Biotechnol. 93:99-108.

Fang, H.H.P., Liu, H. and Zhang, T. 2005. Phototrophic hydrogen production from acetate and butyrate in wastewater. Int. J. Hydrogen Energy 30(7):785-793.

Feick, R., Shiozawa, J.A. and Ertlmaier, A. 1995. Biochemical and spectroscopic properties of the reaction center of the green filamentous bacterium *Chloroflexus aurantiacus*. *In*: R. Blankenship, M.T. Madigan and C. Bauer (eds.) Anoxygenic Photosynthetic Bacteria, Kluwer Academic, Netherlands. pp. 699-708.

Filatova, L., Berg, I. E., Krasil'nikova, A., Tsygankov, T., Laurinavichene, and Ivanobsky R. N. 2005. A study of the mechanism of acetate assimilation in purple nonsulfur bacteria lacking the glyoxylate shunt: Acetate assimilation in *Rhodobacter sphaeroides*. Microbiol. 74:265–269.

Firsow, N.N. and Drew, G. 1977. Differentiation of the intracytoplasmic membrane of *Rhodopseudomonas palustris* induced by variations of oxygen patial pressure or light intensity. Arch. Microbiol. 115:299-306.

Fissler, J., Schirra, C., Kohring, G.W. and Giffhorn, F. 1994. Hydrogen production from aromatic acids by *Rhodopseudomonas palustris*. Appl. Microbiol. Biotechnol. 41:395-399.

Flynn, T., Ghirardi, M.L. and Seibert, M**.** 2002. Accumulation of multiple O_2-tolerant phenotypes in H_2-producing strains of *Chlamydomonas reinhardtii* by sequential application of chemical mutagenesis and selection. Int. J. Hydrogen Energy 27**:**1421-1430.

Franchi, E., Tosi, C., Scolla, G., Penna, G.D., Rodriguez, F. and Pedroni, P.M. 2004. Metabolically engineered *Rhodobacter sphaeroides* RV strains for improved biohydrogen photoproduction combined with disposal of food wastes. Marine Biotechnol. 19:552–565.

Frankenberg, N., Erskine, T.P., Cooper, B.J., Shoolingin-Jordan, M.P., Jahn, D. and Heinz, W.D. 1999. High resolution crystal structure of a Mg^{2+}-dependent porphobilinogen synthase. J. Mol. Biol. 289:591-602.

Freist, W., Gauss, D.H., Söll, D. and Lapointe, J. 1997. Glutaminyl-tRNA synthetase. Biol.Chem. 378:1313-1329.

Frere, F., Schubert, W., Stauffer, F., Frankengerg, N., Neier, R., Jahn, D. and Heinz, W.D. 2002. Structure of porphobilinogen synthase from *Pseudomonas aeruginosa* in complex with 5-fluorolevulinic acid suggests a double Schiff base mechanism. J. Mol. Biol. 320:237-247.

Fuji, T., Tarusawa, M., Miyanaga, M., Kiyota, S., Watanabe, T. and Yabuki, M. 1987. Hydrogen production from alcohols, malate and mixed electron donors by *Rhodopseudomonas* sp. No. 7. Agric. Biol. Chem. 51(1):1–7.

Fukada, H., Casas, A. and Batlle, A. 2005. Aminolevulinic acid: from its unique biological function to its star role in photodynamic therapy. Int. J. Biochem. Cell Biol. 37:272-276.

Gacond, S., Frere, F., Nentwich, M., Faurite, J.P., Frankenberg-Dinkel, N. and Neier, R. 2007. Synthesis of bisubstrate inhibitors of porphobilinogen synthase from *Pseudomonas aeruginosa*. Chem. Biodivers. 4:189-202.

Ganapathy, K., Narayana, V. and Subramanyan, B. 1998. Problem Solving Techniques, Quality Circle Forum of India, Andhra Pradesh, India. pp. 177–202.

Gest, H. and Kamen, M.D. 1949. Photoproduction of molecular hydrogen by *Rhodospirillum rubrum*. Science 109:558-559.

Gest, H., Kamen, M.D. and Brego, N. 1950. Studies on the metabolism of photosynthetic bacteria. V. Photoproduction of hydrogen and nitrogenfixation by *Rhodospirillum rubrum*. J. Biol. Chem. 182:153–70.

Gogotov, I.N. 1986. Hydrogenases of phototrophic microorganisms. Biochimie 68:181-187

Greasham, R.L. 1983. Media for microbial fermentations, Bioprocessing. *In*: H.J. Rehm, G. Read, A. Puhler and P. Stagler, Editors, Biotechnology vol. 3**.** VCH Publisher Inc., New York. pp. 128–139.

Grothe, E., Young, M.M. and Chisti, Y. 1999. Fermentation optimization for the production of poly(β-hydroxybutyric acid) microbial thermoplastic. Enzyme and Microbial. Technol. 25:132-141.

Guo, W.-Q. Ren, N.Q., Wang, X.J., Xiang, W.S., Ding, J., You, Y. and Liu, B.F. 2009. Optimization of culture conditions for hydrogen production by *Ethanoligenens harbinense* B49 using response surface methodology. Bioresour. Technol. 100**:**1192–1196.

Hallenbeck, P, C. and Benemann, J.R. 2002. Biological hydrogen production; fundamentals and limiting processes. Int. J.Hydrogen Energy 27:1185-1193.

Hansel, A. and Lindblad, P. 1998. Mini-review: toward optimization of cyanobacteria as biotechnologically relevant producers of molecular hydrogen, a clean energy source. Appl Environ Microbiol. 50:153–60.

Harlow, E., and D. Lane. 1999. Using Antibodies: A Laboratory Manual. Cold Spring Harbor Laboratory Press, Cold Spring Harbor.

Harwood, C.S. Nitrogenase-catalyzed hydrogen production by purple non sulfur photosynthetic bacteria. *In*: Bioenergy, Wall J.D., Harwood, C.S. and Demain, A. Eds.: ASM Press, Washington.

He, D., Bultel, Y., Magnin, J.P., Roux, C. and Willison, J.C. 2005. Hydrogen photosynthesis by *Rhodobacter capsulatus* and its coupling to a PEM fuel cell. J. Power Sources 141:19-23.

He, G.Q., Kong, Q. and Ding, L.X. 2004. Response surface methodology for optimization the fermentation medium of *Clostridium butyricum*. Lett. Appl. Microbiol. 39:363–368.

Hillmer, P. and Gest, H. 1977. Hydrogen metabolism in photosynthetic bacterium *Rhodopseudomonas capsulata*: production and utilization of H_2 by resting cells. J. Bacteriol. 129:732-739.

H-Kittikul, A., Prasertsan, P., Srisuwan, K., Jitbunjerdkul, S. and Thonglimp, W. 1994. Oil recovery from palm oil mills waste water. Proceeding Oil Loss Prevention in Palm Oil Industry. Suratthani, Thailand. 7-14.

Howarth, D. C. and Codd, G. A. 1985. The uptake and production of molecular hydrogen by unicellular cyanobacteria. J. Gen. Microbiol. 131:1561-1569.

Hustede, E., Steinbuchel, A. and Schlegel, H.G. 1993. Relationship between the photoproduction of hydrogen and the accumulation of PHB in non-sulfur purple bacteria. Appl. Microbiol. Biotechnol. 39:87-93.

Ilag, L.L., Kumar, A.M. and Söll, D. 1994. Light regulation of chlorophyll biosynthesis at the level of 5-aminolevulinic acid formation in *Arabidopsis*. The Plant Cell 6:265-275.

Imhoff, J.F. and Trüper, H.G. 1992. The genus *Rhodospirillum and* related genera *In* The prokaryotes: A handbook on the biology of bacteria ecophysiology, isolation, identification, application Vol III. (2nd edition). B. Genera. H.G. Truper, M. Dworkin, W. Harder. And K.H. Schleifer (Eds). Springer-Verlag, New York. p. 2141-2155

Imhoff, J.F. and Trüper, H.G.1989. Purple nonsulfur bacteria (*Rhodospirillaceae* Pfennig and Truper 1971, 17AL). *In*: Staley J T Bergey's Manual of Systematic Bacteriology. Williams & Wilkins, Baltimore. pp 1658-1682.

Imhoff, J.F., Trüper, H.G. and Pfennig, N. 1984. Rearrangement of species and genera of phototrophic " Purple Nonsunfur Baacteria". Int. J. Sys. Bacteriol. 34:304-343.

Ivanovsky, R.N., Krasilnikova, E.N. and Fal, Y.I. 1993. A pathway of the autotrophic CO_2 fixation in *Chloroflexus aurantiacus*. Arch. Microbiol. 159:257-264.

Jahn, D., Verkamp, E. and Söll, D. 1992. Glutamyl-transfer RNA: a precursor of heme and chlorophyll biosynthesis. J. Trends in Biochemical Sciences 17(6):215-218.

James, B.D., Baum, G.N., Perez, J., Buam, K.N. 2009. Technoeconomic boundary analysis of biological pathways to hydrogen production. US Department of Energy: September 2009.

Jamil, Z., Annuar, S.M.M., Ibrahim, S. and Vikineswary, S. 2009. Optimization of phototrophic hydrogen production by *Rhodopseudomonas palustris* PBUM001 *via* statistical experimental design. Int. J. Hydrogen Energy 34:7502-7512.

Jarret, C., Stauffer, F., Henz, E.M., Marty, M., Luond, M.R., Bobalova, J., Schurmann, P. and Neier, R. 2000. Inhibition of *Escherichia coli* porphobilinogen synthase using analogs of postulated intermediates. Chem. Bio. 7:185-196.

Jerrold, E. M., and Weinstein, A. 1985. Calculus. Springer-*Verlag*, New York.

Jessee, J. 1986. New subcloning efficiency competent cells: >1 x 10^6 transformants/μg. Focus 8**:**9.

Jo, J., Lee, D. and Park, J. 2006. Modeling and optimization of photosynthetic hydrogen gas production by green alga *Chlamydomonas reinhardtii* in sulfur-deprived circumstance. Biotechnol. Progress 22:431–437.

Johansson, M.W, Keyser, P., Sritunyalucksana, K. and Söderhäll, K. 2000. Crustacean haemocytes and haematopoiesis. Aquaculture 191:45-52.

Jouanneau, Y., Wong, B. and Vignalis, P.M. 1985. Stimulation by light of nitrogenase synthesis in cell of *Rhodopseudomona capsulate* growing in N-limited continuous cultures. Biochem. Biophys. Acta 808:149-155.

Kaneko, S., Aoki, T., Nanato, H., Miyoshi, N., Houki, S. and Fukuda, Y. 1998. Intraoperative photodynamic diagnosis of human glioma using 5-ALA induced protoporphyrin IX. Iwamizawa-siritu Sougou Byouin-shi 24:71-79

Karube, I., Matsunaga, T., Tsuni, S. and Suzuki, S. 1976. Continuous hydrogen production by immobilized whole cell of *Clostridium byturicum*. Biochem. Biophys. Acta 44:338-345.

Kemavongse, K., Prasertsan, P., Upaichit, A. and Methacanon, P. 2008. Poly-β-hydroxyalkanoate production by halotolerant *Rhodobacter sphaeroides* U7. World J. Microbiol. Biotechnol. 24:2073–2085.

Kern, M., Klipp, W. and Klemme, J.H. 1994. Increased nitrogenase-dependent H_2 photoproduction by *hup* mutants of *Rhodospirillum rubrum*. Appl. Env. Microbiol. 60:1768-1774.

Khatipov, E., Miyake ,M., Miyake, J. and Asada, Y. 1998. Accumulation of poly-hydroxybutyrate by *Rhodobacter sphaeroides* on various carbon and nitrogen substrates. FEMS Microbiol. Lett.162:39–45.

Kim, J.-N., Yun, J.-S. and Ryu, H.-W. 2001. Simultaneous determination of δ-aminolevulinic acid, porphobilinogen, levulinic acid and glycine in culture broth by capillary electrophoresis. J. Chromato. A. 938:137-143.

Kim, J.S., Ito, K. and Takahashi, H. 1980. The relationship between nitrogenase activity and hydrogen evolution in *Rhodopseudimonas palustris*. Agric. Biol. Chem. 44:827-833.

Kim, M.-K. and Harwood, C.S. 1991. Regulation of benzoate-CoA ligase in. *Rhodopseudomonas* palustris. FEMS Microbiol. Lett. 83:199–204.

Kirk, R.E., Othmer, D.F., Grayson M. and Eckroth, D. 1985. Concise encyclopedia of chemical technology XIII. New York Wiley Interscience. p. 838-893.

Klemme, J.H. 1993. Photoproduction of hydrogen by purple bacteria: a critical evolution of the rate limiting steps. Z .Naturforsch. 48c:482-487.

Koku, H. Eroğlu, İ., Gündüz,U., Yüce,l M. and Türker, L. 2002. Aspects of the metabolism of hydrogen production by *Rhodobacter sphaeroides*. Int J Hydrogen Energy 2:1315–1329.

Koku,H., Eroğlu,İ., Gündüz, U., Yücel, M. and Türker, L. 2003. Kinetics of biohydrogen production by the photosynthetic bacterium *Rhodobacter spheroids* O.U. 001, Int J Hydrogen Energy 28:381–388.

Koller, M., Bona, R., Chiellini, E., Fernandes, E.G., Horvat, P., Kutschera, C., Hesse, P. and Braunegg, G. 2008. Polyhydroxyalkanoate production from whey by *Pseudomonas hydrogenovora*. Bioresour. Technol. 99:4854–4863.

Kovach, M.E., Phillips, R.W., Elzer, P.H., Roop II, R.M. and Peterson, K.M. 1994. pBBR1MCS: A broad-host-range cloning vector. *BioTechniques* 16:800-802.

Kranz, R.G., Gabbert, K.K., Locke, T.A. and Madigan, M.T. 1997. Polyhydroxyalcanoates production in *Rhodobacter capsulatus*: genes, mutants, expression, and physiology. Appl. Environ. Microb. 63(8):3003–3009.

Kumar, N. and Das D. 2001. Continuous hydrogen production by *Enterobacter cloacae* IIT-BT08 using lignocelluloses materials as solid matrices. Enzyme microbiol.Technol. 29:280-287.

Kuramochi, H., Konnai, M., Tanaka, T. and Hotta, Y.1997. Method for improving plant salt tolerance. US patent 5 661 111.

Lascelles, J. 1978. Regulation of pyrrole synthesis. *In* Clayton, R.K., Sistrom W.R. (eds). The photosynthetic bacteria. Plenum Press, New York. pp. 795-808.

Lee, C., Qiao, X., Goeger, D.E. and Anderson, K.E. 2004. Fluorometric measurement of 5-aminolevulinic acid in serum. Clinica Chimica Acta 347:183-188.

Lee, C.M., and Hung, K.T. Hydrogen production using *Rhodopseudomonas palustris* WP3–5 with hydrogen fermentation reactor effluent. *In:* Proceedings of the 16th WHEC, Lyon, France. 13–14 June 2006.

Lee, C.M., Chen, P.C., Wang, C.C. and Tung, Y.C. 2002. Photohydrogen production using purple nonsulfur bacteria with hydrogen fermentation reactor effluent. Int. J. Hydrogen Energy 27:1297-1302.

Lee, S.Y. and Söderhäll K. 2002. Early events in crustacean innate immunity. Fish Shellfish Immunol. 12:421-437.

Lehninger, A., Cox, M. Nelson. D. L. *2008*. Lehninger Principles of Biochemistry, 5th Edition. W.H. Freeman and Company, The United State of America.

Lemoigne, M. 1926. Produits de deshydration et de polymerization de l'acid ,β-oxybutyrique. Bull. soc. chim. biol. 8:770-782.

Levin, D.B., Pitt, L. and Love, M. 2004. Biohydrogen production: prospects and limitations to practical application. Int. J. Hydrogen Energy 29:173-185.

Levin, D.B., Zhum H., Beland, M., Cicek, N. and Holbein. B.E. 2007. Potential for hydrogen and methane production from biomass residues in Canada. Bioresour Technol. 98:654-660.

Li, Q., Sritharathikhum, P., Oshima, M. and Motomizu, S. 2008. Development of a novel detection reagent for simple and sensitive determination of trace amounts of formaldehyde and its application to flow injection spectrophotometric analysis. Analytica Chimica Acta 612:165-172.

Li, R.Y. and Fang, H.H.P. 2008. Hydrogen production characteristics of photoheterotrophic *Rubrivivax gelatinosus* L31. Int. J. Hydrogen Energy. 33:974–980.

Luengo, J.M., Garcia, B., Sandoval, A., Noharro G. and Olivera, E.R. 2003. Bioplastics from microorganisms. Curr. Opin. Microbiol. 6:1–10.

Madigan, M.T., Martinko, J.M., Dunlap, P.V. and Clark D.P. 2009. Brock Biology of Microorganisms, 12th Edition. Benjamin Cummings, San Francisco.

Madmarn, W. 2002. Increased yield of 5-aminolevulinic acid from photosynthetic bacterial mutant strain and its application in sex-reverse nile tilapia (*Oreochromis niloticus* Linn.). Master of Science Thesis in Biotechnology. Prince of Songkla University, Thailand.

Maeda, I., Miyasaka, H., Umeda, F., Kawase, M. and Yagi, K. 2003. Maximization of hydrogen production ability in high-density suspension of *Rhodovulvum sulfidophillum* cells using intracellular poly(3-hydroxybutyrate) as sole substrate. Biotechnol. Bioen. 81:474-481.

Maeda, I., Idehara, K., Okayama, N., Miura, Y., Yagi, K. and Mizoguchi, T. 1997. Poly(3-hydroxybutyrate) as an endogenous substrate for H_2 evolution in *Rhodovulum sulphidophilum*. Biotechnol. Lett. 19:1209-1212.

Makhneva, Z.K., Erokhin, Y.E. and Moskalenko,A.A. 2008. Assembly of LH2 light-harvesting complexes in *Rhodopseudomonas palustris* cells illuminated by blue and red light. Microbiol. 77:339-347.

Maness, P.C. and Weaver, P.F. 2001. Evidence for three distinct hydrogenase activities for *Rhodospirillum rubrum*. Appl. Microbiol. Biotechnol. 57:751–756.

Manish, S. and Banerjee, R. 2008. Comparison of biohydrogen production processes. Int. J. Hydrogen Energy. 33:279–286.

Maruyama, K. and Kitamura, H. 1975. Some effects of propionate on the growth of *Rhodopseudomonas sphaeroides* S. Agr. Biol. Chem. 39:1521-1526.

Masukawa, H., Nakamura,K., Mochimaru, M. and Sakurai, H. 2001. Photobiological hydrogen production and nitrogenase activity in some heterocystous cyanobacteria, p. 63-66. *In* J. Miyake, T. Matsunaga, and A. San Pietro (ed.), Biohydrogen II. Elsevier Science Ltd., Oxford, United Kingdom.

Masukawa, H., Mochimaru, M. and Sakurai, H. 2002. Hydrogenase and photobiological hydrogen production utilizing nitrogenase enzyme system in cyanobacteria. Int. J. Hydrogen Energy 27:1471–1474.

Mauzerall, M. and Granick, S. 1956. The occurrence and determination of 5-aminolevulinic acid and porphobilinogen in urine. J. Biol. Chem. 219:435-437.

McCarty, P.L. 1982. One hundred years of anaerobic treatment. In: Hughes DE, Stafford, D.A., Wheatley, B.I, Baader, W., Lettinga, G., Nyns, E.J., Verstraete, W., and Wenthworth, R.L. (eds) Anaerobic digestion 1981. Elsevier Biomedical Press, Amsterdam. pp 3–22.

Meinhardt, S.W., Kiley, P.J., Kaplan, S., Crofts, A.R. and Harayama, S. 1985. Characterization of light-harvesting mutants of *Rhodopseudomonas sphaeroides*. I. Measurement of the efficiency of light energy transfer from light-harvesting complexes to the reaction center. Arch. Biochem. Biophys. 236**:**130-139.

Melis, A., Zhang, L.P., Forestier, M., Ghirardi, M.L. and Seibert, M. 2000. Sustained photobiological hydrogen gas production upon reversible inactivation of oxygen evolution in the green algae *Chlamydomonas reinhardtii*, Plant Physiology 122:1-27.

Meyer, J., Kelley B.C. and Vicnais, P.M. 1978. Effect of light on nitrogenase function and synthesis in *Rhodopseudomonas capsulata*. J Bacteriol. 136:201-208.

Miyake, J. and Kawamura, S. 1987. Efficiency of light energy conversion to hydrogen by the photosynthetic bacterium *Rhodobacter sphaeroides*. Int. J Hydrogen Energy 2:147-149.

Miyake, J., Wakayama, T., Schnackenberg, J., Arai, T. and Asada, Y. 1999. Simulation of the daily sunlight illumination pattern for bacterial photo-hydrogen production. J. Biosci. Bioeng. 6:659-663.

Moser, J., Schubert, W.D., Beier, V., Bringemeier, I., Jahn, D. and Heinz, D.W. 2001. V-shaped structure of glutamyl-tRNA reductase, the first enzyme of tRNA-dependent tetrapyrrole biosynthesis. The EMBO J. 20:6583-6590.

Mu, Y., Wang, G. and Yu, H.-Q. Response surface methodological analysis on biohydrogen production by enriched anaerobic cultures Enzyme Microb. Tech. 38:905-913.

Mukhopadhyay M., Patra, A. and Paul, A.K. 2005. Production of poly(3-hydroxybutyrate) and poly(3-hydroxybutyrate-co-3-hydroxyvalerate) by *Rhodopseudomonas palustris* SP5212. World J. Microbiol. Biotechnol. 21:765–769.

Nakada, E, Nishikata, S., Asada Y. and Miyake, J. 1999. Photosynthetic bacterial hydrogen production combined with a fuel cell. Int. J. Hydrogen Energy 24:1053–1057.

Nath, K. and Das, D. 2004. Improvement for fermentative hydrogen production: various approaches. Appl. Microbiol. Biotechnol. 65:520–529.

Naveena, B.J., Altaf, Md., Bhadriah K. and Reddy, G. 2005. Selection of medium components by Plackett–Burman design for production of *l*(+) lactic acid by *Lactobacilus amylophilus* GV-6 in SSF using wheat bran, Bioresour. Technol. 96:485–490.

Neidle, L.E. and Kaplan, S. 1993. Expression of the *Rhodobacter sphaeroides hemA* and *hemT* genes, encoding two 5-aminolevulinic acid synthease isozymes. J. Bacteriol. 175:2292-2303.

Ni M., Leung D., Leung M. and Sumathy K. 2006. An overview of hydrogen production from biomass. Fuel Process. Technol., 87:461-472.

Nishikawa, S., Watanabe, K., Tanaka, T., Miyachi, N., Hotta, Y. and Murooka, Y. 1999. *Rhodobacter sphaeroides* mutants which accumulate 5-aminolevulinic acid under aerobic and dark conditions. J. Biosci. Bioeng. 87:798-804.

Oda, Y., Samanta, S. K., Rey, F. E., Wu, L,. Liu, X,. Yan, T., Zhou, J,. and Harwood, C. S.. 2005. Functional genomic analysis of three nitrogenase isozymes in the photosynthetic bacterium *Rhodopseudomonas palustris*. J. Bacteriol. 187:7784-7794.

Ogata, T. and Yamanaka, K. 1982. Butyrate activation in *Rhodopseudomonas palustris* No.82. Agri. Biol. Chem. 46:2593-2594.

Oh, Y.K., Seol, E.H., Lee, E.Y. and Park, S. 2004. Photoproduction of hydrogen production by a new chemoheterotrophic bacterium, *Rhodopseudomonas palustris* P4. Int. J. Hydrogen Energy. 29:1115-1121.

Oishi, H., Nomiyama, H., Nomiyama, K. and Tomokuni, K. 1996. Fluorometric HPLC determination of delta-aminolevulinic acid (ALA). J. Anal. Toxicol. 20:106-110.

Ooshima, H., Takakuwa, S. and Katsuda, T. 1998. Production of hydrogen by a hydrogenase-deficient mutant of *Rhodobacter capsulatus*. J. Ferment. Bioeng. 85:470-475.

Ormerod, J. G. 1956. The use of radioactive carbon dioxide in the measurement of carbon dioxide fixation in Rhodo*spirillum rubrum*. Biochem. J. 64:373-380.

Ormerod, J. G. and Gest, H.1962. Hydrogen photosynthesis and alternative metabolic pathways in photosynthetic bacteria. Bact. Rev. 26:51–66.

O-Thong, S., Prasertsan, P., Intrasungkha, N., Dhamwichukorn, S. and Birkeland, N.K. 2008. Optimization of simultaneous thermophilic fermentative hydrogen production and COD reduction from palm oil mill effluent by Thermoanaerobacterium-rich sludge. Int. J. Hydrogen Energy 33:1221-1231.

O-Thong, S., Prasertsan, P., Karakashev, D. and Angelidaki, I. 2008. Thermophilic fermentative hydrogen production by the newly isolated *Thermoanaerobacterium thermosaccharolyticum* PSU-2. Int. J. Hydrogen Energy 33:1204-1214.

Owen, W.F., Stuckey, D. C.,Healy, J.B., Jr., Young, L.Y. and McCarty, P.L. 1979. Bioassay for monitoring biochemical methane potential and anaerobic toxicity Water Res. 13:485−492.

Pansomboon, P. 1998. Hydrogen production by the photosynthetic bacterium *Rhodopseudomonas sphaeroides* 3701. Master of Science Thesis in Microbiology. Graduate School, Kasetsart University. Bangkok.

Peters, V., and Rehm, B.H.A. 2005. In vivo monitoring of PHA granule formation using GFP-labeled PHA synthase. FEMS Microbiol. Lett. 248:93-100.

Plackett B.J. and Burman J.P. 1994. The design of optimum multifactor experiments. Biometrika 33:305-325.

Prasertsan, P., Choorit, W. and Suwanno, S. 1993. Optimization for growth of *Rhodocyclus gelatinosus* in seafood processing effluents. World J. Microbiol. Biotechnol. 9:593-596.

Rahman, S.H.A., Choudhury, J.P. and Ahmad, A.L. 2006. Production of xylose from oil palm empty fruit bunch fiber using sulfuric acid. Biochem. Eng. J. 30:97-103.

Ramachandran, R. and Menon, R.K. 1998. An overview of industrial uses of hydrogen. Int. J. Hydrogen Energy 23:593-598.

Rebeiz, C. A., Juvik, J. A. and Rebeiz, C. C. 1988. Porphyric insecticides. I. Concepts and phenomenology. Pestic. Biochem. Physiol. 30:11-27.

Rebeiz, C. A., Montazer-Zouhool, A., Hopen, H. and Wu, S. M. 1984. Photodynamic herbicides. I Concepts and phenomenology. Enzyme Microb. Technol. 6:390-401.

Ren, N.Q., Liu, B.F., Ding, J. and Xie, G.J. 2009. Hydrogen production with *Rhodopseudomonas faecalis* RLD-53 isolated from freshwater pond sludge. Bioresour Technol. 100(1):484-487.

Riansa-ngawong, W. 2004. Effect of protein hydrolysate on production of 5-aminolevulinic acid from two strains of photosynthetic bacteria and use as an insecticide. Senior project. Faculty of Agro-Industry. Prince of Songkla University, Thailand.

Rieble, S., Ormerod, G.J. and Beale, I.S. 1989. Transformation of glutamate to 5-aminolevulinic acid by soluble extracts of *Chlorobium vibrioforme.* J. Bacteriol. 171:3782-3787.

Rosselló-Mora, R. and Amann, R. 2001. The species concept for prokaryotes. FEMS Microbiol. Rev. 25**:**39-67.

Sambrook, J., Fritsch, E. F. and Maniatis, T. 1989. Molecular Cloning: a Laboratory Manual, 2nd (Eds).Cold Spring Harbor, New York.

Sangkharak, K. and Prasertsan, P. 2007. Optimization of polyhydroxybutyrate production from a wild type and two mutant strains of *Rhodobacter sphaeroides* using statistical method. J. Biotechnol. 132:331-340.

Sasaki, K., Ikeda, S., Nishizawa, Y. and Hayashi, M. 1987. Production of 5-aminolevulinic acid by photosynthetic bacteria. J. Ferment. Technol. 65:511-515.

Sasaki, K., Tanaka, T., Nishizawa, Y. and Hayashi, M. 1991. Enhanced production of 5-aminolevulinic acid by repeated addition of levulinic acid and supplement of precursors in photoheterotrophic culture of *Rhodobacter sphaeroides*. J. Ferment. Bioeng. 71:403-406.

Sasaki, K., Tanaka, T., Nishizawa, Y. and Hayashi, Y. 1990. Production of herbicide, 5-aminolevulinic acid by *Rhodobacter sphaeroides* using the effluent of swine wastes from an anaerobic digester. Appl. Microbiol. Biotechnol. 32:727-731.

Sasaki, K., Watanabe, T., Tanaka, T. and Tanaka, T. 2002. Biosynthesis, biotechnological production and applications of 5-aminolevulinic acid. Appl. Microbiol. Biotechnol. 58:23-29.

Sasaki, T. 1998. Hydrogen and 5-aminolevulinic acid production by photosynthetic bacteria. *In*: O.R. Zaborsky, Editor, Biohydrogen, Plenum Press, London, pp. 133–142.

Sasikala, C.H. and Ramana, C.H. 1995. Biotechnological potentials of anoxygenic phototrophic bacteria II. Biopolyesters, biopesticide, biofuel, and biofertilizer. Advances Appl. Microbiol. 41:227-278.

Sasikala, K. and Ramana, C.V. 1991. Photoproduction of hydrogen from waste water of a lactic acid fermentation plant by a purple non-sulfur photosynthetic bacterium, *Rhodobacter sphaeroides* O.U. 001. Indian J. Experimental. Biol. 29:74–75.

Sasikala, K., Ramana, C.V. and Rao, P.R. 1992. Photoproduction of hydrogen from the wastewater of a distillery by *Rhodobacter sphaeroides* O.U.001. Int. J. Hydrogen Energy 17:23–27.

Sasikala, K., Ramana, C.V., Rao, P.R. and Kovacs, K.L. 1993. Anoxygenic phototrophic bacteria: physiology and advances in hydrogen production technology. Adv. Appl. Microbiol. 38:211–95.

Sasikala. K., Ramana, C.V., Rao, P.R. and Subrahmanyam, M. 1990. Effect of gas phase on the photoproduction of hydrogen and substrate conversion efficiency in the photosynthetic bacterium *Rhodobacter sphaeroides* O.U. 001. Int. J. Hydrogen Energy 15:795–797.

Sattayasmithstid, S. 2002. Optimization for production of 5-aminolevulinic acid from Halotolerant Photosynthetic Bacteria *Rhodobacter capsulatus* SS3. Master of Science Thesis in Biotechnology, Prince of Songkla University, Thailand.

Sawangsaeng, P. 2005. Strain improvement of halotolerant photosynthetic bacteria and optimization for production of 5-aminolevulinic acid. Master of Science Thesis in Biotechnology, Prince of Songkla University, Thailand.

Shi, X. and Yu, H. 2004. Hydrogen production from propionate by *Rhodopseudomonas capsulate*. Appl. Biochem. Biotechnol. 117:143-154.

Shi, X. and Yu, H. 2005. Optimization of volatile fatty acid compositions for hydrogen production by *Rhodopseudomonas capsulata*. J. Chem. Technol. and Biotechnol. 80:1198-1203.

Shi, X.Y. and Yu, H.Q. 2006. Conversion of individual and mixed volatile fatty acids to hydrogen by *Rhodopseudomonas capsulate.* Int. Biodet. Biodeg. 58:82-88.

Shively, J.M., Davidson, T. and Marrs, B.L. 1984. Derepression in the synthesis of the intermediate and large forms of ribulose 1,5-bisphosphate carboxylase/oxygenase in *Rhodopseudomonas capsulata*. Arch. Microbiol. 138:233–236.

Simon, R., U. Priefer, and A. Puhler. 1983. A broad host range mobilization system for in vivo genetic engineering: transposon mutagenesis in Gram-negative bacteria. Bio/Technology 1:37-45.

Sistrom, W. R. 1960. A requirement for sodium in the growth of *Rhodopseudomonas sphaeroides*. J. Gen. Microbiol. 22**:**778-785.

Sithisarankul, P., Cadorette, M., Davoli, C.T., Serwint, J.R., Chisolm, J.J. and Strickland, P.T. 1999. Plasma 5-aminolevulinic acid concentration and lead exposure in children. Environ Res 80:41-49.

Sreenath, H.K., Koegel, R.G., Moldes, A.B., Jeffries, T.W. and Straub, R.J. 2001. Ethanol production from alfalfa fiber fractions by saccharification and fermentation. *Process Biochem.* 36**:**1199–1204.

Stanier, R.Y., Doudoroff, M., Kunisawa, R. and Contopoulou, R. 1959. The role of organic substrate in bacterial photosynthesis. Biochem.45: 1246-1260.

Stewart, C.S. 1975. Some effects of phosphate and volatile fatty acids salts on the growth of rumen bacteria. J. Gen. Microbiol. 89:319-326.

Stiffler, H.J. and Gest, H. 1954. Effects of light intensity and nitrogen growth source on hydrogen metabolism in *Rhodospirillum rubrum*. Science 120:1024-1026.

Strobel, R, and Sullivan, G. 1999. Experimental design for improvement of fermentations. *In*: Demain AL, Davies JE, eds. Manual of Industrial Microbiology and Biotechnology. Washington: ASM Press, pp. 80-93.

Sunita, M. and Mitra, C.K. 1993. Photoproduction of hydrogen by photosynthetic bacteria from sewage and wastewater. J. Biosci 18:155–160.

Suwansaard, M. 2004. Effect of mineral salt on production of 5-aminolevulinic acid from halotolerant photosynthetic bacteria and use as plant growth stimulator. Senior project. Faculty of Agro-Industry. Prince of Songkla University, Thailand.

Suwanto, A. 2002. Effects of *hemB* antisense RNA on gamma-aminolevulinic acid production in *Rhodobacter sphaeroides*. Hayati 9:15-18.

Sweet, W.J. and Burris, R.H. 1981. Inhibition of nitrogenase activity by NH_4^+ in *Rhodospirillum rubrum*. J. Bacteriol. 145:824-831.

Taguchi. F., Chang, J.D., Takiguchi, S. and Morimoto, M. 1992. Efficient hydrogen production from starch by a bacterium isolated from termites. J. Ferment. Bioeng. 73:224-225.

Tai, T.N., Moore, M.D. and Kaplan, S. 1988. Cloning and characterization of the 5-aminolevulinate gene(s) from *Rhodobacter sphaeroides*. Gene 70:139-51.

Tait, G.H. 1973. 5-aminolevulinate synthetase of *Micrococcus denitrificans.* Biochem. J. 131:389-403.

Takabatake, H., Suzuki, K., Ko, I.B. and Noike, T. 2004. Characteristics of anaerobic ammonia removal by a mixed culture of hydrogen producing photosynthetic bacteria. Bioresour. Technol. 95:151-158.

Tamagnini, P., Axelsson, R., Lindberg, P., Oxelfelt, F., Wunschiers, R. and Lindblad, P. 2002. Hydrogenases and hydrogen metabolism in cyanobacteria. Microbiol Mol Biol Rev. 66:1–20.

Tanaka, T., Sasaki, K., Noparatanaraporn, N. and Nishio, N. 1994. Utilization of volatile fatty acids from the anaerobic digestion liquor of sewage sludge for 5-aminolevulinic acid production by photosynthetic bacteria. World. J. Microbiol. Biotechnol. 10:667-680.

Tanaka, T., Takahashi, K., Hotta, T., Takeuchi, Y. and Konnai, M. 1992. Promotive effects of 5-aminolevulinic acid on yield of several crops. In: Proceedings of the 19th annual meeting of plant growth regulator Society of America, San Francisco. Plant Growth Regulator Society of America, Washington DC, pp 237-241.

Tanaka, T., Watanabe, K., Hotta, Y., Lin, D., Sasaki, K. and Nagai, S. 1991. Formation of 5-aminolevulinic acid under aerobic/dark conditions by a mutant of *Rhodobacter sphaeroides*. Biotech. Lett. 13:589-594.

Tangprasitipap, A. 2005. Production of 5-aminolevulinic acid (ALA) from *Rhodobacter sphaeroides* SH5 on growth, survival and immune performance of black tiger shrimp, *Penaeus monodon*. Doctor Philosophy of Science Thesis in Biotechnology, Prince of Songkla University, Thailand.

Tao, Y., He, Y., Wu, Y., Liu, F., Li, X. Zong, W. and Zho, Z. 2008. Characteristics of a new photosynthetic bacterial strain for hydrogen production and its applications in wastewater treatment. Int. J. Hydrogen Energy 33:936-973.

Toch, D.C. and Cantu, M. 1980. Changes in the regulation of *Rhodospirillum rubrum* nitrogenase as influenced by nutritional and environmental factors. J. Bacteriol. 142:899-907.

Tsygankov, A.A. and Gogotov I.N. 1982. Influence of temperatureand pH of the medium on the nitrogenase and hydrogenase activity of *Rhodobacter capsulata* in nitrogen fixation. Microbiol. 51:325-330.

Tubb. R.S. 1974. Glutamine synthesis and ammonium regulation of nitrogenase synthesis in *Klebsiella*. Nature 251:481-485.

Türkarslan, S.,Yücel, M., Gündüz, U., Türker, L. and Eroğlu, İ**.** 2002. Identification of hydrogenase from *Rhodobacter* species and hydrogen gas production in photobioreactors. *In*: Abstract Book, BioHydrogen 2002 Conference, The Netherlands. April 21-24, 2002.

van der werf, M.J. and Zeikus, J.G. 1996. 5-Aminolevulinate production by *Escherichia coli* containing the *Rhodobacter sphaeroides hemA* gene. Appl. Envir. Microbiol. 62:3560-3566.

van Niel, C.B.1944. The culture, general physiology, morphology, and classification of the non-sulfur purple and brown bacteria. *Bacterial Rev.* 8:1-118.

Vignais, P.M., Colbeau, A., Willson, J.C. and Jouanneau, Y. 1985. Hydrogenase, nitrogenase and hydrogen metabolism in photosynthetic bacteria. Adv Microbiol Physiol. 26:154-234.

Wakayama, T. and Miyake, J. 2002. Light shade bands for the improvement of solar hydrogen production efficiency by *Rhodobacter sphaeroides* RV. Int. J. Hydrogen Energy 27:1495–1500.

Watanabe, K., Kim, J. S., Ito, K., Buranakarl, L., Kampee, T. and Takahashi, H. 1981. Thermostable nature of hydrogen production by non-sulfur purple photosynthetic bacteria isolated in Thailand. J. Agric. Biol. Chem. 45(1):17-222.

Wu, X., Wang, X., Yang, H. and Gou, L. 2010. A comparison of hydrogen production among three photosynthetic bacterial strains. Int. J. Hydrogen Energy doi:10.1016/j.ijhydene.2009.12.141.

Xu, L.P., Sun, Y.Z., Shi, Y., Wu, H., Zhang, B. and Zhao, D.Q. 2008. Optimization of cultivation conditions for extracellular polysaccharide and mycelium biomass by *Morchella esculenta* As 51620. Biochem. Eng. J. 39:66–73.

Yan, Q., Sun, Y., Ruan, L.F., Chen, J. and Yu, P.H.F. 2005. Biosynthesis of short-chain-length-polyhydroxyalkanoates during the dual-nutrient-limited zone by *Ralstonia eutropha*. World J. Microbiol. Biotechnol. 21:17–21.

Yetis, M., Gündüz, U., Eroglu, I., Yücel, M. and Türker, L. 2000. Photoproduction of hydrogen from sugar refinery wastewater by *Rhodobacter sphaeroides* O.U. 001. Int. J. Hydrogen Energy 25:1035-1041.

Yokoi, H., Maki, R., Hirose, J. and Hayashi, S. 2002. Microbial production of hydrogen from starch-manufacturing wastes. Biomass Bioenerg. 22:389-395.

Yokoi, H., Tokoshige, T., Hirose, J., Hyashi, S. and Takasaki, Y. 1997. Hydrogen production by immobilited cells of aciduric *Enterobacter aerogenes* strain HO-35. J. Ferment. Bioeng. 83: 484-491.

Zabut, B., El-Kahlout, K., Yücel, M., Gündüz, U., Türker, L. and Eroğlu, I. 2006. Hydrogen gas production by combined systems of *Rhodobacter sphaeroides* O.U.001 and *Halobacterium salinarum* in a photobioreactor. Int. J Hydrogen Energy 31:1553-1562.

Zeilstra-Ryalls, J.H. 2008. Chapter 42. Regulation of the tetrapyrrole biosynthetic pathway. *In*: The Purple Phototrophic Bacteria**.** C. Neil Hunter, Fevzi Daldal, Marion C. Thurnauer and J. Thomas Beattty (eds). Springer. The Netherlands.

Zeilstra-Ryalls, J.H. and Kaplan, S. 1995. Regulation of 5-Aminolevulinic acid synthesis in *Rhodobacter sphaeroides* 2.4.1: the genetic basis of mutant H-5 auxotrophy. J. Bacteriol. 177:2760-2768.

Zhang, Zh., Schwartz, S., Wagner, L. and Miller, W. 2000. A greedy algorithm for aligning DNA sequences. J. Comput. Biol. 7(1-2):203-214.

Zheng, X.J. and Yu, H.Q. 2005. Inhibitory effects of butyrate on biological hydrogen production with mixed anaerobic cultures. J. Environ. Management 74: 65-70.

Zhu, H., Suzuki, T., Tsygankov, A.A., Asada, Y. and Miyake, J. 1999. Hydrogen production from tofu wastewater by *Rhodobacter sphaeroides* immobilized in agar gels. Int. J. Hydrogen Energy 24:305–10.

Zorin, N.A. 1986. Redox properties and active center of phototrophic bacteria hydrogenases. Biochimie 68:97-101.

Zurrer, H. and Bachofen, R. 1979. Hydrogen production by the photosynthetic bacterium *Rhodospirillum rubrum*. Appl. Environ. Microbiol. 37 (5):789–793.

APPENDICES

Appendix A

Standard curve of cell dry weight

1. The culture of *Rba.sphaeroides* SH5 (pMS3) and *Rps. palustris* TN1, cultured under anaerobic-light (300 lux) at 37°C for 36 h, was adjusted the turbidometrically at the wavelength of 660 nm (OD_{660}) to be 0.2-0.8.
2. Cell pellet was harvested and twice washed with 20 mM Tris(HCl) pH 7.4. by centrifuge (8,000 *xg* for 10 min).
3. Cell pellet remaining in tubes were baked at 105°C for 12 h. and weighted the dry cell until their constantly weight (Saski *et al.,* 1987).

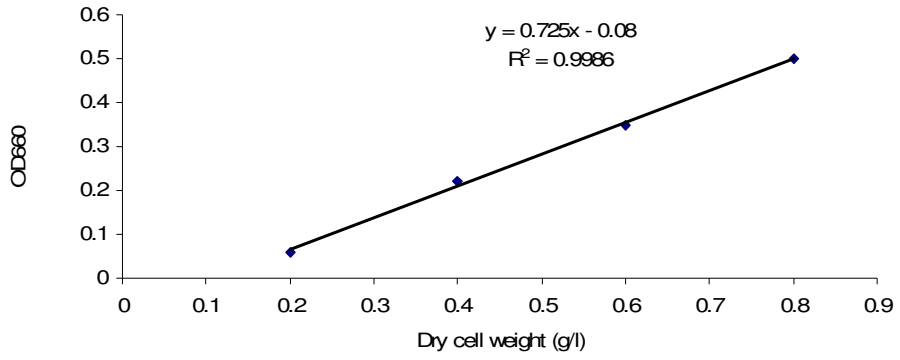

Figure A1. Standard curve of dry cell weight of *Rps. palustris* TN1.

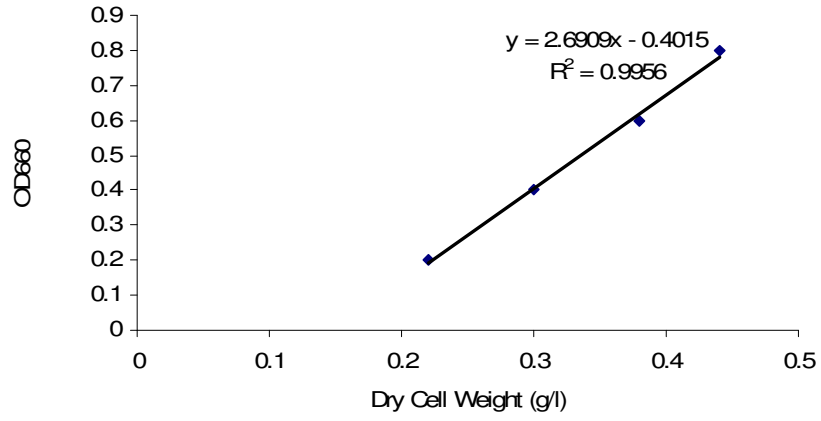

Figure A2. Standard curve of dry cell weight of *Rps. sphaeroides* SH5 (pMS3).

Appendix B

ALA assay

1. Standard curve of chemical assay of ALA

1.1 Chemical Preparation

- 1 M Acetate buffer pH 4.6

This buffer consists of 68.04g sodium acetate tri hydrate in 26.6ml acetic acid. The volume was adjusted to 1 liter with distilled water.

- Modified Ehrlich's reagent

Consistes of 1g p – dimethyl – aminobenzaldehyde (DMAB)
30ml glacial acetic acid
8ml 70% perchloric acid

Make volume to 50ml with glacial acetic acid

1.2 Standard curve preparation

1.2.1 Commercial ALA (0.1 mM) was prepared in distilled water and diluted by serial dilution.

1.2.2 Determined ALA by colorimetric method (Mauzerall and Granick, 1956). Plot the standard curve by the relationship of ALA and $OD_{553.}$

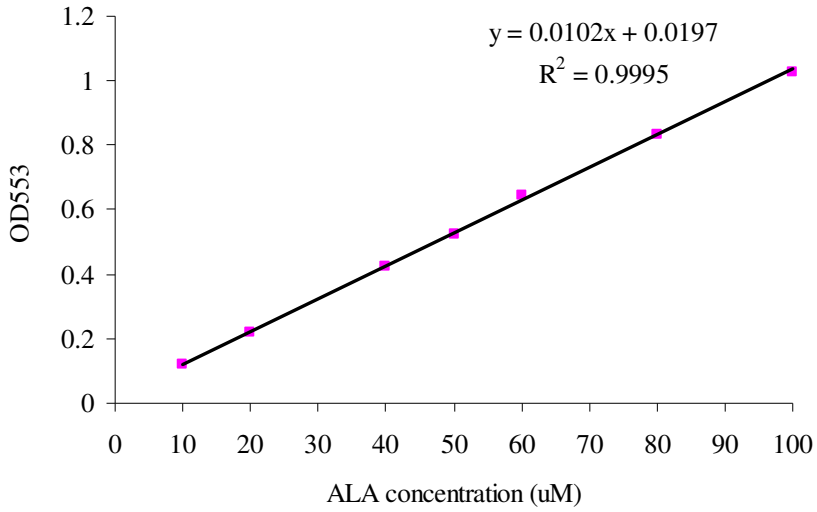

Figure B1. Standard curve of extracellular ALA (μM) by chemical assay.

2. HPLC assay of ALA

2.1 A Fluorescent derivative of ALA preparation

50 µl of sample was reacted with 3.5 ml of acetylacetone reagent, acetylacetone:ethanol:water (15:10:75 by vol) containing 0.4% NaCl, and 0.45 ml formaldehyde solution (8.5% v/v). This mixture was heated for 30 min at 100°C and then cooled in an ice bath. It was left to stand in the dark until analysis by HPLC with a fluorescence detector

2.2 HPLC Assay

Condition: Mobile phase: methanol and 2.5% (w/v) acetic acid (60:40 v/v)

Injection: 20 µl

Column: Inertsil ODS-3 column (5 µm, 250 × 150 mm) (GL Science Inc, Tokyo, Japan).

Operation temperature and flow rate: 40°C, flow rate of 0.6 ml min^{-1}

Fluorescence detection: excitation (363) and emission (473) nm.

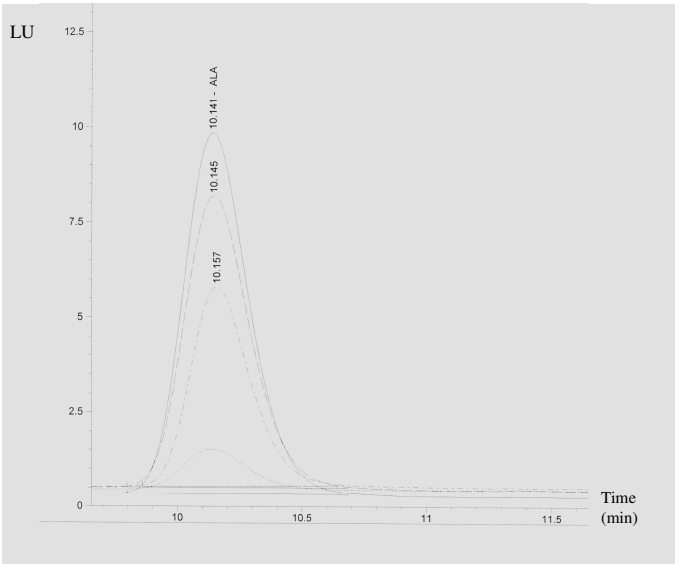

Figure B2. Chromatogram of standard ALA (µM) at 473 nm detected by HPLC.

3. ALA Bioassay

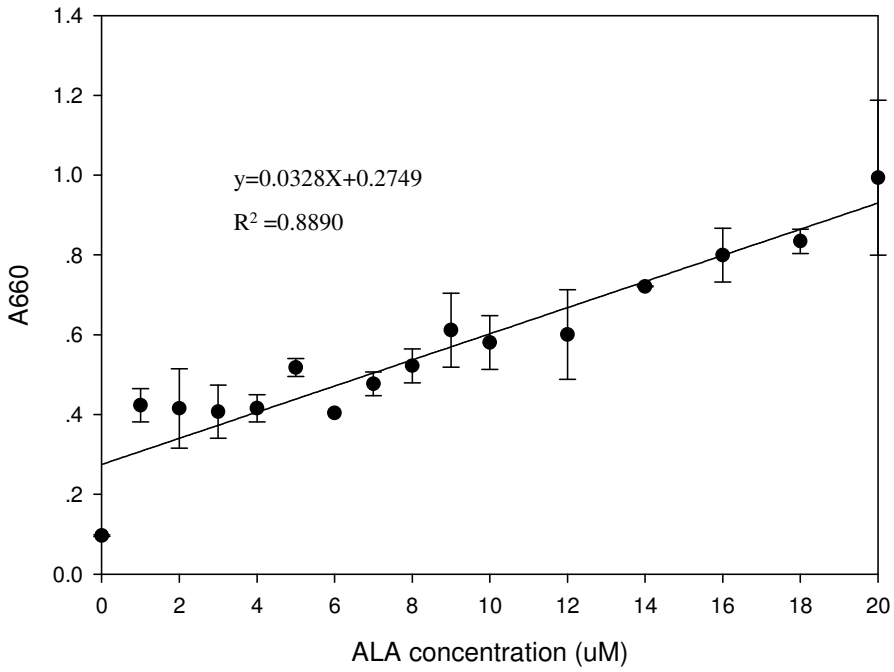

Figure B3. Standard curve of *Rba. Sphaeroides* AT1 growth *versus* ALA concentration in SIS medium supplemented with streptinomycin/spectromycin.

Appendix C

Hydrogen detection

1. Standard curve of Hydrogen

- Inject pure hydrogen (99%) to MX2100 OLDHAM gas detector at different volume.
- Plot the standard curve by the relationship of hydrogen volume and hydrogen concentration

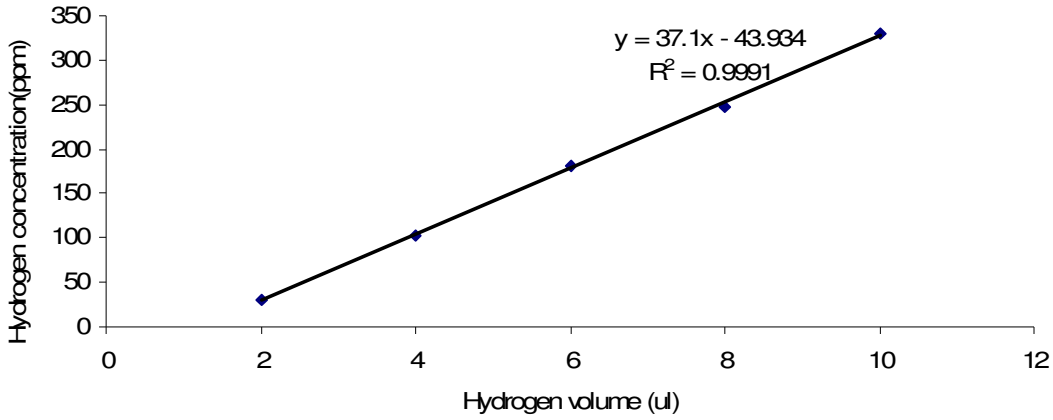

Figure C1. Standard curve of hydrogen concentration (ppm) detected by MX2100 OLDHAM gas detector.

2. Hydrogen calculation correlated to standard curve

Bacterial cell produce total biogas of 200 ml. 1 ml of biogas was withdrawn to determine hydrogen concentration (ppm) by injection into gas detector 1ml. The 170 ppm hydrogen concentration was detected by gas detector. Calculate hydrogen volume correlated to standard curve.

$$y\,(ppm) = 37.1x(\mu l) - 43.9$$
$$170\ ppm = 37.1x - 43.9$$
$$x = 3.40\ \mu l$$

Therefore 1 ml of injection contains hydrogen 3.40 µl

200 ml of total biogas contains hydrogen = 3.40 x 200 = 680 µl

Appendix D

Volatile fatty acid determination by GC

Condition: Injection: 1µl

Column: Stabilwax®-DA, Restek GC columns

Operation temperature at injection and detector port: 230 and 250°C

Oven: hold at 70°C for 3 min, (ii) ramp for 5 min at 20°C min^{-1} to a final temperature of 235°C, (iii) hold at 235°C for 3 min.

Carrier gas: Helium at flow rate 1.2 ml min^{-1}. .

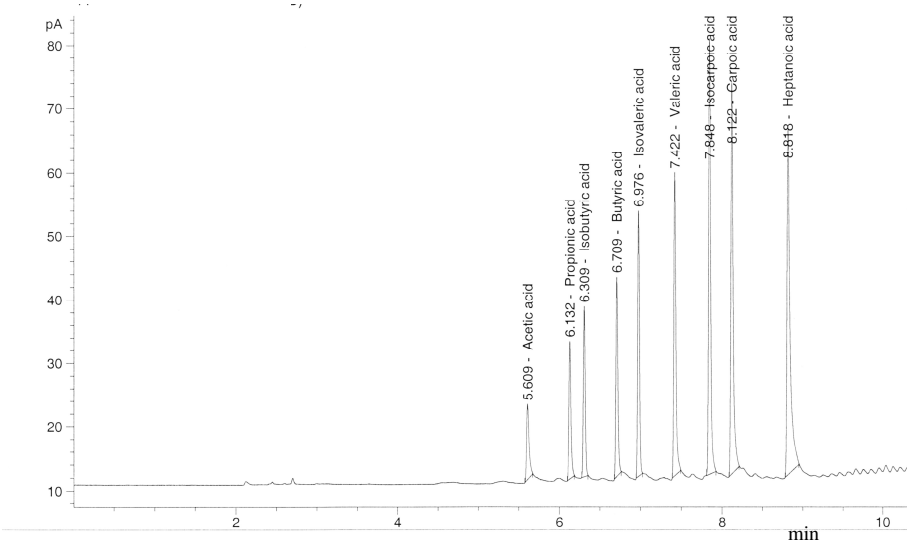

Figure D1. Chromatogram of volatile fatty acids by GC-FID.

Applendix E

Porphobilinogen activity assay

Assay Procedure

1. Add buffer 900 µl enzyme volume.
2. Preincubate assay mixture at 37˚C for 10 minutes.
3. At time 0, add 100 µl of 0.1 M ALA, Vortex quickly and replace in 37˚C of 5 minutes.
4. Stop the reactions by adding 500 µl of stop reagent, mixing quickly. Set at room temperature.
5. Add 100 µl of 0.1 M ALA- HCl, Vortex vigorously.
6. Centrifuge 5000 rpm for 3 minutes, keep solution in the dark.
7. Take 800 µl of supernatant and add 800µl of Ehrlich's reagent and vortex wall
8. Determine pink color at OD 555.

VITAE

Name Miss Maneewan Suwansaard

Student ID 4883006

Education Attainment

Degree	Name of Institution	Year of Graduation
B.Sc. Agro-Industry (1^{st} Class honors)	Prince of Songkla University	2004

Scholarship Awards during Enrolment

The Royal Golden Jubilee Ph.D. Scholarship (RGJ)

The Joint Graduate School of Energy and Environment (JGSEE) Research Fund

The Graduate School, Prince of Songkla University

List of Publications and Proceedings

Publications

Suwansaard, M., Choorit, W., Zeilstra-Ryalls, J.H. and Prasertsan, P. 2009. Isolation of anoxygenic photosynthetic bacteria from Songkhla Lake for use in a two-staged biohydrogen production process from palm oil mill effluent. Int. J. Hydrogen Energy. 34: 7523-7529.

Suwansaard, M., Choorit, W., Zeilstra-Ryalls, J.H.and Prasertsan, P. Photothrophic Hydrogen Production by Newly Isolated *Rhodopsuedomonas palustis* TN1 and Its Characteristics. Biotechnol. Lett. (Accepted).

Suwansaard, M., Prasertsan, P. and Zeilstra-Ryalls, J.H. Optimization of phototropic hydrogen production by *Rhodopsuedomonas palustris* TN1 using statistical methodology (In preparation).

Suwansaard, M., Prasertsan, P. and Zeilstra-Ryalls, J.H. Statistical approach for medium optimization of phototropic hydrogen production by *Rhodopseudomonas palustris* TN1 (In preparation).

Suwansaard, M., Prasertsan, P. and Zeilstra-Ryalls, J.H. Hydrogen and 5-aminolevulinic acid production by two strains of photosynthetic bacteria (In preparation).

Suwansaard, M., Prasertsan, P. and Zeilstra-Ryalls, J.H. Improvement of 5-aminolevulinic acid production by genertically engineered *Rhodobacter sphaeroides* SH5 (In preparation).

Presentations

Suwansaard, M., Prasertsan, P., Choorit, W. 2008. Selection of Hydrogen-Producing Photosynthetic Bacteria Isolated from Songkhla Lake using Mathematical Model. Proceeding of International Workshop on Biohydrogen Production Technology IWBT Conference on February 7-9, 2008, Indian Institue of Karaphur, India (Oral Presentation)

Suwansaard, M., Prasertsan, P., Choorit, W. 2008. Isolation and Selection Hydrogen- Producing Photosynthetic Bacteria from Songkhla Lake. Proceeding of RGJ congress IX on April 4-5, 2008, Pattaya, Thailand (Oral Presentation)

Suwansaard, M., Prasertsan, P., Choorit, W. 2008. Photothrophic Hydrogen Production by Newly Isolated *Rhodopsuedomonas palustis* TN1 and Its Characteristics. Proceeding of International Biotechnology Symposium (IBS) on October 12-17, 2008, Dalian, China (Poster Presentation)

Suwansaard, M., Prasertsan, P. and Zeilstra-Ryalls, J.H. 2009. Optimization of phototropic hydrogen production by *Rhodopsuedomonas palustris* TN1 using statistical methodology. Participate in 109th General meeting of American Society For Microbiology (ASM) on May 17-21, 2009 in Pennsylvania convention center, Philadelphia, Pennsylvania, USA (Poster presentation)

Suwansaard, M., Prasertsan, P. and Zeilstra-Ryalls, J.H. 2009. Hydrogen and 5-aminolevulinic acid production by two strains of photosynthetic bacteria. Participate in The 2009 Asian Bio-Hydrogen Symposium on August 26-28, 2009 in Khon Kaen, Thailand (Oral presentation)

Suwansaard, M., Prasertsan, P. and Zeilstra-Ryalls, J.H. 2009. Statistical Optimization for phototropic hydrogen production by *Rhodopseudomonas palustris* TN1. Participate in RGJ Seminar Series LXIV: Science Technology for Substainable Development on September 4, 2009 in Faculty of Science, Prince of Songkla University, Thailand (Oral presentation)

Suwansaard, M., Prasertsan, P. and Zeilstra-Ryalls, J.H. 2009. Statistical approach for medium optimization of phototropic hydrogen production by *Rhodopseudomonas palustris* TN1. Participate in 14th Europian Congress on Biotechnology on September 13-16, 2009 in Barcelona, Spain (Poster presentation)